Stable Isotope Analysis of Archaeological and Modern Micromammals from the Greater Cape Floristic Region near Pinnacle Point, on the South Coast of South Africa

by

Hope Marie Williams

A Dissertation Presented in Partial Fulfillment
of the Requirements for the Degree
Doctor of Philosophy

Approved November 2015 by the
Graduate Supervisory Committee:

Curtis W. Marean, Co-Chair
Kelly J. Knudson, Co-Chair
Kaye Reed

ARIZONA STATE UNIVERSITY

December 2015

ABSTRACT

The Middle Stone Age archaeological record from the south coast of South Africa contains significant evidence for early modern human behavior. The south coast is within the modern Greater Cape Floristic Region (GCFR), which in the present-day encompasses the entirety of South Africa's Winter Rainfall Zone (WRZ) and contains unique vegetation elements that have been hypothesized to be of high utility to hunter-gatherer populations. Extant paleoenvironmental proxy records for the Pleistocene in the region often indicate evidence for more open environments during the past than occur in the area in the present-day, while climate models suggest glacial presence of the WRZ that would support maintenance of C_3-predominant GCFR vegetation.

These paleoenvironmental proxies sample past environments at geographic scales that are often regional. The GCFR flora is hyper-diverse, and glacial climate change-driven impacts on local vegetation could have been highly variable over relatively small geographic scales. Proxy records that are circumscribed in their geographic scale are thus key to our understanding of ancient environments at particular MSA archaeological localities.

Micromammal fossil teeth are now recognized as an abundant potential reservoir of paleoenvironmental proxy data at an extremely local scale. This study analyzed modern micromammal teeth obtained from raptor pellets at three locations on the south coast. Stable carbon isotope analysis indicates that the modern micromammals from the taxa sampled consume a wide range of $\delta^{13}C_{plant}$ on the landscape when it is available, and thus stable carbon isotope analysis of micromammal teeth should act as a proxy for the range of available $\delta^{13}C_{diet}$ in a circumscribed area of vegetation.

Micromammal stable carbon isotope data obtained from specimens from one of the few well-dated MIS6-MIS5 sequences in the region (Pinnacle Point sites 13B, 30, and 9C). $\delta^{13}C_{enamel}$ values for the taxa sampled indicate diets that are primarily C_3, and there is almost no evidence for a dietary C_4 grass component in any of the sampled specimens. This indicates that, at a minimum, pockets of C_3 vegetation associated with the GCFR were likely available to hunter-gatherers at Pinnacle Point throughout the Middle and Late Pleistocene.

ACKNOWLEDGEMENTS

Data collection for this dissertation was supported by a grant from Late Lessons from Early History; a School of Human Evolution and Social Change (SHESC) Graduate Research Award; and a SHESC dissertation writing fellowship. Destructive analysis permits that enabled that isotope analysis of specimens were granted by the South African Heritage Resource Agency (SAHRA Export permits 80/12/03/012/52; 80/12/03/013/52; 80/12/03/014/52)

I would first like to thank my committee for their invaluable support during the data collection and writing process.

The archaeological and fossil micromammal specimens analyzed were collected as a part of a truly massive research endeavor headed by C.W. Marean, the South African Coast Paleoclimate, Paleoenvironment, Paleoecology, Paleoanthropology Project (SACP4). Various SACP4 scientists and staff have provided advice, data, and logistical support over the years. I would like to thank the SACP4 crew for their invaluable assistance, and without whom none of the archaeological material would be available for analysis. I also thank Bettina Gennari for her laboratory and catalogue assistance at the Diaz Museum. Thalassa Matthews provided modern owl pellets (collected by herself, N. Baker, and J. Sharples, and by Cape Nature) for sampling. She also provided advice and comments on the interpretation of the micromammal material.

Erich Fisher provided the data from the coastline portion of the Paleoscape Model for the South Coast, and Kerstin Braun kindly shared $\delta^{13}C$ data from unpublished Pinnacle Point speleothem. The unpublished large fauna stable isotope data presented in

Chapter 4 was generously provided by Julia Lee-Thorp. Thalassa Matthews and Julia Lee-Thorp also provided comments, corrections and edits to earlier drafts of Chapter 4.

Alexandra Miller, Andrew Sommerville, and Anthony Michaud provided advice and assistance with the sample preparation and data collection of the Wilderness and Wolwe River modern micromammal data; Kelly Knudson provided laboratory space and training in the Archaeological Chemistry Laboratory (Arizona State University). David Dettman and the Environmental Isotope Laboratory in the Department of Geosciences performed the instrumental analysis of the Rein's Nature Reserve modern sample. I also thank Benjamin Passey and Naomi Levin for access to and training on the LA-GC-IRMS at Johns Hopkins University, and to Heather Williams for logistical support in Baltimore. Andrew Jackson helpfully answered several cold e-mails about the use of SIAR in single isotope systems.

Curtis Marean, Kerstin Braun, Erich Fisher, Alastair Potts, Simen Oestmo, Ben Schoville, Amy Rector, Kaye Reed, Kyle Brown, Jocelyn Bernatchez, and countless others provided stimulating discussion over the years about the archaeology and paleoecology of the Pinnacle Point region.

Kyle Miaso, Jeremy Heartberg, Stephanie Vallentine, Sarah Lansing, and Elisabeth Cully are to be thanked for their encouragement and pep talks. Finally, I would like to thank my mother Brenda Williams, my father Steve Williams, and my sister Heather Williams for all of their love and encouragement throughout this process. Last, but most certainly not least, Chris Vitch provided endless support, love, and perspective through the writing of this dissertation, for which I am truly grateful.

TABLE OF CONTENTS

CHAPTER Page

CHAPTER Page

CHAPTER Page

CHAPTER Page

CHAPTER Page

CHAPTER Page

CHAPTER Page

LIST OF TABLES

Table Page

Table Page

Table Page

Table Page

Table Page

Table Page

LIST OF FIGURES

Figure Page

Figure Page

Figure Page

1. Background to the Research

Paleoenvironmental records of the habitats of all hominin groups, including those of early anatomically modern *Homo sapiens*, are central to understanding the timing and geographic distributions of adaptive behaviors in those populations. The habitats hominin populations occupy determine the availability of both plant and animal food resources; influence the availability of raw materials and lithic procurement strategies (Ambrose, 2006; Minichillo, 2006; Brown, 2011); impact the potential for technological innovation (Brown *et al.*, 2009; Brown *et al.*, 2012); and may affect population density, structure, and social organization (Ambrose and Lorenz, 1990), and consequently the development of unique cultural behaviors and adaptions associated with *Homo sapiens*.

Middle Pleistocene fossils attributed to early *Homo sapiens* occur across the continent: in North Africa (Jebel Irhoud, at 190-105 ka; Grun and Stringer, 1991), East Africa (Herto, between 160 - 154 ka; Clark *et al.*, 2003; White *et al.*, 2003), and in southern Africa (Border Cave - Pearson and Grine, 1996). Genetic evidence also indicates that *Homo sapiens* emerged in Africa between 100ka and 200ka (Cann, 1988; Tishkoff and Verrelli, 2003; Relethford, 2008). In all cases, early *Homo sapiens* are associated with lithic technologies assigned to the African Middle Stone Age (MSA), although it is likely that some MSA archaeological occurrences are the work of contemporaneous populations of other closely-related Middle Pleistocene *Homo*, as the earliest MSA technologies appear to pre-date the fossil and genetic evidence for the appearance of *Homo sapiens* (McBrearty and Brooks, 2000; Tryon and McBrearty, 2002; Wilkins *et al.*, 2012).

The evolution of anatomically modern *Homo sapiens* from a population of Middle Pleistocene *Homo* could potentially have occurred in any region in which early fossils of *Homo sapiens* occur, and workers in various regions of Africa have suggested that the origins of modern humans may be tied to population fragmentation resulting from general aridification of the continent (but c.f. Sjodin *et al.*, 2012). This 'refugium hypothesis' (Lahr and Foley, 1994; Lahr and Foley, 1998; Marean, 2010; Marean, 2011) suggests that proto-*Homo sapiens* were resitricted to areas of relative environmental stability during the Middle Pleistocene, when changing glacial and interglacia environmental conditions in Africa may have resulted in habitat fragmentation, limiting gene flow between populations. Adaptation to these new niches and limited gene flow then may have ultimately resulted in speciation in Middle Pleistocene *Homo*, and early *Homo sapiens* would have evolved in one or a few of the postulated refugia.

Marean (2010) has suggested that one such potential refugium for early modern humans is the south coast of South Africa. While the fossil record for early *Homo sapiens* in southern Africa is sparse prior to MIS5e (see McBrearty and Brooks, 2000 for detailed overview), the region has a dense archaeological record, and has provided much of the evidence for complex behavior in early modern humans. Archaeological sites dating the MIS6 are somewhat rare (although this may be an artifact of earlier limitations in geochronometry), and while Border Cave in KwaZulu Natal (Grun and Beaumont, 2001) and Twin Rivers in Zambia (Barham and Smart, 1996) date to this time period, on the south coast only the older deposits at Pinnacle Point 13B (PP13B) are MIS6 in age (Marean *et al.*, 2007; Marean *et al.*, 2010). This is in part due to the fact that, along the south Coast, many low-lying caves were likely washed clean of artifact-bearing deposits

by the MIS5e high sea stand; the abundance of sites immediately post-dating MIS6 suggests an enduring hominin presence in the region during the period that has only been minimally intersected by the archaeological record. Researchers (Van Andel, 1989; Marean *et al.*, 2007; Marean, 2010) have suggested that the presence of tuber-rich fynbos vegetation, shellfish, and relative environmental richness along the south coast during the 128-195 ka period may have provided a refuge environment for the earliest modern humans during harsh glacially-driven climatic change, while in later periods (~65-90 ka, or MIS5b to MIS 4), ecological instability may have stimulated novel behavioral adaptations (Bar-Matthews *et al.*, 2010). Southern African MIS6 MSA deposits have yielded evidence of exploitation of ochre (Watts, 2002) and possible coastal adaptations (Marean *et al.*, 2014; Marean, 2014), while excavation of MIS5 deposits has resulted in evidence for heat treatment of raw materials (Brown *et al.*, 2009), bead production (Henshilwood *et al.*, 2004; d'Errico *et al.*, 2005), ochre processing (Henshilwood *et al.*, 2011) and engraving (Henshilwood *et al.*, 2009).

The south coast of South Africa in the present day is part of the Greater Cape Floristic Region (GCFR), a floristic region that is comprised of the winter-rainfall fynbos and related vegetation traditionally included in the Cape Floral Kingdom (CFK) and the remaining winter-rainfall vegetation of the Karoo, the Namib, and Namaqualand (Born *et al.*, 2007). The flora of the GCFR has a high diversity of edible plants that are appealing to hunter-gatherer populations, particulary in the form of numerous under ground storage organs (USO)-producing plants (Goldblatt, 1997; Proches *et al.*, 2006). GCFR vegetation is hyper-diverse (Goldblatt, 1997; Born *et al.*, 2007), and this diversity appears to be quite ancient, suggesting in turn that there have been extant centers of GCFR floral

endemism since the late Miocene (Cowling *et al.*, 2009; Verboom *et al.*, 2009). Fynbos pollens have also been recovered from Pliocene Langebaanweg deposits (Scott *et al.*, 1995).

Marean *et al.* (2014) argue that the presence of the GCFR is of import to paleoanthropologists studying the origins of *Homo sapiens* because of the combination of the unique vegetation resources of the GCFR, the types of faunal prey resources such vegetation supports, and the presence of a productive marine coastline combine to create a hunter-gatherer habitat quite different from what is found in other parts of Africa.

Thus, the presence of the GCFR across a geographic area abundant with Middle Stone Age archaeological localities raises a number of questions about the nature of hominin adaptation in these environments. However, the habitats in which hunter-gatherers make foraging decisions are not monolithic entities, but are composed of local patches of vegetation (and fauna and other resources) that vary not only over geographic space but also temporally in response to both seasonal variation and longer-term changes in local environmental conditions.

There are a number of lines of evidence, particularly from climate models, that suggest that the Winter Rainfall Zone (WRZ) may have shifted during past glacials. The presence of the WRZ is due to the action of the westerlies (west-east blowing winds which in the present day occur between ~30° and ~60° S latitude) (Chase and Meadows, 2007). During the glacial periods that characterize the Pleistocene, the westerlies likely shifted equator-wards by as much as ~10° (Deacon, 1983; Tyson, 1999), redistributing the WRZ northwards and inland (Van Zinderen Bakker, 1976; Reason and Rouault, 2005; Chase and Meadows, 2007). Some models posit an expansion of winter rain and co-

occuring C_3 plants during glacial periods, while other models—notably that of van Zinderen Bakker (1976)—suggest that the WRZ moved so far northwards that the south coast during glacial stages would have been under the influence of a bimodal year-round rainfall regime (Figure 1.1); the siginicant input of summer rainfall into such a regime might favor the expansion of C_4 plants into areas along the south coast that are today dominated by winter-rainfall associated C_3 flora. Conversely, GCFR co-occurrence with and 'preference' for winter rain (Cowling *et al.*, 1992) leads to the hypothesis that GCFR floral communities may have expanded and contracted with the shifting WRZ during the duration of the Pleistocene.

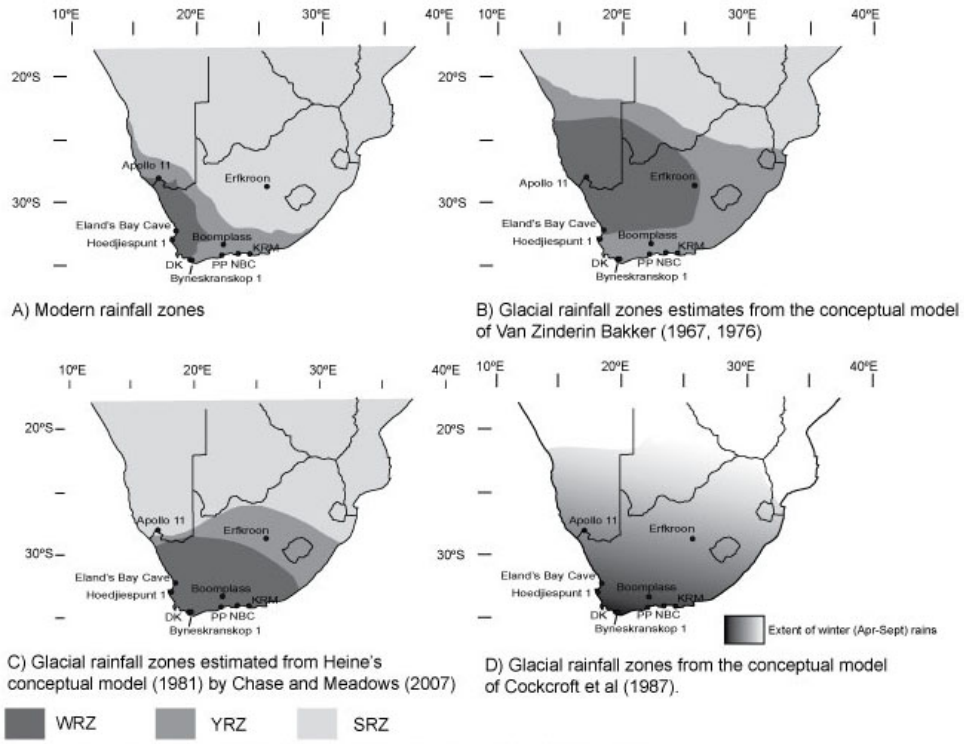

Figure 1.1. Locations of selected Holocene and Pleistocene archaeological localities, superimposed upon the rainfall models summarized by Chase and Meadows (2007, Figure 5) (A) modern southern African rainfall zones, (B-D) some of the models that have been proposed to explain the rainfall distribution and seasonality during glacial periods Modified from Chase and Meadows (2007, Figure 5)

The predominance of C_3 or C_4 floral elements in a region is also partially determined by aridity, with increasing dryness favoring the stomatal anatomy of C_4 grasses. The temperate nature of the present-day south coast of the continent is determined by the presence of the Agulhas current, which circulates warm Indian Ocean water into the southern oceans off the southwest Cape (Lutjeharms *et al.*, 2001). Paleoceanographic proxy data indicates that there are no major disruptions in the flow of the Agulhas along the south Cape during the entirety of the Pleistocene (Rau *et al.*, 2002; Peeters *et al.*, 2004), however variability in the sea surface temperatures (SST's), with sharp declines during glacials (Peeters *et al.*, 2004) suggests reductions in the warm-water input of the Agulhas to Cape coastal environments during glacial periods that may have reduced the amount of rainfall in the region in general. These conflicting models and proxy records raise the issue of whether vegetation communities during MIS6 – MIS3 were comparably stable (and likely GCFR in character), or whether there was episodic replacement of C_3 Cape floral components with C_4 grasses associated with drier, summer rainfall conditions.

Due to a dearth of MIS6-aged fossil and archaeological material along the south coast of South Africa, most of the available paleoenvironmental proxy data for changing glacial and interglacial environments derives from material aged to MIS5 – MIS3, with Last Glacial Maximum (LGM) age material sometimes acting as a potential model for 'peak glacial' conditions. Browsing fauna, which consume bush, shrub, and tree vegetation, are common in Pleistocene faunal assemblages, but some workers argue that they are replaced by grazing taxa during the LGM (Klein, 1980; Faith, 2013), suggesting an expansion of more open grassland vegetation into the region. Analysis by Rector and

Verelli (2010) however finds that there is no change in the relative proportion of grazers and browsers in MIS5- MIS 1 assemblages from the GCFR, and argue that the presence of browsers and grazers in faunal communities in the Western Cape is not strictly related to glacial/interglacial cycling. There is also limited change in the diversity of micromammalian communities during MIS5 to MIS 3 (Avery, 1999), although relative species abundance in archaeological micromammal assemblages has been used to suggest changing vegetation compositions in the Cape Folded Mountains and on the south coast (Avery, 1983).

Conversely, large mammal isotope data supports an expansion of the C_4 vegetation into the western Cape during the late Pleistocene (Lee-Thorp and Beaumont, 1995; Sealy, 1996), but indicate the maintenance of C_3-dominated vegetation during MIS5 (Luyt *et al.*, 2000), while pollen records also indicate an expansion of open-vegetation floral communities during the LGM (Scott *et al.*, 1995). Speleothem $\delta^{13}C$ data from Pinnacle Point on the south coast, meanwhile, shows highly variable changes in the relative proportions of C_4 grasses over the course of the Late Pleistocene, with marked increase in C_4 inputs during MIS 4 and at the MIS5c-5b transition (Bar-Matthews *et al*., 2010), a pattern that appears to extend back further into the Middle Pleistocene (Braun, personal communication).

Marean *et al*. (2014) have argued that the exposure of the Paleo-Agulhas Plain during glacial periods, and the disappearance of the Paleo-Agulhas during interglacials, is the major abiotic factor impacting south coast environmental conditions and floral and faunal community composition; marine transgression and regression thus may be driving

the mixture of changes observed in Middle and Late Pleistocene and Early Holocene proxy paleoenvironmental records for the GCFR.

Even though changes in past distributions of vegetation types would have had substantial implications for hominin adaptation, the paleoenvironmental proxy records for GCFR are often contradictory, suggesting that there is significantly more complexity to the relationship between glacial cycling and vegetation community structure than a simple glacial = open, interglacial = closed formula. This is especially true in the cases where climate models suggest an expansion of the WRZ during glacial periods at the same time that other proxy records suggest an expansion of C_4 vegetation into the present-day expanse of the GCFR. Given the complex paleoenvironmental picture that arises from the terminal Pleistocene proxy record, development of paleoenvironmental records for earlier glacial periods becomes even more important: in order to understand the ways in which the behavioral ecology of early *Homo sapiens* (and other hominins) was linked to local environments along the south coast of South Africa, it is necessary to establish whether vegetation communities similar to those found in the region were extant in the past; where and whether these vegetation communities persisted locally versus where and when they were possibly replaced by other vegetation communities, such as C4 grasslands; and how these vegetation communities responded, at a local scale, to changing climatic inputs during Pleistocene glacial and interglacial cycles.

There must also exist a synthesized paleoenvironmental record that takes geographic scale into consideration: were foraged resources (such as large prey items or lithic raw materials) acquired from habitats similar to those found in the immediate vicinity of archaeological localities? How much did site-proximate environments vary

over geographic scales covered by daily and annual hunter-gatherer foraging rounds? These are "big picture" questions that are difficult for any single study or given paleoenvironmental proxy to address directly, but they form the impetus for producing paleoenvironmental proxy data on a number of different geographic scales.

Thus, understanding the relationship between the adaptive strategies and cultural innovations of early *Homo sapiens* and the habitats they occupied during the Middle and Late Pleistocene ultimately requires multi-proxy, high-resolution paleoenvironmental records that are tied directly to fossil and archaeological occurrences. In the case of the GCFR, there are several compelling reasons to attempt to develop large carbon and oxygen stable isotope data sets from micromammalian remains that might have utility as proxies for past vegetation and/or rainfall. Micromammals are abundant in all extant environments, and many species have large geographic distributions that cover multiple South African biomes, permitting vegetation comparisons to be made. Specimen abundance in archaeological and fossil localities is also often high, due to taphonomic effects (e.g. their aggregation by predators such as raptors in cave and rock shelter localities). In archaeological sites, specimen abundance is also divorced from the intensity of human activities such as hunting, *contra* large mammal abundance, although it is tied to the intensity of raptor occupation at a site. Since micromammals occur in archaeological deposits regardless of human activities, analysis will provide information about periods of occupation and non-occupation within sites. Furthermore, the isotopic composition of micromammals will act as an extremely local paleoenvironmental proxy, because most genera of small mammals do not range widely (when compared to the

ranges of many large fauna), and their agents of collection (primarily owls and small carnivores) have a limited range.

My dissertation thus seeks to expand the (paleo)environmental proxy record for the south coast of South Africa in the following ways: Chapter 2 presents a meta analysis of extant published floral stable carbon isotope data from the Greater Cape Floristic Region, as contextual data for interpreting modern and archaeological micromammal stable carbon isotope data, with a particular focus on the south coast. Chapter 3 presents $\delta^{13}C_{enamel}$ and $\delta^{18}O_{enamel}$ data obtained by sampling modern micromammal specimens from the raptor pellets collected along the south coast near Pinnacle Point, and interprets this data in the context of floral $\delta^{13}C$ data aggregated in Chapter 2. Chapter 4 presents the results of stable isotope analyses of fossil micromammal specimens from Pinnacle Point 30 (PP30), a fossil hyena den, and compares them to the stable carbon and stable oxygen isotope data from PP30 large fauna specimens produced by Julia Lee-Thorp. Chapter 5 presents the $\delta^{13}C_{enamel}$ data from micromammal specimens excavated from MIS6 and MIS5e depositional units at Pinnacle Point 13B (PP13B) and Pinnacle Point 9c (PP9C), while Chapter 6 summarizes the entire $\delta^{13}C_{enamel}$ record from the whole PP13B sequence, which spans from MIS7/6 to MIS5d. This record is then compared to the larger paleoenvironmental proxy record produced for the PP region. Lastly, Chapter 7 reviews and summarizes the data presented and the conclusions drawn in this dissertation, and discusses them in the context of the larger issues in paleoenvironmental reconstruction and MSA archaeology in the region.

Chapter 1 References:

Ambrose, S. H. (2006). "Howiesons Poort lithic raw material procurement patterns and the evolution of modern human behavior: A response to…" J Hum Evolution **50**(3), 365-369

Ambrose, S. H. and K. G. Lorenz (1990). Social and ecological models for the middle stone age in southern africa. The emergence of modern humans: an archaeological perspective. Edinburgh, Edinburgh University Press**:** 3-33.

Avery, D. M. (1983). "Palaeoenvironmental implications of the small Quaternary mammals of the fynbos region." Deacon, HJ, Hendey, QB & Lambrechts, JJN (eds.) Fynbos palaeoecology: a preliminary synthesis. S. Afr. Nat1. Scient. Progress Rep **75**: 139-155.

Avery, D. M. (1999). "A re-appraisal of micromammalian data from South Africa." Quaternary International **57-58**: 175-183.

Bar-Matthews, M., C. W. Marean, Z. Jacobs, P. Karkanas, E. C. Fisher, A. I. R. Herries, . . . A. Ayalon (2010). "A high resolution and continuous isotopic speleothem record of paleoclimate and paleoenvironment from 90 to 53 ka from Pinnacle Point on the south coast of South Africa." Quaternary Science Reviews **29**(17): 2131-2145.

Barham, L. S. and P. L. Smart (1996). "Current events: An early date for the Middle Stone Age of central Zambia." Journal of Human Evolution **30**(3): 287-290.

Born, J., H. Linder and P. Desmet (2007). "The greater cape floristic region." Journal of Biogeography **34**(1): 147-162.

Brown, K. S. (2011). The Sword in the Stone: Lithic Raw Material Exploitation in the Middle Stone Age at Pinnacle Point Site 5-6, Southern Cape, South Africa. PhD, University of Cape Town.

Brown, K. S., C. W. Marean, A. I. R. Herries, Z. Jacobs, C. Tribolo, D. Braun, . . . J. Bernatchez (2009). "Fire as an engineering tool of early modern humans." Science **325**(5942): 859-862.

Brown, K. S., C. W. Marean, Z. Jacobs, B. J. Schoville, S. Oestmo, E. C. Fisher, . . . T. Matthews (2012). "An early and enduring advanced technology originating 71,000 years ago in South Africa." Nature **491**(7425): 590-593.

Cann, R. L. (1988). "DNA and human origins." Annual Review of Anthropology **17**: 127-143.

Chase, B. M. and M. E. Meadows (2007). "Late Quaternary dynamics of southern Africa's winter rainfall zone." Earth-Science Reviews **84**(3-4): 103-138.

Clark, J. D., Y. Beyene, G. WoldeGabriel, W. K. Hart, P. R. Renne, H. Gilbert, . . . K. R. Ludwig (2003). "Stratigraphic, chronological and behavioural contexts of Pleistocene Homo sapiens from Middle Awash, Ethiopia." Nature **423**(6941): 747-752.

Cowling, R. M., P. M. Holmes and A. G. Rebelo (1992). "The ecology of fynbos: nutrients, fire and diversity." Cape Town.: Oxford Univ. Press 411pp.. Contents include: Flora and vegetation, by RM Cowling & PM Holmes: 23-61.

Cowling, R. M., S. Proches and T. C. Partridge (2009). "Explaining the uniqueness of the Cape flora: incorporating geomorphic evolution as a factor for explaining its diversification." Molecular Phylogenetics and Evolution **51**(1): 64-74.

d'Errico, F., C. Henshilwood, M. Vanhaeren and K. van Niekerk (2005). "Nassarius kraussianus shell beads from Blombos Cave: evidence for symbolic behaviour in the Middle Stone Age." Journal of Human Evolution **48**(1): 3-24.

Deacon, H. J. (1983). "Another look at the Pleistocene climates of South Africa." South African Journal of Science **79**: 325-328.

Faith, J. T. (2013). "Taphonomic and paleoecological change in the large mammal sequence from Boomplaas Cave, western Cape, South Africa." Journal of Human Evolution **65**(6): 715-730.

Goldblatt, P. (1997). "Floristic diversity in the Cape Flora of South Africa." Biodiversity and Conservation **6**(3): 359-377.

Grun, R. and P. Beaumont (2001). "Border Cave revisited: a revised ESR chronology." Journal of Human Evolution **40**(6): 467-482.

Grun, R. and C. B. Stringer (1991). "Electron spin resonance dating and the evolution of modern humans." Archaeometry **33**(2): 153-199.

Henshilwood, C., F. D'Errico, M. Vanhaeren, K. van Niekerk and Z. Jacobs (2004). "Middle Stone Age Shell Beads from South Africa." Science **304**(5669): 404.

Henshilwood, C. S., F. d'Errico, K. L. van Niekerk, Y. Coquinot, Z. Jacobs, S. E. Lauritzen, . . . R. Garcia-Moreno (2011). "A 100,000-year-old ochre-processing workshop at Blombos Cave, South Africa." Science **334**(6053): 219-222.

Henshilwood, C. S., F. d'Errico and I. Watts (2009). "Engraved ochres from the middle stone age levels at Blombos cave, south Africa." Journal of Human Evolution **57**(1): 27-47.

Klein, R. G. (1980). "Environmental and ecological implications of large mammals from upper pleistocene and holocene sites in southern africa." Annals of the South African Museum **81**: 223-283.

Lahr, M. M. and R. Foley (1994). "Multiple dispersals and modern human origins." Evolutionary Anthropology: Issues, News, and Reviews **3**(2): 48-60.

Lahr, M. M. and R. A. Foley (1998). "Towards a theory of modern human origins: geography, demography, and diversity in recent human evolution." Yearbook of Physical Anthropology **41**: 137-176.

Lee-Thorp, J. A. and P. B. Beaumont (1995). "Vegetation and seasonality shifts during the late Quaternary deduced from 13C/12C ratios of grazers at Equus Cave, South Africa." Quaternary Research **43**(3): 426-432.

Lutjeharms, J. R. E., P. M. S. Monteiro, P. D. Tyson and D. Obura (2001). "The oceans around southern Africa and regional effects of global change." South African Journal of Science **97**: 119-130.

Luyt, J., J. Lee-Thorp and G. Avery (2000). "New light on Middle Pleistocene west coast environments from Elandsfontein, Western Cape Province, South Africa." South African Journal of Science **96**(7).

Marean, C.W. (2010). "Pinnacle Point Cave 13B (Western Cape Province, South Africa) in context: the Cape floral kingdom, shellfish, and modern human origins." Journal of Human Evolution **59**(3): 425-443.

Marean, C.W. (2011). “Coastal South Africa and the co-evolution of the modern human lineage and coastal adaptations.” Trekking the Shore: Changing Coastlines and the Antiquity of Coastal Settlement. N. Bicho, J. A. Haws and L. G. Davis. New York, Springer: 421-440.

Marean, C. W. (2014). "The origins and significance of coastal resource use in Africa and Western Eurasia." Journal of Human Evolution **77**(0): 17-40.

Marean, C. W., Z. Assefa and A. B. Stahl (2005). The Middle and Upper Pleistocene African record for the biological and behavioral origins of modern humans African Archaeology. New York, Blackwell**:** 93-129.

Marean, C. W., M. Bar-Matthews, J. Bernatchez, E. Fisher, P. Goldberg, A. I. R. Herries, . . . H. M. Williams (2007). "Early human use of marine resources and pigment in South Africa during the Middle Pleistocene." Nature **449**: 905-908.

Marean, C. W., M. Bar-Matthews, E. Fisher, P. Goldberg, A. Herries, P. Karkanas, . . . E. Thompson (2010). "The stratigraphy of the Middle Stone Age sediments at Pinnacle Point Cave 13B (Mossel Bay, Western Cape Province, South Africa)." Journal of Human Evolution **59**(3-4): 234-255.

Marean, C. W., H.C. Cawthra, R.M. Cowling, K.J. Esler, E. Fisher, A. Milewski, A.J. Potts, E. Singels, and J. De Vynck (2014). "Stone Age People in a Changing South African Greater Cape Floristic Region". Fynbos: Ecology, Evolution, and Conservation of a Megadiverse Region. N. Allsopp, J. F. Colville and T. Verboom. Oxford, Oxford University Press: 164-199.

McBrearty, S. and A. S. Brooks (2000). "The revolution that wasn't: a new interpretation of the origin of modern human behavior." Journal of Human Evolution **39**: 453-563.

Minichillo, T. (2006). "Raw material use and behavioral modernity: Howiesons Poort lithic foraging strategies." Journal of Human Evolution **50**(3): 359-364.

Pearson, O. M. and F. E. Grine (1996). "Morphology of the Border Cave hominid ulna and humerus." South African Journal of Science **92**(5): 231-236.

Peeters, F. J., R. Acheson, G.-J. A. Brummer, W. P. De Ruijter, R. R. Schneider, G. M. Ganssen, . . . D. Kroon (2004). "Vigorous exchange between the Indian and Atlantic oceans at the end of the past five glacial periods." Nature **430**(7000): 661-665.

Proches, S., R. M. Cowling, P. Goldblatt, J. C. Manning and D. A. Snijman (2006). "An overview of the Cape geophytes." Biological Journal of the Linnean Society **87**(1): 27-43.

Rau, A. J., J. Rogers, J. R. E. Lutjeharms, J. Giraudeau, J. A. Lee-Thorp, M. T. Chen and C. Waelbroeck (2002). "A 450-kyr record of hydrological conditions on the western Agulhas Bank Slope, south of Africa." Marine Geology **180**(1-4): 183-201.

Reason, C. and M. Rouault (2005). "Links between the Antarctic Oscillation and winter rainfall over western South Africa." Geophys. Res. Lett **32**(7): L07705.

Rector, A. L. and B. C. Verrelli (2010). "Glacial cycling, large mammal community composition, and trophic adaptations in the Western Cape, South Africa." Journal of Human Evolution **58**(1): 90-102.

Relethford, J. H. (2008). "Genetic evidence and the modern human origins debate." Heredity **100**(6): 555-563.

Scott, L., E. S. Vrba, G. H. Denton, T. C. Partridge and L. H. Burckle (1995). Pollen evidence for vegetation and climatic change in southern Africa during the Neogene and Quaternary. Paleoclimate and evolution, with emphasis on human origins. New Haven and London, Yale University Press**:** 65-76.

Sealy, J. (1996). "Seasonality of rainfall around the Last Glacial Maximum as reconstructed from carbon isotope analyses of animal bones from Nelson Bay Cave." South African Journal of Science **92**: 441-444.

Tishkoff, S. A. and B. C. Verrelli (2003). "Patterns of human genetic diversity: implications for human evolutionary history and disease." Annual Review of Genomics and Human Genetics **4**(1): 293-340.

Tryon, C. A. and S. McBrearty (2002). "Tephrostratigraphy and the Acheulian to Middle Stone Age transition in the Kapthurin Formation, Kenya." Journal of Human Evolution **42**(1/2): 211-236.

Tyson, P. D. (1999). "Atmospheric circulation changes and paleoclimates of southern Africa." South African Journal of Science **95**: 194-201.

Van Andel, T. H. (1989). "Late Pleistocene Sea Levels and the Human Exploitation of the Shore and Shelf of Southern South Africa." Journal of Field Archaeology **16**(2): 133-155.

Van Zinderen Bakker, E. (1976). "The evolution of Late-Quaternary palaeoclimates of southern Africa." Palaeoecology of Africa **9**: 160-202.

Verboom, G. A., J. K. Archibald, F. T. Bakker, D. U. Bellstedt, F. Conrad, L. L. Dreyer, . . . J. F. Henning (2009). "Origin and diversification of the Greater Cape flora: ancient species repository, hot-bed of recent radiation, or both?" Molecular Phylogenetics and Evolution **51**(1): 44-53.

Watts, I. (2002). "Ochre in the Middle Stone Age of southern Africa: Ritualized display or hide preservative?" South African Archaeological Bulletin **57**: 1-14.

White, T. D., B. Asfaw, D. DeGusta, H. Gilbert, G. D. Richards, G. Suwa and F. Clark Howell (2003). "Pleistocene Homo sapiens from Middle Awash, Ethiopia." Nature **423**(6941): 742-747.

Wilkins, J., B. J. Schoville, K. S. Brown and M. Chazan (2012). "Evidence for early hafted hunting technology." Science **338**(6109): 942-946.

2. Isotope ecology of the modern Greater Cape Floristic Region, with particular focus on the Pinnacle Point area: metadata analysis of the modern floral stable carbon isotope record and the production of the GCFR-specific Stable Carbon Isotope Metadata Set (GSCIMS).

Introduction

Interpretation of isotopic proxy records of past continental environments requires not only an understanding of the chemical and physical processes that result in isotope fractionation, but contextual data which can shed light on the fidelity with which relatively 'simple' isotope records can record the interaction of complex environmental factors. This is especially true in regions where vegetation communities can be characterized as complex and in which both C_3 and C_4 grasses are present or are hypothesized to have been present; or in regions where seasonal rainfall regimes converge or are hypothesized to have shifted over geologic time; or where landscape evolution and/or the exposure or inundation of low-lying areas has occurred; or where changes in mammalian communities has occurred over time. At Pinnacle Point almost all of these conditions are present or occurred over the course of the last 300,000 years.

Where mammalian tissue stable isotope data is used as a proxy for past environments, the best contextual data for interpreting ancient signals is modern data of the same or similar type. For example, where the stable carbon isotope values of enamel from large ungulate gazers from the Pliocene is used as a proxy for relative percentages of C_3 and C_4 grasses in a given past environment, modern contextual data should exist that links different $\delta^{13}C_{enamel}$ values of given grazing taxa to given vegetation communities (and further, the stable carbon isotope composition of plants within those communities should also be known).

Isotopic characterization of changes in vegetation communities in regions where C_4 grasses have almost completely replaced C_3 grasses by the Late Miocene or Early Pliocene is theoretically straightforward; samples enriched in ^{13}C suggest the presence of C_4 grasses, whilst samples depleted in ^{13}C suggest the presence of bushier, closed C_3 vegetation communities. Conversely, grazer tissue $\delta^{13}C$ values at the margins of C_3 grass and C_4 grass communities can suggest the varying proportions of photosynthetic pathways present, as grazers ('ideally') consume *only* grass, and thus have no "bush" signal as a component of their tissue $\delta^{13}C$ values. In present-day regions where C_4 grasses are totally absent, variation in the $\delta^{13}C$ values of C_3 plant tissue (with a range of ~-35‰ VPDB to – 22‰ VPDB; O'Leary, 1988) are dependent upon factors such as aridity and plant litter recycling in closed-canopy environments (Farquhar *et al.*, 1989; Kohn, 2010); variation in $\delta^{13}C_{C3\ plant}$ values are reflected (accounting for diet-tissue offsets) in $\delta^{13}C_{tissue}$ values of primary consumers.

Vegetation in the Greater Cape Floristic Region (the GCFR) is often categorized as primarily C_3 due to the predominance of the "fine bush" (fynbos) plants in many of the vegetation communities (Cowling *et al.,* 1997), but this is somewhat misleading. "Relative grass cover" as a percentage of total vegetation varies within GCFR floral communities (Cowling, 1983; Rebelo *et al.*, 2006), such that some structural communities, such as "grassy fynbos" or "restioid fynbos"(Cowling *et al.,* 1997) have comparably low shrub-cover and comparable high graminoid cover. There is also significant taxonomic diversity in the non-shrub understory of the GCFR plant communities, and the frequency of C_4 grasses in this portion of the vegetation increases in relationship to abiotic factors such as higher mean annual precipitation (MAP),

frequency of summer rainfall, increased growing season temperature, soil fertility, and slope aspect (Vogel *et al.,* 1978; Cowling, 1983); along the south coast in particular, aspect is a key drving factor, as south-facing slopes receive less solar radiation, resulting in cooler temperatures where C_3 grasses outcompete C_4 grasses and thus predominate (Colwing, 1983). Problematically, although the individual vegetation communities within the GCFR are well-characterized (Cowling, 1992; Cowling and Richardson, 1995; Cowling *et al.*, 1997; Rebelo *et al.*, 2006), relative frequency data for grasses and endemic fynbos taxa are sparse.

Unlike in eastern and central Africa (Cerling and Harris, 1999; Cerling *et al.,* 2003; Cerling *et al.,* 2004) and the savanna areas of South Africa (Codron *et al.,* 2005), there has been as of yet no systematic attempt to characterize the range of isotopic variation in GCFR plant communities, likely in part due to the high diversity and species richness of the GCFR. Stable carbon isotope data exists, but is patchily distributed through the botany literature. The primary exception to this is the data presented in Rundel *et al.* (1999), which characterizes the carbon isotope discrimination (Δ, sensu Farquhar *et al.,* 1989) of plants in the Richterveld Succulent Karroo. Carr *et al.* (2014) also report n-alkane distributions for a large (>200) plant dataset from the fynbos bioregion within the GCFR, but have not yet published bulk tissue $\delta^{13}C$ data for those specimens.

In order to attempt to characterize the range of $\delta^{13}C$ values found in modern GCFR vegetation in the absence of systematic survey, I performed an analysis of the extant botany and isotope ecology literature to aggregate it into a GCFR-specific Stable Caron Isotope Metadata Set (here abbreviated as “GSCIMS” for brevity). Stable carbon

isotope data was incorporated into GSCIMS if it met the following criteria: $\delta^{13}C_{plant}$ or Δ values were available for plant material at least at the familial, and ideally at the generic level. Some sources reported only bulk average values only for C_3 or C_4 vegetation as a 'group' and were thus excluded from this data set. The stable carbon isotope data was for taxa known to occur in GCFR plant communities, and (with the exception of some C_4 grasses, see below), plant samples were taken from within the geographic boundaries of the modern GCFR.

Fourteen data sources were identified that included taxon-specific $\delta^{13}C$ data for species of flora that occur within GCFR plant communities. Data was included from studies whose sampling localities were either explicitly described as within the geographic boundaries of the GCFR (Sealy and Van der Merwe, 1986; Boom *et al.,* 2014; Lötter *et al.,* 2014) or whose geographic coordinates were given in the text (Rundel *et al.,* 1999; West *et al.,* 2001; Agenbag, 2006; Latimer *et al.,* 2009; Araya *et al.,* 2010; Robb *et al.,* 2012; Reinecke, 2013; Van den Heuvel and Midgley, 2014), and determined to be within the boundaries of the GCFR by GIS analysis (Figure 2.1). Some important older publications (Mooney *et al.,* 1977; Vogel *et al.,* 1978) report taxon-specific data but provided only non-coordinate town and provincial locality information. Most of these sampling localities could be identified using Google Earth using the town or area names provided in the relevant literature, and approximate coordinates for all localities in these two data sets were generated by dropping a Google "pin" in the area closest to the map center that was outside the developed towns themselves. Sampling locations from Mooney *et al.* (1997) and Vogel *et al.* (1978) were then also entered into a GIS database, and only localities that fell within the boundaries of the GCFR were included.

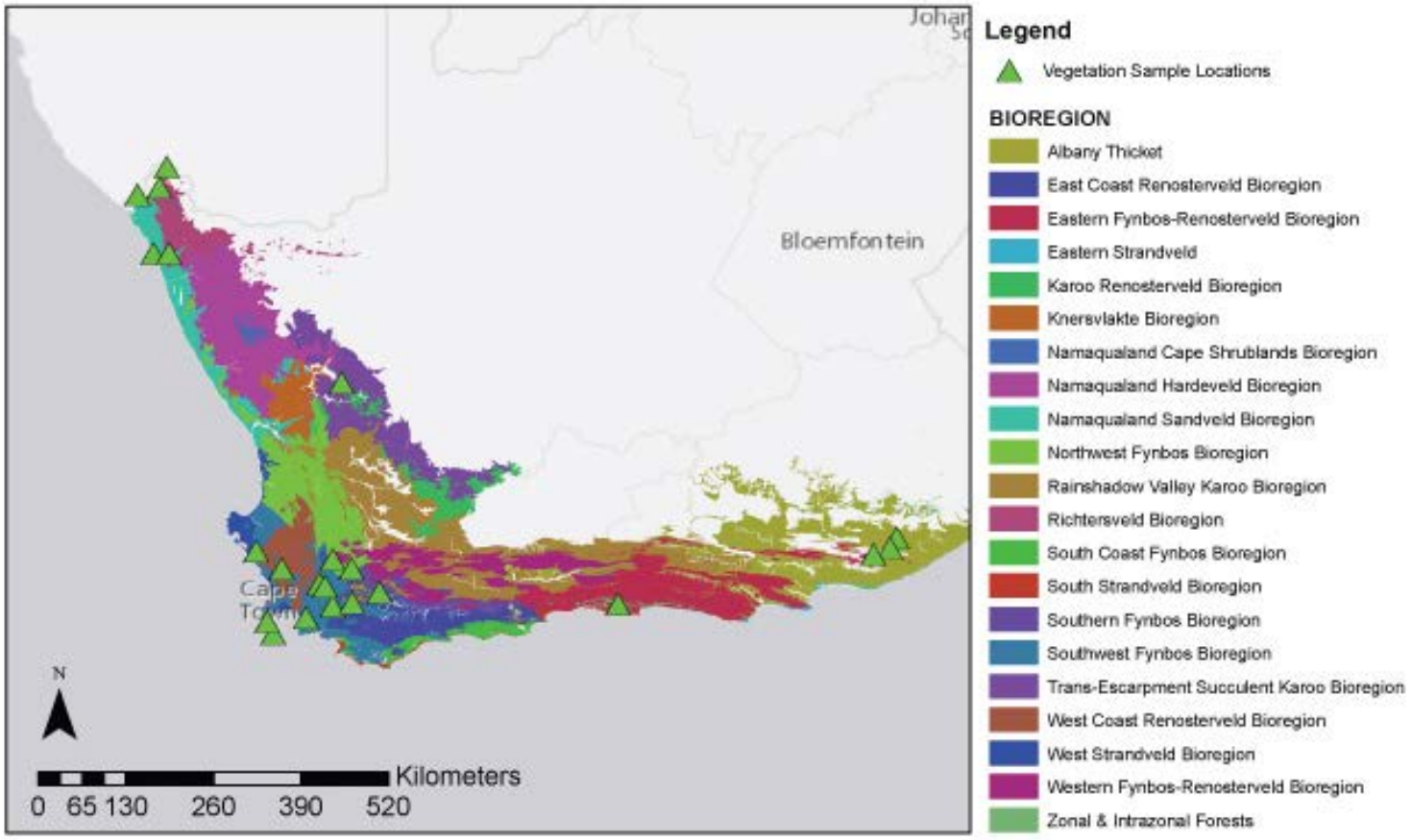

Figure 2.1. Location(s) (green triangles) of the available data for GCFR plant $\delta^{13}C_{tissue}$ values from the literature, superimposed over GCFR floral bioregions (Mucina and Rutherford, 2006). Does not include non-GCFR sampling localities used for C_4 $\delta^{13}C_{tissue}$ values, or localities given in Latimer *et al.* for *Protea* specimens (Latimer *et al.*, 2009, Figure 1)

The $\delta^{13}C$ plant tissue data reported the in the literature above is heavily weighted towards C_3 foliar tissue, and includes only three specimens of C_4 grasses. The best systematic survey of southern African grasses was produced by Schulze *et al.* (1996), but their sampling explicitly focused on grasses in Namibian ecosystems, outside of the geographic range of the GCFR. There is, however, significant taxonomic overlap in grasses between the two regions, and while differences in latitude and aridity can impact the $\delta^{13}C_{tissue}$ composition of C_3 plants (Tieszen *et al.,* 1979; Farquhar *et al.,* 1982; Körner *et al.,* 1991; Heaton, 1999; Weiguo *et al.,* 2005; Kohn, 2010), variation in $\delta^{13}C_{tissue}$ values of C_4 plants is primarily related to differences in structural "leakiness" (gas-permeability) of the bundle sheath, where carbon fixation occurs (Farquhar *et al.,* 1989). Furthermore, it is generally agreed that there is minimal association between $\delta^{13}C_{tissue}$ in C_4 plants and measures of aridity/rainfall, and the Swap *et al.* (2004) study of $\delta^{13}C_{tissue}$ variation in C_3 and C_4 plants from southern Africa found no relationship between MAP and $\delta^{13}C$ in southern African C_4 grasses.

Given that variation in C_4 $\delta^{13}C_{tissue}$ values is primarily structural, rather than ecological, and given that within a given taxon the photosynthetic anatomy will be the same regardless of geographic location, then $\delta^{13}C_{tissue}$ values of a given C_4 taxon near-to-but-outside of the GCFR should be a useful approximation of $\delta^{13}C_{tissue}$ values for that taxon within the GCFR as well. Thus, $\delta^{13}C_{tissue}$ data from taxa that occur both within the Schulze *et al.* (1996) dataset and in Cowling's (1983) list of C_4 grasses present in the western GCFR were included in GSCIMS as reasonable proxy values for C_4 stable carbon isotope tissue data that is not otherwise yet extant in the literature. Similarly, C_4

grass taxa that appear in Vogel *et al.* (1978) outside of the GCFR but in the Cowling (1983) list or as fynbos taxa in (Rebelo *et al.*, 2006) were also included here.

The resultant dataset contains 346 unique entries (Appendix A); some taxa have multiple entries where the data derives from different research groups, which were included in order to capture the range of $\delta^{13}C$ values for each taxon. Data in Appendix A is organized alphabetically by plant taxon. Two fields for descriptive information about the plant types are included for reference ("plant description" and "plant description 2"). "Plant description 1" provides general structural information about the taxonomic entry (e.g. monocot, dicot, tree, shrub, succulent), while "plant description 2" contains any secondary information that may be of interest. The field "part" describes, where noted in the literature, which part of the plant was sampled, as there is some intra-organismal variation in $\delta^{13}C_{tissue}$ values due to variable fractionation of carbon. Photosynthetic pathway is noted for all taxa: C_3, C_4, CAM, and, following the Boom *et al.*, (2014) notation, FCAM for facultative CAM plants that switch between C_3 and CAM photosynthetic pathways. One specimen (*Hydnora africana*) is an achlorophyllous parasite, and does not perform photosynthesis (and is thus neither C_3 nor C_4) .

The $\delta^{13}C$ values for the Rundel et al (1999) dataset were converted from Δ values by algebraic substitution from the following formula (from Farquhar *et al.*, 1989):

$$\Delta = \frac{\delta_a - \delta_p}{1+\delta_p}, \text{ such that } \delta_p = \frac{\delta_a - \Delta}{\Delta + 1}$$

where the carbon isotopic composition of the atmosphere, δ_a= -7.8‰ (or -0.0078); Δ is the given value of carbon isotope discrimination by the plant in ‰ (thus values reported as X are entered into the equation above as X(10^{-3}); and where the stable carbon isotopic composition of the plant tissue, δ_p is the resultant $\delta^{13}C_{tissue}$ value of the plant in per mil (and thus $\delta^{13}C_{tissue}$ ‰ = $\delta_p * 1000$). The exact floral $\delta^{13}C$ values from Robb *et al.*, 2013 are not reported in the original text, and were digitized from the figures using WebPlotDigitizer (Rohatgi, 2010). The same is true for the available native tree data from the Knysna forests (West *et al.,* 2001), for the *Protea* data from Latimer et al (2009), and the data from Reinecke (2013) and Lotter *et al.,* (2014). One specimen from Rundel *et al.* (1999) has no taxonomic identification beyond "succulent"; it is included in Appendix A, but excluded from further analysis.

The GCFR flora metadata set is dominated by specimens of CAM/FCAM plants (*n* =155). This is an overrepresentation relative to the frequency of succulents in GCFR floral communities, and is at least partially due to the frequency of sampling localities occurring in the Succulent Karoo bioregion. There are however 186 entries for non-CAM plants (C_3 *n* = 157, C_4 *n* = 29). The large sample size of this metadata set in all functional plant categories thus provides good initial coverage, although, given the extreme diversity of taxa present in the GCFR, it is clearly incomplete. It is treated here as an initial approximation of the range of end member $\delta^{13}C$ values for GCFR vegetation.

Furthermore, GSCIMS is missing one major category of C_3 plants, the genus *Erica*, which forms the primary shrub component of many of the 'heathland' fynbos vegetation communities (see below). The non-sampling of this genus is problematic, as it is hyper-prevalent in plant communities along the south coast (Rebelo *et al.,* 2006), and

the lack of stable carbon isotope data for *Erica* is likely to be an artifact of plant sampling having been concentrated in the southwestern Cape (Figure 2.1). $\delta^{13}C_{plant}$ values for species of *Erica* from the northern hemisphere suggest an approximate range of -24.9‰ to -26.8‰ VPDB (Llorens *et al.*, 2003a; Llorens *et al.*, 2003b; Saura *et al.*, 2010; Werner and Maguas, 2010). While data from Llorens *et al.* (2003a) indicates that there is no intraspecific effect of aridity or temperature of the $\delta^{13}C_{tissue}$ values of some species of *Erica*, given the vast geographic distance between these *Erica* communities and those found in Southern Africa, I argue that these available stable carbon isotope values cannot be used as anything other than indefinite preliminary proxies for GCFR *Erica*.

Summary of GSCIMS metadata:

GCFR C_3 Plants:

GCFR C_3 plant $\delta^{13}C$ values range from -31.3‰ VPDB to -18.30‰ (mean -25.9‰, σ = 2.39). The GCFR C_3 plants appear to lack the lowest portion of the world-wide range of stable carbon isotope values for C_3 plants (i.e. -35‰ to -31‰): in most regions of the world, the most ^{13}C-depleted specimens are found in closed-canopy forests which, with the exception of the Southern Afrotemperate Forest (Mucina and Rutherford 2006 code FOz1) relicts in the Knysna Area, are absent from the GCFR.

There are 25 $\delta^{13}C_{tissue}$ values for 14 species of trees in the GCFR stable carbon isotope metadata set. Tree samples come from across the GCFR; from Knysna (West *et al.*, 2001), from the southwestern Cape within about 150km of Cape Town (Reinecke, 2013), from the northwest (Rundel *et al.*, 1999), and from the Eastern Cape near

Grahamstown (Mooney *et al.,* 1977). $\delta^{13}C_{tissue}$ values for three species of trees from the Diepwalle Forest, Knysna (West *et al.,* 2001) sampled both open and closed canopy environments, as well as mature and juvenile trees; mean $\delta^{13}C$ = -26.27‰ (n = 11, σ = 2.35) (see West *et al.,* 2001 for discussion of reletive depletion/enrichment in ^{13}C in relation to open/closed canopies in the Knysna Forest). Stable carbon isotope samples of trees from riparian contexts in the Northern Cape (Rundel *et al.,* 1999) have mean $\delta^{13}C$ values of -24.53‰ (n = 7, σ = 1.899); the tree taxa sampled from the Western Cape have a mean $\delta^{13}C$ value of -28.87‰ (n = 6, σ = 1.063) (Reinecke, 2013), and a lone shrubby tree from an Albany thicket context (*Boscia oleoides*) has a $\delta^{13}C_{tissue}$ value of -24.1‰ VPDB (Mooney *et al.,* 1977).

Overall, the GCFR tree values overlap with, but are somewhat higher than, the mean $\delta^{13}C$ value of -27.8‰ VPDB reported for open canopy forest environments in East Africa (Cerling *et al.,* 2003). Although the FOz1 trees are on average 1.68‰ more depleted in ^{13}C than the riparian Northern Cape trees, the difference in $\delta^{13}C$ values between the populations is not significant (t-test p = 0.1391). The Western Cape trees are significantly depleted relative to trees from the Northern Cape and Knysna (ANOVA F = 7.04, r^2 = 0.4103, p = 0.0039). All GCFR tree 'populations' however have mean $\delta^{13}C$ values that are significantly higher than the east African closed canopy forest $\delta^{13}C$ mean value of -31.4‰ VPDB (Cerling *et al.,* 2003) (one-sample t-test for each comparison, p = 0.0021 or smaller).

In the GSCIMS data set, grasses, restios, and geophytes all also have comparably low $\delta^{13}C_{tissue}$ values with more restricted ranges of stable carbon isotope variation (Figure

2.2, Table 2.1). Only 2 $\delta^{13}C$ values are extant in the current literature for 'true' C_3 grass; both values are quite low: *Dregeochloa calviniensis* from Loriesfontein (MAP 0-200mm) $\delta^{13}C$ = -26.3‰, *Lasiochloa longifolia* from Ceres (MAP 801-100) $\delta^{13}C$ = -27.6‰. Despite the comparably large difference in mean annual precipitation between the sampling localities, the difference in $\delta^{13}C$ between the two grass samples is only 1.3‰. *Restio* taxa are often included in the graminoids for GCFR vegetation units (e.g. Rebelo *et al.*, 2006), a category that includes sedges and rushes as well as the 'true grasses'. *Restio* and the true grasses in the sample have similar values of $\delta^{13}C$ (Table 2.1).

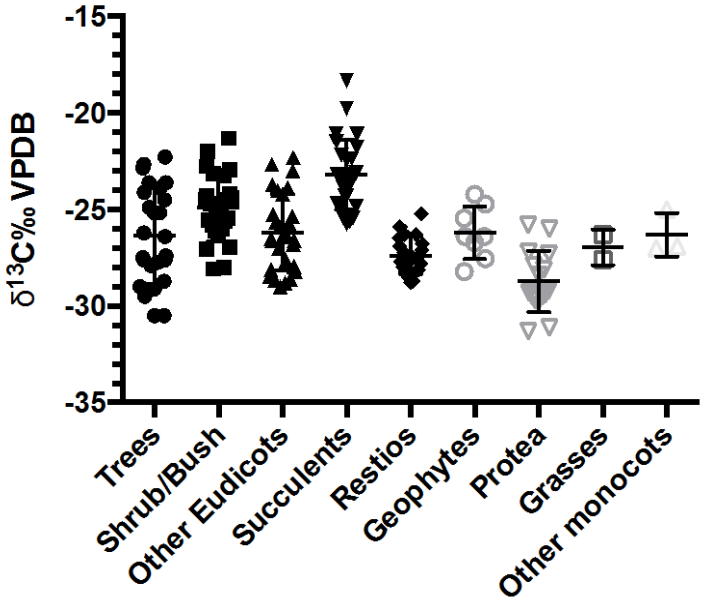

Figure 2.2. $\delta^{13}C_{tissue}$ values of C_3 plants from the GCFR metadata set. $\delta^{13}C_{tissue}$ values from sources cited in Appendix A.

C_3 plants	Trees	Shrub/ Bush	Other Eudicots	Succulents	Restios	Protea	Geophytes	Grasses	Other monocots
n	25	25	28	27	21	16	8	2	3
Minimum	-30.5	-28.07	-29	-25.73	-28.8	-31.3	-28.2	-27.6	-27
Median	-26.4	-24.86	-26.45	-23.33	-27.5	-29.25	-26.4	-26.95	-26.9
Maximum	-22.27	-21.31	-22.3	-18.3	-25.2	-25.8	-24.2	-26.3	-25
Mean	-26.33	-24.9	-26.18	-23.2	-27.37	-28.71	-26.2	-26.95	-26.3
Std. Deviation	2.512	1.732	1.984	1.809	0.9567	1.589	1.36	0.9192	1.127
Lower 95% CI	-27.37	-25.61	-26.95	-23.92	-27.8	-29.56	-27.33	-35.21	-29.1
Upper 95% CI	-25.3	-24.18	-25.41	-22.49	-26.93	-27.87	-25.06	-18.69	-23.5

Table 2.1. $\delta^{13}C_{tissue}$ values (‰, VPDB) for structural categories of C_3 plants in the GCFR. Data from sources cited in Appendix A.

The most ^{13}C-depleted average plant values are found among members of the genus *Protea* ($\delta^{13}C\ \overline{x}$ = -28.1‰, σ=1.59). *Protea* are significantly depleted in ^{13}C when compared to all other C_3 plant groups except *Restio* (ANOVA, F=19.74, r^2 =0.4530, p < 0.0001, with Tukey's post-hoc test: Table 2.2). Conversely, succulents reported in the literature as using C_3 photosynthesis are significantly enriched in ^{13}C when compared to all other GCFR C_3 plants. *Restio* $\delta^{13}C_{tissue}$ values are significantly lower than those of shrub/bush GCFR plants, but not of trees, geophytes or other dicots. Broadly, trees, shrub/bushes, and all other dicotylous plants have stable carbon isotope values that are not significantly enriched or depleted in ^{13}C relative to one another (Table 2.2).

Tukey's multiple comparisons test	difference between means	95% CI of difference	Significant?
Trees vs. Shrub/Bush	-1.43	-2.994 to 0.1188	No
Trees vs. Other Eudicots	-0.15	-1.666 to 1.362	No
Trees vs. Succulents	-3.12	-4.656 to -1.602	Yes
Trees vs. Restios	1.03	-0.5946 to 2.663	No
Trees vs. Protea	2.38	0.6183 to 4.141	Yes
Trees vs. Geophytes	-0.13	-2.370 to 2.100	No
Shrub/Bush vs. Other Eudicots	1.28	-0.2284 to 2.800	No
Shrub/Bush vs. Succulents	-1.69	-3.218 to -0.1640	Yes
Shrub/Bush vs. Restios	2.47	0.8429 to 4.100	Yes
Shrub/Bush vs. Protea	3.81	2.056 to 5.579	Yes
Shrub/Bush vs. Geophytes	1.30	-0.9326 to 3.537	No
Other Eudicots vs. Succulents	-2.97	-4.461 to -1.493	Yes
Other Eudicots vs. Restios	1.18	-0.4024 to 2.774	No
Other Eudicots vs. Protea	2.53	0.8075 to 4.256	Yes
Other Eudicots vs. Geophytes	0.0168	-2.189 to 2.223	No
Succulents vs. Restios	4.16	2.562 to 5.764	Yes
Succulents vs. Protea	5.50	3.773 to 7.245	Yes
Succulents vs. Geophytes	2.99	0.7788 to 5.209	Yes
Restios vs. Protea	1.34	-0.4800 to 3.172	No
Restios vs. Geophytes	-1.16	-3.455 to 1.117	No
Protea vs. Geophytes	-2.51	-4.897 to -0.1324	Yes

Table 2.2. Matrix of post-hoc multiple comparisons (Tukey's) for ANOVA of GCFR C_3

Other researchers have found a weak relationship between $\delta^{13}C_{tissue}$ values of C_3 plants and mean annual rainfall (MAP) (Stewart *et al.,* 1995; Swap *et al.,* 2004; Weiguo *et al.,* 2005). Using the 2001 annual rainfall data for South Africa (AGIS, 2007) as a proxy for all MAP in a given sampling locality over the years covered by the literature review, approximated MAP (AMAP) values were assigned to each locality from which C_3 $\delta^{13}C_{tissue}$ data was reported within the GCFR metadata set (Table 3). Precipitation varies across the study area from a low of 0-200mm annually on the northernmost West Coast, to a high of approximately 1000mm/yr ~60km due east of Cape Town (AGIS, 2007). MAP ranges for given areas are in 200mm 'bins'; for all sampling localities the centroid of the bin was taken as an AMAP value, with the exception of the data from van den Heuvel and Midgley (2014), where the authors combined the $\delta^{13}C_{tissue}$ data, by taxon, from two different sampling localities, one with a MAP range of 601-800mm ("Redhill") and a second with a MAP of 801-1000mm ("Somerset West"). Van den Heuvel and Midgley (2014) found no significant difference in the within-taxa $\delta^{13}C_{tissue}$ values between these localities; in order to accommodate this data, the combined data from both of these localities was assigned an AMAP value of 800mm. Latimer *et al.* (2009) reported exact precipitation values; these were rounded to the nearest hundred for AMAP binning.

Region	Locality Specific	MAP range (mm/yr)	AMAP (mm/yr)	Rainfall	Citation
Western Cape	Diepwalle Forest	1000	1000	year-round	West *et al.,* 2001
Western Cape	33.25°S, 18.25°E	201-400	300	winter	Robb *et al.,* 2013
Western Cape	Ceres	801-1000	900	winter	Vogel *et al.,* 1978
Western Cape	New Years Peak	1000	1000	winter	Araya *et al.,* 2010
Western Cape	Riverlands	201-400	300	winter	Araya *et al.,* 2010
Western Cape	Somerset West/Redhill	601-800/801-1000	800	winter	van den Heuvel & Midgley, 2014
Western Cape	Villiersdorp	801-1000	900	winter	Mooney *et al.,* 1977
Western Cape	Nature's valley	1100	1100	winter	Latimer *et al.,* 2009
Western Cape	Swartberg Pass	840	800	winter	Latimer *et al.,* 2009
Western Cape	Jonaskop 744m	438	400	winter	Latimer *et al.,* 2009
Western Cape	Jonaskop 950m	782	800	winter	Latimer *et al.,* 2009
Western Cape	Jonaskop 1550	1407	1400	winter	Latimer *et al.,* 2009
Western Cape	Jonaskop 950m	782	800	winter	Latimer *et al.,* 2009
Western Cape	Molenaars	1000	1000	winter	Reinecke 2013
Western Cape	Sanddrifskloof	201-400	300	winter	Reinecke 2013
Northern Cape	Akkerdisdraai	0-200	100	winter	Rundel *et al.,* 1999
Northern Cape	Brandkaros	0-200	100	winter	Rundel *et al.,* 1999
Northern Cape	Hellskloof	0-200	100	winter	Rundel *et al.,* 1999
Northern Cape	Loeriesfontein	0-200	100	winter	Vogel *et al.,* 1978
Little Karroo	Robertson Karroo	201-400	300	winter	Mooney *et al.,* 1977
Eastern Cape	Fish River Karroid Scrub	401-600	500	year-round	Mooney *et al.,* 1977
Eastern Cape	Grahamstown - Pluto's Vale	401-600	500	year-round	Mooney *et al.,* 1977

Table 2.3. MAP and AMAP values for all localities in GSCIMS with C_3 $\delta^{13}C$ data.

Analysis of the available but very coarse-grained data suggests a weak, albeit significant, relationship between $\delta^{13}C_{tissue}$ values and MAP; a similar relationship to that found by Swap *et al.* (2004) for non-winter rainfall regions of southern Africa. GCFR C_3 $\delta^{13}C_{tissue}$ values and mean annual precipitation are negatively correlated (*Pearson's r* = -0.4935, r^2 = 0.2435, $p < 0.0001$; Figure 2.3); however, much of the strength of the correlation is driven by the very low $\delta^{13}C_{plant}$ values of *Protea*. There is no correlation between MAP and $\delta^{13}C$ when comparing flora from areas that receive < 600mm annually (p= 0.5951) to one another (*Pearson's r* =-0.03565, r^2 = 0.001271, p = 0.7445) or when comparing areas with MAP > 800 mm annually to one another (*Pearson's r* = -0.1885, r^2 = 0.03554, p = 0.1898).

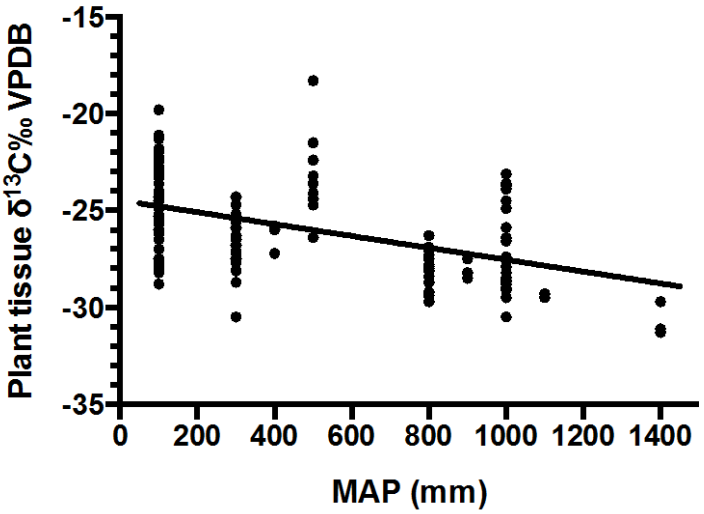

Figure 2.3. $\delta^{13}C_{tissue}$ values (‰, VPDV) of C_3 plants from the GCFR (data from Appendix A) compared to approximated mean annual precipitation data (from AGIS, 2007).

This weak relationship between C_3 $\delta^{13}C_{tissue}$ values and MAP in the GCFR suggests that while caution should be used when comparing $\delta^{13}C_{tissue}$ values from areas

with significantly different amounts of annual precipitation, $\delta^{13}C_{tissue}$ values from C_3 taxa in one region of the GCFR can likely be cautiously used as proxies for $\delta^{13}C_{tissue}$ values of the same taxa in other regions of the GCFR, as long as rainfall is controlled for.

A dataset specifically designed to test for changing within-taxon $\delta^{13}C_{tissue}$ values across the GCFR precipitation gradient(s) is necessary to more rigorously test the relationship between MAP and C_3 $\delta^{13}C_{tissue}$, but the preliminary analysis indicates that precipitation alone is not the primary source of variation in C_3 $\delta^{13}C$ across the GCFR, as the range of variation in C_3 $\delta^{13}C_{tissue}$ values within MAP bins is larger than the mean differences in C_3 $\delta^{13}C_{tissue}$ between the most arid and well-watered regions. This suggests that, although aridity clearly impacts C_3 plant tissue carbon isotope composition, in the absence of more detailed bioregion specific data, the $\delta^{13}C_{tissue}$ values for given taxa can be a useful approximation of individual end-member $\delta^{13}C$ values of GCFR floral communities.

GCFR C_4

Twenty-nine grasses known to occur in GCFR floral communities are included in the metadata set in Appendix A. $\delta^{13}C_{tissue}$ values for the C_4 plants range from -9.96‰ to -15.6‰, with mean C_4 $\delta^{13}C_{tissue}$ = -12.34‰ VPDB (σ = 1.12). The difference between the C_3 and C_4 grass $\delta^{13}C$ means is 13.5‰. As is the pattern worldwide, there is no overlap in $\delta^{13}C$ between C_4 grasses and any of the C_3 plants in the GCFR (Figure 2.4).

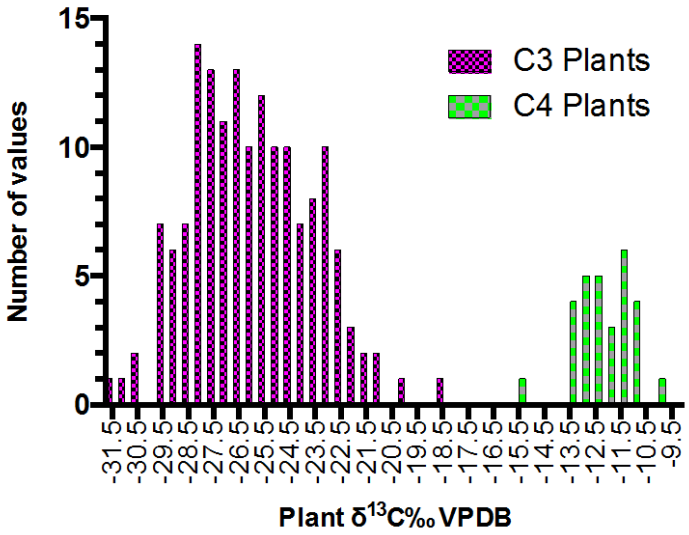

Figure 2.4. Frequency distribution of C_3 and C_4 $\delta^{13}C_{tissue}$ values.

GCFR CAM and FCAM Plants

CAM plants (including those that are facultatively CAM, e.g. plants that switch between C_3 and CAM photosynthetic pathways) are usually excluded from consideration in the isotope ecology literature either because they are not common in the geographic study area of interest, or because they are presumed to be unpalatable to most fauna. However, CAM plants are common in the succulent Karoo (Milton *et al.*, 1997) and thicket (Hoare *et al.*, 2006) vegetation in the GCFR; characteristic plants common in the latter include *Portulacaria afra* (Spekboom) which 'switches' between C_3 and CAM photosynthetic pathways, and members of the genus *Euphorbia.* CAM plants also occur within fynbos vegetation communities, especially in regions prone to low rainfall (Rebelo *et al.*, 2006). CAM plants comprise slightly more than 50% of the entries in the metadata

set compiled here. One hundred nine plants are categorized as CAM and 46 taxa are classified as facultatively CAM (FCAM).

$\delta^{13}C_{tissue}$ values of obligate CAM plants range from -10.6‰ to -18.7‰ VPDB, with a mean $\delta^{13}C_{tissue}$ of -14.37‰ ($\sigma = 1.72$). $\delta^{13}C_{tissue}$ values of FCAM plants are comparably depleted in ^{13}C and have $\delta^{13}C_{tissue}$ values between -16.7‰ and -27.6‰ VPDB, with a mean $\delta^{13}C_{tissue}$ of -20.41‰ ($\sigma = 2.793$); GCFR CAM and FCAM plants are significantly different in $\delta^{13}C_{tissue}$ values ($p < 0.0001$). The lowest $\delta^{13}C$ values for FCAM plants are almost certainly the result of sampling plants that were actively using C_3 photosynthesis, rather than crasseulean acid metabolism.

Obligate CAM $\delta^{13}C_{tissue}$ values overlap appreciably with those of the C_4 grasses found in the GCFR (Figure 2.5), although the mean carbon isotope ratios of the plant groups are significantly different (t-test, $p < 0.0001$). Overlap in $\delta^{13}C_{tissue}$ values between C_3 and obligate CAM plants is functionally non-existent (the lowest CAM $\delta^{13}C_{tissue}$ value is -18.7‰ VPDB while the highest C_3 value is -18.3‰ VPDB). Predictably, FCAM plants engaged in C_3 photosynthesis have $\delta^{13}C_{tissue}$ values that overlap with pure C_3 plants (Figure 2.5). In the GCFR, plants with $\delta^{13}C_{tissue} < \sim 20‰$ are utilizing C_3 photosynthesis, while plants with $\delta^{13}C_{tissue} > \sim 18‰$ are utilizing either CAM or C_4 photosynthetic pathways. This 'trough' in the frequency distribution of $\delta^{13}C_{tissue}$ values between the plant groups suggests a clear boundary for isotopic ecology studies in the GCFR: isotopic reconstructions of "pure C_3" vegetation must have at a minimum a $\delta^{13}C_{plant}$ of less than 20‰ VPDB (after adjusting for the Suess effect). "Pure C_3" in this sense must necessarily include FCAM plants utilizing the C_3 metabolic pathway, and so cannot

dismiss all succulents from the vegetation reconstruction, but it does allow for the positive exclusion of all obligate CAM and C_4 vegetation.

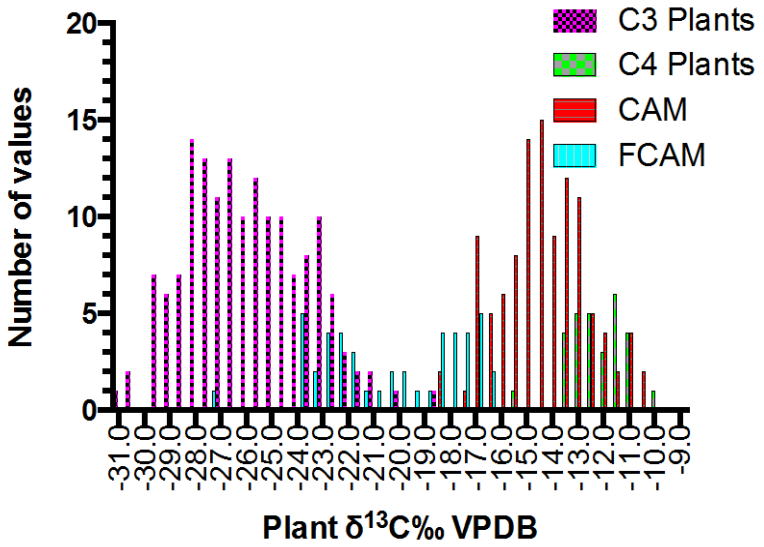

Figure 2.5. Frequency distribution $\delta^{13}C_{tissue}$ values for all photosynthetic types.

GSCIMS-Hypothesized variability in the range of stable carbon isotope plant tissue values available in different southern Cape Vegetation communities

Depending on the changes in vegetation structure, the range of $\delta^{13}C_{plant}$ values available in the form of plant tissue should vary in a given a region across both time and space. The range of available plant $\delta^{13}C_{tissue}$ values in a vegetation community is composed of the known or inferred $\delta^{13}C_{plant}$ values of all the constituent floral taxa. Analysis of the GSCIMS data set suggests that there are some differences in the range of $\delta^{13}C_{plant}$ values available to primary consumers on the landscape between given GCFR vegetation units. Given what is known about the stable carbon isotope composition of structural categories of plants, the following are hypothesized:

H1: In the case of GCFR floral communities, among shrubby plants, reduction in the frequency of *Protea* or true trees occurring in the vegetation at a given locality will result in slightly higher average $\delta^{13}C_{C3\text{-}plant}$ values, as plants with the most depleted tissues will be absent or less common in the environment.

H2: A reduction in the availability of succulent plants or woody shrubs (including all the non-Ericoid taxa found in the metadata set) will result in consistently more depleted plant tissues occurring on the landscape, as those C_3 plants that are most enriched in ^{13}C would not be present.

The exact frequencies of these different types of non-graminoid C_3 vegetation may be impossible to tease apart on any sort of larger geographic or temporal scale, due to heterogeneity within floral communities, but the tissues of browsers should at least partly reflect contractions in the stable carbon isotope values of available plants—at the very least, consumer tissue $\delta^{13}C$ values that imply plant tissue $\delta^{13}C$ values concentrated around -28 to -30‰ VPDB would suggest a reduction in frequency of palatable succulents and many of the shrub genera on the landscape.

A similar but simpler relationship should exist in regards to the frequency of different graminoid flora in a given vegetation community:

H3: Where C_4 grass taxa are rare, the range of $\delta^{13}C_{plant}$ values contracts, as the most ^{13}C-enriched components of the vegetation are no longer present. Grazer tissue $\delta^{13}C$ values will be higher.

H4: Where C_3 grass and *Restio* taxa are rare, the range of $\delta^{13}C_{plant}$ values available on the landscape to grazing primary consumers will be higher (even while C_3 browse is abundant), and grazer tissue $\delta^{13}C$ values will be higher, reflecting the relative scarcity of ^{13}C-depleted graminoid plant tissue in the landscape.

As a simple proxy for the range of $\delta^{13}C$ values found in a given vegetation community, the most depleted and enriched in ^{13}C plant taxa from each photosynthetic group (C_3, C_4, and CAM) can be used as end member vegetation values. This works around the lack of published data on the relative frequencies of specific plant taxa within a vegetation community, and instead lets us predict a range of values that will be present in a given floral community. This is still a time-consuming task, as lists of endemic taxa from a specific vegetation community must be compared with taxonomic entries in the stable carbon isotope metadata set. To attempt to do so for the entirety of the GCFR is time-prohibitive. Instead, C_3, CAM, and C_4 $\delta^{13}C_{plant}$ ranges have been produced for the vegetation communities proximate to this dissertation's study area only—e.g. vegetation communities within approximately 50km of either Pinnacle Point proper, or those near to the three localities from which modern micromammal specimens were collected (Figure 2.6).

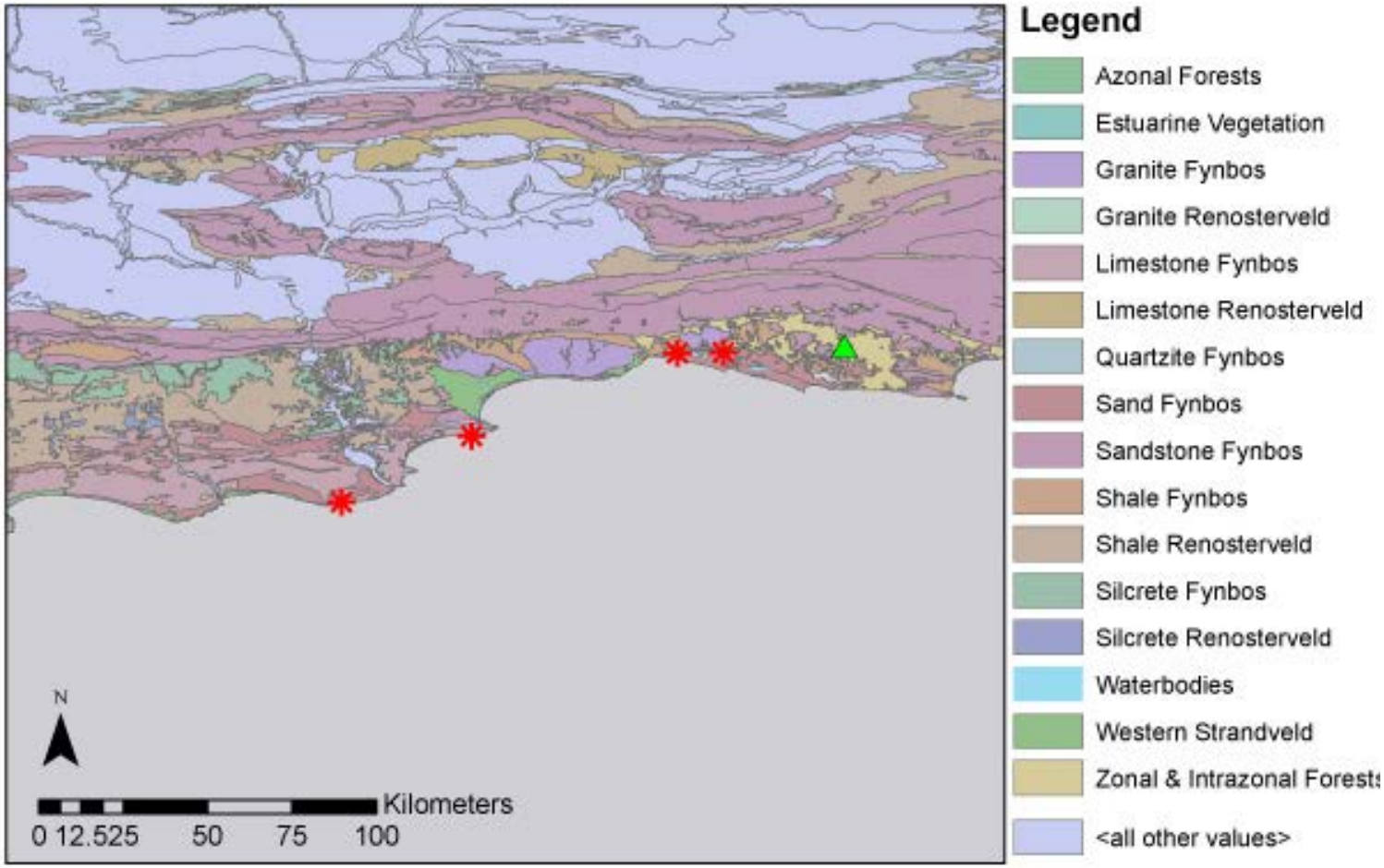

Figure 2.6. Modern GCFR vegetation in the Pinnacle Point study region (vegetation distribution data from Mucina and Rutherford, 2006) . Red stars represent modern micromammal sampling locations and Pinnacle Point. The green triangle is the location of the Knysna Forest vegetation samples from West *et al.* (2001).

Summary of available GSCIMS data for the Major Vegetation Groups Proximate to Pinnacle Point

Major vegetation groups were identified using the GIS data from Mucina and Rutherford (2006) (Figure 2.6). Seventeen vegetation communities were identified within 50km of the Pinnacle Point region. Using the "Important Taxa" and "Endemic Taxa" lists from Rebelo *et al.* (2006), provisional end-member C_3, C_4, and CAM $\delta^{13}C$ values were compiled for each vegetation type. Because the $\delta^{13}C_{plant}$ metadata set is limited in its scope, these are preliminary designations that ultimately should be ground-truthed by vegetation sampling and isotopic analysis. Given the hyperdiversity of the flora in the GCFR, often there are no stable carbon isotope data extant for a particular species, but data from other members of the genus are available. When this generic data is applicable (i.e. it comes from a similar area of MAP as the target vegetation community) it is included in the summaries below and noted with an asterisk.

North Langeberg Sandstone Fynbos

North Langeberg Sandstone Fynbos (Mucina and Rutherford 2006 code FFs 11) is dominated by proteoid and restioid fynbos (Rebelo *et al.*, 2006). It exists across a large rainfall gradient (250 – 1200 mm/yr, Rebelo *et al.*, 2006). Taxa that occur in FFs 11 for which there is $\delta^{13}C$ data are shown in Table 2.4. GSCIMS lacks several key genera, including the C_3 grasses *Erharta* and *Pentaschistis*, for which there are only data from the summer rainfall zone (Vogel *et al.*, 1978; Schulze *et al.*, 1996), and *Erica*, a 'heathland' C_3 plant group found in many fynbos vegetation communities.

Plant Type	Taxon	δ^{13}C ‰ VPDB	σ
C_3			
	*Aspalathus **	-26.9	1.56
restioid	*Calopsis**	-26.9	
restioid	*Cannomois **	-27.5	
restioid	*Elegia**	-27	0.77
restioid	*Hypodiscus**	-28.0	0.21
annual	*Indigofera sp.*	-22.7	
restioid	*Ischyrolepis capensis*	-28.2	
	Leucadendron salignum	-28.5	
	Leucadendron salignum	-25.9	
	*other Leucadendron**	-26.9	2.25
	*Pelargonium**	-24.9	0.00
restiod	*Restio**	-26.8	0.83
restioid	*Senecio**	-22.2	
restioid	*Staberoha cernua*	-26.3	
restioid	*Thamnochortus **	-28.2	
	Thesium sp	-26.8	
annual	*Ursinia sp.*	-28.1	
restioid	*Willdenowia **	-28.8	
shrub	*Zygophyllum**	-24.1	1.02
tall shrub	*Protea**	-27.9	1.35
C_4			
grass	*Heteropogon contortus*	-12.1	
CAM/FCAM			
succulent	*Adromischus**	-13.6	1.33
succulent	*Crassula (CAM)**	-14.6	1.29
succulents	*Crassulaceae(CAM)**	-15.3	0.35
leaf succulent	*Drosanthemum (CAM)**	-15.8	
leaf succulent	*Antimima sp.(FCAM)*	-19.5	
	*Crassula (FCAM)**	-18.8	1.38
succulent	*Crassulaceae (FCAM)**	-22.8	0.57
leaf succulent	*Drosanthemum (FCAM)**	-22.5	0.44
leaf succulent	*Senecio (FCAM)**	-17.5	

Grass Genera w/o GCFR δ^{13}C values	
Genus	
Ceratocaryum	C_3
Ehrhata	C_3
Ficinia	C_3
Mastersiella	C_3
Merxmuellera	C_3
Pentameris	C_3
Pentaschistis	C_3
Platycoaulos	C_3
Rhodocoma	C_3
Tetraria	C_3
Thamnochortus	C_3

Table 2.4. Extant $\delta^{13}C_{tissue}$ data (‰, VPDB) for genera of plants found in the North Langeberg Sandstone Fynbos. Data derived from sources listed in Appendix A. Floral taxonomic presence determined from Rebeleo *et al*. (2006)

South Langeberg Sandstone Fynbos

South Langeberg Sandstone Fynbos (Mucina and Rutherford FFs 16) inhabits areas with slightly wetter MAP (320-1440 mm) than does North Langeberg Sandstone Fynbos, and is dominated by ericaceous, restioid and proteoid fynbos (Rebelo *et al.*, 2006). Members of the genus *Erica* are common, but problematically there is no stable carbon isotope data for the genus from southern Africa. FFs 16 vegetation communities appear to lack the *Crassula* common in the North Langeberg Sandstone Fynbos (Rebelo *et al.* 2006). As in the case of the North Langeberg Sandstone Fynbos, the stable carbon isotope dataset also does not have coverage for *Pentaschistis* and *Erharta* C_3 grasses.

The available $\delta^{13}C$ data for South Langeberg Sandstone Fynbos taxa are shown in Table 2.5. Again, it is stressed that the common genus *Erica* is not represented in the currently available data.

North Outeniqua Sandstone Fynbos

North Outeniqua Sandstone Fynbos (Mucina and Rutherford 2006 FFs18) is a moderately dense shrubland vegetation composed primarily of *Protea* and restioid fynbos that receives MAP of 520mm (Rebelo *et al.*, 2006). Taxonomic coverage of the shrub component of FFs18 is poor in GSCIMS; however, the majority of the important graminoid genera (*sensu* Rebelo *et al.*, 2006) appear. The available $\delta^{13}C$ data for North Outeniqua Sandstone Fynbos taxa are shown in Table 2.6.

Plant Type	Taxon	$\delta^{13}C$ ‰ VPDB	σ
C_3			
restioid	*Anthochortus crinalis*	-25.2	
	Aspalathus *	-26.9	1.56
restioid	*Calopsis* *	-26.9	
	*Cyphia**	-23.0	
restioid	*Elegia filacea*	-26.3	
restioid	*Elegia filacea*	-28.0	
	*other Elegia**	-26.9	0.49
	*Hypodiscus**	-28.0	0.21
restioid	*Ischyrolepis capensis*	-28.2	
annual	*Indigofera sp.*	-22.7	
	Leucadendron salignum	-28.5	
	Leucadendron salignum	-25.9	
	*other Leucadendron**	-26.9	2.25
	Othonna *	-25.0	1.02
	*Pelargonium**	-24.9	0.00
	Podalyria sp	-27.0	
	*Protea**	-28.6	0.96
	*Restio**	-26.8	0.83
leaf succulent	*Senecio* *	-22.2	
restioid	*Staberoha cernua*	-26.3	
annual	*Ursinia sp.*	-28.1	
C_4			
grass	*Cymbopogon**	-12.2	1.02
grass	*Eragrostis capensis*	-13.2	
grass	*Themeda triandra*	-11.6	
CAM/FCAM			
	*Pelargonium (CAM)**	-16.9	

Grass Genera w/o GCFR $\delta^{13}C$ values	
Genus	
Ceratocaryum	C_3
Chrysitrix	C_3
Ehrhata	C_3
Pentachistis	C_3
Pentameris	C_3
Tetraria	C_3

Table 2.5. Extant $\delta^{13}C_{tissue}$ data (‰, VPDB) for genera of plants found in the South Langeberg Sandstone Fynbos. Data derived from sources listed in Appendix A. Floral taxonomic presence determined from Rebeleo *et al*. (2006)

Plant Type	Taxon	$\delta^{13}C$ ‰ VPDB	σ
C_3			
	Aspalathus *	-26.9	1.56
restioid	*Cannomois* *	-27.5	
	*Elegia**	-27	0.77
restioid	*Hypodiscus* *	-28.0	0.21
	*Leucadendron**	-27.0	1.93
	Podalyria sp	-27.0	
annual	*Oxalis sp.*	-27.9	
annual	*Oxalis spp.*	-26.4	
bush	*Protea**	-28.6	0.96
	*Restio**	-26.8	0.83
	Zygophyllum *	-24.1	1.02
C_4			
grass	*Aristida* *	-11.0	
grass	*Brachiaria* *	-11.5	
grass	*Heteropogon contortus*	-12.1	
grass	*Themeda triandra*	-11.6	
CAM			
	Haworthia *	-12.6	0.64

Grass Genera w/o GCFR $\delta^{13}C$ values	
Genus	
Pentaschistis	C_3
Mastersiella	C_3
Merxmuellera	C_3
Rhodocomoa	C_3

Table 2.6. Extant $\delta^{13}C_{tissue}$ data (‰, VPDB) for genera of plants found in the North Outeniqua Sandstone Fynbos. Data derived from sources listed in Appendix A. Floral taxonomic presence determined from Rebeleo *et al*. (2006)

South Outeniqua Sandstone Fynbos

South Outeniqua Sandstone Fynbos (FFs 19) is a shrubby proteoid/restioid fynbos with a significant 'grassy' component. Mean rainfall is 785mm/yr (Rebelo *et al.,* 2006). Taxonomic coverage of the isotopic composition of the grasses in this vegetation community is sparse, especially in contrast with the database's coverage of the grasses from the North Outeniqua Sandstone Fynbos. This is partially due to the larger number of graminoid species (n = 45) reported by Rebelo *et al.* (2006) that are present in the vegetation community, in combination with the comparably limited available C_3 grass

isotope data. $\delta^{13}C_{plant}$ data for taxa found in FFs19 vegetation communities is presented in Table 2.7.

Plant Type	Taxon	$\delta^{13}C$ ‰ VPDB	σ
C_3			
	*Aspalathus **	-26.9	1.56
restioid	*Anthochortus **	-25.2	
restioid	*Cannomois **	-27.5	
restioid	*Elegia**	-27.0	0.77
restioid	*Hypodiscus**	-28.0	0.21
restioid	*Ischyrolepis**	-27.2	0.49
	Leucadendron salignum	-28.5	
	Leucadendron salignum	-25.9	
	*other Leucadendron**	-26.9	2.25
annual	*Osteospermum **	-25.6	
bush	*Protea**	-28.6	0.96
	*Restio**	-26.8	0.83
	*Staberoha**	-27.4	1.56
restioid	*Thamnochortus **	-28.2	
	Thesium sp	-26.8	
annual	*Ursinia sp.*	-28.1	
corm annual	*Watsonia **	-23.9 to -29.2	
restioid	*Willdenowia **	-28.8	
C_4			
	*Andropogon **	-11.8	
grass	*Themeda triandra*	-11.6	
FCAM			
	*Senecio**	-19.9	3.29

Grass Genera w/o GCFR $\delta^{13}C$ values	
Genus	
Anthochortus	C_3
Chrysitrix	C_3
Epischoenus	C_3
Ehrhata	C_3
Ficinia	C_3
Mastersiella	C_3
Merxmuellera	C_3
Pentameris	C_3
Pentaschistis	C_3
Platycaulos	C_3
Staberoha	C_3
Tetraria	C_3

Table 2.7. Extant $\delta^{13}C_{tissue}$ data (‰, VPDB) for genera of plants found in the South Outeniqua Sandstone Fynbos. Data derived from sources listed in Appendix A. Floral taxonomic presence determined from Rebeleo *et al*. (2006)

Albertinia Sand Fynbos

This vegetation community (FFd 9, Mucina and Rutherford, 2006) grows on sandy substrates adjacent to limestone fynbos communities along the south Coast, and is primarily an open shrubby proteoid-dominated vegetation (Rebelo *et al.*, 2006). Rainfall is comparably low compared to other vegetation units previously discussed (MAP 230-620mm, Rebelo *et al.*, 2006). Many of the FFd 9 succulent taxa have not been sampled for carbon isotopes; although there is substantial shrub $\delta^{13}C$ data for taxa such as *Leucadendron*, the resulting table of stable carbon isotopic composition (Table 2.8) is heavily biased towards the graminoids present in this vegetation community.

Plant Type	Taxon	$\delta^{13}C$ ‰ VPDB	σ
C_3			
	Aspalathus *	-26.9	1.56
	Bulbine *	-26.4	
restioid	*Calopsis* *	-26.9	
restioid	*Elegia* *	-27.0	0.77
restioid	*Ischyrolepis**	-27.1	0.49
	*Leucadendron**	-27.0	1.93
	Nylandtia spinosa	-22.3	
	*Protea**	-26.3	0.76
leaf succulent	*Senecio* *	-22.2	
restioid	*Staberoha distachyos*	-28.5	
restioid	*Thamnochortus* *	-28.2	
restioid	*Willdenowia* *	-28.8	
C_4			
grass	*Cynodon dactylon*	-12.7	
grass	*Cynodon dactylon*	-15.6	
CAM/FCAM			
	*Senecio (FCAM)**	-17.1	0.58

Grass Genera w/o GCFR $\delta^{13}C$ values	
Genus	
Mastersiella	C_3
Staberoha	C_3

Table 2.8. Extant $\delta^{13}C_{tissue}$ data (‰, VPDB) for genera of plants found in the Albertinia Sand Fynbos. Data derived from sources listed in Appendix A. Floral taxonomic presence determined from Rebeleo *et al.* (2006)

Knysna Sand Fynbos

Knysna Sand Fynbos (Mucina and Rutherford, 2006 FFd 10) receives significantly more rain (MAP ~ 850mm) than the region inhabited by Albertinia Sand Fynbos and has vegetation more similar to Sandstone Fynbos communities than other Sand Fynbos communities (Rebelo *et al.*, 2006). As with the Albertinia Sand Fynbos vegetation, coverage of stable carbon isotope data of C_3 taxa within this vegetation group is poor, with the exception of the graminoids, of which only four reported genera are not included in the dataset. The resulting table (Table 2.9) is heavily biased towards graminoids, but provides an excellent dietary end member $\delta^{13}C$ dataset for researchers looking at grazing mammalian taxa within this environment.

Plant Type	Taxon	$\delta^{13}C$ ‰ VPDB	σ
C_3			
restioid	*Ischyrolepis**	-27.2	0.49
	*Leucadendron**	-27.0	1.93
	*Protea **	-29.0	0.53
restioid	*Thamnochortus **	-28.2	
C_4			
grass	*Aristida **	-11.0	
grass	*Brachiaria serrata*	-11.5	
grass	*Cynodon dactylon*	-12.7	
grass	*Cynodon dactylon*	-15.6	
grass	*Eragrostis capensis*	-13.2	
grass	*Heteropogon contortus*	-12.1	
grass	*Themeda triandra*	-11.6	
grass	*Tristachya **	-11	

Grass Genera w/o GCFR $\delta^{13}C$ values	
Genus	
Ficinia	C_3
Tetraria	C_3

Table 2.9. Extant $\delta^{13}C_{tissue}$ data (‰, VPDB) for genera of plants found in the Knysna Sand Fynbos. Data derived from sources listed in Appendix A. Floral taxonomic presence determined from Rebeleo *et al.* (2006)

Garden Route Shale Fynbos

Garden Route Shale Fynbos (Mucina and Rutherford 2006 FFh 9) is found along the south coast of South Africa on shale-derived soils. The vegetation exists primarily in year-round rainfall zones with a MAP of 301-1120mm (Rebelo *et al.,* 2006). The vegetation grades from grass-predominant fynbos vegetation in area that receive less rainfall to more closed and dense fynbos dominated by *Protea* and *Erica* flora (Rebelo *et al.,* 2006). GSCIMS coverage of the shrub taxa in this vegetation unit is better than in the two previous described, in part because the diversity of *Erica* taxa appears to be lower, and there is $\delta^{13}C_{plant}$ data available for other shrubby vegetation such as *Rhus* and *Pelargonium*. Only two genera of graminoids mentioned by Rebelo *et al.* (2006) are not found in the stable carbon isotope database. The $\delta^{13}C$ data (Table 2.10) for this vegetation community thus should be fairly representative of the range of stable carbon isotopic compositions of plants in the Garden Route Shale Fynbos.

Swellendam Silcrete Fynbos

Swellendam Silcrete Fynbos (Mucina and Rutherford 2006 FFc1) is an asteraceous fynbos found in an area with a mean annual rainfall of 520mm (Rebelo *et al.,* 2006). Absence of *Erica* and *Leucospermum* taxa from the stable carbon isotope data reduces GSCIMS $\delta^{13}C$ coverage of this vegetation community, although the graminoids are comparably well represented (Table 2.11).

Plant Type	Taxon	$\delta^{13}C$ ‰ VPDB	σ
C_3			
restioid	*Elegia* *	-27	0.77
graminoid	*Ischyrolepis**	-27.2	0.49
	*Leucadendron**	-27.00	1.93
leaf succulent	*Pelargonium* *	-24.9	
	*Protea**	-28.6	0.88
	*Restio**	-26.8	0.83
riparian shrub/tree	*Rhus**	-23.4	1.09
C_4			
grass	*Aristida* *	-11.0	
grass	*Brachiaria serrata*	-11.5	
grass	*Cymbopogon**	-12.2	1.02
grass	*Eragrostis capensis*	-13.2	
grass	*Tristachya* *	-11	
grass	*Themeda triandra*	-11.6	
CAM/FCAM			
	*Crassula (CAM)**	-14.6	1.28
	*Crassula (FCAM)**	-18.8	1.38
	Pelargonium *	-16.9	

Important Grass Genera w/o GCFR $\delta^{13}C$ values
Genus
none

Table 2.10. Extant $\delta^{13}C_{tissue}$ data (‰, VPDB) for genera of plants found in the Garden Route Shale Fynbos. Data derived from sources listed in Appendix A. Floral taxonomic presence determined from Rebeleo *et al*. (2006)

Plant Type	Taxon	δ^{13}C ‰ VPDB	σ
C_3			
	Berkheya *	-25.5	
restioid	*Ischyrolepis* *	-27.5	0.70
	*Leucadendron**	-27.0	1.93
	*Protea**	-26.3	0.76
restioid	*Restio**	-26.8	0.83
	Ruschia (C_3)*	-23.4	0.42
C_4			
grass	*Cymbopogon**	-12.2	1.02
grass	*Cynodon dactylon*	-12.7	
grass	*Cynodon dactylon*	-15.6	
grass	*Eragrostis capensis*	-13.2	
grass	*Themeda triandra*	-11.6	
CAM/FCAM			
succulent	*Pelargonium* *	-16.9	
leaf succulent	*Ruschia (CAM)**	-16.5	0.82
leaf succulent	*Ruschia (FCAM)**	-21.2	3.19

Grass Genera w/o GCFR δ^{13}C values	
Genus	
Ehrharta	C_3
Juncus	C_3
Merxmuellera	C_3
Pentaschistis	C_3
Isolepis	C_3

Table 2.11. Extant $\delta^{13}C_{tissue}$ data (‰, VPDB) for genera of plants found in the Swellendam Silcrete Fynbos. Data derived from sources listed in Appendix A. Floral taxonomic presence determined from Rebeleo *et al*. (2006)

Garden Route Granite Fynbos

Garden Route Granite Fynbos (Mucina and Rutherford 2006 FFg 5) receives between 350 – 880 mm MAP, and is a comparably grassy fynbos with some proteoid and ericoid component (Rebelo *et al.,* 2006). With the exception of *Protea, Pelargonium,* and *Leucadendron,* there is no stable carbon isotope data extant for the non-succulent shrub component of this vegetation community. About half of the listed grass genera in this unit (Rebelo *et al.,* 2006)—*Bracharia, Eragrostis, Heteropogon,* and *Themeda*—are C_4 grasses (Table 2.11). Coverage in the $\delta^{13}C$ meta-dataset is heavily biased towards these C_4 grasses, and $\delta^{13}C_{plant}$ values are only available for graminoid C_3 flora from the genus *Restio* for this vegetation community (Table 2.12).

Plant Type	Taxon	$\delta^{13}C$ ‰ VPDB	σ
C_3			
	*Aspalathus **	-26.9	1.56
	*Leucadendron**	-27.0	1.93
	*Pelargonium**	-24.9	0.00
	*Protea **	-27.7	1.22
restiod	*Restio**	-26.8	0.83
	Thesium sp	-26.8	
C_4			
grass	*Brachiaria serrata*	-11.5	
grass	*Eragrostis capensis*	-13.2	
grass	*Heteropogon contortus*	-12.1	
grass	*Themeda triandra*	-11.6	

Grass Genera w/o GCFR $\delta^{13}C$ values	
Genus	
Tetraria	C_3
Ficinia	C_3
Pentaschistis	C_3

Table 2.12. Extant $\delta^{13}C_{tissue}$ data (‰, VPDB) for genera of plants found in the Garden Route Granite Fynbos. Data derived from sources listed in Appendix A. Floral taxonomic presence determined from Rebeleo *et al.* (2006)

Canca Limestone Fynbos

Canca Limestone Fynbos (Mucina and Rutherford 2006 FFl 3) is the predominant vegetation type proximate to the Pinnacle Point locality. The vegetation occurs on shallow limestone soils in regions receiving a mean of 485 mm of rainfall annually. Vegetation is dominated by proteoid, restioid and asteraceous fynbos, and ericoids are rare (Rebelo *et al.*, 2006). Despite this, there is no stable carbon isotope data for many of the flora found in the Canca Limestone Fynbos, likely because vegetation sampling has largely been focused in the southwest Cape (see Figure 2.1). All of the graminoids listed by Rebelo *et al.*, (2006) are C_3 taxa (Table 2.13).

Plant Type	Taxon	$\delta^{13}C$ ‰ VPDB	σ
C_3			
	Aspalathus *	-26.9	1.56
restioid	*Elegia* *	-27.0	0.77
annual	*Indigofera sp.*	-22.7	
restioid	*Ischyrolepis* *	-27.5	0.70
	*Leucadendron**	-27.0	1.93
	*Protea**	-26.3	0.76
	Ruschia (C_3)*	-23.4	0.42
	Sutera *	-24.5	
restioid	*Thamnochortus* *	-28.2	
CAM/FCAM			
	Haworthia *	-12.6	0.64
	*Ruschia (CAM)**	-16.5	0.82
	*Ruschia (FCAM)**	-21.0	3.42

Grass Genera w/o GCFR $\delta^{13}C$ values	
Genus	
Ceratocaryum	C_3
Ficinia	C_3
Pentaschistis	C_3

Table 2.13. Extant $\delta^{13}C_{tissue}$ data (‰, VPDB) for genera of plants found in the Canca Limestone Fynbos. Data derived from sources listed in Appendix A. Floral taxonomic presence determined from Rebeleo *et al*. (2006)

Eastern Ruens Shale Renosterveld

Eastern Ruens Shale Renosterveld (Mucina and Rutherford FRs 13) is found on soils derived from the Bokkeveld shale in areas of year-round rainfall (MAP 270-540 mm; Rebelo *et al.*, 2006). Many of the constituent grasses are C_3, for which no GCFR-specific data exists. Stable carbon isotope data available for FRs 13 flora are found in Table 2.14.

Plant Type	Taxon	$\delta^{13}C$ ‰ VPDB	σ
C_3			
	*Aspalathus **	-26.9	1.56
leaf succulent	*Drosanthemum**	-18.3	
annual	*Oxalis sp.*	-27.9	
annual	*Oxalis spp.*	-26.4	
	*Rhus**	-23.4	1.09
	Thesium sp	-26.8	
stem succulent	*Trichodiadema*	-23.6	
annual	*Ursinia sp.*	-28.1	
C_4			
grass	*Cymbopogon**	-12.2	1.02
grass	*Eragrostis curvula*	-13.4	
grass	*Eragrostis curvula*	-13.04	
grass	*Themeda triandra*	-11.6	
CAM/FCAM			
	Aloe ferox	-14.7	
	Aloe ferox	-13.3	
leaf succulent	*Drosanthemum (CAM)**	-15.8	
	*Haworthia **	-12.6	0.64
	*Drosanthemum (FCAM)**	-22.5	0.44

Grass Genera w/o GCFR $\delta^{13}C$ values	
Genus	
Merxmuellera	C_3
Ehrhata	C_3
Festuca	C_3
Koeleria	C_3
Tribolium	C_3

Table 2.14. Extant $\delta^{13}C_{tissue}$ data (‰, VPDB) for genera of plants found in the Eastern Ruens Shale Renosterveld. Data derived from sources listed in Appendix A. Floral taxonomic presence determined from Rebeleo *et al*. (2006)

Mossel Bay Shale Renosterveld

Mossel Bay Shale Renosterveld (Mucina and Rutherford 2006 FFs 14) is dominated by the presence of renosterbos (*Elytropappus rhinocerotis*) (Rebelo *et al.*, 2006), for which there is no published $\delta^{13}C_{plant}$ values. Boom *et al.* (2004) have published $\delta^{13}C$ values for "Asteraceae" from the GCFR, which have been here used provisionally as a proxy for renosterbos values. Coverage of the stable carbon isotope metadata set for FFs 14 is otherwise excellent; in the graminoids, only *Ehrharta* and *Pentaschistis* lack $\delta^{13}C$ data points, and most shrub species are represented (Table 2.15).

Uniondale Shale Renosterveld

Uniondale Shale Renosterveld (Mucina and Rutherford 2006 FRs 16) is also dominated by renosterbos vegetation, in tandem with a grassy understory to the shrub vegetation (Rebelo *et al.*, 2006). *Acacia karoo* also occurs in this vegetation community. GSCIMS coverage of this vegetation unit is moderate: there is $\delta^{13}C$ data for a number of the shrub and succulent shrub taxa (Table 2.16), but there is no GCFR-specific $\delta^{13}C$ data for two of the three C_3 grass taxa (*Erharta* and *Melica*) mentioned by Rebelo *et al.* (2006).

Plant Type	Taxon	$\delta^{13}C$ ‰ VPDB	σ
C_3			
	Asteraceae (Renosterbos proxy)	-29.0	
evergreen shrub	*Blepharis capensis*	-22.0	
	Carpabrotus sp.	-23.2	
leaf succulent	*Drosanthemum (C_3)**	-18.3	
annual	*Indigofera sp.*	-22.7	
restioid	*Ischyrolepis **	-27.5	0.70
riparian tree/shrub	*Rhus **	-23.4	1.09
leaf succulent	*Senecio **	-22.2	
annual	*Ursinia sp.*	-28.1	
C_4			
grass	*Brachiaria serrata*	-11.5	
grass	*Sporobolus africanus*	-13.1	
grass	*Themeda triandra*	-11.6	
CAM/FCAM			
succulent	*Aloe ferox*	-14.7	
succulent	*Aloe ferox*	-13.3	
succulent	*Aloe speciosa*	-17.0	
succulent	*Crassula perforata*	-13.1	
leaf succulent	*Drosanthemum (CAM)**	-15.8	
succulent	*Aloe speciosa*	-20.3	
succulent	*Drosanthemum (FCAM)**	-22.5	0.44
leaf succulent	*Senecio **	-17.1	0.58

Grass Genera w/o GCFR $\delta^{13}C$ values	
Genus	
Ehrhata	C_3
Pentaschistis	C_3

Table 2.15. Extant $\delta^{13}C_{tissue}$ data (‰, VPDB) for genera of plants found in the Mossel Bay Shale Renosterveld. Data derived from sources listed in Appendix A. Floral taxonomic presence determined from Rebeleo *et al*. (2006)

Plant Type	Taxon	$\delta^{13}C$ ‰ VPDB	σ
C_3			
tree	*Acacia cf karoo*	-27.7	
	Asteraceae (Renosterbos proxy)	-29.0	
leaf succulent	*Drosanthemum (C_3)**	-18.3	
tree/shrub	*Rhus **	-23.4	1.09
	Thesium sp	-26.8	
evergreen shrub	*Zygophyllum **	-24.1	1.02
C_4			
true grass	*Aristida **	-11.0	
CAM/FCAM			
	Aloe ferox	-14.7	
	Aloe ferox	-13.3	
	Aloe microstigma	-14.6	
	Aloe microstigma	-14.5	
	*Crassula (CAM)**	-14.6	1.29
leaf succulent	*Drosanthemum (CAM)**	-15.8	
	*Crassula (CAM)**	-19.0	1.55
leaf succulent	*Crassula muscosa*	-18.2	
succulent	*Drosanthemum (FCAM)**	-22.5	0.44
perrenial	*Galenia africana*	-23.8	

Grass Genera w/o GCFR $\delta^{13}C$ values	
Genus	
Ehrhata	C_3
Melica	C_3

Table 2.16. Extant $\delta^{13}C_{tissue}$ data (‰, VPDB) for genera of plants found in the Uniondale Shale Renosterveld. Data derived from sources listed in Appendix A. Floral taxonomic presence determined from Rebeleo *et al*. (2006)

Langkloof Shale Renosterveld

Langkloof Shale Renosterveld (Mucina and Rutherford 2006 Frs 17) has somewhat dense graminoid vegetation with a large renosterbos component (Rebelo *et al.*, 2006). The shrubby component of this vegetation unrepresented in the GSCIMS database. The graminoid component of this renosterveld vegetation is however better sampled, with extant stable carbon isotope data from the literature available for approximately half of the grass taxa listed (Table 2.17).

Plant Type	Taxon	δ^{13}C ‰ VPDB	σ
C_3			
	*Aspalathus **	-26.9	1.56
	*Asteraceae (Renosterbos proxy)**	-29.0	
annual	*Indigofera sp.*	-22.7	
leaf succulent	*Senecio (C_3)**	-22.2	
C_4			
grass	*Brachiaria serrata*	-11.5	
grass	*Cymbopogon**	-12.2	1.02
grass	*Sporobolus africanus*	-13.05	
grass	*Themeda triandra*	-11.6	
FCAM			
leaf succulent	*Senecio (FCAM)**	-17.1	0.58

Grass Genera w/o GCFR δ^{13}C values	
Genus	
Ehrhata	C_3
Festuca	C_3
Ficinia	C_3
Hellictotrichon	C_3
Merxmuellera	C_3
Pentaschistis	C_3

Table 2.17. Extant $\delta^{13}C_{tissue}$ data (‰, VPDB) for genera of plants found in the Langkloof Shale Renosterveld. Data derived from sources listed in Appendix A. Floral taxonomic presence determined from Rebeleo *et al.* (2006)

Grootbrak Dune Strandveld

Grootbrak Dune Strandveld (Mucina and Rutherford 2006 FS 9) has dense tall shrub with only a sparse grass understory (Rebelo *et al.*, 2006). The stable carbon isotope metadata set for GCFR plants has excellent coverage for most of the taxa in this vegetation community (Table 2.18).

Southern Cape Dune Fynbos

Southern Cape Dune Fynbos (Mucina and Rutherford 2006 FFd 11) occurs on stabilized dunes along the southern coast, and is dominated by restios and heath-shrub vegetation (Rebelo *et al.*, 2006). Many of the shrub species present in this vegetation community have not been sampled for carbon isotope analysis, and coverage of the metadata base for this vegetation type is poor-to-moderate. $\delta^{13}C_{plant}$ values extant for FFd11 flora are shown in Table 2.19.

Southern Afrotemperate Forest

Southern Afrotemperate Forest (Mucina and Rutherford FOz 1) is found primarily along the south Coast of South Africa near Knysna. Its understory (described in Rebelo *et al.*, 2006) is under-sampled in terms of isotopic analysis. Available published $\delta^{13}C$ data primarily comes from tree species but is not extensive, and there is some sparse grass data as well (Table 2.20).

Plant Type	Taxon	$\delta^{13}C$ ‰ VPDB	σ
C_3			
	Carpabrotus sp.	-23.2	
riparian tree	*Euclea* *	-25.2	
	Grewia *	-24.7	
riparian tree/shrub	*Rhus* *	-23.4	1.09
riparian tree	*Schotia afra*	-22.8	
leaf succulent	*Tetragonia* *	-23.3	
evergreen shrub	*Zygophyllum* *	-24.1	1.02
C_4			
grass	*Cynodon dactylon*	-12.7	
grass	*Cynodon dactylon*	-15.6	
grass	*Panicum* *	-12.1	0.95
CAM/FCAM			
	*Aloe**	-15.4	1.64
succulent	*Cotyledon orbiculata*	-13.7	
succulent	*Cotyledon orbiculata*	-11.0	
succulent	*Cotyledon orbiculata*	-10.9	
succulent	*Crassula perforata*	-13.1	
shrub, succulent	*Euphorbia mauritanica*	-16.9	
shrub, succulent	*Euphorbia mauritanica*	-16.0	
succulent	*Pelargonium peltatum*	-16.9	
stem succulent	*Sarcostemma viminale*	-13.2	
succulent	*Crassula expansa*	-20.3	
succulent	*Euphorbia burmannii*	-18.3	
succulent	*Euphorbia mauritanica*	-22.8	
shrub, succulent	*Euphorbia mauritanica*	-22.0	
succulent	*Senecio radicans*	-16.7	

Grass Genera w/o GCFR $\delta^{13}C$ values	
Genus	
Ehrhata	C_3
Ficinia	C_3
Stipa	C_3

Table 2.18. Extant $\delta^{13}C_{tissue}$ data (‰, VPDB) for genera of plants found in the Gootbrak Dune Strandveld. Data derived from sources listed in Appendix A. Floral taxonomic presence determined from Rebeleo *et al*. (2006)

Plant Type	Taxon	δ^{13}C ‰ VPDB	σ
C_3			
	Aspalathus *	-26.9	1.56
annual	*Indigofera sp.*	-22.7	
restioid	*Ischyrolepis* *	-27.5	0.70
	Leucadendron salignum	-28.5	
	Leucadendron salignum	-25.9	
	Pelargonium(C_3)*	-24.9	0
riparian shrub	*Rhus populifolia*	-24.2	
riparian tree	*Rhus undulata*	-22.7	
restioid	*Thamnochortus* *	-28.2	
	Thesium sp	-26.8	
CAM			
	*Pelargonium (CAM)**	-16.9	

Grass Genera w/o GCFR δ^{13}C values	
Genus	
Ehrhata	C_3
Ficinia	C_3
Pentaschistis	C_3
Tetraria	C_3
Tribolium	C_3

Table 2.19. Extant $\delta^{13}C_{tissue}$ data (‰, VPDB) for genera of plants found in the Southern Cape Dune Fynbos. Data derived from sources listed in Appendix A. Floral taxonomic presence determined from Rebeleo *et al*. (2006)

Plant Type	Taxon	$\delta^{13}C$ ‰ VPDB	σ
C_3			
tree	*Afrocarpus falcatus*	-29.1	
tree	*Afrocarpus falcatus*	-24.5	
tree	*Afrocarpus falcatus*	-24.9	
tree	*Brabejum stellatifolium*	-29.5	
tree	*Brabejum stellatifolium*	-28.7	
tree	*Metrosideros angustifolia*	-27.9	
tree	*Metrosideros angustifolia*	-27.6	
tree	*Olea capensis macrocarpa*	-26.4	
tree	*Olea capensis macrocarpa*	-30.5	
tree	*Olea capensis macrocarpa*	-27.4	
tree	*Olea capensis macrocarpa*	-27.6	
tree	*Podocarpus latifolis*	-23.6	
tree	*Podocarpus latifolis*	-27.5	
tree	*Podocarpus latifolis*	-23.6	
tree	*Podocarpus latifolis*	-23.9	
restioid	*Ischyrolepis* *	-27.5	0.70
annual	*Oxalis sp.*	-27.9	
annual	*Oxalis spp.*	-26.4	

Grass Genera w/o GCFR $\delta^{13}C$ values	
Genus	
Schoenoxiphium	C_3
Other Understory Taxa	
Amauropelta	
Asparagus	
Clivia	
Freesia	
Gerbera	
Laurophyllus	
Liparis	
Mystacidium	
Polystichum	
Streptocarpus	

Table 2.20. Extant $\delta^{13}C_{tissue}$ data (‰, VPDB) for genera of plants found in the Southern Afrotemperate Forest. Data derived from sources listed in Appendix A. Floral taxonomic presence determined from Rebeleo *et al*. (2006)

Conclusions

In the extant GCFR vegetation communities in the southern Cape, the available stable carbon isotope data from GSCIMS suggests that across all 17 plant communities discussed here, there is a wide range of $\delta^{13}C_{plant}$ values present. There are however several small differences between the vegetation communities that should be highlighted.

For most of the vegetation communities presented here, $\delta^{13}C_{plant}$ values for C_3 plants range from ~ -29‰ to -22.0‰ VPDB (with outliers in either direction present in some individual vegetation communities, Figure 2.7). There are two notable exceptions to this: the $\delta^{13}C_{tissue}$ values for C_3 plants from the Knysna Sand Fynbos and from the Grootbrak Dune Strandveld.

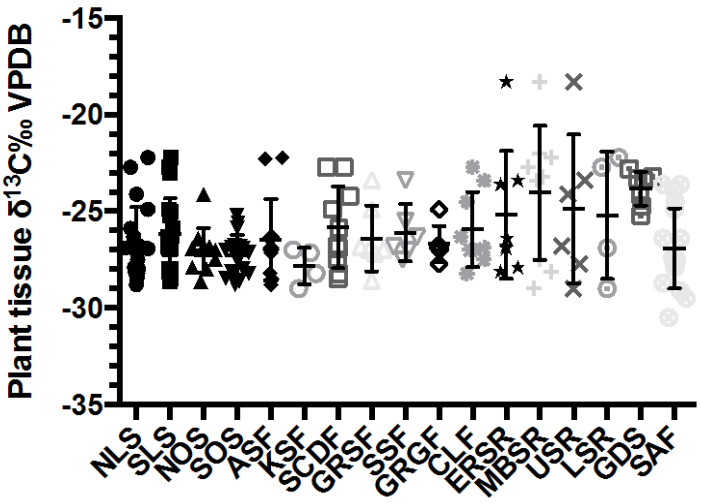

Figure 2.7. $\delta^{13}C_{plant}$ values available in the literature for C_3 plants, by vegetation community. Key to veg community codes: NLS = North Langeberg Sandstone Fynbos; SLS = South Langeberg Sandstone Fynbos; NOS = North Outeniqua Sandstone Fynbos; SOS = South Outeniqua Sandstone Fynbos; ASF = Albertinia Sand Fynbos; KSF = Knysna Sand Fynbos; SCDF = Southern Cape Dune Fynbos; GRSF = Garden Route Shale Fynbos; SSF = Swellendam Shale Fynbos; GRGF = Garden Route Granite Fynbos; CLF = Canca Limestone Fynbos; ERSR= Eastern Ruens Shale Renosterveld; MBSR = Mossel Bay Shale Renosterveld; USR = Uniondale Shale Renosterveld; LSR = Langkloof Shale Renosterveld; GDS = Grootbrak Dune Strandveld; SAF = Southern Afromontaine Forest.

At least with regard to the data available in the GSCIMS data set, C_3 plants with higher $\delta^{13}C_{tissue}$ values appear to be absent from the Knysna Sand Fynbos. Graminoids were overrepresented in the stable carbon metadata set for this vegetation community, and given the comparably lower $\delta^{13}C_{tissue}$ values for *Restio* and true C_3 grasses relative to shrubs and bushes in the GCFR (Figure 2.2), it is possible that this truncation of the range of C_3 $\delta^{13}C_{plant}$ values in the Knysna Sand Fynbos is an artifact of poor taxonomic coverage by GSCIMS. *Protea* and *Leucadendron* shrubs are however present in this vegetation type, and both are quite depleted in ^{13}C.

Conversely, the GSCIMS taxonomic coverage of the Grootbrak Dune Strandveld does not miss major categories of plants. While the $\delta^{13}C_{tissue}$ values of the common C_3 grass genera (*Ehrhata*, *Ficinia*, and *Stipa*) are not available for the GCFR, there are no *Restio* taxa present, and the non-grass C_3 taxa that are the most depleted in ^{13}C (e.g. *Protea*, large trees, Table 2.18) are absent from the Grootbrak Dune Strandveld (see Rebelo *et al.*, 2006). Thus, although it could be possible for grazing taxa in the Grootbrak Dune Strandveld to have lower $\delta^{13}C$ tissue values if the C_3 grasses turn out to be quite depleted, provisionally there is no source vegetation for browsing taxa that is lower than -25.2‰ VPDB (e.g. consumer $\delta^{13}C_{enamel}$ values could be no lower than about -12‰).

Although GCFR vegetation communities are often described as "primarily C_3" (in part because of their relative 'shrubby'ness, and in part because of the higher frequency of C_3 grasses present in GCFR vegetation communities than found in summer rainfall regions (Vogel *et al.*, 1978)), C_4 grass occurs in almost all of the 17 vegetation communities surveyed here. The major exception is the Southern Afrotemperate Forest

vegetation, which appears to have an understory composed of only C_3 plant genera (Table 2.20; Rebelo *et al.,* 2006). Thus, primary consumers obtaining their diet entirely within the Knysna Forests, for example, will have $\delta^{13}C_{tissue}$ values that reflect a pure C_3 diet, as C_4 grasses are not present.

For most fynbos vegetation communities (with the exception of the comparably small region discussed in Cowling, 1983), there is only broad categorical information about the relative frequency of C_3 versus C_4 grasses (e.g. Vogel *et al.,* 1978), and the only available data for most vegetation units is the species richness of grass genera. This is not an ideal proxy, as the grassy understory of vegetation communities may be speciose yet dominated by a single taxon. At the same time, the relative frequency of C_4 grass taxa in a given vegetation unit does have an impact on the amount of available vegetative biomass that is enriched in ^{13}C. Using the taxonomic lists from Rebelo *et al.*, (2006), counts of C_3 and C_4 graminoid taxa (including *Restio*) in each of the 17 surveyed vegetation communities were tallied (Table 2.21).

Per the literature, C_4 grasses are absent not only from the Southern Afrotemperate Forest, but from the Canca Limestone Fynbos and the Southern Cape Dune Fynbos. Assuming that C_4 grasses are in fact absent from these vegetation communities, fauna consuming only flora from any of these vegetation communities should have $\delta^{13}C_{tisse}$ values that reflect pure C_3 vegetation. Non-C_3 $\delta^{13}C_{fauna}$ values would indicate consumption of CAM/FCAM plants only, or in the case of the Southern Afrotemperate forest, that the animals were non-local.

Conversely, C_4 grasses are comparably quite speciose in the renosterveld communities of the south coast, and as well as in the Knysna Sand Fynbos, in the Grootbrak Dune Strandveld, and the Garden Route Shale Fynbos (Table 2.21). This increased speciosity of C_4 grasses in these vegetation communities should be reflected in comparably higher $\delta^{13}C_{tissue}$ values of grass consumers in the renosterveld, strandveld and shale fynbos regions, and significantly lower $\delta^{13}C_{tissue}$ values in grass feeders from the Afrotemperate Forest or the Canca Limestone Fynbos vegetation communities.

Aggregation from the literature of the available plant stable carbon isotope data for GCFR floral taxa thus provides a necessary framework to interpret the dietary signals contained in the $\delta^{13}C_{tissue}$ values of modern fauna from the region. This modern faunal data can in turn then be used to contextualize and interpret stable carbon isotope data from fossil specimens, which are abundant in South Africa.

Vegetation Community	C_3 grass taxa n	% C_3 of total	C_4 grass taxa n	% C_4 of total
North Langeberg Sandstone Fynbos	63	98.4%	1	1.6%
South Langeberg Sandstone Fynbos	32	91.4%	3	8.6%
North Outeniqua Sandstone Fynbos	9	69.2%	4	30.8%
South Outeniqua Sandstone Fynbos	42	95.5%	2	4.5%
Albertinia Sand Fynbos	13	92.9%	1	7.1%
Knysna Sand Fynbos	4	36.4%	7	63.6%
Southern Cape Dune Fynbos	8	100.0%	0	0.0%
Garden Route Shale Fynbos	4	40.0%	6	60.0%
Swellendam Silcrete Fynbos	6	54.5%	5	45.5%
Garden Route Granite Fynbos	4	50.0%	4	50.0%
Canca Limestone Fynbos	8	100.0%	0	0.0%
Eastern Ruens Shale Renosterveld	7	70.0%	3	30.0%
Mossel Bay Shale Renosterveld	4	57.1%	3	42.9%
Uniondale Shale Renosterveld	2	66.7%	1	33.3%
Langkloof Shale Renosterveld	6	54.5%	5	45.5%
Grootbrak Dune Strandveld	3	60.0%	2	40.0%
Southern Afrotemperate Forest	1	100.0%	0	0.0%

Table 2.21. Absolute counts of grass taxa and relative frequency of C_3 and C_4 grass taxa in each vegetation unit. Data compiled from Rebelo *et al.* (2006).

Chapter 2 References:

Agenbag, L. (2006). A Study on an altitudinal gradient investigating the potential effects of climate change on Fynbos and the Fynbos Succulent Karoo Boundary Masters Thesis, University of Stellenbosch.

AGIS. (2007). "Agricultural Geo-Referenced Information System." Retrieved Jan, 2015, from http://www.agisagric.za.

Araya, Y. N., J. Silvertown, D. J. Gowing, K. McConway, P. Linder and G. Midgley (2010). "Variation in $\delta^{13}C$ among species and sexes in the family Restionaceae along a fine-scale hydrological gradient." Austral Ecology **35**(7): 818-824.

Boom, A., A. S. Carr, B. M. Chase, H. L. Grimes and M. E. Meadows (2014). "Leaf wax n-alkanes and δ13C values of CAM plants from arid southwest Africa." Organic Geochemistry **67**: 99-102.

Carr, A. S., A. Boom, H. L. Grimes, B. M. Chase, M. E. Meadows and A. Harris (2014). "Leaf wax n-alkane distributions in arid zone South African flora: environmental controls, chemotaxonomy and palaeoecological implications." Organic Geochemistry **67**: 72-84.

Cerling, T. E. and J. M. Harris (1999). "Carbon isotope fractionation between diet and bioapatite in ungulate mammals and implications for ecological and paleoecological studies." Oecologia **120**(3): 347-363.

Cerling, T. E., J. M. Harris and B. H. Passey (2003). "Diets of East African Bovidae based on stable isotope analysis." Journal of Mammalogy **84**(2): 456-470.

Cerling, T. E., J. A. Hart and T. B. Hart (2004). "Stable isotope ecology in the Ituri Forest." Oecologia **138**(1): 5-12.

Codron, J., D. Codron, J. A. Lee-Thorp, M. Sponheimer, W. J. Bond, D. de Ruiter and R. Grant (2005). "Taxonomic, anatomical, and spatio-temporal variations in the stable carbon and nitrogen isotopic compositions of plants from an African savanna." Journal of Archaeological Science **32**(12): 1757-1772.

Cowling, R. and D. Richardson (1995). Fynbos: South Africa's Unique Floral Kingdom. Cape Town, University of Cape Town Press.

Cowling, R., D. Richardson and P. Mustart (1997). Fynbos. Vegetation of Southern Africa. R. M. Cowling, D. M. Richardson and S. M. Pierce. Cambridge, Cambridge University Press.

Cowling, R. M. (1983). "The occurrence of C_3 and C_4 grasses in fynbos and allied shrublands in the South Eastern Cape, South Africa." Oecologia **58**(1): 121-127.

Cowling, R. M. (1992). The Ecology of Fynbos: Nutrients, Fire and Diversity. Cape Town, Oxford.

Farquhar, G., M. O'Leary and J. Berry (1982). "On the Relationship Between Carbon Isotope Discrimination and the Intercellular Carbon Dioxide Concentration in Leaves." Functional Plant Biology **9**(2): 121-137.

Farquhar, G. D., J. R. Ehleringer and K. T. Hubick (1989). "Carbon isotope descrimination and photosynthesis." Annual Review of Plant Physiology and Plant Molecular Biology **40**: 503-537.

Flanagan, L. B., J. R. Brooks, G. T. Varney, S. C. Berry and J. R. Ehleringer (1996). "Carbon isotope discrimination during photosynthesis and the isotope ratio of respired CO_2 in boreal forest ecosystems." Global Biogeochemical Cycles **10**(4): 629-640.

Heaton, T. H. E. (1999). "Spatial, Species, and Temporal Variations in the $^{13}C/^{12}C$ Ratios of C_3 Plants: Implications for Palaeodiet Studies." Journal of Archaeological Science **26**(6): 637-649.

Hoare, D. B., L. Mucina, M. C. Rutherford, J. H. J. Vlok, D. I. W. Euston-Brown, A. R. Palmer, . . . R. A. Ward (2006). Albany Thicket Biome. The Vegetation of South Africa, Lesotho, and Swaziland. Pretoria, South African National Biodiversity Institute**:** 540-567.

Kohn, M. J. (2010). "Carbon isotope compositions of terrestrial C_3 plants as indicators of (paleo)ecology and (paleo)climate." Proceedings of the National Academy of Sciences of the United States of America **107**(46): 19691-19695.

Körner, C., G. D. Farquhar and S. C. Wong (1991). "Carbon isotope discrimination by plants follows latitudinal and altitudinal trends." Oecologia **88**(1): 30-40.

Latimer, A. M., J. A. Silander Jr, A. G. Rebelo and G. F. Midgley (2009). "Experimental biogeography: the role of environmental gradients in high geographic diversity in Cape Proteaceae." Oecologia **160**(1): 151-162.

Llorens, L., J. Peñuelas and M. Estiarte (2003a). "Ecophysiological responses of two Mediterranean shrubs, Erica multiflora and Globularia alypum, to experimentally drier and warmer conditions." Physiologia Plantarum **119**(2): 231-243.

Llorens, L., J. Penuelas and I. Filella (2003b). "Diurnal and seasonal variations in the photosynthetic performance and water relations of two co-occurring

Mediterranean shrubs, Erica multiflora and Globularia alypum." Physiologia Plantarum **118**(1): 84-95.

Lötter, D., E. A. van Garderen, M. Tadross and A. J. Valentine (2014). "Seasonal variation in the nitrogen nutrition and carbon assimilation in wild and cultivated Aspalathus linearis (rooibos tea)." Australian Journal of Botany **62**(1): 65-73.

Milton, S., R. Yeaton, W. Dean and J. Vlok (1997). "Succulent karoo." Vegetation of southern Africa **649**.

Mooney, H. A., J. H. Troughton and J. A. Berry (1977). "Carbon isotope ratio measurements of succulent plants in southern Africa." Oecologia **30**(4): 295-305.

O'Leary, M. H. (1988). "Carbon isotopes in photosynthesis." BioScience: 328-336.

Rebelo, A. G., C. Boucher, N. Helme, L. Mucina and M. C. Rutherford (2006). Fynbos Biome. The Vegetation of South Africa, Lesotho, and Swaziland. Pretoria, South African National Biodiversity Institute**:** 52-219..

Reinecke, M. K. (2013). Links between lateral riparian vegetation zones and flow. PhD, Stellenbosch University.

Rohatgi, A. (2010). "WebPlotDigitizer." 3.6. 2014, from http://arohatgi.info/WebPlotDigitizer.

Rundel, P. W., Esler, K. J., & Cowling, R. M. (1999). “Ecological and phylogenetic patterns of carbon isotope discrimination in the winter-rainfall flora of the Richtersveld, South Africa”. Plant Ecology, **142**(1-2), 133-148

Saura, A., S. Mas and F. Lloret (2010). "Foliar stable carbon and nitrogen isotopes in woody Mediterranean species with different life form and post-fire regeneration." Plant Biology **12**(1): 125-133.

Schulze, E. D., R. Ellis, W. Schulze, P. Trimborn and H. Ziegler (1996). "Diversity, metabolic types and $\delta^{13}C$ carbon isotope ratios in the grass flora of Namibia in relation to growth form, precipitation and habitat conditions." Oecologia **106**(3): 352-369.

Sealy, J. C. and N. J. Van der Merwe (1986). "Isotope Assessment and the Seasonal-Mobility Hypothesis in the Southwestern Cape of South Africa [and Comments and Replies]." Current Anthropology: 135-150.

Stewart, G. R., M. H. Turnbull, S. Schmidt and P. D. Erskine (1995). "^{13}C natural abundance in plant communities along a rainfall gradient: a biological integrator of water availability." Functional Plant Biology **22**(1): 51-55.

Swap, R. J., J. N. Aranibar, P. R. Dowty, W. P. Gilhooly and S. A. Macko (2004). "Natural abundance of ^{13}C and ^{15}N in C_3 and C_4 vegetation of southern Africa: patterns and implications." Global Change Biology **10**(3): 350-358.

Tieszen, L. L., M. M. Senyimba, K. I. Simeon and J. H. Troughton (1979). "The Distribution of C_3 and C_4 Grasses and Carbon Isotope Discrimination along an Altitudinal and Moisture Gradient in Kenya." Oecologia **37**(3): 337-350.

Van den Heuvel, I. M. and J. J. Midgley (2014). "Towards an isotope ecology of Cape Fynbos small mammals." African Zoology **49**(2): 195-202.

Vogel, J. C. (1978). Recycling of carbon in a forest environment, Oecologia Plantarum **13:** 89-94.

Vogel, J. C., A. Fuls and R. P. Ellis (1978). "The geographical distribution of Kranz grasses in South Africa." South African Journal of Science **74**: 209-215.

Weiguo, L., F. Xiahong, N. Youfeng, Z. Qingle, C. Yunning and A. N. Zhisheng (2005). "$\delta^{13}C$ variation of C_3 and C_4 plants across an Asian monsoon rainfall gradient in arid northwestern China." Global Change Biology **11**(7): 1094-1100.

Werner, C. and C. Maguas (2010). "Carbon isotope discrimination as a tracer of functional traits in a Mediterranean macchia plant community." Functional Plant Biology **37**(5): 467-477.

West, A. G., J. J. Midgley and W. J. Bond (2001). "The evaluation of $\delta^{13}C$ isotopes of trees to determine past regeneration environments." Forest Ecology and Management **147**(2): 139-149.

3. Isotope Ecology of the modern Greater Cape Floristic Region: the modern micromammal record, with particular attention to new Pinnacle-Point Area-proximate data.

Introduction

The best contextual data for interpreting ancient stable isotope records is isotope data from modern specimens belonging to the same taxonomic groups. Micromammal data is increasingly being collected by researchers studying the isotope ecology of many communities (e.g. Thackeray *et* al., 2003; Hopley *et al.* 2006; Robb *et al.*, 2012; Symes *et al.*, 2013; Van den Heuvel and Midgley, 2014; Codron *et al.* 2015), including those found within the confines of the GCFR. This section summarizes the modern microfaunal stable isotope records available for the region, and presents new data generated from samples of populations of micromammals from different vegetation contexts along the south coast of South Africa.

Modern Micromammals

The isotopic ecology of micromammals is a small but growing transdisciplinary field. Many recent isotopic studies of modern rodent communities use hair clippings as the sample material (Robb *et al.*, 2012; Symes *et al.*, 2013; Van den Heuvel and Midgley, 2014; Codron *et al.*, 2015) This is logistically convenient for researchers, as it enables live-trapping of small mammals rather than sacrifice of individuals, but more importantly, isotopic hair analysis yields carbon, nitrogen, oxygen, and hydrogen stable

isotope data (depending on the analytical method used). Having access to these four isotope systems allow workers to investigate a multiplicity of research questions including but not limited to diet (carbon and nitrogen); trophic position (nitrogen and hydrogen); water use and respiration (oxygen and hydrogen); and plant-part consumption (carbon and oxygen). It also allows for the use of more sophisticated dietary mixing models (Phillips *et al.,* 2014) in modern ecological studies.

This reliance on hair provides no difficulties then for workers investigating the isotopic ecology of single modern micromammal taxa or of small mammal communities, but it becomes quickly problematic for workers looking to translate this isotopic ecology into the paleoenvironmental arena. Analysis of fossil micromammal specimens must be singularly reliant upon enamel, as it is the only tissue suitable for analysis of biogenic isotope ratios that is preserved relatively unaltered through time and across depositional environments (Lee-Thorp and Van Der Merwe, 1987; Lee-Thorp, 1989; Wang and Cerling, 1994; Kohn *et al.,* 1999; Sponheimer and Lee-Thorp, 1999; Hedges, 2002; Lee-Thorp, 2002). Bone apatite is likely to be suitable for analysis of modern and peri-modern specimens, although even modern specimens from *Bubo sp.* pellets in East Africa show some chemical alteration of the mineral matrix of bone (Dauphin *et al.,* 2003), and the small size of postcranial remains decreases the thickness of cortical bones, exposing more relative depth of the tissue to diagenetic processes.

Enamel's chemical structure limits the light stable isotope systems available for analysis to two (carbon and oxygen). Previous enamel stable isotope data obtained from modern micromammal specimens from various areas of the world was primarily limited to oxygen isotope data ($\delta^{18}O_p$) obtained from the phosphate group of hydroxyapatite; the

$\delta^{18}O_p$ data is often generated from micromammals to examine the relationship between $\delta^{18}O_p$ and local meteoric water (e.g Lindars *et al.,* 2001; Longinelli *et al.,* 2003; Navarro *et al.,* 2004; Royer *et al.,* 2013). Isotopic analysis of the carbonate phase of enamel apatite in both fossil and modern micromammals had been relatively rare until very recently, likely due to the difficulty in obtaining sufficient powdered enamel for phosphoric acid digestion (the 'conventional' chemical method for producing carbon and oxygen isotope data) and/or the relatively late development of *in situ* sampling techniques that targeted carbon (Cerling and Sharp, 1996; Sharp and Cerling, 1996; Passey and Cerling, 2006). This is especially true in the case of fossils, where obtaining enamel from very small specimens without complete destruction of the sample was difficult: indeed a number of the various fossil taxa that had been sampled for carbon and oxygen and reported in the literature are more rightly classified as "small mammals" rather than "micromammals" (e.g. pocket gophers analysed by Rogers and Wang, 2002; the fossil lagomorphs in Tutken *et al.,* 2006; fossil Cryptomys data reported by Yeakel *et al.,* 2007) and are more easily mechanically sampled than the smaller murine rodents.

As a result, study of the isotope ecology and isotope niches of micromammals is in its infancy, and for many taxa, there are significant questions that need to be resolved. This is especially true for researchers aiming to use micromammal stable isotope values to investigate past environmental changes, who need to know, as a baseline, whether the isotopic composition of a taxon's diet will change over vegetative space, or whether rodent dietary niches are so strictly partitioned that a given taxon will always consume vegetation with a comparably narrow range of $\delta^{13}C$.

Assessing this can be approached in two ways: first, by selection of sample taxa that are both generalists in their habitat preferences and non-specific in their diets (e.g. they are not dietary specialists focused on the seeds of a specific plant genus), and second, via the acquisition of $\delta^{13}C_{micromammal}$ data from a number of modern vegetation communities whose isotopic compositions are known to vary. Thus for example, taxa known to be gramnivores should sample, as a population, the range of grass types available in a given vegetation community. If the vegetation community is comprised of pure C_4 grasses the carbon isotope ratio data from the micromammalian taxon should also indicate "pure C_4" diets; the $\delta^{13}C_{tissue}$ values of that same taxon however, when sampled from a C_3 grass dominated vegetation community will reflect a strong C_3 dietary component.

For southern Africa, the only published study that explicitly samples the same micromammal taxon across a wide range of modern vegetation communities is Thackeray *et al.* (2003), in which specimens of the Namaqua Rat Mouse (*Aethomys namaquensis,* also sometimes attributed to the genus *Michaelamys*) were sampled along a SW-NE transect across the entire sub-continent. *A. namaquensis* is primarily a grass feeder, although it does consume leaves and seeds (Kesner *et al.*, 2013). Given the changing frequencies of C_3 and C_4 grasses across that range, it was expected that 1) the $\delta^{13}C_{tissue}$ values of *A. namaquensis* will change across space over that range and 2) that $\delta^{13}C_{tissue}$ values will vary in a way that reflects changing percentages of C_3 and C_4 flora in the vegetation communities across that transect. This is broadly the pattern seen in the results from Thackeray *et al.* (2003), with the lowest values of *A. namaquensis* $\delta^{13}C$ found in the Western Cape, and the highest $\delta^{13}C$ values occurring in specimens from

areas that have significant C_4 input into the vegetation biomass. This variability in $\delta^{13}C_{tissue}$ values in *A. namaquensis* occurs across biogeographic vegetative space (Thackeray *et al.*, 2003), in spite of the fact that on smaller geographic scales Codron *et al.* (2015) found no difference in median $\delta^{13}C_{hair}$ values between *A. namaquensis* from wooded and grassveld habitats in the Cradle Nature Reserve.

The work by Thackeray *et al.* (2003) is proof-of-concept for the idea that although the niche partitioning within micromammal communities at given localities may be relatively stable (Codron *et al.*, 2015), the stable carbon isotope values of generalist herbivorous micromammals will vary across changing vegetative isoscapes. Problematically, there are not yet similar studies for other micromammal taxa, nor have researchers yet begun to explore intra-specific $\delta^{13}C_{tissue}$ variation across different vegetation communities within the GCFR. What does exist in the literature are stable carbon isotope values obtained from a number of different micromammal taxa at specific localities both within and outside of the GCFR as part of localized isotope ecology research (Appendix B).

None of the published modern micromammal $\delta^{13}C$ data comes from specimens from the vicinity of Pinnacle Point. Furthermore, the one taxon, *A. namaquensis*, which is explicitly known to vary across changing vegetation communities is comparably rare in the Pinnacle Point fossil assemblages (Matthews *et al.*, 2009; Matthews *et al.*, 2011; Matthews, n.d.). In order to provide modern contextual stable carbon and oxygen isotope data for micromammals from the Pinnacle Point region, modern micromammal specimens from four species and three collection localities were analyzed for carbon and oxygen isotopes. This data is then compared to published $\delta^{13}C$ values for the same taxa

from other regions of South Africa, and to predicted carbon isotopic ratios found in the local vegetation communities from which they were sampled.

Description of Taxa Chosen For Sampling

Micromammal communities tend to be speciose, although the taxonomic composition of micromammal communities varies based on changing ecological and climatic conditions (Avery, 1982; Thackeray, 1987; Avery, 1988; Cuenca Bescos, 2003; Reed, 2003; Matthews, 2004). Some taxa that have specific habitat preferences are thus restricted in time and space; other taxa are more 'catholic' in their habit preferences and have broad geographic distributions and/or occur throughout long temporal sequences.

Specific criteria were developed for selecting both modern and fossil micromammal taxa for isotopic analysis for this study. A species must have a cosmopolitan distribution throughout South Africa, or minimally within large areas of the modern GCFR.

1. The species must be non-specific in some aspect of its habitat preference, such that it inhabits a broad range of modern vegetation communities. The first and second criteria together ensure that taxa will be locally persistent even in changing ecological conditions.
2. The approximate diet of a given species is known, and that within the broad constraints of its feeding behavior it is not a specialist feeder. This criterion allows for selected taxa to be, for example, grass feeders, as long as there is no known

preference for specific grass taxa only, or to be consumers of geophytes if it shows no preference for specific geophytic types.

3. Micromammal species must be herbivorous. This significantly restricts the pool of available micromammal genera available for sampling, but is important for a number of reasons. These include: A) Diet-to-tissue offsets will be more consistent across taxa than when comparing taxa occupying different trophic niches. The isotopic composition of dietary protein and the bulk diet should also be similar, thus minimizing the impact of tissue-specific routing. B) There is trophic fractionation of carbon and oxygen, but the diet-tissue offsets of insects is not well characterized for South African ecosystems. Thus the relationship between $\delta^{13}C_{insectivore}$ and $\delta^{13}C_{plant}$ values is more complex. C) In omnivorous diets, diet-to-tissue offsets are partially dependent upon concentration-dependent mixing (Phillips and Koch, 2002). When plant foods (with high ratio of C:N) form a small portion of a diet compared to animal food (with a low C:N ratio), the isotopic signal of food concentrated in carbon may swamp the signal of low-carbon food, even when it makes up only a small and possibly geo-temporally restricted portion of the diet (Phillips and Koch, 2002). Excluding insectivores from the analysis and including only herbivorous taxa produces a simpler and somewhat more straightforward vegetation proxy.

4. Species or genera selected for analysis must not be rare in the Pinnacle Point fossil assemblages. This criterion allows for intra-specific analysis of changing $\delta^{13}C_{diet}$ values through time at a fixed geographic point. Since, within a given vegetation community, different micromammal taxa may differentially sample the range of

available $\delta^{13}C_{plant\ tissue}$ values, comparing only intra specific values through time or across space controls for niche-partitioning and other ecological factors.

Four modern taxa from three genera were determined to meet these criteria, and were sampled for stable carbon and oxygen isotope analysis.

Bathyergus suillus

The Cape Dune Mole Rat (*B. suillus*) is a terrestrial burrowing rodent whose current distribution is limited to the southwestern coast of the Cape of South Africa (Skinner and Chimimba, 2005; Maree *et al*., 2008). Adult individuals weigh between 670g and 900g (Skinner and Chimimba, 2005). The genus *Bathyergus* is at least early Miocene in age and is found in the Mio-Pliocene Langebaanweg fossil deposits in the Western Cape (Matthews, 2004). *B. suillus* is herbivorous and its diet consists primarily of geophytes (Bennett and Faulkes, 2000), as well as aboveground vegetation that is pulled into the burrows from below (Jarvis, 2013). Stable carbon isotopic composition of *B. suillus* tissues is expected to reflect the $\delta^{13}C$ values of geophytic and graminoid taxa within a given vegetation community. *B. suillus* are a water-independent taxon that obtains H_2O from consumed plant material (Bennett and Faulkes, 2000); as such $\delta^{18}O_{tissue}$ values will reflect the oxygen isotopic composition of consumed plant material, rather than meteoric water.

Gerbilliscus afra

The Cape Gerbil (*G. afra*) has a modern distribution throughout the southwestern Cape (Granjon and Dempster, 2013). *G. afra* does not occur in the Mio-Pliocene deposits at Langebaanweg (Matthews, 2004), but is common in Middle Pleistocene fossil assemblages in the Western Cape (Matthews, 2004; Matthews *et al.*, 2005). It has a diet similar to that of *B. suillus*, and consumes grasses, bulbs and roots (Skinner and Chimimba, 2005; Granjon and Dempster, 2013); as such the $\delta^{13}C_{tissue}$ values for this taxon should reflect an admixture of the underground storage organ (USO) component of the diet and the C_3/C_4 fraction of graminoid floral taxa.

Otomys irroratus

The Southern African Vlei Rat (*O. irroratus*) has a present-day distribution throughout the GCFR and into the north eastern veld and savanna environments of South Africa (Taylor, 2013); generic *Otomys* specimens occur in South African Pliocene deposits (Skinner and Chimimba, 2005; Taylor, 2013), and the taxon is common throughout the Pinnacle Point deposits (Matthews *et al.*, 2009; Matthews *et al.*, 2011; Matthews, n.d.). *O. irroratus* is a preferential grass feeder, although it also consumes herbaceous plants (Taylor, 2013). $\delta^{13}C_{tissue}$ values of *O. irroratus* should primary reflect the relative frequency of C_3 and C_4 graminoids in the diet, with a small component of other foliage included.

Otomys saundersiae

Saunder's Vlei Rat (*Otomys saundersiae*) has a somewhat more restricted modern range than *O. irroratus* (Taylor, 2013). Less is known about its diet, but the Otomyinae as a group have a dentition specialized for grass feeding, and *O. saundersiae* has a general habitat preference for grassy or *Restio*-dominated vegetation (De Graaff, 1981; Taylor, 2013). *O. saundersiae* diets are therefore likely to be similar to those of *O. irroratus*, and $\delta^{13}C_{tissue}$ data from this taxon should primarily reflect the relative contribution of C_4 plants to the grassy or graminoid component of local plant communities.

It should be noted that none of the micromammalian taxa sampled have known diets that include CAM or FCAM vegetation (unless there are tuberous succulents on the landscape such as *Bulbine caulescens*, in which case a small proportion of the diet of *G. afra* or *B. suillus* might include a CAM signal). The general lack of dietary CAM in the sampled taxon provides the added benefit of end-member $\delta^{13}C$ separation, with a 13.5‰ VPDB difference between the C_3 and C_4 dietary components.

Modern Specimen Sampling Localities

Modern micromammal specimens sampled for isotopic analysis derive from three sampling localities, all along the south coast of South Africa, and all less then 70km from Pinnacle Point.

Rein's Nature Reserve is located near the coast approximately 37 km southwest of Pinnacle Point (Figure 3.1). The collection locality is a private nature reserve located primarily on Canca Limestone Fynbos, which is described as 'uncontaminated' by alien vegetation (Matthews, personal communication). Micromammal specimens derive from Spotted Eagle Owl (*Bubo africanus*) pellets collected by T. Matthews approximately 10m from a nesting site. Strandveld and Albertinia Sand Fynbos vegetation both occur less than 3km from the collection locality.

The Amisrus (Island Lake, Wilderness) specimens derive from collections made by T. Matthews, N. Baker, and J. Sharples in January and June of 2006 near a barn owl (*Tyto Alba*) roost site. The collection locality is surrounded by Southern Afrotemperate Forests (Matthews, personal communication), and is less than 3km from occurrences of Southern Cape Dune Fynbos and Garden Route Shale Fynbos (Figure 3.2).

The Wolwe River specimens were collected in 1984 by Cape Nature. The collection locality has been approximated, but vegetation in the area is predominantly either Southern Cape Dune Fynbos, or Knysna Sand Fynbos (Figure 3.2). Some stands of Southern Afrotemperate Forest occur within 3km of the site. Micromammal specimens were derived from African Grass Owl (*Tyto capensis*) pellets.

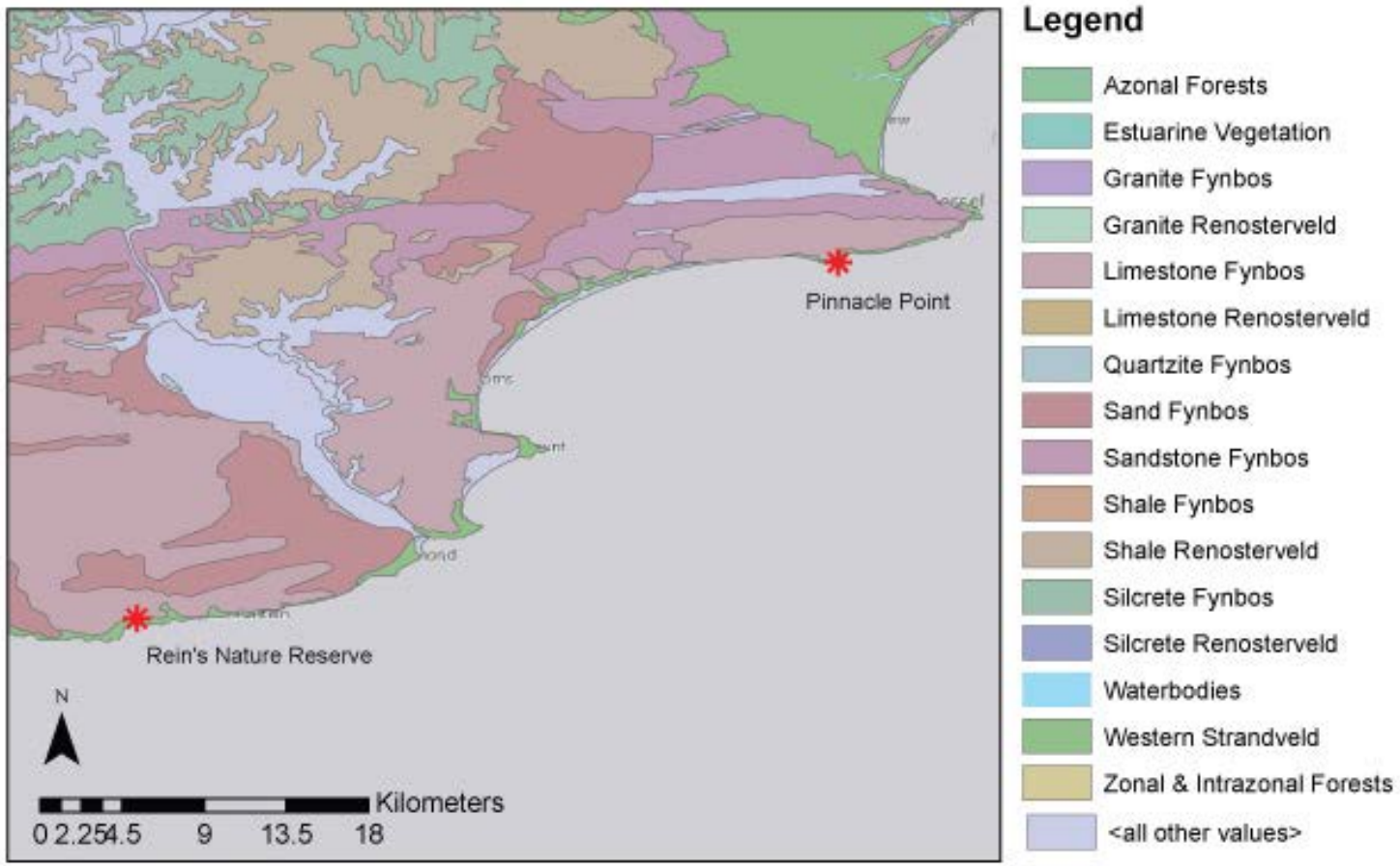

Figure 3.1. Location of the modern micromammal sampling locality Rein's Nature Reserve, relative to Pinnacle Point. Vegetation distribution data from Mucina and Rutherford (2006).

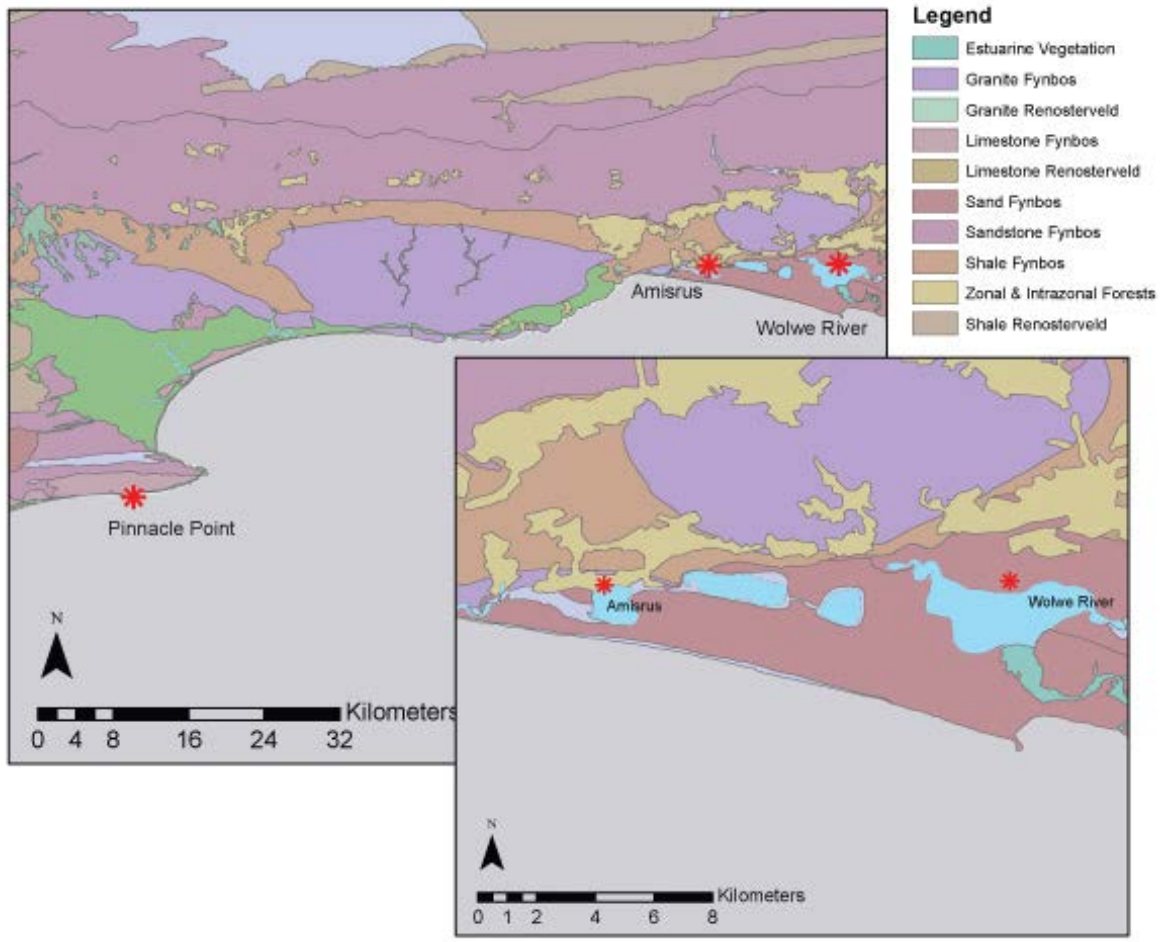

Figure 3.2. Locations of the modern micromammal sampling localities Amisrus, Wilderness, and Wolwe River, relative to Pinnacle Point. Inset: zoomed in view of sampling localities, with vegetation community types more visible due to scale. Vegetation distribution data from Mucina and Rutherford (2006).

Materials and Methods

Specimen Selection, Sampling, and Pretreatment:

Modern specimens were visually examined prior to isotope analysis, and specimens that were significantly discolored or otherwise appeared altered were not sampled.

Enamel apatite was obtained by mechanical sampling of unaltered posterior teeth (*O. irroratus* and *O. saundersiae*) or well-mineralized erupted portions of incisor teeth (*G. afra* and *B. suillus*). All cleaning and pre-treatment of modern micromammal materials was performed at the Archaeological Chemistry Laboratory, Arizona State University (ASU). Fifteen specimens from Amisrus, 12 specimens from Wolwe River, and 10 specimens from Rein's Nature Reserve were selected for analysis (Table 24).

Prior to sampling, all specimens were sonicated in individual baths of 18.2 Ω H_2O and allowed to air dry. Specimens were then mechanically cleaned using a Dremel Minimite hand drill equipped with a carbide dental burr. Once cleaned, teeth from micromammal specimens from Amisrus and Wolwe River were extracted from the dental arcade to avoid accidental "clipping" of the alveolar bone with the drill during sampling. Teeth from individual specimens were then mechanically sampled using the Dremel hand drill, and carbide burrs were switched out between individual specimens to avoid cross-contamination. In most cases, it was impossible to obtain sufficient enamel from individual teeth using this drilling method; therefore powder from multiple posterior teeth from individual specimens was aggregated into bulk enamel samples for most of the micromammal specimens from Amisrus and Wolwe River.

Cleaned micromammal specimens from Rein's Nature Reserve were also extracted from the dental arcade, but were mechanically processed in a different manner from the Amisrus and the Wolwe River specimens. Individual posterior tooth specimens were placed into an agate mortar and briefly smashed (not ground) with the agate pestle to produce large fragments, which separated enamel shards from the tooth. Shards of enamel were then separated from dentine underneath a light microscope. The enamel shards were then returned to a clean agate mortar and ground to a fine powder with the pestle. Agate mortar and pestle were thoroughly cleaned between specimens using 18.2 MΩ H_2O and dried with KimWipes.

Enamel powders produced by both sampling methods underwent chemical pretreatment to remove remaining organic material and any possible adhering secondary carbonates (Nielsen-Marsh and Hedges, 2000). Powdered specimen enamel was weighed and placed into new 2.0 mL centrifuge tubes. All tubes were marked with the specimen identification number, a sample number, and the weight of enamel power (in mg). To remove organic contaminants from the sample powder, 0.04 mL 2% NaOCL per mg enamel powder was pipetted into each specimen tube, and enamel specimens were soaked for 24 hours. Specimen tubes were then centrifuged, the NaOCL solution was decanted, and enamel powders were each rinsed 3x in 0.50 mL 18.2 MΩ H_2O. In order to remove any non-structural carbonate from the enamel powder, 0.04ml of 0.1 molar CH_3COOH per mg enamel was pipetted into each specimen tube. Samples were allowed to react for 24 hours, centrifuged, and the CH_3COOH solution was decanted. Specimens were then rinsed 3 more times in 0.50 mL 18.2 MΩ H_2O, and kept in a 50°C laboratory oven until dry (ACL internal laboratory procedures, Knudson n.d.).

Instrumentation

Instrumentation for the Amisrus and Wolwe River modern micromammal specimens was performed at the W.M. Keck Foundation Laboratory for Environmental Biogeochemistry at ASU using a Thermo Delta Plus Advantage mass spectrometer. Samples were introduced to the IRMS via a Gas Bench system. Following the procedures outlined by Michaud *et al.* (2007), specimen powder was weighed into vials; specimen vials were then flushed with He to remove atmospheric contamination (in particular atmospheric CO_2). Samples were then reacted with >100% H_3PO_4 at 70°C for a minimum of 6 hours prior to introduction into the mass spectrometer. The long reaction time was necessary to ensure complete evolution of sample CO_2 and to avoid fractionation due to incomplete reaction. $\delta^{13}C$ and $\delta^{18}O$ data points output by instrumentation are normalized to VPDB (Michaud, 2007).

Given the low CO_3% by weight in enamel apatites (Koch *et al.,* 1997), in order to evolve sufficient CO_2 via phosphoric acid reaction to produce accurate and/or replicable stable carbon and oxygen isotope ratio measurements, the minimum sample size by weight for the gas bench introduction system was ~5mg (Michaud, personal communication). It was difficult to produce enamel samples of this size from the comparably small micromammal teeth without aggregating multiple posterior teeth, and it was clear this analytical method would not work at all for fossil material, as it resulted in the complete destruction of the greater part of the posterior dentition of a specimen.

In order to reduce the sample size for the remaining modern specimens, the enamel powder obtained from the Rein's micromammals was sent to the Environmental Isotope Laboratory at the University of Arizona (UofA) for analysis. The introduction

system at the UofA is a Kiel III carbonate device; use of the Kiel III device significantly reduces the necessary powdered carbonate or enamel sample size (Thermo Finnigan, 2002). Specific information regarding the analytical procedures and precision of the isotope measurements at the UofA Environmental Isotope Lab can be found at http://www.geo.arizona.edu/node/153.

Stable carbon and oxygen isotope ratio measurements were successfully obtained from 27 modern specimens from sampling localities proximate to Pinnacle Point (Table 3.1). All stable isotope ratios are reported using delta notation (δ):

$$\delta = \left(\frac{R_{sample} - R_{standard}}{R_{standard}}\right) * 1000 \qquad R = \frac{^{heavy}X}{^{light}X}$$

where R is the measured ratio of the heavy to light isotope, R_{sample} is the measured ratio in the sample, and $R_{standard}$ is the measured isotope ratio of the standard. Measured values of $\delta^{13}C$ are normalized the VPDB, and values of $\delta^{18}O$ are normalized to SMOW. Where initial data output for $\delta^{18}O$ has been previously normalized to VPDB, $\delta^{18}O$ VSMOW values have been calculated using the following formula: $\delta^{18}O_{VSMOW} = 1.03092(\delta^{18}O_{VPDB}) + 30.92$.

Taxon	Locality	Laboratory #	SPEC ID	Tooth Sampled	n
O. irroratus	Amisrus	ACL-0479	WA-0001	M1-M3	IE
O. saundersiae	Amisrus	ACL-0480	WA-0002	M1-M3	2
O. irroratus	Amisrus	ACL-0480B	WA-0003	M1-M3	IE
O. irroratus	Amisrus	ACL-0488	WA-0004	M1-M3	1
O. irroratus	Amisrus	ACL-0489	WA-0005	M1-M3	1
O. irroratus	Amisrus	ACL-0491	WA-0006	M1-M3	1
O. irroratus	Amisrus	ACL-0492	WA-0007	M1-M3	IE
O. irroratus	Amisrus	ACL-0493	WA-0008	M1-M3	1
O. irroratus	Amisrus	ACL-0494	WA-0009	M1-M3	IE
O. irroratus	Amisrus	ACL-0495	WA-0010	M1-M3	1
O. irroratus	Amisrus	ACL-0496	WA-0011	M1-M3	IE
O. irroratus	Amisrus	ACL-0497	WA-0012	M1-M3	1
O. irroratus	Amisrus	ACL-0498	WA-0013	M1-M3	1
O. irroratus	Amisrus	ACL-0499	WA-0014	M1-M3	IE
O. irroratus	Amisrus	ACL-0500	WA-0015	M1-M3	IE
B. suillus	Rein's	ACL-6094	SPEO(A)	incisor	1
G. afra	Rein's	ACL-6087	SPEO(E)2	incisor	1
G. afra	Rein's	ACL-6089	SPEO(E)3	incisor	SL
O. saundersiae	Rein's	ACL-6091	SPEO(D)1	ML1	1
O. saundersiae	Rein's	ACL-6095	SPEO(E)1	ML1	1
O. saundersiae	Rein's	ACL-6088	SPEO(G)	ML1	1
O. saundersiae	Rein's	ACL-6092	SPEO(F)1	MU1	1
O. saundersiae	Rein's	ACL-6086	SPEO(F)2	MU1	1
O. saundersiae	Rein's	ACL-6090	SPEO(F)3	ML1	1
O. saundersiae	Rein's	ACL-6093	SPEO(F)4	ML1	1
O. irroratus	Wolwe River	ACL-0501	WLR-0001	M1-M3	1
O. irroratus	Wolwe River	ACL-0502	WLR-0002		IE
O. irroratus	Wolwe River	ACL-0503	WLR-0003	M1-M3	1
O. irroratus	Wolwe River	ACL-0504	WLR-0004	M1-M3	1
O. irroratus	Wolwe River	ACL-0505	WLR-0005	M1-M3	2
O. irroratus	Wolwe River	ACL-0506	WLR-0006	M1-M3	1
O. irroratus	Wolwe River	ACL-0507	WLR-0007	M1-M3	1
O. irroratus	Wolwe River	ACL-0508	WLR-0008		IE
O. irroratus	Wolwe River	ACL-0509	WLR-0009	M1-M3	1
O. irroratus	Wolwe River	ACL-0510	WLR-0010	M1-M3	1
O. irroratus	Wolwe River	ACL-0511	WLR-0011	M1-M3	1
O. irroratus	Wolwe River	ACL-0512	WLR-0012	M1-M3	1

Table 3.1. Species, tooth type, and lab ID for modern specimens sampled from Amisrus, Wolwe River, and Rein's Nature Reserve. IE = insufficient enamel remaining after pretreatment. SL= specimen lost due to failed analytical run during instrumentation.

Results*:*

Carbon:

Rein's Nature Reserve Micromammals

Stable carbon isotope ratios were obtained from 10 micromammal specimens from the Rein's Nature Reserve sampling locality: $\delta^{13}C_{enamel}$ data was acquired for one specimen each of *B. suillus* and *G. afra,* and from 8 specimens of *O. saundersiae*. Enamel powder from an additional gerbillid specimen was lost due to instrument malfunction. *B. suillus* $\delta^{13}C_{enamel}$ = -13.51‰ VPDB . *G. afra* $\delta^{13}C_{enamel}$ = -8.9‰. *O. saundersiae* $\delta^{13}C_{enamel}$ ranges from -15.19 to -17.23‰ ($\overline{x}$ $\delta^{13}C_{enamel}$ = -16.01‰, σ = 0.092).

Amisrus Micromammals

Carbon isotope ratio data was obtained from 7 specimens of *O. irroratus* and 1 specimen of *O. saundersiae*. $\delta^{13}C_{enamel}$ of the *O. saundersiae* specimen was -12.0‰ VPDB, while the range of $\delta^{13}C_{enamel}$ values for *O. irroratus* from Amisrus are from -7.1 to -21.2‰ VPDB.

Wolwe River Micromammals

Ten specimens of *O. irroratus* yielded sufficient enamel for isotope analysis. *O. irroratus* $\delta^{13}C_{enamel}$ values range from -10.1‰ VPDB to -18.3‰ VPDB ($\overline{x}$ $\delta^{13}C_{enamel}$ = -14.17‰, σ = 2.829).

Oxygen:

Rein's Nature Reserve Micromammals

The oxygen isotope ratios of the micromammals from Rein's Nature Reserve range from 20.92‰ VSMOW to 33.88‰. The *G. afra* $\delta^{18}O_{enamel}$ value (30.33‰ VSMOW) and the *O. saundersiae* $\delta^{18}O_{enamel}$ range (between 32.37‰ and 33.88‰) are close together, but *B. suillus* is depleted in ^{18}O by more than 10‰ ($\delta^{18}O_{enamel}$ = 20.92‰).

Amisrus Micromammals

The $\delta^{18}O_{enamel}$ of the *O. saundersiae* specimen from Amisrus is 21.0‰ VSMOW. *O. irroratus* $\delta^{18}O$ values range from 25‰ to 27.9‰ ($\overline{x}$ $\delta^{18}C_{enamel}$ = 26.29‰, σ = 0.871).

Wolwe River Micromammals

$\delta^{18}O_{enamel}$ values for the Wolwe River *O. irroratus* range from 24.9‰ to 29.9‰, with a mean $\delta^{18}O_{enamel}$ of 27.15‰ VSMOW (σ=1.679).

Discussion

South Coast Modern Carbon Isotope Data:

The micromammals from the different study localities have a wide range of $\delta^{13}C_{enamel}$ values, both intra- and inter- specifically and between localities. Ranges of $\delta^{13}C_{enamel}$ values are quite wide for the sampled populations from Amisrus and Wolwe River, and comparably narrow at Rein's Nature Reserve.

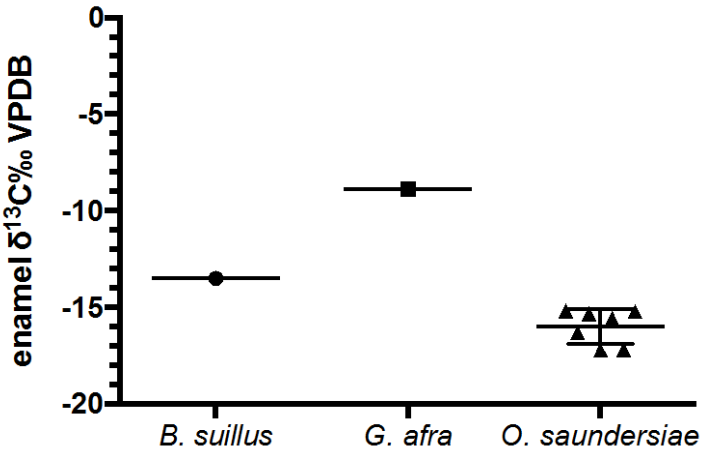

Figure 3.3. Stable carbon isotope ratio data for the sampled micromammals from Rein's Nature Reserve

At Rein's Nature reserve the $\delta^{13}C_{enamel}$ values of the *O. saundersiae* are lower than those of the *B. suillus* or *G. afra* specimens (Figure 3.3). Using the measured $\delta^{13}C_{enamel}$ for *B. suillus* and *G. afra* as hypothetical population means for a one-sample t-test, the Rein's *O. saundersiae* specimens are in fact significantly more depleted in ^{13}C than either of these taxa (one-sample t-test, $p_{B.\ suillus} = 0.0003$, $p_{G.\ afra} < 0.0001$).

Enamel $\delta^{13}C$ is offset from dietary $\delta^{13}C$ by an enrichment factor ($\varepsilon^*_{apatite\text{-}diet}$) that reflects metabolic fractionation of carbon; $\delta^{13}C_{diet}$ can be approximated by use of the formula below (which uses algebraic substitution of the formulae in Cerling and Harris, 1999 to solve for δ_{diet}):

$$\delta_{diet} = \left(\frac{1000 + \delta_{enamel}}{1 + \frac{\varepsilon^*_{enamel\text{-}diet}}{1000}} \right) - 1000$$

$\varepsilon^*_{apatite\text{-}diet}$ is the representation of the non-equilibrium carbon isotope enrichment factor between enamel and diet (see Cerling and Harris, 1999). $\varepsilon^*_{apatite\text{-}diet}$ values have been experimentally determined to be between 10‰ and 14‰ for most mammalian taxa (Lee-

Thorp and Van Der Merwe, 1987; Lee-Thorp, 1989; Cerling and Harris, 1999; Passey *et al.,* 2005).

All of the *Otomys* specimens from Rein's have values of enamel $\delta^{13}C$ indicative of pure C_3 diets; using the lowest diet-tissue enrichment factor suggested in the literature for small mammals (11‰; Hynek *et al.,* 2012) to convert the most enriched $\delta^{13}C_{enamel}$ value of *O. saundersiae* results in an inferred $\delta^{13}C_{diet}$ of -24.91‰, well below the -20‰ threshold for GCFR C_3 plants suggested by the GSCIMS analysis (Chapter 2). Binary mixing model calculations using a number of different assumptive end-member values to calculate dietary C_4 fraction (Table 3.2.a) support the conclusion that the *Otomys* specimens from Rein's are all C_3-consumers.

Given the dietary preference of *O. saundersiae* for grasses and their association with somewhat more open habitats, this dietary signal is consistent with Canca Limestone Fynbos vegetation (from which the specimens were collected), which has asteraceous and restioid components but is generally lacking in shrubby *Erica* taxa (Rebelo *et al.*, 2006). Canca Limestone Fynbos is also lacking in C_4 grasses (Table 3.3), which is also consistent with the lack of evidence for a dietary C_4 component in the $\delta^{13}C_{enamel}$ of the Rein's *Otomys*.

a) Rein's Nature Reserve							
Taxon	**$\delta^{13}C_{enamel}$**	**$\delta^{13}C_{diet}$ (ε^* = 11‰)**	**%C_4 (case 1)**	**%C_4 (case 2)**	**$\delta^{13}C_{diet}$ (ε^* = 14‰)**	**%C_4 (case 1)**	**%C_4 (case 2)**
O. saundersiae	-16.32‰	-27.02‰	0%*	0%*	-29.90‰	0%*	0%*
O. saundersiae	-17.23‰	-27.92‰	0%*	0%*	-30.80‰	0%*	0%*
O. saundersiae	-15.19‰	-25.91‰	0%	0%*	-28.79‰	0%*	0%*
O. saundersiae	-15.35‰	-26.06‰	0%*	0%*	-28.94‰	0%*	0%*
O. saundersiae	-17.19‰	-27.88‰	0%*	0%*	-30.76‰	0%*	0%*
O. saundersiae	-15.23‰	-25.94‰	0%*	0%*	-28.83‰	0%*	0%*
O. saundersiae	-15.57‰	-26.28‰	0%*	0%*	-29.16‰	0%*	0%*
B. suillus	-13.51‰	-24.24‰	13.15%	0%*	-27.13‰	0%*	0%*
G. afra	-8.9‰	-19.68‰	49.14%	4.08%	-22.58‰	26.25%	0%*
b) Amisrus							
Taxon	**$\delta^{13}C_{enamel}$**	**$\delta^{13}C_{diet}$ (ε^* = 11‰)**	**%C_4 (case 1)**	**%C_4 (case 2)**	**$\delta^{13}C_{diet}$ (ε^* = 14‰)**	**%C_4 (case 1)**	**%C_4 (case 2)**
O. irroratus	-12.7‰	-23.4‰	19.5%	0%*	-26.3‰	0%*	0%*
O. irroratus	-7.1‰	-17.9‰	63.2%	27.0%	-20.8‰	40.3%	0%*
O. irroratus	-12.3‰	-23.0‰	22.6%	0%*	-25.9‰	0%*	0%*
O. irroratus	-11.5‰	-22.3‰	28.9%	0%*	-25.1‰	6.0%	0%*
O. irroratus	-18.1‰	-28.8‰	0%*	0%*	-31.7‰	0%*	0%*
O. irroratus	-16.0‰	-26.7‰	0%*	0%*	-29.6‰	0%*	0%*
O. irroratus	-21.2‰	-31.8‰	0%*	0%*	-34.7‰	0%*	0%*
O. saundersiae	-12.0‰	-22.7‰	24.9%	0%*	-25.6‰	2.1%	0%*
c) Wolwe River							
Taxon	**$\delta^{13}C_{enamel}$**	**$\delta^{13}C_{diet}$ (ε^* = 11‰)**	**%C_4 (case 1)**	**%C_4 (case 2)**	**$\delta^{13}C_{diet}$ (ε^* = 14‰)**	**%C_4 (case 1)**	**%C_4 (case 2)**
O. irroratus	-15.0‰	-25.7‰	1.5%	0%*	-28.6‰	0%*	0%*
O. irroratus	-14.7‰	-25.4‰	3.9%	0%*	-28.3‰	0%*	0%*
O. irroratus	-15.0‰	-25.7‰	1.5%	0%*	-28.6‰	0%*	0%*
O. irroratus	-10.7‰	-21.5‰	35.1%	0%*	-24.4‰	12.2%	0%*
O. irroratus	-18.3‰	-29.0‰	0%*	0%*	-31.9‰	0%*	0%*
O. irroratus	-14.3‰	-25.0‰	7.0%	0%*	-27.9‰	0%*	0%*
O. irroratus	-15.1‰	-25.8‰	0.7%	0%*	-28.7‰	0%*	0%*
O. irroratus	-10.8‰	-21.6‰	34.3%	0%*	-24.5‰	11.5%	0%*
O. irroratus	-10.1‰	-20.9‰	39.8%	0%*	-23.8‰	16.9%	0%*
O. irroratus	-17.7‰	-28.4‰	0%*	0%*	-31.3‰	0%*	0%*

Table 3.2. %C_4 in diet. $\delta^{13}C_{diet}$ was calculated assuming $\varepsilon^*_{enamel\text{-}diet}$ of either 11‰ or 14‰. %C_4 = ($\delta^{13}C_{diet}$ - $\delta^{13}C_{C3}$)/($\delta^{13}C_{C4}$ - $\delta^{13}C_{C3}$)*100. Case 1: $\delta^{13}C_{C3}$ = -25.91‰ (mean GSCIMS C_3); $\delta^{13}C_{C4}$ = -12.24‰ (mean GSCIMS C_4). Case 2: $\delta^{13}C_{C3}$ = -20‰ (hypothetical max GCFR C_3), $\delta^{13}C_{C4}$ =-12.24‰. %C_4 values of 0%* indicate inferred $\delta^{13}C_{diet}$ values than are lower than the assumed end member $\delta^{13}C$ value of C_3 plants.

Plant Type	Taxon	$\delta^{13}C$ ‰ VPDB	σ
C_3			
	Aspalathus *	-26.9	1.56
restioid	*Elegia* *	-27.0	0.77
annual	*Indigofera sp.*	-22.7	
restioid	*Ischyrolepis* *	-27.5	0.70
	*Leucadendron**	-27.0	1.93
	*Protea**	-26.3	0.76
	*Ruschia (C_3)**	-23.4	0.42
	Sutera *	-24.5	
restioid	*Thamnochortus* *	-28.2	
CAM/FCAM			
	Haworthia *	-12.6	0.64
	*Ruschia (CAM)**	-16.5	0.82
	*Ruschia (FCAM)**	-21.0	3.42

Grass Genera w/o GCFR $\delta^{13}C$ values	
Genus	
Ceratocaryum	C_3
Ficinia	C_3
Pentaschistis	C_3

Table 3.3. Extant $\delta^{13}C_{tissue}$ data (‰, VPDB) for genera of plants found in the Canca Limestone Fynbos. Data derived from sources listed in Appendix A. Floral taxonomic presence determined from Rebeleo *et al.* (2006)

The *B. suillus* $\delta^{13}C_{enamel}$ value suggests a $\delta^{13}C_{diet}$ of -24.24‰ ($\varepsilon^*_{apatite\text{-}diet}$ = 11‰) to -27.13‰ ($\varepsilon^*_{apatite\text{-}diet}$ = 14‰), which is also consistent with a limited input of C_4 grass into the diet of this specimen. Linear mixing models (Table 3.2.a) suggest a 0-13% dietary fraction of C_4 grass for this specimen, while Bayesian modeling using Stable Isotope Analysis in R (SIAR) (Parnell and Jackson, 2013) suggests a dietary C_4 grass fraction for this specimen of 0-26%. *B. suillus* is a burrowing taxon, and the soils on which Canca Limestone Fynbos grows tend to be shallow (Rebelo *et al.*, 2006); this, in tandem with the paucity of C_4 grasses in the Canca Limestone Fynbos suggest that the *B. suillus* specimen may have come from a different vegetation community nearby. Strandveld and Albertinia Sand Fynbos vegetation communities are both found with the foraging radius of the aggregating predator (*Bubo africanus*) from the pellet collection

locality, and occur on comparably deeper sandy substrates. Both of these vegetation communities contain C_4 grasses such as *Cynodon* and *Panicum* (Tables 3.4), Albertinia Sand Fynbos contains a number of C_3 restios taxa, and both vegetation communities contain C_3 geophytes such as *Bulbine sp.*

Plant Type	Taxon	$\delta^{13}C$ ‰ VPDB	σ
C_3			
	Aspalathus *	-26.9	1.56
	Bulbine *	-26.4	
restioid	*Calopsis* *	-26.9	
restioid	*Elegia* *	-27.0	0.77
restioid	*Ischyrolepis**	-27.2	0.49
	*Leucadendron**	-27.0	1.93
	Nylandtia spinosa	-22.3	
	*Protea**	-26.3	0.76
leaf succulent	*Senecio* *	-22.2	
restioid	*Staberoha distachyos*	-28.5	
restioid	*Thamnochortus* *	-28.2	
restioid	*Willdenowia* *	-28.8	
C_4			
grass	*Cynodon dactylon*	-12.7	
grass	*Cynodon dactylon*	-15.6	
CAM/FCAM			
	*Senecio (FCAM)**	-17.1	0.58

Grass Genera w/o GCFR $\delta^{13}C$ values	
Genus	
Mastersiella	C_3
Staberoha	C_3

Table 3.4. Extant $\delta^{13}C_{tissue}$ data (‰, VPDB) for genera of plants found in the Albertinia Sand Fynbos. Data derived from sources listed in Appendix A. Floral taxonomic presence determined from Rebeleo *et al.* (2006)

The higher $\delta^{13}C_{enamel}$ value (-8.9‰VPDB) obtained from the specimen of *G. afra* from Rein's Nature reserve is indicative of mixed feeding: approximate $\delta^{13}C_{diet}$ ranges between -19.86‰ ($\varepsilon^*_{apatite\text{-}diet}$ = 11‰) and -22.58‰ ($\varepsilon^*_{apatite\text{-}diet}$ = 14‰). *G. afra* consumes primarily bulbs, roots and grasses, and the highest C_3 $\delta^{13}C_{plant}$ values suggested

by GSCIMS for any of the Rein's vegetation communities come from *Nylandtia spinosa* (Tortoise Berry Bush, -22.3‰ VPDB), and *Indigofera sp.* (-22.7‰). Unless this *G. afra* specimen fed exclusively on these or similar plants, it is likely that its diet included a fraction of the C_4 grasses available in the sand fynbos or strandveld vegetation communities. Calculations of dietary C_4 fraction (fC_4) that assume the C_3 component of the *G. afra* diet is the GSCIMS-calculated GCFR mean of -25.91‰ indicate that more than 26% of the gerbillid's diet was C_4 grasses (Table 3.2.a). Bayesian modeling using SIAR (Parnell and Jackson, 2013) of diet of the *G. afra* specimen using non-CAM end member values from Albertinia Sand Fynbos (Appendix A) suggest that C_4 grasses were between 26 and 62% of the diet of the *G. afra* specimen.

No *B. suillus* or *G. afra* were sampled from the Amisrus locality, but stable carbon isotope data from 12 specimens of *Otomys* from this location suggests a wider range of available plant $\delta^{13}C$ values on the landscape within the foraging radius of the aggregating predator (Table 3.2.b). The most depleted specimen (*O. irroratus*, $\delta^{13}C_{enamel}$ = -21.2‰) has a minimum inferred $\delta^{13}C_{diet}$ value of -31.85‰, a value more depleted than any non-tree value in the GSCIMS data set. Values of $\delta^{13}C_{plant}$ are vertically stratified within closed-canopy forests, such that understory plants are depleted in ^{13}C relative to leaves from the top of the canopy or C_3 plants from open environments (Vogel, 1978; Tieszen and Boutton, 1989; Flanagan *et al.,* 1996; Cerling *et al.,* 2004); the $\delta^{13}C_{enamel}$ value of -21.2‰ for this specimen of *O. irroratus* is suggestive of a diet comprised of understory grasses or plants from very closed environments. Two other *O. irroratus* specimens have $\delta^{13}C_{enamel}$ values (-18.1‰, -16.0‰) that are indicative of pure C_3 diets, which is consistent with feeding on vegetation either from the forest or from the nearby

Southern Cape Dune Fynbos, which also lacks an extensive C_4 component (Table 3.5), or alternately, within a microhabitat in the Garden Route Shale Fynbos that locally lacked C_4 elements.

Plant Type	Taxon	$\delta^{13}C$ ‰ VPDB	σ
C_3			
	Aspalathus *	-26.9	1.56
annual	*Indigofera sp.*	-22.7	
restioid	*Ischyrolepis* *	-27.5	0.70
	Leucadendron salignum	-28.5	
	Leucadendron salignum	-25.9	
	Pelargonium(C_3)*	-24.9	0
riparian shrub	*Rhus populifolia*	-24.2	
riparian tree	*Rhus undulata*	-22.7	
restioid	*Thamnochortus* *	-28.2	
	Thesium sp	-26.8	
CAM			
	*Pelargonium (CAM)**	-16.9	

Grass Genera w/o GCFR $\delta^{13}C$ values	
Genus	
Ehrhata	C_3
Ficinia	C_3
Pentaschistis	C_3
Tetraria	C_3
Tribolium	C_3

Table 3.5. Extant $\delta^{13}C_{tissue}$ data (‰, VPDB) for genera of plants found in the Southern Cape Dune Fynbos. Data derived from sources listed in Appendix A. Floral taxonomic presence determined from Rebeleo *et al.* (2006)

One specimen of *O. irroratus* from Amisrus has a higher $\delta^{13}C_{enamel}$ value of -7.1‰, which is indicative of a comparably large dietary fraction of C_4 grass (Table 3.2.b, Appendix B). C_4 grasses are rare or non-existent in the Southern Afrotemperate Forests or in the Southern Dune Cape Fynbos, thus this *Otomys* specimen is unlikely to have been feeding in either of these vegetation contexts. Instead, it likely came from nearby vegetation from the Garden Route Shale Fynbos, which occurs less than 3km

from the pellet collection locality, well within the foraging range of the aggregating raptor. Garden Route Shale Fynbos vegetation communities can contain up to six genera of C_4 grasses (Rebelo *et al.*, 2006)(Table 3.6), and would provide a comparably plentiful dietary source of C_4 grasses. Three additional specimens of *O. irroratus* and one specimen of *O. saundersiae* from the Amisrus pellets also have $\delta^{13}C_{enamel}$ values that suggest some dietary C_4 grass component. (Table 3.2.b), and thus were likely not occupying a habitat composed of exclusively C_3 floral elements when the enamel of their posterior teeth was formed.

The difference between the most depleted and most enriched *Otomys* stable carbon isotope ratios from Amisrus specimens is 14.1‰, and the inferred $\delta^{13}C_{diet}$ values suggest that the *Otomys* specimens are likely sampling two different vegetation communities proximate to the pellet collection locality, which is located within the Southern Afrotemperate Forest. Understory plants in closed forests such as those found near Amisrus tend to be quite depleted in ^{13}C, and on the south coast of South Africa this vegetation community contains little-to-no C_4 vegetation as part of its understory; vegetation from the nearby Southern Cape Dune Fynbos is also largely lacking in C_4 elements. Thus the likely C_4 grass component of the diets of some of the modern *Otomys* specimens more likely came from vegetation outside these plant communities, possibly from that of the nearby Garden Route Shale Fynbos. Conversely, no plant taxa found in the Garden Route Shale Fynbos that have been sampled for carbon isotopic analysis and reported in the literature (Table 3.6) have $\delta^{13}C_{tissue}$ values depleted enough in ^{13}C to be the source carbon for the most ^{13}C-depleted *Otomys* specimen(s) from this locality. Thus the range of $\delta^{13}C_{enamel}$ values found in the Amisrus *Otomys* specimens suggests that the

micromammals sample the multiple vegetation communities extant near the collection locality and within the range of the aggregating predator.

Plant Type	Taxon	$\delta^{13}C$ ‰ VPDB	σ
C_3			
restioid	*Elegia* *	-27.0	0.77
graminoid	*Ischyrolepis**	-27.2	0.49
	*Leucadendron**	-27.0	1.93
leaf succulent	*Pelargonium* *	-24.9	
	*Protea**	-28.6	0.88
	*Restio**	-26.8	0.83
riparian shrub/tree	*Rhus**	-23.4	1.09
C_4			
grass	*Aristida* *	-11.0	
grass	*Brachiaria serrata*	-11.5	
grass	*Cymbopogon**	-12.2	1.02
grass	*Eragrostis capensis*	-13.2	
grass	*Tristachya* *	-11	
grass	*Themeda triandra*	-11.6	
CAM/FCAM			
	*Crassula (CAM)**	-14.6	1.28
	*Crassula (FCAM)**	-18.8	1.38
	Pelargonium *	-16.9	

Grass Genera w/o GCFR $\delta^{13}C$ values
Genus
none

Table 3.6. Extant $\delta^{13}C_{tissue}$ data (‰, VPDB) for genera of plants found in the Garden Route Shale Fynbos. Data derived from sources listed in Appendix A. Floral taxonomic presence determined from Rebeleo *et al.* (2006)

Ten specimens assigned to *O. irroratus* were sampled from the Wolwe River pellet collection locality. Similar to their conspecifics from the Amisrus locality, the Wolwe River *Otomys* have a range of $\delta^{13}C_{enamel}$ values that is almost 10‰ (Figure 3.4). Three Wolwe River *O.* irroratus specimens have $\delta^{13}C_{enamel}$ values between -11‰ and -10‰, which is enriched when compared to the pure C_3 *Otomys* from Rein's Nature Reserve or the most ^{13}C-depleted specimens from Amisrus. Reconstructed dietary C_4

fraction suggests that these specimens are likely to have engaged in some mixed feeding (Table 3.2.c) and are thus indicative of the presence of C_4 grass in one of the local vegetation communities. None of the remaining seven *Otomys* specimens from this locality have $\delta^{13}C_{enamel}$ values depleted enough to suggest a closed-forest dietary component (Table 3.2.c), although all seven of these more depleted specimens are likely to be primarily C_3 consumers. Two non-forest GCFR vegetation communities occur within the foraging radius of *Tyto capensis* from the collection locality: the Southern Cape Dune Fynbos, and the Knysna Sand Fynbos. The presence of a C_4 component in the diet of about a third of the specimens sampled suggests that they likely come from Knysna Sand Fynbos vegetation contexts, as the Southern Cape Dune Fynbos is comparably lacking in C_4 elements, while seven C_4 grass genera are present in the Knysna Sand Fynbos (Table 3.7). It is impossible to determine which vegetation community the other specimens derived from, as these individuals could have been feeding either in the Southern Cape Dune Fynbos or (given the small ranges of *Otomys*) in a microhabitat patch of Knysna Fynbos that by chance locally lacked C_4 elements.

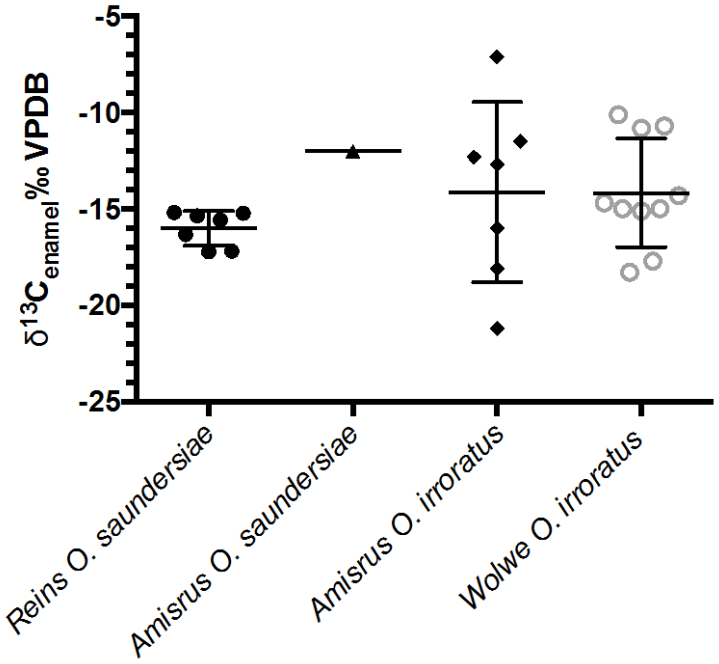

Figure 3.4. $\delta^{13}C_{enamel}$ values of sampled *Otomys* specimens from Rien's Nature Reserve, Amisrus, and Wolwe River.

Plant Type	Taxon	δ13C ‰ VPDB	σ
C_3			
restioid	*Ischyrolepis**	-27.2	0.49
	*Leucadendron**	-27.0	1.93
	*Protea **	-29.0	0.53
restioid	*Thamnochortus **	-28.2	
C_4			
grass	*Aristida **	-11.0	
grass	*Brachiaria serrata*	-11.5	
grass	*Cynodon dactylon*	-12.7	
grass	*Cynodon dactylon*	-15.6	
grass	*Eragrostis capensis*	-13.2	
grass	*Heteropogon contortus*	-12.1	
grass	*Themeda triandra*	-11.6	
grass	*Tristachya **	-11	

Grass Genera w/o GCFR δ13C values	
Genus	
Ficinia	C_3
Tetraria	C_3

Table 3.7. Extant $\delta^{13}C_{tissue}$ data (‰, VPDB) for genera of plants found in the Knysna Sand Fynbos. Data derived from sources listed in Appendix A. Floral taxonomic presence determined from Rebeleo *et al.* (2006)

The means of the *Otomys* $\delta^{13}C_{enamel}$ samples from the three different sampling localities are not significantly different from one another (ANOVA $F = 86.54$ $r^2 = 0.076$, $p = 0.435$), but Bartlett's test indicates that the population $\delta^{13}C_{enamel}$ variance is significantly different between sampling localities (Bartlett's statistic = 11.4, $p = 0.0030$). The *Otomys* sample from Rein's Nature reserve is composed entirely of *O. saundersiae*, while the *Otomys* samples from the other two localities are primarily *O. irroratus*. Small differences in feeding ecology between *O. saundersiae* and *O. irroratus* could be responsible for the contracted range of $\delta^{13}C_{enamel}$ values in the Rein's sample, but this seems unlikely, given the $\delta^{13}C_{enamel}$ value of -12‰ for the *O. saundersiae* specimen from Amisrus.

Instead, I hypothesize that the contracted range of $\delta^{13}C_{enamel}$ values for the *Otomys* specimens from Rein's Nature Reserve reflect a known narrow range of $\delta^{13}C_{plant}$ on the landscape near the collection site, while the wider ranges of the *Otomys* specimens from Amisrus and Wolwe River are indicative of more C_4 plants (and thus more frequent occurrences of high $\delta^{13}C_{plant}$ values) in the vegetation communities near those sites. The stable carbon isotope data for specimens from all collection localities is consistent with what is known about the taxonomic and isotopic composition of the flora from vegetation groups at or near the sites.

The entire range of carbon isotope ratios among all modern micromammal taxa from the study area is comparably wide: $\delta^{13}C_{enamel}$ values range from -7.1‰ to -21.2‰. Much of this variation is not the result of differences in $\delta^{13}C$ between sampling localities, as this entire range of stable carbon isotope values is found in a single population of

O. irroratus from the Amisrus collecting locality. This 14.1‰ difference in specimens most depleted and most enriched in ^{13}C is considerably larger than found in many (but not all) large mammal taxa for which there are large sample sizes (Ambrose and DeNiro, 1986; Bocherens *et al.*, 1996; Cerling *et al.*, 2003; Thackeray *et al.*, 2003; Codron *et al.*, 2006). Hynek et al (2012) report similarly wide ranges of $\delta^{13}C_{enamel}$ for small mammals from the Mio-Pliocene in Argentina (between 10‰ and 18‰, depending on stratigraphic unit) and suggest that wide ranges of enamel carbon isotope ratios in micromammals indicate that generalist micromammal taxa have the potential to sample an entire range of available $\delta^{13}C_{plant}$ values on a given landscape. The carbon isotope data from the modern South African localities reported here appears to support this hypothesis, and are also suggestive of the idea that comparably *narrow* $\delta^{13}C$ ranges in micromammal taxa reflect a greatly reduced range of available $\delta^{13}C_{plant}$ in an environment (although larger sample sizes from geographic areas with relatively restricted ranges of available $\delta^{13}C_{plant}$ values are needed to further test this latter hypothesis).

PP-proximate Micromammal Carbon Isotope Data in Context: Other South African records

The stable carbon isotope data from micromammals from the modern collection localities in the Pinnacle Point region along the south coast of South Africa suggest that *Otomys*, *Bathyergus*, and *Gerbilliscus* $\delta^{13}C_{enamel}$ values, where treated as "populations" of values rather than individual data points, reflect the ranges of plant types (and thus the range of $\delta^{13}C_{plant}$ values) over a relatively circumscribed geographic space. However, one of the drawbacks of sampling modern taxa from fixed vegetation communities is that it is

difficult to demonstrate whether or not the isotope ecology of each taxon would vary over a changing isoscape, or whether niche partitioning would obscure larger environmental signals. Kimura *et al.* (2013) found evidence of niche partitioning between larger and smaller murine rodents in Miocene Pakistan, but the changing environmental and dietary signal through time was still retained in the micromammal community. That micromammal taxa with similar diets sample slightly different portions of local vegetation is also supported by Codron *et al.* (2015), and is further suggested in the significantly different $\delta^{13}C_{enamel}$ in *Otomys*, *Bathyergus*, and *Gerbilliscus* found in this study (although it is important to stress that the sample sizes here are quite small and further study is clearly needed).

This potential for niche partitioning between micromammal taxa underscores the need to compare $\delta^{13}C_{enamel}$ values over time or across space within likely no higher a taxonomic level than the genus. It also suggests significant potential for the development of isotopic community structure analysis of entire micromammal communities, which could potentially result in fine scale differentiation between similar vegetation communities.

To address whether the $\delta^{13}C_{tissue}$ values of specific micromammal taxa vary over larger regional-scale vegetation changes that could not be captured within the relatively restricted geographic scope of Pinnacle Point region, the modern micromammal data reported here was compared to all currently published stable carbon isotope data from southern Africa (Appendix B.a-d). This $\delta^{13}C$ data exists in a number of forms; as data obtained from the analysis of hair (Robb *et al.*, 2012; Symes *et al.*, 2013; Van den Heuvel and Midgley, 2014; Codron *et al.*, 2015); as stable carbon isotope data obtained from

collagen (Sealy and Van der Merwe, 1986; Thackeray *et al.*, 2003); and as data obtained by sampling enamel apatite, either by using traditional or laser techniques (Hopley *et al.*, 2006; Yeakel *et al.*, 2007; Henry *et al.*, 2012). The Hopley *et al.* 2006 data is from an Iron Age assemblage but has been included here in the "modern" data.

Metabolic fractionation and routing of carbon is tissue-specific, and so $\varepsilon^*_{\text{tissue-diet}}$ values are different between tissue types: as a result $\delta^{13}C_{hair}$ data and $\delta^{13}C_{collagen}$ data are not directly comparable with $\delta^{13}C_{enamel}$ values. The tissue-specific offsets however have been measured in some small mammals, and so to compare the modern enamel apatite data reported here to the published hair and collagen stable carbon isotope ratios, all $\delta^{13}C_{tissue}$ values have been 'converted' to approximate $\delta^{13}C_{diet}$ values. Because all taxa sampled in this study are herbivorous, it is assumed that dietary protein and dietary carbohydrate sources are the same, have approximately equal $\delta^{13}C$, and thus do not result in different values of micromammal bulk tissue $\delta^{13}C$ and protein-derived tissue $\delta^{13}C$ (Arneson and MacAvoy, 2005).

Although there are a range of published values for $\varepsilon^*_{\text{collagen-other tissue}}$ (see Crowley *et al.*, 2010), the published values likely to reflect the influence of body size and digestive physiology on the diet-tissue spacing have here been chosen (following the arguments made by Hynek *et al.*, 2012). The wood rats sampled by Podelsak et al (2008) are both small in body size, and more importantly, strictly herbivorous in their digestive physiology: the mean $\varepsilon^*_{\text{enamel-diet}}$ value obtained by Podelsak *et al.* was 11‰. A $\varepsilon^*_{\text{collagen-keratin}}$ value of 2.7‰ has been taken from Tieszen and Farge's (1993) laboratory mouse

data (these mouse specimens were also fed a plant-based diet). The $\Delta_{collagen\text{-}diet}$ value of 5.4‰ (Jim *et al.*, 2004) has been used to approximate $\varepsilon^*_{collagen\text{-}diet}$.

Conversion of $\delta^{13}C_{keratin}$ (hair) or $\delta^{13}C_{collagen}$ values to $\delta^{13}C_{diet}$ values was performed by sequential calculation. $\delta^{13}C_{diet}$ is calculated from $\delta^{13}C_{collagen}$ and $\varepsilon^*_{collagen\text{-}diet}$ using the formula $\delta_{diet}=[(1000+\delta_{collagen})/(1+(\varepsilon^*/1000)]-1000$. $\delta^{13}C_{hair}$ undergoes the same algebraic transformation with an additional preliminary calculation of $\delta^{13}C_{collagen}$ using $\delta^{13}C_{hair}$ and $\varepsilon^*_{collagen\text{-}keratin}$ through the formula $\delta_{collagen}=[(1+(\varepsilon^*/1000))^*(1000+\delta_{keratin})]-1000$. All formulae used above are algebraically derived from the formulae (1) (see Cerling and Harris, 1999; Passey *et al.*, 2005) and (2) (see Craig, 1954; Passey *et al.*, 2005) which results in formula (3):

$$(1)\quad \alpha^*_{tissue\text{-}diet} = \frac{1000 + \delta_{tissue}}{1000 + \delta_{diet}} \qquad (2)\quad \varepsilon^*_{tissue\text{-}diet} = \left(\alpha^*_{tissue\text{-}diet}-1\right)^*1000$$

$$(3)\quad \delta_{diet}=\left(\frac{1000+\delta_{tissue}}{1+\frac{\varepsilon^*_{\bar{x}}}{1000}}\right)-1000$$

There are 29 published values for modern or near-modern specimens of *B. suillus* (*n* =16), *G. afra* (*n* = 1), and members of the genus *Otomys* (*O. irroratus n* = 3, *O. angoniensis n* = 1, *Otomys sp. n* = 8) It should be noted that some of these reported values are means of sampled populations (e.g. Codron *et al.*, 2015; van den Heuvel and Midgley, 2014). All of the published *Bathyergus* specimens (Sealy and Van der Merwe, 1986; Yeakel *et al.*, 2007) derive from Western Cape GCFR contexts (Figure 3.5); this taxon has a geographic distribution restricted to this region. The one published $\delta^{13}C$ value

for *G. afra* also comes from the Western Cape (–34.1385°S, 18.9228°E) and was collected from an area where the vegetation is Koegelberg Sandstone Fynbos (van den Heuvel and Midgley, 2014). Published *Otomys* specimens come from a diversity of geographic locations that span vegetation communities with both C_3 and C_4 grass predominance (Hopley *et al.*, 2006; Henry *et al.*, 2012; Van den Heuvel and Midgley, 2014; Codron *et al.*, 2015).

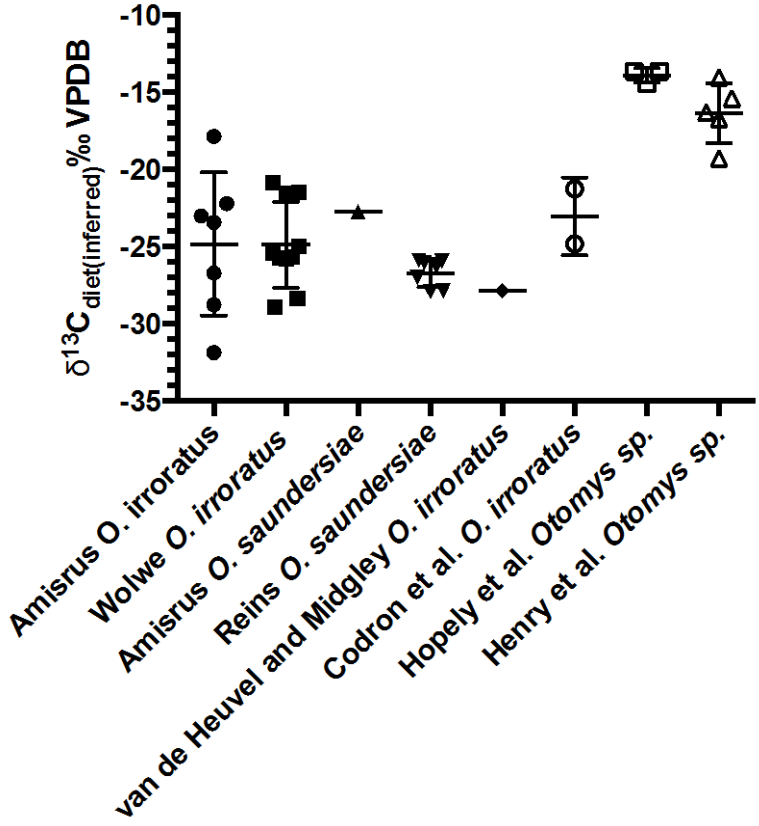

Figure 3.5. $\delta^{13}C_{diet(inferred)}$ values of the sampled *Otomys* specimens from Amisrus, Wolwe Rivier, and Rien's Nature Reserve, compared to the transformed $\delta^{13}C_{diet(inferred)}$ data for *Otomys* from the southwestern Cape (van den Heuvel and Midgley, 2014), and northeastern South Africa (Codron *et al.*, 2015; Hopley *et al.*, 2006; Henry *et al.*, 2012). The plotted $\delta^{13}C$ values from Codron et al (2015) represent the median dry- and wet-season values (post-transformation). Values from Hopley *et al.*, and Henry *et al.* represent raw data reported in those respective publications.

Yeakel *et al.* (2007) sampled the bone apatite of 11 *Bathyergus* specimens from the southwestern Cape, and observed a wide range of $\delta^{13}C_{apatite}$ values (~7‰, from -3.3‰ to -10.3‰). These values are between 3.2‰ and 10.2‰ more enriched in ^{13}C than the Rein's *B. suillus* specimen sampled here (Figure 3.6). Robb *et al.* (2012) sampled the hair of nine individuals who have an approximate mean $\delta^{13}C_{hair}$ value of -20‰ (Robb *et al.* applied a 2.3‰ enrichment factor to compare the hair values to vegetation that has been removed from the approximate mean $\delta^{13}C_{hair}$ discussed here); this corresponds to a mean $\delta^{13}C_{diet}$ value of ~ -22.3‰ for the *B. suillus* specimens they report.

The Reins *B. suillus* specimen $\delta^{13}C_{enamel}$ value (-13.51‰ VPDB) is similar to collagen values reported by Sealy and van der Merwe (1986) once tissue-specific enrichment factors have been controlled for, and all values have been transformed to approximate dietary $\delta^{13}C$ (Table 3.8, Figure 3.7).

Yeakel *et al.* (2007) attribute the higher values of $\delta^{13}C_{apatite}$ in their modern specimens to heavy consumption of *Cynodon* (a C_4 grass), and Robb *et al.* (2012) argue that analysis of their *B. suillus* hair $\delta^{13}C$ values also suggests a significant albeit variable (18-47%) C_4 grass component in this taxon's diet. The comparably high values of $\delta^{13}C_{deit}$ for the Yeakel *et al.,* (2007) *B. suillus* specimens, when compared to the Reins *B. suillus* specimen and the values of $\delta^{13}C$ obtained by Sealy and van der Merwe (1986) suggests that that the relative fraction of C_4 vegetation in *B. suillus* diets will vary over time and space, probably as a function of the prevalence of C_4 grasses over (and thus able to be pulled into) the burrow space.

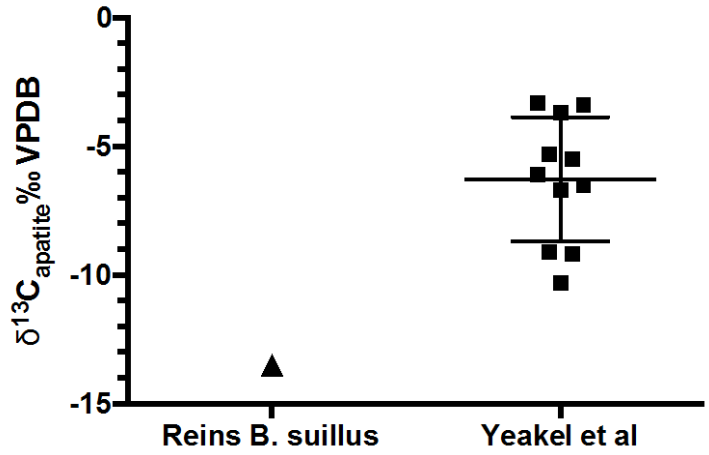

Figure 3.6. $\delta^{13}C_{enamel}$ values of the sampled *B. suillus* specimen from Rien's Nature Reserve compared to the $\delta^{13}C_{apatite}$ data for *B. suillus* from the southwestern Cape reported by Yeakel *et al.* (2007).

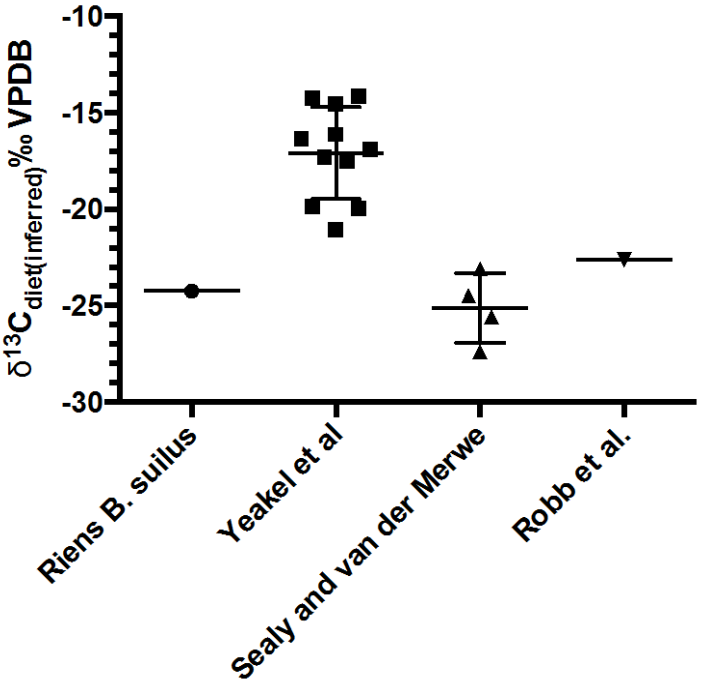

Figure 3.7. $\delta^{13}C_{diet(inferred)}$ values of the sampled *B. suillus* specimen from Rien's Nature Reserve compared to the transformed $\delta^{13}C_{diet(inferred)}$ data for *B. suillus* from the southwestern Cape.

Stable carbon isotope data for specimens of *G. afra* are almost non-existent in the literature. One additional hair value is available from van den Heuvel and Midgley (2014; Table 3.9). That specimen derives from Koegelberg Sandstone Fynbos, and has an approximated $\delta^{13}C_{diet}$ value of -24.95‰, which is distinctively C_3 and consistent with the predominance of proteoid and restioid components of that vegetation type. In contrast, the *G. afra* specimen from Rein's Nature Reserve has a $\delta^{13}C_{diet}$ value of -19.68‰ VPDB, which suggests that a reasonable fraction of this individual's diet was comprised of C_4 grasses, consistent with vegetation communities found in the region today. The available *G. afra* data suggests that *Gerbilliscus* $\delta^{13}C_{tissue}$ values may capture the presence or absence of C_4 plants in a given area, and that these $\delta^{13}C_{tissue}$ values should vary accordingly across geographic space. However, given that the currently available data includes only two specimens, this is clearly a hypothesis in need of further testing.

Data on the stable carbon isotope ratios of *Otomys* tissues are comparably more abundant, likely due to the broad distribution of this genus across southern Africa (Table 3.10). Eighteen stable carbon isotope data points exist for specimens of *Otomys irroratus* sampled from within the confines of the GCFR; two additional median $\delta^{13}C_{hair}$ values representing 17 specimens from the Cradle Nature Reserve have been reported by Codron *et al.* (2015). *Otomys saundersiae* $\delta^{13}C$ have only been obtained by the study reported here, but there are additional *Otomys sp.* values (n = 7) of $\delta^{13}C$ for modern and Iron Age specimens from Gauteng and Limpopo provinces (Hopley *et al.,* 2006; Henry *et al*., 2012).

Taxon	n	δ^{13}C ‰ VPDB hair	δ^{13}C ‰ VPDB collagen	δ^{13}C ‰ VPDB enamel	δ^{13}C ‰ VPDB "diet"	Citation
B. suillus	9	-20‰			-22.6‰	Robb *et al.,* 2012
B. suillus	1		-22.1‰		-27.4‰	Sealy & van der Merwe, 1986
B. suillus	1		-20.3‰		-25.6‰	Sealy & van der Merwe, 1986
B. suillus	1		-17.8‰		-23.1‰	Sealy & van der Merwe, 1986
B. suillus	1		-19.2‰		-24.5‰	Sealy & van der Merwe, 1986
B. suillus	1			-5.3‰	-16.1‰	Yeakel et al 2007
B. suillus	1			-3.4‰	-14.2‰	Yeakel et al 2007
B. suillus	1			-9.2‰	-12.0‰	Yeakel et al 2007
B. suillus	1			-5.5‰	-16.3‰	Yeakel et al 2007
B. suillus	1			-6.1‰	-16.9‰	Yeakel et al 2007
B. suillus	1			-3.3‰	-14.1‰	Yeakel et al 2007
B. suillus	1			-6.7‰	-17.5‰	Yeakel et al 2007
B. suillus	1			-3.7‰	-14.5‰	Yeakel et al 2007
B. suillus	1			-6.5‰	-17.3‰	Yeakel et al 2007
B. suillus	1			-9.1‰	-19.9‰	Yeakel et al 2007
B. suillus	1			-10.3‰	-21.1‰	Yeakel et al 2007
B. suillus	1			-13.5‰	-24.2‰	Williams, this thesis

Table 3.8. Published δ^{13}C values for *B. suillus* specimens. Approximate $\delta^{13}C_{diet}$ values calculated using the values of ε* discussed in the text.

Taxon	n	δ^{13}C ‰ VPDB hair	δ^{13}C ‰ VPDB collagen	δ^{13}C ‰ VPDB enamel	δ^{13}C ‰ VPDB "diet"	Citation
G. afra	3	-22.32			-25.0	van den Heuvel & Midgley, 2014
G. afra	1			-8.90	-19.7	Williams, this thesis

Table 3.9. Published δ^{13}C values for *G. afra* specimens. Approximate $\delta^{13}C_{diet}$ values calculated using the values of ε* discussed in the text.

When all values of $\delta^{13}C_{tissue}$ have been converted to approximate $\delta^{13}C_{diet}$ values using the formulae described above, it is clear that there is some separation between the stable carbon isotope composition of *Otomys* specimens from the GCFR when compared to $\delta^{13}C_{diet}$ values of specimens obtained from different vegetation contexts. (Figure 3.7).

The population of $\delta^{13}C_{diet}$ values for the *Otomys* specimens from the GFCR contexts (Amisrus, Wolwe Rivier, Rein's, and the van den Heuvel and Midgley data) all overlap with one another, and sampled populations from each of the four contexts all have at least some specimens whose stable carbon isotope ratios are consistent with C_3-exclusive diets.

Codron *et al.* (2015) suggest that in the Cradle Nature Reserve in Gauteng, the $\delta^{13}C$ values obtained from *O. irroratus* indicate that the taxon occupies a 'preferred' C_3 isotopic niche and expands its diet breadth to include C_4 grasses in the dry season when preferred resources become scarcer. Indeed, the range of values for *O. irroratus* reported in that study is significantly wider for specimens sampled during the dry season ($\delta^{13}C_{hair}$ values range from ~ -14.3‰ to ~ -23.2‰, Codron *et al.*, 2015 - Figure 1) than for those sampled during the wet season ($\delta^{13}C_{hair}$ values range from ~ -20‰ to ~ -22.8‰, Codron *et al.*, 2015 - Figure 1), although the authors note that this may be in part due to locational sampling bias.

Taxon	n	δ^{13}C ‰ VPDB hair	δ^{13}C ‰ VPDB enamel	δ^{13}C ‰ VPDB "diet"	Citation
O. irroratus	2	-25.24		-27.9	van den Heuvel & Midgley, 2014
O. irroratus	1		-12.7	-23.4	Williams, this thesis
O. irroratus	1		-7.1	-17.9	Williams, this thesis
O. irroratus	1		-12.3	-23.0	Williams, this thesis
O. irroratus	1		-11.5	-22.2	Williams, this thesis
O. irroratus	1		-18.1	-28.8	Williams, this thesis
O. irroratus	1		-16.0	-26.7	Williams, this thesis
O. irroratus	1		-21.2	-31.9	Williams, this thesis
O. irroratus	1		-15.0	-25.7	Williams, this thesis
O. irroratus	1		-14.7	-25.4	Williams, this thesis
O. irroratus	1		-15.0	-25.7	Williams, this thesis
O. irroratus	1		-10.7	-21.5	Williams, this thesis
O. irroratus	1		-18.3	-28.9	Williams, this thesis
O. irroratus	1		-14.3	-25.0	Williams, this thesis
O. irroratus	1		-15.1	-25.8	Williams, this thesis
O. irroratus	1		-10.8	-21.6	Williams, this thesis
O. irroratus	1		-10.1	-20.8	Williams, this thesis
O. irroratus	2		-17.7	-28.4	Williams, this thesis
O. irroratus	8	-18.63		-21.3	Codron *et al.,* 2015
O. irroratus	9	-22.19		-24.8	Codron *et al.,* 2015
O. saundersiae	1		-16.3	-27.0	Williams, this thesis
O. saundersiae	1		-17.2	-27.9	Williams, this thesis
O. saundersiae	1		-15.2	-25.9	Williams, this thesis
O. saundersiae	1		-15.4	-26.1	Williams, this thesis
O. saundersiae	1		-17.2	-27.9	Williams, this thesis
O. saundersiae	1		-15.2	-25.9	Williams, this thesis
O. saundersiae	1		-15.6	-26.3	Williams, this thesis
O. saundersiae	2		-12.0	-22.8	Williams, this thesis
Otomys sp.			-3.6	-14.4	Hopley *et al.,* 2006
Otomys sp.			-2.8	-13.7	Hopley *et al.,* 2006
Otomys sp.			-2.8	-13.7	Hopley *et al.,* 2006
Otomys sp.	1		-3.2	-14.0	Henry *et al.,* 2012
Otomys sp.	1		-8.5	-19.3	Henry *et al.,* 2012
Otomys sp.	1		-5.5	-16.3	Henry *et al.,* 2012
Otomys sp.	1		-5.9	-16.7	Henry *et al.,* 2012
Otomys sp.	1		-4.6	-15.4	Henry *et al.,* 2012

Table 3.10. Published δ^{13}C values for *Otomys* specimens. Approximate $\delta^{13}C_{diet}$ values calculated using the values of ε* discussed in the text. Hopley *et al.,* 2006 values are Iron Age in age.

When the ranges of $\delta^{13}C_{tissue}$ values (as represented by minimum and maximum measured values) obtained from *Otomys* specimens from different sampling contexts are "standardized" to $\delta^{13}C_{diet}$ and compared (Figure 3.8), there is significant overlap between the ranges of approximated $\delta^{13}C_{diet}$ values of populations of *Otomys* from the GCFR contexts of Amisrus and Wolwe River, and the 'seasonally averaged' palimpsest range from the Cradle Nature Reserve *Otomys* sampled by Codron *et al.* (2015) The more depleted populations of *Otomys* from the GCFR contexts at Rein's Nature reserve and the van den Heuvel & Midgley sampling fall outside the range of even the most depleted, C_3 consuming *O. irroratus* specimens from the Cradle Nature Reserve. In fact, once diet-tissue offsets are controlled for, 14 of the 26 Otomys stable carbon isotope data points from GCFR contexts are more depleted than the most depleted specimen from the Cradle Nature Reserve sample.

Other stable carbon isotope values for *Otomys irroratus* or *Otomys saundersiae* do not currently occur in the literature. *Otomys sp.* specimens from non-GCFR contexts in southern Africa have however been reported by Hopley *et al.,* (2006) and Henry *et al.,* (2012, in the supplemental material). These specimens (Table 3.10, Figure 3.8) are quite enriched in ^{13}C when compared to their GCFR congeners (after controlling for diet-tissue offsets), and the specimens all have $\delta^{13}C_{tissue}$ values that are suggestive of diets composed exclusively of C_4 plant matter. The most ^{13}C-depleted specimens of the sample population from Malapa Roost reported by Henry *et al.* (2012) overlap with the most ^{13}C-enriched portions of the Amisrus *O. irroratus* and the Codron *et* al. (2015) Cradle Nature Reserve *O. irroratus* populations, consistent with the identification of specimens in both populations as having diets with significant C_4 components. There is no apparent overlap

between the range of $\delta^{13}C_{diet}$ values from the Hopley et al (2006) Iron Age *Otomys sp.* population and any reported population of *Otomys* except that sampled from Malapa Roost.

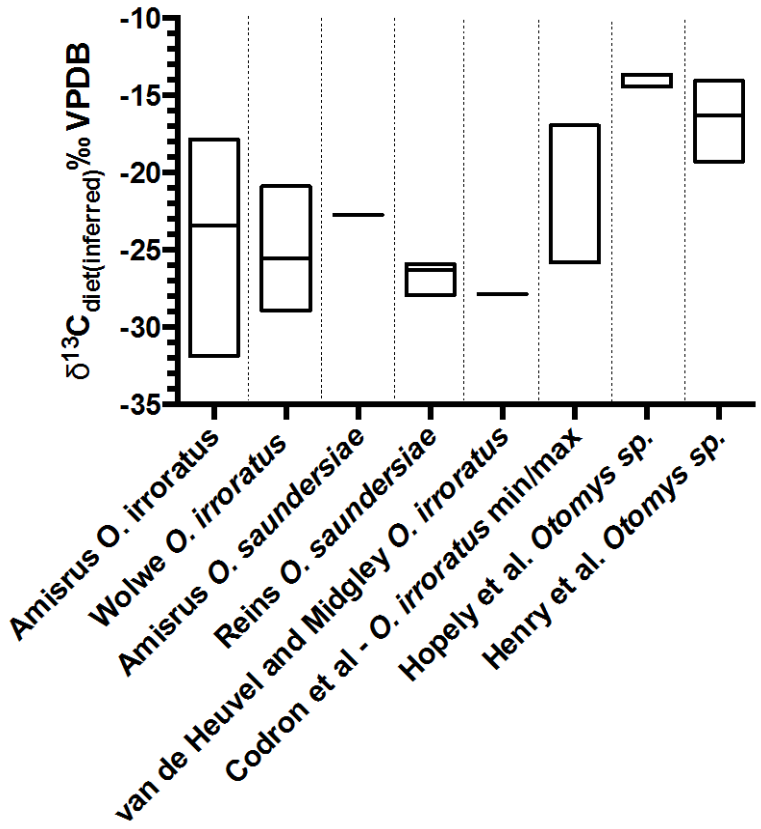

Figure 3.8. $\delta^{13}C_{diet(inferred)}$ values of the sampled *Otomys* specimens from Rien's Nature Reserve, Amisrus, and Wolwe Rivier, compared to the transformed $\delta^{13}C_{diet(inferred)}$ data for *Otomys* from the southwestern Cape (van den Heuvel and Midgley, 2014), and northeastern South Africa (Codron *et al.*, 2015; Hopley *et al.*, 2006; Henry *et al.*, 2012). Box plots represent maximum and minimum measured values, horizontal lines are population means. The combined wet/dry season data from Codron *et al.* (2015) uses only the approximate maximum and minimum values of $\delta^{13}C_{hair}$ (transformed to $\delta^{13}C_{diet(inferred)}$) reported from Figure 1 of that publication.

ANOVA (with Tukey's multiple comparisons post hoc test) of the published datasets for which there are sufficient data points available indicates that there are significant differences between the different populations of $\delta^{13}C_{diet}$ values ($F = 19.2$, $r^2 = 0.7399$, $p < 0.0001$). The Amisrus and Wolwe River *O. irroratus* populations, and the Rein's Nature Reserve *O. saundersiae* population are not significantly different from one another; nor are the Iron Age *Otomys* sp. and Malapa Roost *Otomys sp.* populations significantly different from one another in terms of $\delta^{13}C_{diet}$. The latter two populations of *Otomys* however both have mean $\delta^{13}C$ values that are significantly different from those obtained from *Otomys* from any of the GCFR contexts. This underscores the fact that the vegetation sampled by these populations has distinctively different stable carbon isotope ratios.

The comparison of the stable carbon isotope data obtained from geographically disparate populations of *Otomys* specimens suggests several things. In both primarily C_3 contexts and primarily C_4 contexts, populations of *Otomys* can sample either a wide range of $\delta^{13}C_{plant}$ values (C_3 contexts: Amisrus, Wolwe River (this study); C_4 contexts: Cradle Nature Reserve (Codron *et al.*, 2015), or a comparably narrow range of $\delta^{13}C_{plant}$ values (C_3 contexts: Rein's Nature Reserve (this study), van den Heuvel and Midgley (2014); C_4 contexts: Malapa Roost (Henry *et al.*, 2012), Limpopo Iron Age (Hopley *et al.*, 2006)).

However, there is also a real difference in the absolute ranges of $\delta^{13}C_{diet}$ values between different populations of *Otomys* from different regions of South Africa. Even the "preferentially C_3" *Otomys* specimens sampled by Codron *et al.* (2015) do not appear to have intersected plant matter with very low values of $\delta^{13}C_{plant}$, whereas at least some specimens from *all* GCFR contexts are very depleted in ^{13}C. Conversely, almost no

GCFR *Otomys* specimens, even those with quite high values of $\delta^{13}C_{tissue}$, have stable isotope ratios as enriched in ^{13}C as the specimens from the Limpopo Iron Age (Hopley *et al.,* 2006) or the Malapa Roost site (Henry *et al.,* 2012). The higher $\delta^{13}C_{tissue}$ values obtained from the Iron Age and Malapa Roost specimens is the result of the consumption of almost no C_3 plant matter.

Thus, although the breadth of the isotopic niche in rodents is likely to be influenced by a number of factors that researchers are just beginning to explore, the ultimate niche breadth is constrained by the vegetation in a given habitat, and the 'placement' of that isotopic niche (along a C_3/C_4 continuum) in *Otomys,* at least, also appears to vary across vegetative space.

Conclusions

A number of recent studies have found that micromammal stable carbon isotope data can act as paleoenvironmental indicators (Hopley *et al.,* 2006; Hynek *et al.,* 2012; Kimura *et al.,* 2013). The new Pinnacle Point-proximate data presented here suggest that modern micromammal remains from pellets at a single predator roost location can sample a wide range of vegetation in a region, including vegetation communities proximate to but different from those on which the sampling locality itself is located.

Codron et al (2015) suggest that, based on their Cradle Nature Reserve data, within a taxon, there may be a relationship between the comparable breadths of a sampled isotopic niche and whether the specimens were feeding during the wet or dry seasons. If this pattern holds to be true across a number of vegetative domains, it could

have interesting implications for the study of micromammals from individual fossilized pellets, could they be recovered as such. There is unfortunately no such seasonal control on the collection of the Pinnacle Point-proximate modern pellets, and so whether the isotopic niche breadth differences between the Amisrus and the Rein's samples reflects a difference in seasonal feeding ecology cannot be tested.

However, intra-generic variation in modern $\delta^{13}C_{tissue}$ values across space suggests that, within the micromammal taxa sampled here, $\delta^{13}C_{tissue}$ values probably reflect both changes in niche-breadth due to local climatic factors, as well as differences in available $\delta^{13}C_{plant}$ between vegetation communities in different habitats.

What does this mean for the interpretation of stable carbon isotope data obtained from archaeological and fossil specimens? When measured isotopic niche breadth is wide, it would be impractical to assume wet-season aggregation (due to the palimpsest nature of these assemblages), but it would indicate that the entire population of micromammals being measured is more likely to sample the range of vegetation that was extant upon a landscape. Conversely, when the measured isotope niche of a particular taxon in a fossil locality is comparably narrow, caution in excluding other vegetation types from the paleoenvironmental reconstruction must be exercised. The data presented here, as well as the data available from the extant literature suggests that intra-generic narrow isotopic niches can occur in quite different vegetation contexts (so that the mean population values of $\delta^{13}C_{tissue}$ are quite different from one another, even when the breadth of both population values is quite narrow; see above, and also Thackeray *et al.*, 2003).

Chapter 3 References

Ambrose, S. and M. DeNiro (1986). "The isotopic ecology of East African mammals." Oecologia **69**(3): 395-406.

Arneson, L. S. and S. E. MacAvoy (2005). "Carbon, nitrogen, and sulfur diet-tissue discrimination in mouse tissues." Canadian Journal of Zoology **83**(7): 989-995.

Avery, D. M. (1982). "Micromammals as palaeoenvironmental indicators and an interpretation of the Late Quaternary in the southern Cape Province, South Africa." Annals of the South African Museum **85**: 183-374.

Avery, D. M. (1988). "Micromammals and paleoenvironmental interpretation in southern Africa." Geoarchaeology **3**(1): 41-52.

Bennett, N. C. and C. G. Faulkes (2000). African mole-rats: ecology and eusociality, Cambridge University Press.

Bocherens, H., P. L. Koch, A. Mariotti, D. Geraads and J.-J. Jaeger (1996). "Isotopic Biogeochemistry (^{13}C, ^{18}O) of Mammalian Enamel from African Pleistocene Hominid Sites." Palaios **11**(4): 306-318.

Cerling, T. E. and J. M. Harris (1999). "Carbon isotope fractionation between diet and bioapatite in ungulate mammals and implications for ecological and paleoecological studies." Oecologia **120**(3): 347-363.

Cerling, T. E., J. M. Harris and B. H. Passey (2003). "Diets of East African Bovidae based on stable isotope analysis." Journal of Mammalogy **84**(2): 456-470.

Cerling, T. E., J. A. Hart and T. B. Hart (2004). "Stable isotope ecology in the Ituri Forest." Oecologia **138**(1): 5-12.

Cerling, T. E. and Z. D. Sharp (1996). "Stable carbon and oxygen isotope analysis of fossil tooth enamel using laser ablation." Palaeogeography, Palaeoclimatology, Palaeoecology **126**(1-2): 173-186.

Codron, D., J. A. Lee-Thorp, M. Sponheimer, D. de Ruiter and J. Codron (2006). "Inter- and intrahabitat dietary variability of chacma baboons (Papio ursinus) in South African savannas based on fecal δ13C, δ15N, and% N." American Journal of Physical Anthropology **129**(2): 204-214.

Codron, J., K. J. Duffy, N. L. Avenant, M. Sponheimer, J. Leichliter, O. Paine, . . . D. Codron (2015). "Stable isotope evidence for trophic niche partitioning in a South African savanna rodent community." Current Zoology **61**(3): 397-411

Craig, H. (1954) “Carbon-13 in plants and the relationships between carbon-13 and carbon-14 variations in nature” Journal of Geology **62**:115–149

Crowley, B. E., M. L. Carter, S. M. Karpanty, A. L. Zihlman, P. L. Koch and N. J. Dominy (2010). "Stable carbon and nitrogen isotope enrichment in primate tissues." Oecologia **164**(3): 611-626.

Cuenca Bescos, G. (2003). "The micromammal record as proxy of palaeoenvironmental changes in the Pleistocene of the Sierra de Atapuerca (Burgos, Spain)." Quaternary climatic changes and environmental crises in the Mediterranean Region: 133-138.

Dauphin, Y., P. Andrews, C. Denys, Y. Fernandez-Jalvo and T. Williams (2003). "Structural and chemical bone modifications in a modern owl pellet assemblage from olduvai gorge (tanzania)." Journal of Taphonomy **1**: 209-232.

De Graaff, G. (1981). "The rodents of southern Africa." Durban: Butterworths.

Faith, J. T. (2011). "Ungulate community richness, grazer extinctions, and human subsistence behavior in southern Africa's Cape Floral Region." Palaeogeography, Palaeoclimatology, Palaeoecology **306**(3): 219-227.

Granjon, L. and E. R. Dempster (2013). Genus Gerbilliscus: Gerbils. Mammals of Africa. J. Kingdon, D. Happold, T. Butynskiet al, Bloomsbury. Volume **III**.

Hedges, R. E. M. (2002). "Bone diagenesis: an overview of processes." Archaeometry **44**(3): 319-328.

Henry, A. G., P. S. Ungar, B. H. Passey, M. Sponheimer, L. Rossouw, M. Bamford, . . . L. Berger (2012). "The diet of Australopithecus sediba; Supplementary Information." Nature **487**(7405): 90-93.

Hopley, P. J., A. G. Latham and J. D. Marshall (2006). "Palaeoenvironments and palaeodiets of mid-Pliocene micromammals from Makapansgat Limeworks, South Africa: a stable isotope and dental microwear approach." Palaeogeography, Palaeoclimatology, Palaeoecology **233**(3): 235-251.

Hynek, S. A., B. H. Passey, J. L. Prado, F. H. Brown, T. E. Cerling and J. Quade (2012). "Small mammal carbon isotope ecology across the Miocene-Pliocene boundary, northwestern Argentina." Earth and Planetary Science Letters **321-322**(0): 177-188.

Jarvis, J. U. M. (2013). Bathyergus suillus (Cape Dune Mole Rat). Mammals of Africa. J. Kingdon, D. Happold, T. Butynskiet al, Bloomsbury **III:** 646-648.

Jim, S., S. H. Ambrose and R. P. Evershed (2004). "Stable carbon isotopic evidence for differences in the dietary origin of bone cholesterol, collagen and apatite: implications for their use in palaeodietary reconstruction." Geochimica et Cosmochimica Acta **68**(1): 61-72.

Kesner, M., A. V. Linzey and C. T. Chimimba (2013). "*Aethomys namaquensis* (Namaqua Veld Rat)". Mammals of Africa. J. Kingdon, D. Happold, T. Butynski*et al.* **III:** 370-371.

Kimura, Y., L. L. Jacobs, T. E. Cerling, K. T. Uno, K. M. Ferguson, L. J. Flynn and R. Patnaik (2013). "Fossil mice and rats show isotopic evidence of niche partitioning and change in dental ecomorphology related to dietary shift in late Miocene of Pakistan." PloS one **8**(8): e69308.

Koch, P. L., N. Tuross and M. L. Fogel (1997). "The effects of sample treatment and diagenesis on the isotopic integrity of carbonate in biogenic hydroxylapatite." Journal of Archaeological Science **24**(5): 417-429.

Kohn, M. J., M. J. Schoeninger and W. W. Barker (1999). "Altered states: effects of diagenesis on fossil tooth chemistry." Geochimica et cosmochimica acta **63**(18): 2737-2747.

Lee-Thorp, J. and N. J. Van Der Merwe (1987). "Carbon isotope analysis of fossil bone apatite." South African Journal of Science; v. **83**(11) p. 712-715

Lee-Thorp, J. A. (1989). "Stable carbon isotopes in deep time: the diets of fossil fauna and hominids." PhD Dissertation, University of Cape Town.

Lee-Thorp, J. A. (2002). "Two decades of progress towards understanding fossilization processes and isotopic signals in calcified tissue minerals." Archaeometry **44**: 435-446.

Lindars, E. S., S. T. Grimes, D. P. Mattey, M. E. Collinson, J. J. Hooker and T. P. Jones (2001). "Phosphate $\delta^{18}O$ determination of modern rodent teeth by direct laser fluorination: an appraisal of methodology and potential application to palaeoclimate reconstruction." Geochimica et Cosmochimica Acta **65**(15): 2535-2548.

Longinelli, A., P. Iacumin, S. Davanzo and V. Nikolaev (2003). "Modern reindeer and mice: revised phosphate-water isotope equations." Earth and Planetary Science Letters **214**(3-4): 491-498.

Maree, S., Faulkes, C. and Griffin, M. 2008. *Bathyergus suillus*. The IUCN Red List of Threatened Species 2008: e.T2620A9462799 Downloaded August 2012, from http://www.iucnredlist.org/details/2620/0.

Matthews, T. (2004). The taxonomy and taphonomy of Mio-Pliocene and Late Middle Pleistocene micromammals from the Cape west coast, South Africa PhD Thesis, University of Cape Town, South Africa.

Matthews, T. (n.d.). A summary of the micromammal population from PP30 (Brown hyaena den). Unpublished report.

Matthews, T., C. Denys and J. E. Parkington (2005). The palaeoecology of the micromammals from the late Middle Pleistocene site of Hoedjiespunt 1 (Cape Province, South Africa). Journal of Human Evolution **49**(4): 432-451

Matthews, T., C. Marean and P. Nilssen (2009). "Micromammals from the Middle Stone Age (92 - 167 ka) at Cave PP13B, Pinnacle Point, south coast, South Africa." Paleontol. Afr **44**: 112-120.

Matthews, T., A. Rector, Z. Jacobs, A. I. R. Herries and C. W. Marean (2011). "Environmental implications of micromammals accumulated close to the MIS6 to MIS5 transition at Pinnacle Point Cave 9 (Mossel Bay, Western Cape Province, South Africa)." Palaeogeography, Palaeoclimatology, Palaeoecology. **302**(3-4): 213-229

Michaud, A. (2007). "d13C and d18O of Carbonates." 2014, from http://kfleb.asu.edu/Analytical/gIRMS/Instrumentandanalysis/Analytical/Methods/Carbonates.html.

Navarro, N., C. Lécuyer, S. Montuire, C. Langlois and F. Martineau (2004). "Oxygen isotope compositions of phosphate from arvicoline teeth and Quaternary climatic changes, Gigny, French Jura." Quaternary Research **62**(2): 172-182.

Nielsen-Marsh, C. M. and R. E. M. Hedges (2000). "Patterns of diagenesis in Bone II: Effects of acetic acid treatment and the removal of diagenetic CO2/3." Journal of Archaeological Science **27**: 1151-1159.

Parnell, A. and A. Jackson (2013). “Stable Isotope Analysis in R”. https://cran.r-project.org/web/packages/siar/siar.pdf

Passey, B. H. and T. E. Cerling (2006). "In situ stable isotope analysis (13 C, 18 O) of very small teeth using laser ablation GC/IRMS." Chemical Geology **235**: 238-249.

Passey, B. H., T. F. Robinson, L. K. Ayliffe, T. E. Cerling, M. Sponheimer, M. D. Dearing, . . . J. R. Ehleringer (2005). "Carbon isotope fractionation between diet, breath CO2, and bioapatite in different mammals." Journal of Archaeological Science **32**(10): 1459-1470.

Phillips, D. and P. Koch (2002). "Incorporating concentration dependence in stable isotope mixing models." Oecologia **130**(1): 114-125.

Phillips, D. L., R. Inger, S. Bearhop, A. L. Jackson, J. W. Moore, A. C. Parnell, . . . E. J. Ward (2014). "Best practices for use of stable isotope mixing models in food-web studies." Canadian Journal of Zoology **92**(10): 823-835.

Podelsak, D. W., A.-M. Torregrossa, J. R. Ehleringer, M. D. Dearing, B. H. Passey and T. E. Cerling (2008). "Turnover of oxygen and hydrogen isotopes in the body water, CO_2, hair, and enamel of a small mammal." Geochimica et cosmochimica acta **72**(1): 19-35.

Radloff, F. G. T. (2008). The ecology of large herbivores native to the coastal lowlands of the Fynbos Biome in the Western Cape, South Africa, PhD Thesis, Stellenbosch University.

Rebelo, A. G., C. Boucher, N. Helme, L. Mucina and M. C. Rutherford (2006). Fynbos Biome. The Vegetation of South Africa, Lesotho, and Swaziland. Pretoria, South African National Biodiversity Institute**:** 52-219.

Reed, D. N. (2003). Micromammal paleoecology: past and present relationships between African small mammals and their habitats PhD, Stony Brook University.

Robb, G. N., S. Woodborne and N. C. Bennett (2012). "Subterranean sympatry: an investigation into diet using stable isotope analysis." PloS one **7**(11): e48572.

Rogers, K. L. and Y. Wang (2002). "Stable isotopes in pocket gopher teeth as evidence of a Late Matuyama climate shift in the southern Rocky Mountains." Quaternary Research **57**(2): 200-207.

Royer, A., C. Lecuyer, S. Montuire, R. Amiot, S. Legendre, G. Cuenca-Bescos, . . . F. Martineau (2013). "What does the oxygen isotope composition of rodent teeth record?" Earth and Planetary Science Letters **361**: 258-271.

Sealy, J. C. and N.J. van der Merwe (1986). "Isotope Assessment and the Seasonal-Mobility Hypothesis in the Southwestern Cape of South Africa [and Comments and Replies]." Current Anthropology: **27**(2): 135-150.

Sharp, Z. and T. Cerling (1996). "A laser GC-IRMS technique for in situ stable isotope analyses of carbonates and phosphates." Geochimica et Cosmochimica Acta **60**(15): 2909-2916.

Skinner, J. D. and C. T. Chimimba (2005). The mammals of the southern African sub-region, Cambridge University Press.

Sponheimer, M. and J. A. Lee-Thorp (1999). "Alteration of enamel carbonate environments during fossilization." Journal of Archaeological Science **26**(2): 143-150.

Symes, C. T., J. W. Wilson, S. M. Woodborne, Z. S. Shaikh and M. Scantlebury (2013). "Resource partitioning of sympatric small mammals in an African forest-grassland vegetation mosaic." Austral Ecology **38**(6): 721-729.

Taylor, P. J. (2013). “Genus Otomys: Vlei Rats”. Mammals of Africa Volume III: Rodents, Hares and Rabbits .Happold, D. C. D. (ed.). Bloomsbury Publishing, London, United Kingdom,

Thackeray, J. F. (1987). "Late Quaternary environmental changes inferred from small mammalian fauna, southern Africa." Climatic Change **10**(3): 285-305.

Thackeray, J. F., A. van der Venter, J. Lee-Thorp, C. T. Chimimba and J. van Heerden (2003). "Stable carbon isotope analysis of modern and fossil samples of the South African rodent Aethomys namaquensis." Annals of the Transvaal Museum **40**: 43-46.

Thermo Finnigan (2002). Kiel Carbonate Device Operating Manual.

Tieszen, L. L. and T. W. Boutton (1989). Stable carbon isotopes in terrestrial ecosystem research. Stable isotopes in ecological research, Springer**:** 167-195.

Tieszen, L. L. and T. Fagre (1993). Effect of diet quality and composition on the isotopic composition of respiratory CO2, bone collagen, bioapatite, and soft tissues. Prehistoric Human Bone, Springer**:** 121-155.

Tutken, T., T. W. Vennemann, H. Janz and E. P. J. Heizmann (2006). "Palaeoenvironment and palaeoclimate of the Middle Miocene lake in the Steinheim basin, SW Germany: A reconstruction from C, O, and Sr isotopes of fossil remains." Palaeogeography, Palaeoclimatology, Palaeoecology **241**(3-4): 457-491.

Van den Heuvel, I. M. and J. J. Midgley (2014). "Towards an isotope ecology of Cape Fynbos small mammals." African Zoology **49**(2): 195-202.

Wang, Y. and T. E. Cerling (1994). "A model of fossil tooth and bone diagenesis: implications for paleodiet reconstruction from stable isotopes." Palaeogeography, Palaeoclimatology, Palaeoecology **107**(3-4): 281-289.

Yeakel, J. D., N. C. Bennett, P. L. Koch and N. J. Dominy (2007). "The isotopic ecology of African mole rats informs hypotheses on the evolution of human diet." Proceedings of the Royal Society B: Biological Sciences **274**(1619): 1723-1730.

4. Micromammal and macromammal fauna stable isotopes from a MIS6 fossil hyena den Pinnacle Point 30 (south coast of South Africa) reveal differences in relative contribution of C_4 grasses to local paleovegetation on different geographic scales.

Abstract

There are a number of hypotheses about the impact of glacial climate change on southern African paleoenvironments, but proxy records that date to the Middle Pleistocene in particular are relatively scarce, especially along the southern coast of the continent. This study presents integrated micromammal and macromammal stable isotope paleoenvironmental proxy data from one of the few well-dated MIS6 fossil occurrences in the region, a fossil brown hyena (*Parahyena brunnea*) den Pinnacle Point 30 (PP30). Two predators with significantly different foraging ranges aggregated the large and small mammal components of the PP30 fossil assemblage. The large mammal specimens were brought to PP30 by *Parahyena brunnea* (with a likely daily foraging radius in excess of 170km, based on modern analogue; Wiesel 2007; Mills 1990), while the micromammal taxa were deposited at the site primarily by the spotted eagle owl, *Bubo africanus* (Matthews, nd) with a foraging radius of ~3km (Andrews, 1990; Matthews, 2004). Hynek *et al.*, (2012) have argued that micromammal stable isotope data act as a proxy for very local conditions, while large faunal analyses produce data that reflects a broader regional scale; and it is here proposed that the large and small mammal components of the PP30 assemblage also sample paleovegetation at different geographic scales. Comparison of the stable carbon isotope data obtained from the PP30 micromammal and macromammal fossil specimens suggests that these two assemblage components intersected vegetation

with differing proportions of C_4 grasses. Micromammal $\delta^{13}C$ proxy data indicates that, immediately local to the site, a C3 dominated vegetation—likely similar to that extant in the region today—was present at PP30 at 151 ka; large fauna $\delta^{13}C$ proxy data, conversely, shows evidence of a vegetation community with a significant C_4 grass component that likely occurred somewhat more distant from the site itself.

Introduction

Quaternary paleoenvironments in Africa are often contextualized within a framework of glacial/interglacial variation, where aridity during glacial periods significantly impacts the biogeography and diversity of both flora and fauna. However, local proxy records and vegetation modeling both suggest highly variable regional paleoenvironmental responses to changes in major abiotic factors across the continent (Scholz *et al.,* 2007; Cowling *et al.,* 2008; Blome *et al.,* 2012). This is especially true in many parts of southern Africa where the distinctive local climatic and environmental features likely had unique responses to changing global factors, because these features arise independently of the primary drivers of climate/environmental change in the rest of Africa (Muller and Tyson, 1988; Barrable *et al.,* 2002; Stuut *et al.,* 2004; Reason and Rouault, 2005; Chase and Meadows, 2007). A clearer picture of the impact of global Pleistocene climate change on local environment(s) within regions and sub-regions of Africa is especially important to paleoanthropologists because genetic and fossil data suggest that it is near the end of the Middle Pleistocene that modern *Homo sapiens* first appears (Cann, 1988; Ingman *et al.,* 2000; Clark *et al.,* 2003; White *et al.,* 2003;

McDougall *et al.*, 2005). Many workers have hypothesized that the evolution of modern *H. sapiens* was partially driven by adaptive responses of Middle Pleistocene *Homo* to fragmented African environments during MIS6 and MIS7 (Lahr and Foley, 1994; Lahr and Foley, 1998; McBrearty and Brooks, 2000; Henshilwood *et al.*, 2006; Marean, 2010).

Southern Africa has a rich archaeological and fossil hominin record dating back to the Pliocene (Dart, 1925; Klein, 1999; Kuman and Clarke, 2000; Berger *et al.*, 2002; Mitchell, 2002; Marean *et al.*, 2005; Barham and Mitchell, 2008; Berger *et al.*, 2010), and much of the Late Pleistocene evidence for "behavioral modernity" is concentrated along the south coast (Henshilwood *et al.*, 2004; d'Errico *et al.*, 2005; d'Errico and Henshilwood, 2007; Marean *et al.*, 2007; Brown *et al.*, 2009; Henshilwood *et al.*, 2009; Henshilwood *et al.*, 2011; Brown *et al.*, 2012; Marean *et al.*, 2014). However, although there are several Middle Pleistocene archaeological and fossil localities in East Africa, assemblages in southern Africa are rare for this period. Well-dated paleoenvironmental proxy records for the region are even sparser (Marean *et al.*, 2014).

In order to address the gap for the southern Cape of South Africa, presented here are tandem micromammal and macromammal stable carbon and oxygen isotope data for one of only two fossil-bearing localities on the south coast of South Africa that is well-dated to the Middle Pleistocene (Jacobs, 2010; Rector and Reed, 2010; Marean *et al.*, 2014), the MIS6-age fossil hyena den Pinnacle Point 30 (PP30). Tandem micromammal and large mammal isotope data has the potential to provide a more complete picture of local and regional vegetation than either data set alone, as isotopic data from micromammals and large mammals represent the prey of very different accumulators - in the case of PP30, brown hyena (*Parahyena brunnea*; Lansing *et al*., 2009) and owls

(likely the spotted eagle owl, *Bubo africanus,* based on incisor digestion patterns; Matthews, n.d.). Owls and hyenas sample distinct faunal communities and create accumulations that differ significantly in taxonomic representation. These differing prey communities of owls and hyenas also likely sample different parts of the ancient ecosystem, with differing stable isotopic values of plants, and thus considering accumulations of both will significantly enrich our understanding of past environments. The predation ranges of raptors such as owls are comparably small (r =~3km, or ~28.27 km^2) when compared to the ranges of large carnivores such as hyenas (Figure 4.1)(Andrews, 1990; Mills, 1990; Matthews, 2004), and the habitat from which the predator selects prey items is reflected in the isotopic composition of the fossil assemblages.

Furthermore, these herbivorous mammalian taxa have distinctive life histories and foraging ranges. Small fauna tend to have restricted home ranges, while large herbivores, even those not part of migration ecosystems, tend to have significantly larger ranges. Thus micromammals and large mammals should sample different components of both site-local and regional environments (e.g. Hynek *et al*., 2012). In ecotones or other localities where habitat heterogeneity is likely to have been present, direct comparison of the micromammal and large mammal stable isotope data may provide a more comprehensive view of paleovegetation that reflects taxon-specific behavior, herbivore foraging ranges and predator ranges.

Stable carbon and oxygen isotope data obtained from fossil tooth enamel have long been applied as proxies for paleoenvironmental conditions. Most of these data were generated from large mammalian fauna however. Sampling of very small mammalian

fauna to produce stable isotope data sets that are likely to reflect environmental conditions over a narrower geographic range is a relatively recent phenomenon (Hopley *et al.*, 2006; Yeakel *et al.*, 2007; Thackeray *et al.*, 2008; Gehler *et al.*, 2012; Hynek *et al.*, 2012; Kimura *et al.*, 2013). Furthermore, methodological advances in mass spectrometry now permit sampling of very small specimens including the use of laser ablation (Cerling and Sharp, 1996; Sharp and Cerling, 1996; Lindars *et al.*, 2001; Passey and Cerling, 2006; Grimes *et al.*, 2008; Podelsak *et al.*, 2008). Laser ablation gas chromatograph isotope ratio mass spectrometry (LA-GC-IRMS) was here used to acquire the stable carbon and oxygen isotope data from the micromammal specimens recovered from PP30, while 'conventional' H_3PO_4 $\delta^{13}C$ and $\delta^{18}O$ data was acquired by sampling large mammal teeth from the same locality.

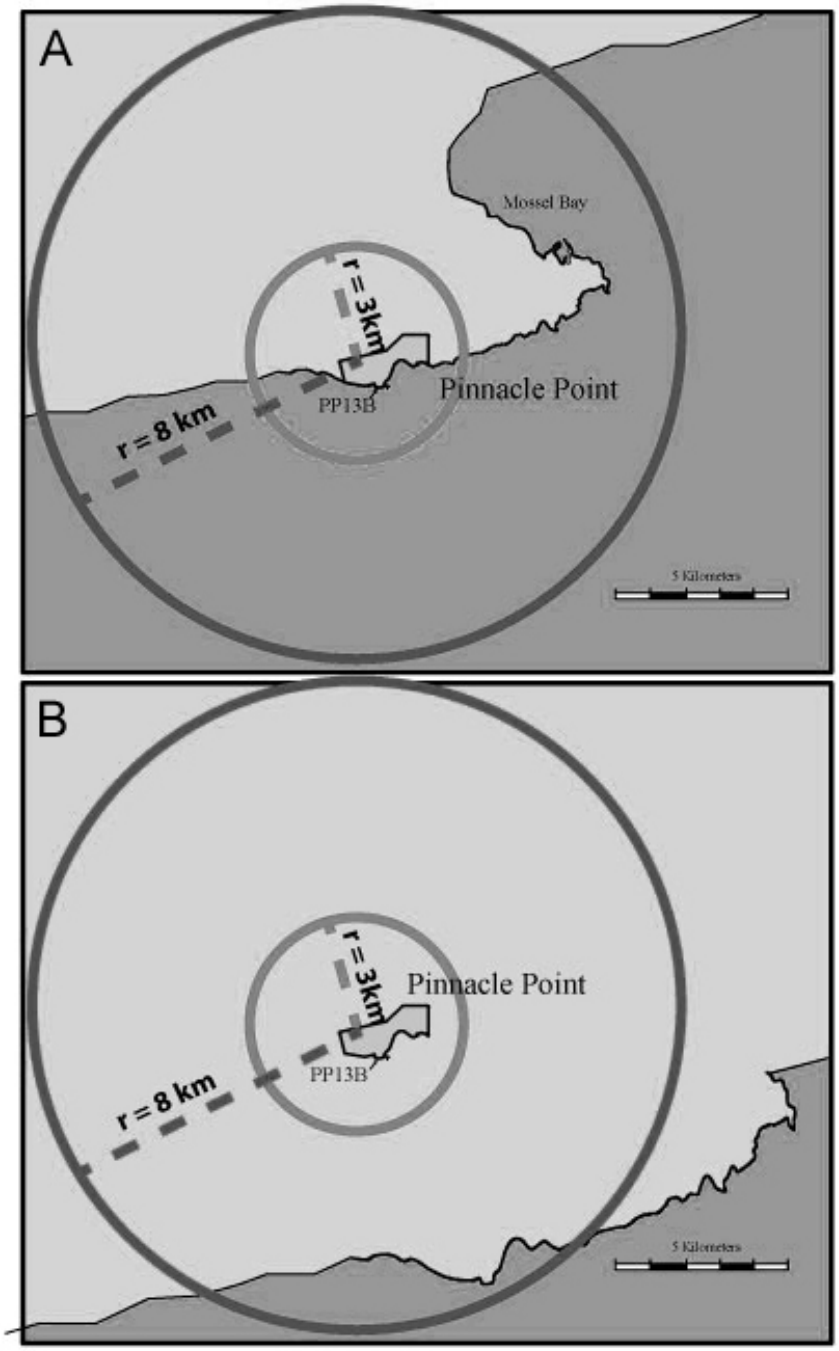

Figure 4.1. Cartoon of the foraging radius of owls (small circle) at PP13B during interglacial (A) and glacial (B) conditions. The larger circle represents the foraging range of large predators, such as hyaenids and humans

Environmental and Climatic Features

Most of southern Africa, with the exception of the southwest and southern Cape, falls under the influence of a summer rainfall regime that ultimately derives from the southward movement of warm wet airflow over the southern African interior (Partridge *et al.*, 1997; Tyson, 1999). Conversely, the southwest tip of Africa is under the influence of a winter rainfall regime that does not penetrate further north, and arises from distinct sea surface temperature patterns and the action of the mid-latitude westerlies, and is strongly affected by processes other than the summer rainfall that arises from the Indian Ocean monsoonal systems (Tyson, 1999). Where the winter and summer rainfall zones converge, which in the present day occurs along the southern coast of the continent, this intersectection produces a zone of year-round rainfall that is less-strongly seasonal.

Both geographic distribution and intensity of rainfall in the winter, year-round and summer rainfall areas are linked to sea surface temperatures (STTs) in the South Atlantic/Antarctic Oceans and the Indian Oceans respectively, as well as the latitudinal location of the prevailing atmospheric systems (see Chase and Meadows, 2007). Pole-ward or equator-ward shifts in the location of the intertropical convergence zone(s) (ITCZ) from which the prevailing winds derive, and as well as fluctuating SSTs over the course of the Pleistocene, likely altered the amount of rainfall and the distribution of winter and summer rain over southern Africa (Van Zinderen Bakker, 1976; Meadows and Baxter, 1999; Chase and Meadows, 2007; Marean *et al.*, 2014).

While the structure of vegetation communities is also constrained by the characteristics of underlying bedrock and soils (Cowling, 1983; Goldblatt, 1997; Cowling

et al., 2009) the impact of geology on vegetation at a given tectonically stable locality can be treated as more or less a constant for the duration of the Pleistocene. Of the variable climatic factors that impact vegetation communities, changing aridity and seasonality of rainfall (along with decreasing atmospheric CO_2 concentrations) is a primary underlying driver of changes in local vegetation communities.

In present-day southern African plant communities there is a strong relationship between the predominant photosynthetic pathway of grasses and the occurrence of winter or bi-model/summer rain (Vogel *et al.*, 1978). Grasses using C_4 photosynthesis are dominant in most of the summer rainfall zone because they require warm growing season temperatures, while C_3 grasses are confined to those areas with cool growing seasons. In the present day, the south coast of South Africa is home to the unique Greater Cape Floristic Region (GCFR), which, partially due to its relatively high proportion of geophytic plants and richly productive coastline, has been hypothesized to have been a potential refugium environment for early modern humans during glacial phases (Marean 2010; Marean, 2011). The GCFR has a variety of biomes, and those in the predominantly winter rainfall regime are dominated by shrubs and grasses that use C_3 photosynthetic pathways, while C_4 grasses are significantly more common in those areas where rain is in the summer (Cowling, 1983; Cowling and Richardson, 1995). Pleistocene changes in the distribution or frequency of winter rainfall in a given region would thus have significantly impacted the composition of local floral communities. Furthermore, if exposure of the now-offshore Agulhas bank (the "Paleo-Agulhas", Figure 4.1) was concomitant with increased summer rainfall in the region, more C_4 grass-dominated

environments might have become available to faunal communities (Bar-Matthews *et al.*, 2010; Marean *et al.,* 2014).

C_3 and C_4 photosynthetic pathways fractionate carbon (as part of CO_2 fixation) such that the tissues of C_4 plants are significantly enriched in $\delta^{13}C$ relative to C_3 plants (Bender, 1971; Smith and Epstein, 1971). Change in the relative contribution of C_4 grasses to paleovegetation communities in a region will be reflected in the isotopic composition of consumer diets and thus by extension consumer tissues, such that taxa with diets with a significant C_4 grass component will be comparably enriched in $\delta^{13}C_{enamel}$ values relative to taxa consuming primarily C_3-vegetation (DeNiro and Epstein, 1978; Lee-Thorp and Van Der Merwe, 1987; Cerling and Harris, 1999; Sponheimer *et al.,* 2003b).

The site

PP30 is a paleontological locality that occurs within a cave in a calcrete layer stratified above the Table Mountain Sandstone cliffs at Pinnacle Point, South Africa (Rector and Reed, 2010). It was excavated as a salvage operation when it was discovered by trenching to lay pipes for a development. Excavations followed most of the procedures typical for excavations at Pinnacle Point (Marean *et al.,* 2004; Bernatchez and Marean, 2011; Oestmo and Marean, 2014) though some strict requirements were relaxed due to the salvage nature of the excavations. All sediments were screened through nested 10mm, 3mm, and 1.5 mm screens, and additional fossil material was thus recovered. Minimal stratigraphic variation, and the uniformity of staining and fossilization of the fauna suggests that the assemblage was accumulated over a comparably short period of

geologic time (Rector and Reed, 2010). Optically stimulated luminescence (OSL) ages from sediment matrix indicate a relatively constricted period of deposition that dates to about 151 ka during the MIS6 glacial (Rector and Reed, 2010).

The presence of carnivore-modified bone, carnivore bones (especially brown hyena) and Brown Hyena (*Parahyaena brunnea*) coprolites indicate that the assemblage was accumulated by *Parahyaena brunnea* (Lansing *et al.,* 2009). The apparent rapid deposition and relatively constrained chronometric ages from PP30 are also consistent with this diagnosis as brown hyena dens are areas of rapid accumulations of large numbers of vertebrate remains (Skinner and Van Aarde, 1991; Skinner *et al.,* 1998). Digestive etching on the PP30 micromammal incisors is most similar to the pattern observed in modern spotted eagle owl (*Bubo africanus*) assemblages, and thus *Bubo africanus* is considered to be the aggregator of the small mammal portion of the assemblage (Matthews, n.d.), although the high frequency of un-etched incisors (23.21% of the assemblage) is uncommon in modern eagle owl collections (Matthews, n.d.).

PP30 is today located proximate to the present-day coast. However, lowered sea levels during glacial intervals in the Pleistocene would have resulted in a retreat of the coastline and exposure of the Paleo-Agulhas Plain. Paleoscape modeling of Pleistocene shorelines in the region (Fisher *et al.,* 2010) puts the coast at c. 151 ka approximately 90km from the site (Figure 4.1). Retreat of the coastline, associated with impacts on regional rainfall, plus possible changes in the seasonality of rainfall suggested by various climate models, may have altered the composition of vegetation communities in the region, both through alteration of the relative proportion of C_3 and C_4 grasses in vegetation communities along the present-day south coast, and the possible introduction

of a grassland ecosystem component on the paleo-Agulhas plain (Marean *et al.,* 2014). Changes in the relative frequency of C_3 and C_4 grass components in both site-local and regional vegetation are difficult to tease apart using either large fauna isotope data or micromammal isotope data alone; given the large ranges and migratory habits of many large grazers, it is often difficult to separate local vs. regional proxy vegetation signals from one another without a baseline to which the large fauna data can be compared (Koch, 1998; Hynek *et al.,* 2012). Conversely, the relatively restricted ranges of both the micromammal taxa and accumulating agents such as owls, would sample a diversity of near-site habitats, but could miss further afield vegetation communities that would be sampled by the larger taxa.

Given that the large faunal fossil assemblage from PP30 contains ungulate taxa indicative of both grassland ecosystems and GCFR vegetation (Rector and Reed, 2010; Marean *et al.,* 2014), the use of complementary large fauna and micromammal isotope data will be especially useful in addressing issues of geographic scale in the paleoenvironmental reconstruction of habitats near PP30 during MIS6.

Materials and Methods

Materials

A large sample of both cranial and post-cranial micromammal remains was recovered from PP30, both *in situ*, and in the screened sediments. One hundred and two specimens were identified to species by Matthews (nd) (Table 4.1). The micromammal assemblage from PP30 is dominated by the Otomyinae (vlei rats), and shows a low taxonomic diversity. All micromammal species present in the assemblage occupy a broad diversity of habits and thus are not themselves diagnostic of any particular paleoenvironmental condition(s) (Matthews, nd).

Micromammal specimens from the PP30 assemblage are housed at the Diaz Museum, Mossel Bay, South Africa. Permission to sample the PP30 micromammals was granted by the South African Heritage Resources Agency (SAHRA export and destructive analysis permit 80/12/03/014/52). Taxonomically identified teeth were examined for signs of surface alteration, burning, staining, or adhering calcretions. One hundred and three micromammal teeth, including those with non-specific taxonomic identifications, were preliminarily identified in the field as suitable for laser ablation GC-IRMS. Of these, approximately half were exported for analysis per the restrictions of the SAHRA permit. Soricidae (*M. varius*) and chiroptera (*Rhinolophus*) from the PP30 assemblage were not sampled because both taxonomic groups are insectivorous. *M. albicaudatus* and *R. pumilio* specimens were also excluded, although the one gerbillid (*G. afra*) specimen was sampled. The resulting taxonomic composition of the micromammal isotope sample (Table 4.2) is thus primarily composed of *Otomys* specimens. However,

the relative species representation in the isotope sample is still comparable to that of the larger assemblage (Figure 4.2).

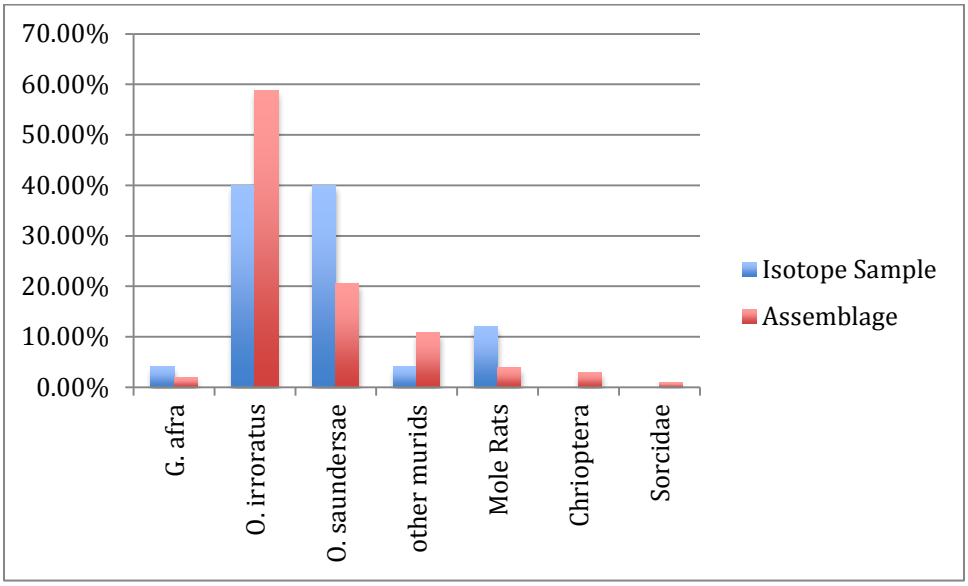

Figure 4.2. Relative representation of taxa in the total micromammal assemblage and in the isotope sample (all sampled specimens).

	n	%
Muridae		
G. afra	2	1.96
M. albicaudatus	4	3.92
R. pumilio	6	5.88
O. saundersiae	21	20.59
O. irroratus	60	58.82
Otomys sp. (saundersiae/irroratus)	1	0.98
Soricidae		
M. varius	1	0.98
Bathyergidae		
G. capensis	1	0.98
C. hottentotus	1	0.98
B. suillus	2	1.96
Chiroptera		
Rhinolopus sp. (? clivosus)	3	2.94
Total	**102**	

Table 4.1. Micromammal species representation at PP30 (from Matthews, nd)

Taxon	Specimen n	Analysis n
G. afra	1	1
O. irroratus	10	12
O. saundersiae	10	13
Indet. mole rat	3	6
Indet. Murid	1	2
Total	25	34

Table 4.2. Taxonmic identifications of sampled specimens (includes all sampled specimens, including those for which data was discarded for quality control reasons).

Sampling Procedures: Micromammals

LA-GC-IRMS was performed at the stable isotope lab at Johns Hopkins University (Baltimore, USA), using the procedures described in detail in Passey and Cerling (2006). Specimens were mounted on an adjustable stand within a vacuum chamber, which was then flushed for a minimum of 4 hours with inert He gas to remove the atmospheric CO_2 from the chamber. Blank measurements were taken at the beginning of each chamber run prior to ablation sampling to ensure that the He flush of the chamber was complete. Blank measurements were also taken at periodic intervals during each sampling run to ensure the integrity of the vacuum chamber (e.g. no leaks that might allow contaminant atmospheric CO_2 into the chamber), to monitor potential CO_2 off gassing from specimens during the course of the sampling run, and to calculate background CO_2 blank fraction for CO_2 peaks produced by specimen ablation (Passey and Cerling, 2006).

Groups of specimen ablations were bracketed with measurement of a reference gas of known isotopic composition which was injected into the chamber. Isotope data obtained from fossil specimens was normalized to VPDB ($\delta^{13}C$) and VSMOW ($\delta^{18}O$), using the reference CO_2 values (Passey and Cerling, 2006). Internal enamel standards of modern large mammal enamel were also included in the sample chambers, and measured at regular intervals.

Specimen ID	**Taxon**	**Tooth Sampled**	**n ablation**	***in situ?***
100464	Indet. mole rat	incisor	2	
100475	Indet. mole rat	incisor	2	
100491	Indet. mole rat	incisor	2	
100486	Indet. mole rat	incisor	2	Y
100584b	*O. saundersiae?*	incisor	2	Y
100584a	*O. saundersiae*	MU3	1	
100583	*O. saundersiae*	MU3	1	
100523	*O. saundersiae*	MU3	2	
100549	*O. saundersiae*	ML1	1	
100559	*O. saundersiae*	ML1	1	
100570	*O. saundersiae*	ML1	1	
100573	*O. saundersiae*	ML1	1	
100575	*O. saundersiae*	ML1	1	
100586	*O. saundersiae*	ML1	2	
100503	*O. irroratus*	MU3	1	
100518	*O. irroratus*	MU3	1	
100574	*O. irroratus*	MU3	1	
100580	*O. irroratus*	MU3	2	
100521b	*O. irroratus*	MU3	1	
100505	*O. irroratus*	ML1	1	
100511	*O. irroratus*	ML1	1	
100522	*O. irroratus*	ML1	1	
100589a	*O. irroratus*	ML1	1	
100589b	*O. irroratus*	ML1	2	
100534a	*G. afra*	MU1	1	

Table 4.3. Tooth type sampled (by SACP4 specimen id number). MU1 = 1st maxillary molar. MU3 = 3rd maxillary molar. ML1 = 1st mandibular molar

Each specimen was ablated using a Photon-Machines Fusions 30 watt CO_2 laser operating at 5% power and with a dwell time of 0.01 seconds. Ablation produces CO_2 gas, which is then transported by carrier He gas, and the gas sample(s) are aggregated and then 'cryofocused' in a liquid nitrogen trap (Cerling and Sharp, 1996; Sharp and Cerling, 1996; Passey and Cerling, 2006). The He carrier gas is then separated from the CO_2 gas in the gas chromatograph and the CO_2 introduced into the mass spectrometer (Passey and Cerling, 2006).

Ablation pit sizes were 30μm in diameter, and between 10 and 40 ablation pits were produced for each specimen-sampling event. The production of multiple ablation pits for each enamel sample is necessary, as single ablation events do not individually produce enough CO_2 gas for analysis by the IRMS (Passey and Cerling, 2006). Ablation pits were produced in a non-overlapping pattern preset for each sample using the laser-targetting software (Figure 4.3). Number of laser shots was increased when Vs area of blanks were slightly larger than ideal, in order to minimize the impact of residual CO_2 on the analytical signal produced by specimen ablation. The specimen stand within each chamber was adjusted between sampling of each specimen in order to rotate the surface of each tooth orthogonal to the path of the laser. Any 'charring' produced during the formation of an ablation pit is indicative of laser combustion of non-enamel organic material (Henry *et al.*, 2012, SOM): six ablation runs from five specimens were eliminated from the final analysis because significant "charring" on the edge of the ablation pits was noted during the analysis.

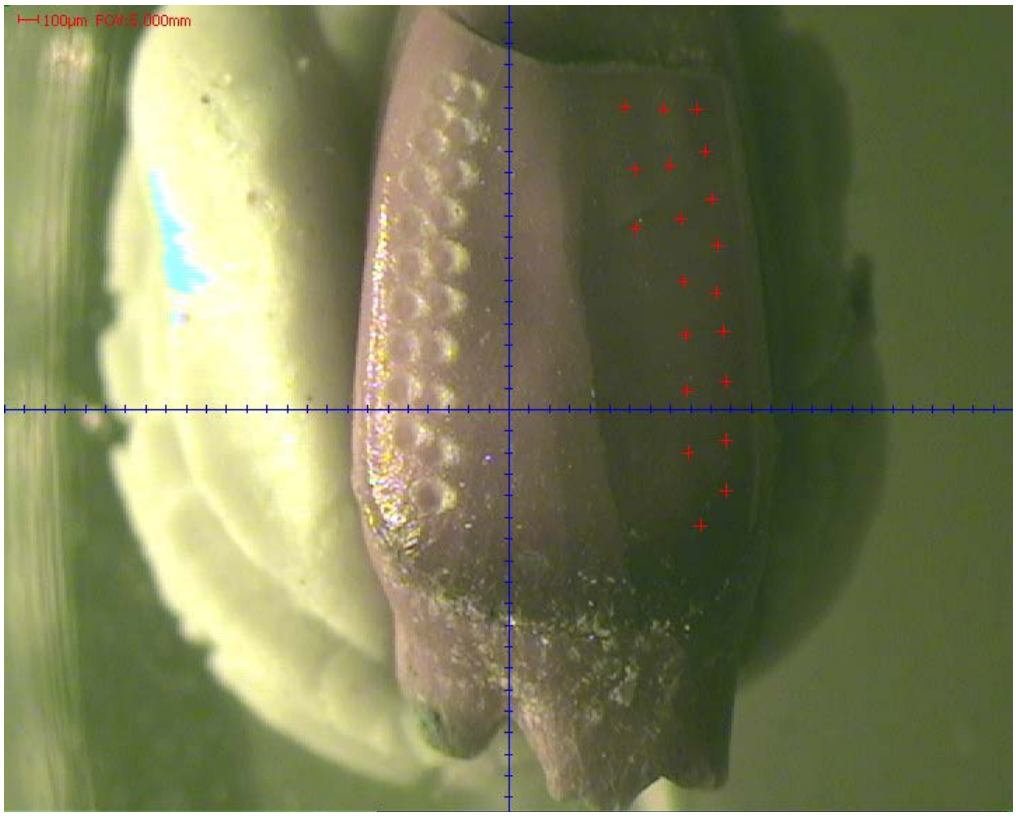

Figure 4.3. Image of a mounted specimen after LA-GC-IRMS sampling. Ablation pits are visible along the left margin of the tooth surface. Note lack of char on pit margins and the non-overlapping nature of the ablation pits.

Replicate measures made on fossil mole rat specimen #100464 produced $\delta^{13}C$ values of -12.4‰ and -11.8‰ VPDB (σ= 0.43), and $\delta^{18}O$ values of 25.2‰ and 25.1‰ (σ=0.05). All replicate data (including specimens not discussed in this paper but obtained during the same sampling period) from 46 replicate sets result in mean σ for $\delta^{13}C$ of 0.39 (range = 0‰ - 1.99‰), and a mean σ for $\delta^{18}O$ of 0.40 (range = 0‰ -1.33‰).

Two sets of replicate LA-GC-IRMS measurements of internal large mammal enamel standards were made during the collection of the PP30 micromammal isotope data (Table 4.4). The dispersion of LA-GC-IRMS carbon and oxygen data obtained from K00-TSV-223-1 and K00-AB-301-1 during the PP30 data collection period is larger than

Sample ID	δ^{13}C‰ VPDB	difference δ^{13}C	mean	σ	δ^{18}O‰ VSMOW	difference δ^{18}O	mean	σ
K00-TSV-223-1	-1.0				25.3			
K00-TSV-223-1	-1.2	0.20	-1.06	0.14	25.2	0.01	25.25	0.01
K00-AB-301-1	-13.5				21.0			
K00-AB-301-1	-11.7	1.74	-12.60	1.23	19.2	1.83	20.08	1.29

Table 4.4. δ^{13}C and δ^{18}O values obtained for internal enamel standards during the period in which the PP30 data was collected. Isotope data are normalized to VPDB (carbon) and VSMOW (oxygen). K00-TSV-223-1 is a modern large grazer (African buffalo (*Syncerus caffer*)) which is more enriched in ^{13}C and consistent with a grazing diet of primarily C_4 plants; K00-AB-301-1 is a modern Black Rhinoceros (*Diceros bicornus*) browser.

that of the replicate measurements made on the fossils themselves, but is within a range of acceptable precision for carbon and oxygen isotope measurements made on carbonates. The carbon and oxygen isotope values of K00-AB-301 and K00-TSV-223-1 are consistent with other LA-GC-IRMs-obtained values from those same specimens over a longer sampling period (unpublished data), and thus the larger range of variation in isotope values obtained from the large fauna enamel standards using LA-GC-IRMS may in part be an effect of sample heterogeneity in the enamel of large fauna (see Sharp and Cerling, 1996).

Modern micromammal specimens were collected from Amisrus, Lake Island, Wilderness and Wolwe River – where the present-day vegetation is some of the most closed/C_3 vegetation in the region (Figure 4.1), and from Rien's Nature reserve, where the sampling locality intersects modern beach vegetation and is proximate to large expanses of limestone fynbos. Identified specimens were selected for analysis based either on the presence of multiple molar teeth, or in-situ incisors.

Specimens were sonicated for 15 minutes in 18.2 MΩ H_2O, and were then dried overnight at 50°C in a laboratory oven. Teeth were extracted from the dental arcade by tweezers. Enamel samples were then collected either by drilling teeth using a Dremel equipped with a clean carbide drill bit, or alternatively, specimen teeth were partially crushed in an agate mortar, enamel was separated from dentine under a light microscope, and separated enamel was then finely ground in a clean agate mortar. In all cases where molars rather than incisors were sampled, multiple posterior teeth from each individual were aggregated to produce enough enamel for analysis.

Once enamel specimens were obtained, enamel pretreatment was performed at the Archaeological Chemistry Laboratory (ASU, USA), following standard in-house procedures. Enamel specimens were soaked in 2% NaOCl at a ratio of 0.04 mL/mg_{sample} for 24 hours to remove organic contaminants. The NaOCl solution was then decanted, samples were rinsed 3x in 0.50 mL 18.2 MΩ H_2O, and 0.04 mL/mg_{sample} of 0.1 M acetic acid (CH_3COOH) was added to the enamel samples to remove any contaminant carbonate material. After 24 hours, the CH_3COOH was decanted, and specimens were again rinsed 3x in 0.50 mL 18.2 MΩ H_2O, before being dried at 50°C until dry.

'Wilderness' micromammal specimens were sampled as part of a pilot project, and were analyzed at the W. M. Keck Foundation Laboratory for Environmental Biogeochemistry (ASU) using a gas bench system to input samples into a Thermo Deltaplus Advantage mass spectrometer. To reduce necessary sample size (see Chapter 3), modern samples obtained from specimens collected from Reins Nature Reserve were analyzed by the University of Arizona Environmental Isotope Laboratory using a Kiel-III attached to a Finnegan MAT252. In both cases, enamel samples were reacted with 100%

H_3PO_4 at 70°C to produce evolved CO_2 for introduction to the mass spectrometer. Resultant stable carbon and oxygen isotope data were normalized using known values of the standards measured during the analytical runs, NBS 18 and NBS 19 (see Chapter 3).

*Sampling Procedures: Large Mammals**

Isotopic analysis of enamel from large herbivores from PP30 was performed by J.A. Lee-Thorp at the University of Bradford Light Stable Isotopes Facility, and the resultant unpublished raw data was provided to Williams for comparison with the PP30 micromammal stable isotope data.

Prior to analysis, the large mammal teeth were mechanically cleaned; enamel samples were then obtained by drilling along the long axis of the tooth, a sampling strategy that averages enamel over the entire growth period of the tooth and thus results in a 'bulk' sample (Lee-Thorp, nd). Enamel powder samples were chemically pretreated following the techniques described in Lee-Thorp *et al*. (1997) and Sponheimer and Lee-Thorp (2001) (Lee-Thorp, nd). Sample CO_2 was evolved via phosphoric acid digestion, and introduced to a Thermo Finnigan Delta V mass spectrometer via Gasbench/GC system: measurement precision for the data provided by Lee-Thorp is better than 0.1‰ for carbon isotope data, and 0.3‰ for oxygen isotope data (Lee-Thorp, nd).

Results

All isotope data are reported using delta notation relative to the standards VPDB (all carbon data, and modern specimen oxygen data prior to transformation) or VSMOW (all fossil oxygen data), following convention.

Micromammals:

Twenty-seven isolated and in situ fossil micromammal teeth were sampled using LA-GC-IRMS; data collected from fifteen specimens was excluded from this analysis on the basis of large blank fractions, which potentially compromised the accuracy of isotope measurements made on those specimens (Passey and Cerling, 2006). Data from an additional five specimens was excluded from analysis due to char on the edges of the ablation pits. The remaining dataset is comprised of 10 isotope measurements made on 9 individual specimens. Excluded large fraction blanked data is however included in a supplementary table (Supplementary Table 1).

Micromammal carbon isotope composition:

The $\delta^{13}C_{enamel}$ VPDB values obtained by laser ablation of the fossil micromammal specimens range from -9.3‰ to -14.1‰ VPDB, and are summarized by taxon in Table 4.5. A normal distribution of the stable carbon isotopic composition of a population of animals from a given taxonomic group (as dietary variability is the driving factor in an individual's enamel isotope ratio) is not assumed; as such, comparisons of the isotopic composition of different populations from different taxonomic groups uses the non-

parametric Kruskal-Wallis (K-W) Test with Dunn's multiple comparison (post hoc) to test for significant differences in stable carbon isotope composition between the *Otomys irroratus*, *Otomys saundersiae*, and mole rat fossil populations reported here.

	n	Minimum δ13C ‰VPDB	Maximum δ13C ‰VPDB	Mean δ13C ‰VPDB	σ
Indet. mole rat	3	-12.4	-9.3	-11.2	1.7
O. irroratus	4	-14.5	-10.7	-12.9	1.6
O. saundersiae	3	-14.1	-11.5	-12.9	1.3

Table 4.5. Summary statistics for the stable carbon isotope data obtained from the PP30 micromammal specimens, by taxon. Table shows only data for which instrumental fraction blanks were smaller than 0.15. Large-blanked data can be found in Supplemental Table 1.

A KW test indicates no significant differences between the stable carbon isotope values of the populations of *O. irroratus*, *O. saundersiae*, and mole rats sampled (H= 2.248, p =0.36) (Figure 4.4). This general pattern is somewhat inconsistent with analyses of other micromammal data from the region (Williams, in prep-a; Williams, in prep b) in which the mole rats are comparably more enriched in ^{13}C than other micromammal taxa, and is likely to be a function of the smaller sample size in this study. Additional mole rat specimens that were excluded from the analysis on the basis of larger fraction blanks during analysis (Supplemental Table 1) do have enamel that is more ^{13}C-enriched, but because this data is less precise, the results are inconclusive.

The mole rat specimen sampled has enamel $\delta^{13}C$ that indicative of a diet composed of C_3 vegetation ($\delta^{13}C$ = -12.1, ±0.4).

The Otomyidae (*O. irroratus, O. saundersiae*) are primarily pure C_3 consumers (*O. irroratus* mean $\delta^{13}C_{enamel}$ = -12.9‰ σ = 1.6 (range -14.5‰ to -10.7‰ VPDB)*; O. saundersiae* mean $\delta^{13}C_{enamel}$ = -12.9‰ σ = 1.3 (range -14.1‰ to -11.5‰ VPDB). *O. irroratus* will consume most vegetation in its habitat (Skinner and Chimimba, 2005), and it appears to be a preferential grazer when grasses are available (De Graaff, 1981; Skinner and Chimimba, 2005). The diet of *O. saundersiae* is less well-understood (Skinner and Chimimba, 2005), but given morphological similarities to other closely related species of *Otomys* it likely shares similar diet breadth to other members of the genus. There are no pure C_4 feeders in the micromammal assemblage, as indicated by the $\delta^{13}C_{enamel}$ values of the specimens sampled here. The Otomyidae stable carbon isotope data is consistent with specimens habitats occuring in a range of local vegetation types that are C_3-predominant.

Once 'corrected' for the fossil fuel effect, which has resulted in the ^{13}C-depletion of the modern atmosphere, $\delta^{13}C_{enamel}$ values obtained via phosphoric acid digestion from eighteen modern Otomyidae specimens from the Wilderness and Wolwe River localities in South Africa (Table 4.6) range from -19.7‰ to -5.6‰. (Wilderness *O. irroratus* $\delta^{13}C_{enamel}$ values range from -19.7‰ to -5.6‰, mean = -12.9‰, σ = 4.69, n= 7; Wilderness *O. saundersiae* $\delta^{13}C_{enamel}$ = -10.5‰ σ = 0.13; Wolwe river *O. irroratus* $\delta^{13}C_{enamel}$ values range from -16.8‰ to -8.6‰, σ = 2.82, n = 10). Four specimens (2 each from Wilderness and Wolwe River) have $\delta^{13}C_{enamel}$ values lower than any of the PP30

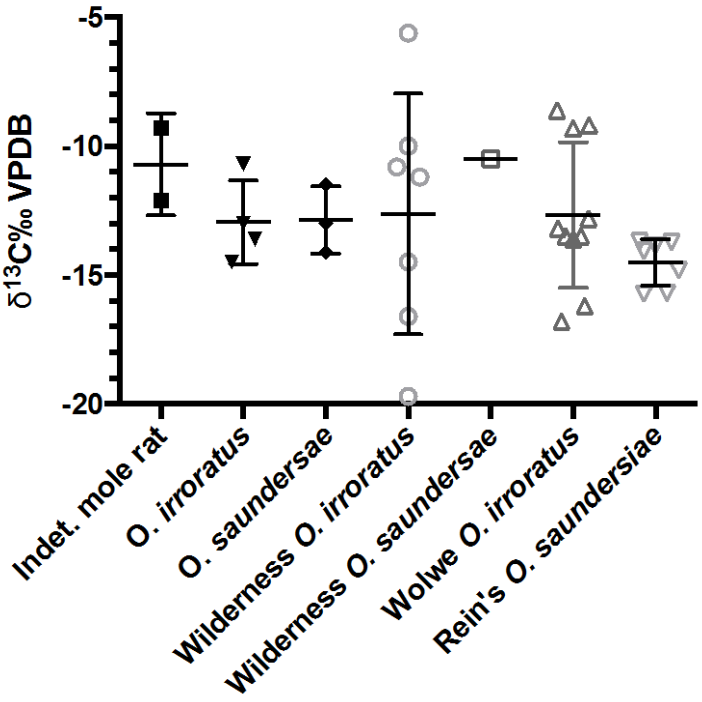

Figure 4.4. $\delta^{13}C_{enamel}$ data from PP30 micromammals (includes both incisors and molar teeth) by taxonomic identification. Mole rat stable carbon isotope values, as a population, are ^{13}C-enriched relative to Otomyids. Fossil specimens are represented by closed shapes on the graph, while open shapes represent $\delta^{13}C_{enamel}$ values obtained from modern pellet collection specimens, corrected for the fossil fuel effect.

fossil micromammal specimens sampled, and some modern specimens have values that are up to 5‰ lower than any PP30 fossil $\delta^{13}C_{enamel}$ value obtained. Although the fossil micromammal *Otomys* specimens from PP30 sample environments where C_3 flora is predominant, none of the PP30 micromammal specimens analyzed here sample microhabitats similar to the most closed environments available in the present-day Cape.

'Corrected' modern micromammal specimens from Rein's Nature Reserve (Table 4.6) $\delta^{13}C_{enamel}$ values range from -15.8‰ to -7.4‰ (*O. saundersiae* $\delta^{13}C_{enamel}$ values range from -15.8‰ to -13.7‰, mean = -14.5‰, σ = 0.9025, *n* = 7; *G. afra* $\delta^{13}C_{enamel}$ =

Taxon	Locality	n	δ13C$_{enamel}$ (‰ VPDB)	δ13C ‰, corrected	δ18O$_{enamel}$ (‰ VSMOW)
B. suillus	Rein's Nature Reserve	1	-13.51	-12.01	20.92
G. afra	Rein's Nature Reserve	1	-8.9	-7.4	30.03
O. irroratus	Amisrus, Wilderness	1	-12.7	-11.2	26
O. irroratus	Amisrus, Wilderness	1	-7.1	-5.6	26.5
O. irroratus	Amisrus, Wilderness	1	-12.3	-10.8	27.9
O. irroratus	Amisrus, Wilderness	1	-11.5	-10	26.3
O. irroratus	Amisrus, Wilderness	1	-18.1	-16.6	26.4
O. irroratus	Amisrus, Wilderness	1	-16	-14.5	25.9
O. irroratus	Amisrus, Wilderness	1	-21.2	-19.7	25
O. irroratus	Wolwe River	1	-15	-13.5	27.2
O. irroratus	Wolwe River	1	-14.7	-13.2	28.1
O. irroratus	Wolwe River	1	-15	-13.5	29.4
O. irroratus	Wolwe River	1	-10.7	-9.2	25.5
O. irroratus	Wolwe River	1	-18.3	-16.8	27.3
O. irroratus	Wolwe River	1	-14.3	-12.8	26.7
O. irroratus	Wolwe River	1	-15.1	-13.6	24.9
O. irroratus	Wolwe River	1	-10.8	-9.3	27.3
O. irroratus	Wolwe River	1	-10.1	-8.6	25.2
O. irroratus	Wolwe River	2	-17.7	-16.2	29.9
O. saundersiae	Rein's Nature Reserve	1	-16.32	-14.82	32.37
O. saundersiae	Rein's Nature Reserve	1	-17.23	-15.73	32.74
O. saundersiae	Rein's Nature Reserve	1	-15.19	-13.69	33.67
O. saundersiae	Rein's Nature Reserve	1	-15.35	-13.85	33.88
O. saundersiae	Rein's Nature Reserve	1	-17.19	-15.69	32.54
O. saundersiae	Rein's Nature Reserve	1	-15.23	-13.73	33.73
O. saundersiae	Rein's Nature Reserve	1	-15.57	-14.07	33.86
O. saundersiae	Amisrus, Wilderness	2	-12	-10.5	21.9

Table 4.6. $\delta^{13}C_{enamel}$ and $\delta^{18}O_{enamel}$ values for modern specimens (data acquired by phosphoric acid digestion of enamel carbonate).

-7.4‰; *B. suillus* $\delta^{13}C_{enamel}$ = -12.0‰). Rein's Nature Reserve is located on the south coast of South Africa, in an area where the predominant modern vegetation is limestone fynbos. None of the modern Rein's specimens are as depleted in ^{13}C as the most depleted Wilderness/Wolwe specimens. *O. saundersiae* specimens have a range of $\delta^{13}C_{enamel}$ values similar to those of modern large fauna from closed habitats in the Western Cape

(Lee-Thorp *et al.*, 1989). All Rein's *Otomys* specimens are more depleted in ^{13}C than any of the PP30 specimens reported here.

Micromammal Data: Oxygen

Although biogenic oxygen isotope ratios can be preserved in many enamels, they are more susceptible to diagenetic alteration (Wang and Cerling, 1994; Sponheimer and Lee-Thorp, 1999), and interpretation of $\delta^{18}O_{enamel}$ data is problematic for a number of reasons, both methodological and ecological. Large offsets in measurement between laser and conventional replicate measurements on fossil and modern enamel occur as a result of the laser bulk-sampling an admixture of carbonate, phosphate and hydroxyl oxygen during ablation (Passey and Cerling, 2006); thus precision in measurement is reduced, although large scale changes in oxygen isotope composition of enamel should be resolvable (Passey and Cerling, 2006). In terms of isotope ecology, a number of different factors can contribute to the oxygen isotope composition of mammalian enamel, including the oxygen isotopic composition of vegetation (which can be impacted by aridity as well as seasonality of rainfall); variability in the oxygen isotopic composition of different plant parts; the isotopic composition of meteoric water and the frequency with which it is ingested ('drinking behavior') (Kohn *et al.*, 1996; Sponheimer and Lee-Thorp, 1999). It would thus be ideal to establish the relationship between environmental water $\delta^{18}O$ and body water/apatite $\delta^{18}O$ for individual species or genera in controlled contexts. Lacking such laboratory studies for the taxa sampled here, inter-specific variation can partially be controlled for by analyzing data by taxon rather than aggregating it.

Laser ablation-obtained oxygen isotope data has here been normalized to VSMOW to facilitate cautious relative comparison to the large fauna oxygen isotope data. Passey and Cerling (2006) observed a mean laser-conventional offset of -6.4‰ ± 0.7 in controlled experiments on fossil enamel. The systematic depletion in ^{18}O of the PP30 fossil micromammal specimens when compared to the large fauna (Figure 4.5) is consistent with this.

$\delta^{18}O_{enamel}$ VSMOW values for the PP30 micromammals range from 21.6‰ to 26.2‰. Comparison of the $\delta^{18}O_{enamel}$ values by taxon (mean values of $\delta^{18}O_{enamel}$ VSMOW for *O. irroratus* = 24.4‰ ± 1.6; for *O. saundersiae* = 23.6‰ ± 1.8; for mole rats = 24.7‰ ± 0.8) shows overlap in the range of $\delta^{18}O$ between taxonomic groups (Figure 4.6). KW test of the *O. irroratus*, *O. saundersiae*, and 'mole rat' populations show no significant difference in the oxygen isotope ratios of those populations of specimens ($H = 0.5030$ $p = 0.8105$).

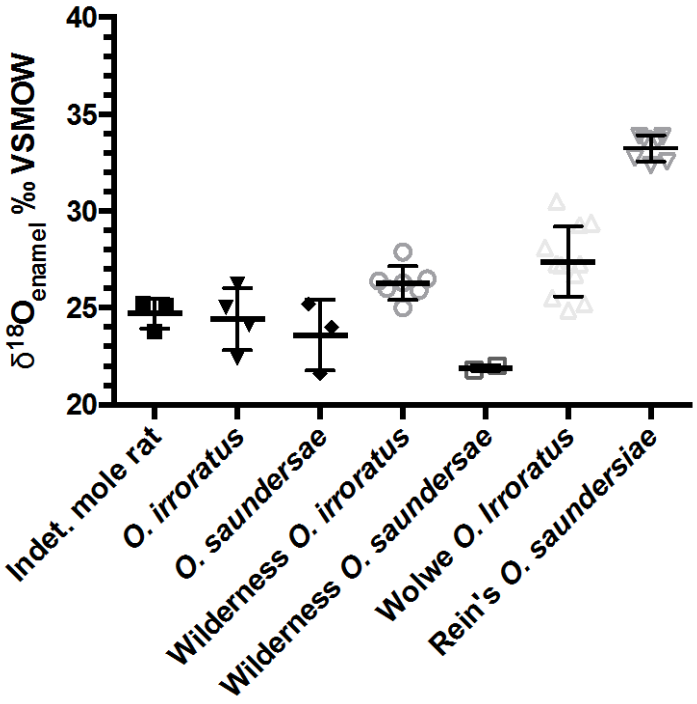

Figure 4.6. $\delta^{18}O_{enamel}$ data from PP30 micromammals (includes both incisors and molar teeth) by taxonomic identification. Fossil specimens are represented by closed shapes on the graph. Open shapes represent $\delta^{13}C_{enamel}$ values obtained from modern pellet collection specimens.

Large Fauna

Fifty-two taxonomically identified fossil teeth from PP30 were sampled by J.A. Lee-Thorp for carbon and oxygen isotope analysis (one specimen, Alcelaphine tooth #67502, was sampled twice, for a total sample *n* = 53).

Taxa sampled for isotopic analysis represent browsing antelope species (*Pelea, R. campestris, R. melanotis*), mixed feeders who primarily consume browse but with significant grass component to their diets (*Antidorcas, R. fulvorufula*), and grazing taxa (*Alcelaphus, Connochaetes, Hippotragus, Damaliscus, R. arundinum*). Three brown hyena specimens (*Parahyena brunnea)* were also analyzed.

The $\delta^{13}C_{enamel}$ VPDB values obtained from the PP30 large fauna specimens range from -9.91‰ to -5.63‰ (Table 4.7). Mean $\delta^{13}C_{enamel}$ values of the browsing taxa (*Pelea, R. campestris, R. melanotis*) are depleted in ^{13}C by only ~1‰ relative to the other large herbivorous taxa from PP30 (browser $\delta^{13}C_{enamel}$ = -9.39, σ = 0.48; mixed feeder $\delta^{13}C_{enamel}$ = -8.53‰, σ = 1.01; grazer $\delta^{13}C_{enamel}$ = -8.23‰, σ = 0.96). No significant differences in the carbon isotope values are detected when specimens are grouped by taxon (KW test, H= 11.60, p 0.1146). However when samples are grouped by feeding behavior (browser, mixed feeder, or grazer), the populations of carbon isotope values are significantly different between browsers and grazers (KW test, H=8.725, p = 0.0127, Dunn's multiple comparison test).

Isotopic variability within these feeding behavior categories also differs. Browser $\delta^{13}C_{enamel}$ values are relatively restricted, ranging from -10.0‰ to -8.8‰, while mixed feeders and grazers exhibit a wider range: mixed feeders between -9.6‰ and -6.1‰, and grazer values from -9.9‰ to -5.6‰ (Figure 4.7). Thus, while there is significant overlap in the lower $\delta^{13}C_{enamel}$ values obtained from all sampled taxa, some specimens of taxa that engage in either obligate or facultative grazing have higher $\delta^{13}C_{enamel}$ values relative to both PP30 browsing taxa and PP30 grazing conspecifics. The higher $\delta^{13}C_{enamel}$ values reflect a larger C_4 grass component in the diets of some, but not all, of the grazers.

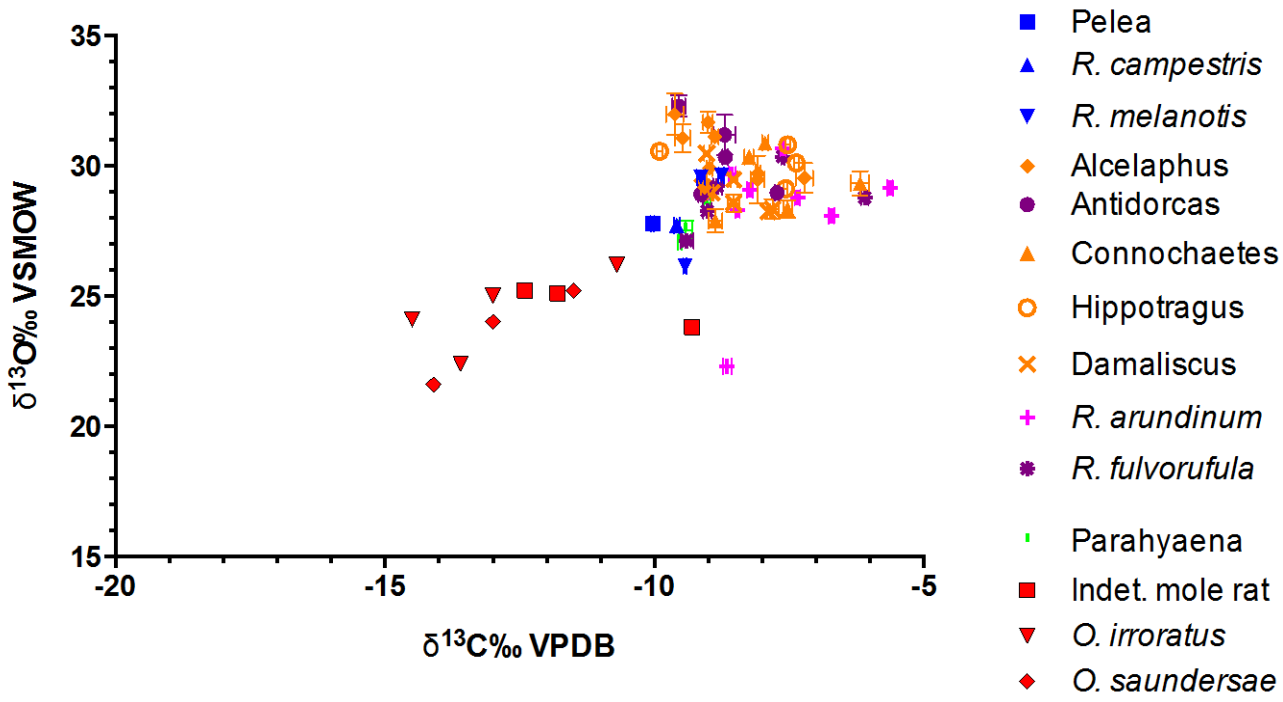

Table 4.5. XY plot of $\delta^{13}C_{enamel}$ and $\delta^{18}O_{enamel}$ values for all sampled PP30 fossil specimens. Micromammal taxa are in red, large fauna who are, by modern analogue, browsers, are in blue, those that are mixed feeders in purple, and those that are considered obligate grazers are in orange

Taxon	PP30 $\delta^{13}C$ ‰VPDB	σ	n	Modern SA $\delta^{13}C$ ‰VPDB [a]	Modern EA $\delta^{13}C$ ‰VPDB [b,c]
Pelea	-10.04		1		
Raphicerus campestris	-9.59		1	-10.8	
Raphicerus melanotis	-9.11	0.35	3		
Alcelaphus	-8.72	0.77	9	2.7	3.7[b], 4.3 - 4.5[c]
Connochaetes	-7.76	1.00	5	1.5 - 2.1	3.4[b], 2.1 – 5.0[c]
Hippotragus	-8.10	1.21	4	1.6 - 3.5	2.5 - 4.1[b]
Damaliscus	-8.55	0.53	7	2.0 - 3.9	1.8 - 3.4[b]
Redunca arundinum	-7.81	1.09	9	2.4	
Redunca fulvorufula	-8.19	1.35	5	2.9	2.5[b]
Antidorcas	-8.81	0.62	6	-8.6	

Table 4.7. Mean stable carbon isotope values for large herbivorous fauna from PP30, and $\delta^{13}C$ data reported in the literature for modern specimens from summer rainfall zones in South Africa (Sponheimer *et al.*, 2003) and East Africa ([b]Cerling *et al.*, 2003; [c]Cerling and Harris, 1999). Entries for modern $\delta^{13}C$ values are left blank when no data exists for a given taxon. Where PP30 fossil specimens have been identified to the genus, modern data for members of the same genus (but not necessarily the same species) have been included in the table. The impact of ^{13}C-depleted modern atmospheric CO_2 has been 'corrected for' by adding 1.5‰ to all reported modern values.

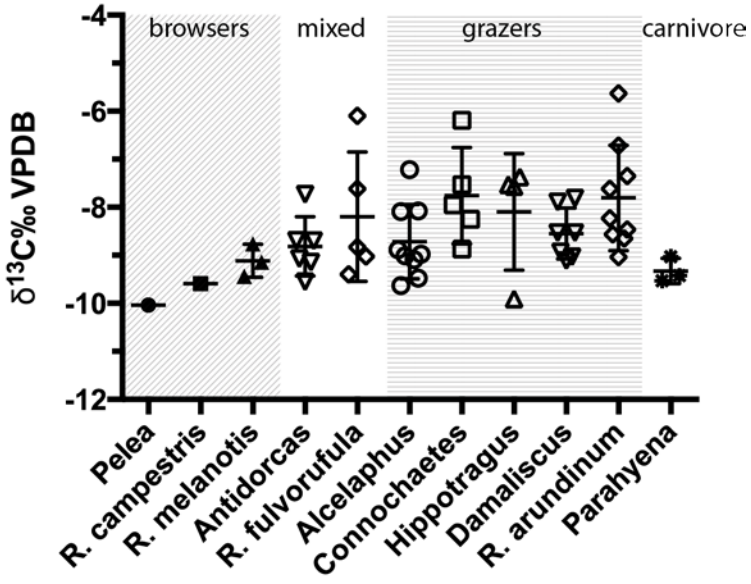

Figure 4.7. $\delta^{13}C_{enamel}$ data from PP30 large fauna. Shaded boxes group taxa by feeding behavior in their modern conspecifics (browser, mixed feeder, grazer, carnivore).

$\delta^{13}C_{enamel}$ values for each large mammal taxonomic group sampled in the PP30 fossil assemblage are more enriched in ^{13}C than other herbivorous taxa from C_3 vegetation communities in South Africa (Lee-Thorp and van der Merwe, 1987; Lee-Thorp et al 1989; Sponheimer et al 2003) and in East Africa (Cerling *et al.,* 2003). The lowest values from PP30 large faunal specimens barely overlap with $\delta^{13}C_{enamel}$ values (-14.9‰ to -9.3‰) reported from the clearly C_3 early Pliocene assemblage of Langebaanweg on the Western Cape, South Africa (Franz-Odendaal *et al.,* 2002).

A number of taxa found in the PP30 assemblage are in the present day associated with specific habitat types. Grysbok (*Raphicerus melanotis*), a browser, is endemic to the GCFR, associated with fynbos vegetation, and prefers dense vegetation cover (Kingdon *et al.,* 2013; Marean *et al.,* 2014); the $\delta^{13}C_{enamel}$ values of fossil *R. melanotis* from PP30 (mean = -9.11‰, $\sigma = 0.35$, $n = 3$) are some of the lower stable carbon isotope values from the PP30 large fauna. Hartebeest (*Alcelaphus*), springbok (*Antidorcas),* and wildebeest (*Connochaetes*) are in particular associated with more open grassland ecosystems in the present day. Mean carbon isotope values for fossil exemplars from PP30 (Table 4.7), while slightly higher relative to *Raphicerus*, still suggest only small C4 grass contributions. In fact, all fossil specimens of grazing taxa (*Alcelaphus, Connochaetes, Hippotragus, Damaluscus)* from PP30 have $\delta^{13}C_{enamel}$ values that are notably depleted in ^{13}C when compared to fossil-fuel effect 'corrected' $\delta^{13}C_{enamel}$ data reported from modern ecosystems dominated by C_4 grasses, such as in the north of South Africa (Sponheimer *et al.,* 2003a) (Table 4.7). Taken together, the large mammal stable carbon isotope data suggests only minor proportions of C_4 grass in the vegetation communities proximate to PP30 at 151ka.

Changes in the relative proportion of winter and summer rain in the western and southern Cape can be observed in changing $\delta^{18}O$ values in proxy records such as speleothem (Bar-Matthews *et al.,* 2010), but analysis of the stable oxygen isotope data obtained from phosphoric acid digestion of enamel carbonate from the PP30 large mammal fauna is constrained by the same theoretical issues described previous in our presentation of the PP30 micromammal oxygen isotope data (above). The oxygen isotope ecology of many of the taxa sampled here is not well understood in modern analogues, and can be significantly impacted by non-climatological factors such as drinking behavior, water-use, and plant part consumption. Therefore, although the $\delta^{18}O_{enamel}$ values obtained from the large mammal fauna are reported here, they are not used to make inferences about relative proportions of winter and summer rain to local meteoric water.

With the exception of one outlier value (*R. arundinum,* $\delta^{18}O_{enamel}$ = 22.30‰ VSMOW), stable oxygen isotope values for all sampled PP30 large fauna range from 26.1‰ to 32.28‰. Although grazers and mixed feeders are somewhat enriched relative to browsers (Figure 4.8), the enrichment is not significant (KW test, H =3.647, $p \cong$ 0.1615).

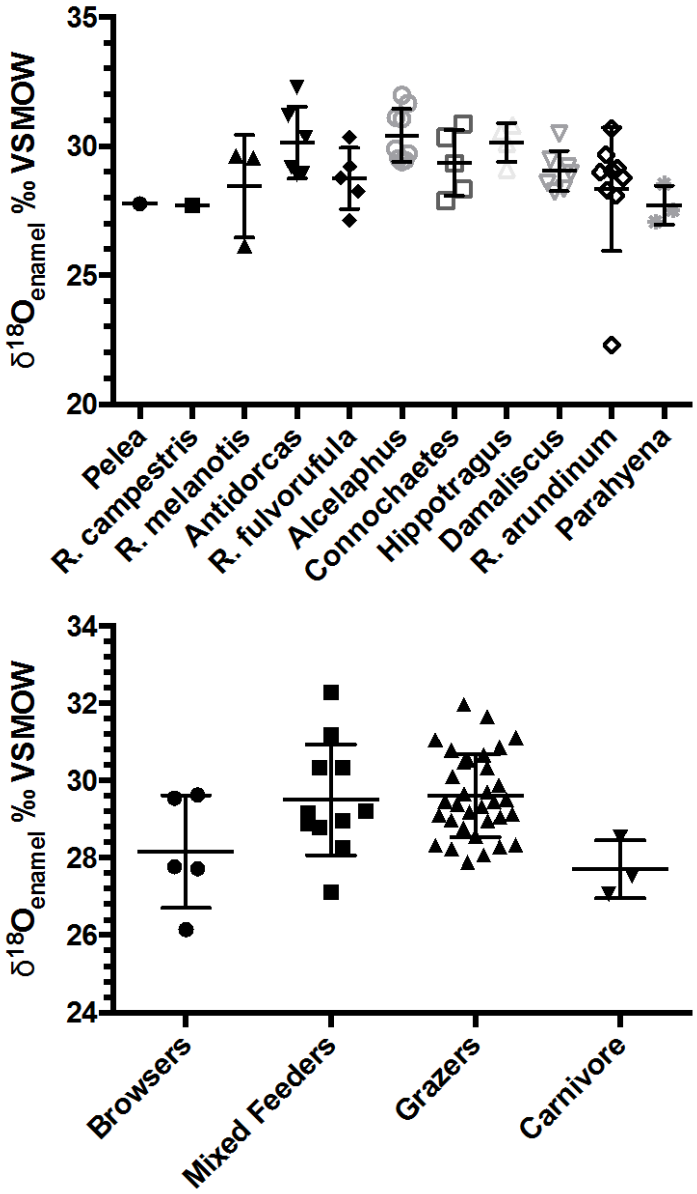

Figure 4.8. $\delta^{18}O_{enamel}$ values obtained from the PP30 large fauna fossil material, grouped by taxon (A), and generalized feeding ecology (B). The outlying stable carbon isotope value for *R. arundinum* seen in "A" has been removed from in the grouped analysis in "B".

Discussion

Because the fossil assemblages from PP30 represent a fairly constrained period of deposition, the micromammal and large faunal material can be treated as contemporaneous (Rector and Reed, 2010) and the isotope data as proxies of paleoenvironmental conditions near to the site at about 151 ka, a phase of MIS6 indicated by deep sea core and ice core records to be a strong phase of glacial cooling. However, taken separately, analyses of the PP30 fossil micromammal carbon and oxygen isotope data and the PP30 fossil large mammal carbon and oxygen isotope data do not appear immediately concordant. Both the $\delta^{18}O$ and $\delta^{13}C$ values obtained from the micromammal fossils are ^{13}C-depleted when compared to even the lowest $\delta^{13}C$ values from the large fauna (Figure 4.5). The means of the micromammal $\delta^{18}O_{enamel}$ isotope populations (analyzed exclusively using LA-GC-IRMS) and the large fauna $\delta^{18}O_{enamel}$ isotope populations (analyzed by H_3PO_4 digestion) are significantly different (unpaired T-test not assuming equal standard deviations, $p < 0.0001$). The difference between the means of these populations of oxygen isotope values is 5.076 ± 0.4771 (95% *CI = 4.037 to 6.114*). Reported analytical offsets for $\delta^{18}O$ between specimens analyzed using both LA-GC-IRMS and 'conventional' H_3PO_4 techniques is −5.1‰ ± 1.2 for fossil specimens (Passey and Cerling, 2006); given that the LA-GC-IRMS-analyzed PP30 micromammal oxygen isotope data is consistently depleted in ^{18}O relative the conventionally-analyzed large fauna by ~4-6‰, it is highly likely that the difference between the means of the PP30 micromammal $\delta^{18}O$ values and the PP30 large fauna $\delta^{18}O$ values is an analytical artifact.

The generally lower $\delta^{13}C_{enamel}$ values of the PP30 micromammals relative to the PP30 large fauna, however, are unlikely to be a result of the different analytical methods used. Reported analytical offsets between laser ablation-obtained and phosporic acid digestion-obtained values for carbon are only $-0.5‰ \pm 0.8$ for fossil specimens (Passey and Cerling, 2006). Hynek *et al.* have argued for a consideration of a reduced tissue-diet enrichment factor ($\varepsilon^*_{enamel\text{-}diet}$) for rodents (Hynek *et al.*, 2012), but even assuming a decrease in tissue-diet enrichment factor as large as 3‰ (an $\varepsilon^*_{enamel\text{-}diet}$ of 11‰ for small mammals vs 14‰ for ungulates, see Cerling and Harris, 1999; Podelsak *et al.*, 2008; Hynek *et al.*, 2012), many PP30 micromammal stable carbon isotope values are still depleted in ^{13}C relative to the large mammal fauna as a whole. It is thus likely that the differences in ^{13}C between the PP30 micromammals and the large mammals are neither a methodological nor an analytical artifact but rather reflects dietary differences in the relative proportions of C_3 and C_4 of these large and small primary consumers during MIS6.

In addition to being comparably enriched in ^{13}C relative to the PP30 micromammals, the intraspecific range of stable carbon isotope values are narrower in the large fauna (Table 4.8). If small mammals act as random isotopic samplers of their immediate environments (Hynek *et al.*, 2012), the wide range of intraspecific $\delta^{13}C$ variation within the fossil *Otomys* species (Table 4.8) is suggestive of a site-local environment that is C_3 vegetation predominated, with varying small contributions of C_4 grasses, possibly dependent on changes in the microhabitats inhabited by individual specimens. The range of *O. saundersiae* and *O. irroratus* $\delta^{13}C_{enamel}$ values (-14.1‰ to -11.5‰, and -14.5‰ to -10.7‰) overlap with the large fauna stable carbon isotope data

reported for the C_3 Pliocene Langebaanweg fossil assemblage (-14.9‰ to -9.3‰, Franz-Odendaal *et al.*, 2002), for modern large C_3 consumers in the Cape (which, when corrected to a 'pre-industial atmosphere' range from approximately -14.5‰ to -11.5‰, Lee-Thorp *et al.*, 1989), and with the modern micromammal *Otomys* $\delta^{13}C$ values from some of the more closed, C_3 environments extant in the present-day southern Cape (fossil fuel effect 'corrected' $\delta^{13}C$ range of -19.7‰ to -5.6‰), and are thus strongly suggestive of C_3 dominated vegetation in the immediate vicinity of PP30 at 151yr.

Taxon	n	min $\delta^{13}C$ ‰VPDB	max $\delta^{13}C$ ‰VPDB	mean $\delta^{13}C$ ‰VPDB	σ	range ‰
Indet. mole rat	3	-12.4	-9.3	-11.2	1.7	3.1
O. irroratus	4	-14.5	-10.7	-12.9	1.6	3.8
O. saundersiae	3	-14.1	-11.5	-12.9	1.3	2.6
Pelea	1			-10.04		
R. campestris	1			-9.59		
R. melanotis	3	-9.44	-8.76	-9.11	0.34	0.68
Antidorcas	6	-9.55	-7.73	-8.81	0.62	1.82
R. fulvorufula	5	-9.4	-6.1	-8.19	1.35	3.30
Alcelaphus	9	-9.63	-7.22	-8.72	0.77	2.41
Connochaetes	5	-8.87	-6.19	-7.76	1.00	2.68
Hippotragus	4	-9.91	-7.37	-8.10	1.21	2.54
Damaliscus	7	-9.11	-7.81	-8.55	0.53	1.30
R. arundinum	9	-9.04	-5.63	-7.81	1.09	3.41
Parahyena	3	-9.53	-9.03	-9.33	0.26	0.50

Table 4.8. Minimum, maximum, and mean $\delta^{13}C_{enamel}$ values obtained from each PP30 fossil taxonomic group.

The mole rat $\delta^{13}C_{enamel}$ values overlap with the most enriched specimen of the Otomyidae, and with the lowest values found in the large fauna dataset. Modern mole rats primarily consume geophytic parts of plants, as well as grasses and sedges, although the taxonomic variability of the flora in the diet varies between species (Davies and Jarvis,

1986). Although there is limited data available, C_3 geophytes are not notably enriched relative to other C_3 plants, nor are C_4 geophytes depleted in ^{13}C relative to C_4 grasses (Codron *et al.,* 2005). Consumption of C_4 geophytes is therefore not the dietary source of the enriched PP30 mole rat stable carbon isotope values observed; instead it is hypothesized that that modest enrichment of mole rat enamel is due to a dietary grass or sedge fraction. Specific identification of the mole rats sampled here was not possible on diagnostic grounds, however the stable carbon isotope values of the PP30 the mole rats (mean $\delta^{13}C_{enamel}$= -11.17‰; range -12.4‰ to -9.3‰ VPDB) are intermediate between values reported for modern *Georychus capensis* (approximately -14.5‰ to -10.0‰ VPDB after a 1.5‰ correction for the fossil fuel effect) and *Bathyergus suillus* (approx.. -7.5‰ to -2.5‰ VPDB, 'corrected') specimens from C_3-dominated vegetation communities in the Western Cape (Yeakel *et al.,* 2007; Robb *et al.,* 2012) .

The stable carbon isotope composition of the most ^{13}C -depleted specimens of the *Otomys* populations sampled here reflect pure C_3 feeding behavior; the $\delta^{13}C_{enamel}$ values of these Otomyid specimens are considerably more depleted in ^{13}C than the lowest values of any large fossil fauna from PP30, including those that are, by modern analogy, browsing species (*Pelea* and *Raphicerus*, Table 4.8). PP30 *Pelea* and *Raphicerus* values ($\delta^{13}C_{enamel}$ range from -10.04‰ to -8.76‰) are about 1.5‰ to 3‰ higher than the values reported for modern C_3-consuming large fauna in the Cape (once they have been corrected for the ^{13}C-depletion of the modern atmosphere) (Lee-Thorp *et al.,* 1989), and overlap only with the most enriched end-members of the range of $\delta^{13}C$ values for herbivorous fossils from Langebaanweg (Figure 4.9). All fossil grazers and mixed-feeding taxa from PP30 fall outside the range of carbon isotope values reported for

modern Cape fauna (e.g. the PP30 fauna is more enriched in ^{13}C). Furthermore, although some specimens of grazing or mixed-feeding taxa (notably specimens of *Hippotragus, Alcelaphus,* and *Antidorcas*) overlap with the most enriched $\delta^{13}C$ values reported from the C_3 Langebaanweg fauna, as a whole these taxa (*Antidorcas, R. fulvorufula, Alcelaphus, Connochaetes, Hippotragus, Damaliscus,* and *R. arundinum*) have stable carbon isotope values that are enriched relative to reported values for modern and fossil C_3 assemblages in the Cape.

Conversely, none of the large mammal fossil specimens from PP30 have $\delta^{13}C_{enamel}$ values as high as modern fauna that live in C_4 grassland ecosystems (Table 4.7, Figure 4.9). This suggests that the large fauna from PP30, especially the obligate grazing species, sampled a paleovegetation that retains a significant C_3 grass component in which C_4 grasses were available for graze; this pattern is what would be expected from bulk enamel $\delta^{13}C$ values if large herbivores were moving between C_3 and C_4 vegetation communities..

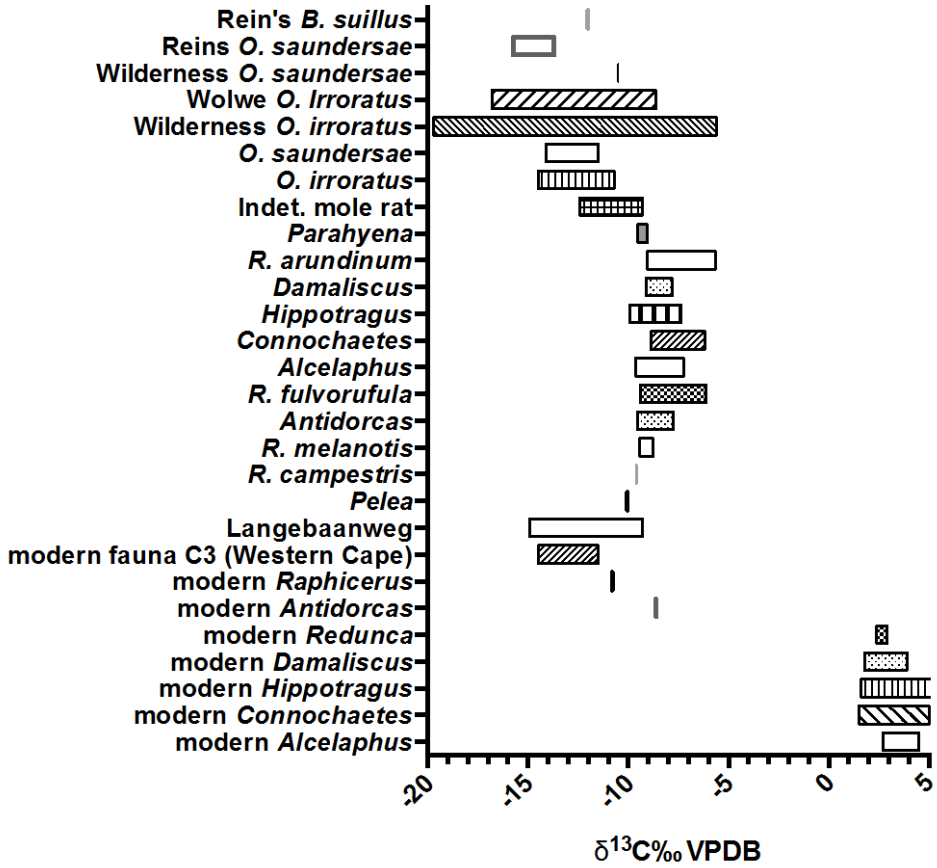

Figure 4.9. Ranges of $\delta^{13}C$ values reported for modern and fossil material, including PP30 (this paper), modern micromammal material (this paper), Langebaanweg fossil material (Franz-Odendaal *et al.*, 2002), modern C_3 consumers in the western Cape (Lee-Thorp *et al.*, 1989), and modern fauna from C_4-predominant environments ("modern C_4) in South and East Africa (Cerling and Harris, 1999; Cerling *et al.*, 2003; Sponheimer *et al.*, 2003)

The hunting range of the aggregating predator (*Bubo africanus* or other closely related owl species) of the micromammal component of the PP30 is comparably small (r=3km, or ~28.27 km^2, (Andrews, 1990; Matthews, 2004)), and likely samples environments immediately proximate to the site itself. The $\delta^{13}C_{enamel}$ data obtained from the micromammal specimens at PP30 suggests the presence of C_3-dominated vegetation, with only a small component of C_4 grasses. This is consistent with a number of GCFR

vegetation community types extant in the region in the present day. The current vegetation surrounding the Pinnacle Point cliffs includes extensive limestone Fynbos on the cliffs. This limestone Fynbos is dominated by C_3 shrubs such as protea, with some rare grasses that can include both C_3 and C_4 types. On the slopes of the dunes along some of the lower portions of the cliffs is Strandveld, which is dominated by C_3 shrubs and trees such as Milkwood (*Sideroxylon inerme*) and various types of geophytes. Stable carbon isotope data from mole rats is within the range of carbon isotope values obtained from modern model rat specimens from the Western Cape: combined with the C_3 fossil *Otomys* carbon isotope signal, the fossil micromammal carbon isotope data does not suggest that this fynbos vegetation at PP30 was replaced during glacial MIS6 by C_4 grasses.

The owls accumulating the micromammals at PP30 would have been sampling a habitat dominated by C_3 vegetation, while the brown hyenas accumulating the large fauna, with their greater foraging radius and preference for large bodied fauna, could have sampled a habitat with the potential for a much wider range of vegetation. The range of the aggregating predator (*Parahyaena brunnea*) of the large mammal faunal sample is considerably larger (>170 km^2, depending on habitat heterogeneity (Wiesel, 2007). Comparison of the fossil large mammal $\delta^{13}C_{enamel}$ data and the fossil micromammal $\delta^{13}C_{enamel}$ data from PP30 strongly suggests that these two assemblage components are sampling distinct vegetation communities. The PP30 micromammal stable carbon isotope values are consistent with C_3 vegetation as common to this area today, while values for the PP30 large fauna indicate that some of the grazers had access to C_4 grass resources that are not reflected in the diets of the small fauna, and thus were not likely to occur in

the area immediate (within ~3km) of the site. Various workers have hypothesized the potential for the development of grasslands on the exposed paleo-Agulhas during glacials such as MIS6 (Goldblatt and Manning, 2002; Marean, 2010; Faith, 2011; Marean *et al.*, 2014); stable isotope evidence for an increased C_4 vegetation component only in the diets of the large fauna from the PP30 151 ka assemblage, while being largely absent from the carbon isotope signature of the PP30 micromammals, is supportive of this hypothesis.

***Acknowledgments**

I would like to thank Julia Lee-Thorp for generously providing the large faunal stable isotope data to be analyzed and presented in tandem with the PP30 micromammal data discussed here. The text of the section "*Sampling Procedures: Large Mammals"* is a brief summary of a much more detailed description of the analytical procedures provided by Lee-Thorp (nd).

This chapter forms the basis of a draft of a multi-authored paper in preparation.

species	SACP4#	fraction blank	δ^{13}C ‰VPDB	δ^{13}C ‰VSMOW
Indet. mole rat	100475	0.18181	-9.7	24.3
Indet. mole rat	100486	0.25528	-8.1	28.8
Indet. mole rat	100486	0.24447	-8.0	28.2
Indet. mole rat	100491	0.17071	-8.0	24.1
Indet. mole rat	100491	0.18103	-7.8	23.7
O. irroratus	100522	0.20619	-12.4	22.8
O. irroratus	100580	0.19338	-11.4	25.4
O. irroratus	100580	0.19057	-11.2	25.4
O. saundersiae	100559	0.18226	-12.5	24.2
O. saundersiae	100584a	0.199	-12.4	25.7
O. saundersiae	100575	0.2005	-9.6	26.8
O. saundersiae	100523	0.21007	-17.1	23.2
O. saundersiae	100586	0.19478	-17.3	19.4
O. irroratus	100589a	0.21301	-15.9	25.5
O. irroratus	100589b	0.18756	-16.1	19.5

Supplemental Table 1. Large-blanked data eliminated from the analysis. This data has fraction blanks >0.15. Large fraction blanks decrease the precision of the laser measurement, and data is included here for archival purposes only.

Chapter 4 References

Andrews, P. (1990). Owls, caves, and fossils: predation, preservation, and accumulation of small mammal bones in caves, with an analysis of the pleistocene cave faunas from westbury-sub-mendip, somerset, UK. Chicago, University of Chicago Press.

Bar-Matthews, M., C. W. Marean, Z. Jacobs, P. Karkanas, E. C. Fisher, A. I. R. Herries, . . . A. Ayalon (2010). "A high resolution and continuous isotopic speleothem record of paleoclimate and paleoenvironment from 90 to 53 ka from Pinnacle Point on the south coast of South Africa." Quaternary Science Reviews **29**(17): 2131-2145.

Barham, L. and P. Mitchell (2008). The first Africans: African archaeology from the earliest toolmakers to most recent foragers, Cambridge University Press.

Barrable, A., M. E. Meadows and B. C. Hewitson (2002). "Environmental reconstruction and climate modelling of the Late Quaternary in the winter rainfall region of the Western Cape, South Africa." South African Journal of Science **98**: 611-616.

Bender, M. M. (1971). "Variations in the $^{13}C/^{12}C$ ratios of plants in relation to the pathway of photosynthetic carbon dioxide fixation." Phytochemistry **10**(6): 1239-1244.

Berger, L. R., D. J. de Ruiter, S. E. Churchill, P. Schmid, K. J. Carlson, P. H. G. M. Dirks and J. M. Kibii (2010). "Australopithecus sediba: A new species of Homo-like australopith from South Africa." Science **328**(5975): 195-204.

Berger, L. R., R. Lacruz and D. J. De Ruiter (2002). "Revised age estimates of Australopithecus-bearing deposits at Sterkfontein, South Africa." American Journal of Physical Anthropology **119**(2): 192-197.

Bernatchez, J. and C. W. Marean (2011). "Total station archaeology and the use of digital photography." SAA Archaeol. Rec **11**: 16-21.

Blome, M. W., A. S. Cohen, C. A. Tryon, A. S. Brooks and J. Russell (2012). "The environmental context for the origins of modern human diversity: A synthesis of regional variability in African climate 150,000 - 30,000 years ago." Journal of Human Evolution **62**(5): 563-592.

Brown, K. S., C. W. Marean, A. I. R. Herries, Z. Jacobs, C. Tribolo, D. Braun, . . . J. Bernatchez (2009). "Fire as an engineering tool of early modern humans." Science **325**(5942): 859-862.

Brown, K. S., C. W. Marean, Z. Jacobs, B. J. Schoville, S. Oestmo, E. C. Fisher, . . . T. Matthews (2012). "An early and enduring advanced technology originating 71,000 years ago in South Africa." Nature **491**(7425): 590-593.

Cann, R. L. (1988). "DNA and human origins." Annual Review of Anthropology **17**: 127-143.

Cerling, T. E. and J. M. Harris (1999). "Carbon isotope fractionation between diet and bioapatite in ungulate mammals and implications for ecological and paleoecological studies." Oecologia **120**(3): 347-363.

Cerling, T. E., J. M. Harris and B. H. Passey (2003). "Diets of East African Bovidae based on stable isotope analysis." Journal of Mammalogy **84**(2): 456-470.

Chase, B. M. and M. E. Meadows (2007). "Late Quaternary dynamics of southern Africa's winter rainfall zone." Earth-Science Reviews **84**(3-4): 103-138.

Clark, J. D., Y. Beyene, G. WoldeGabriel, W. K. Hart, P. R. Renne, H. Gilbert, . . . K. R. Ludwig (2003). "Stratigraphic, chronological and behavioural contexts of Pleistocene Homo sapiens from Middle Awash, Ethiopia." Nature **423**(6941): 747-752.

Codron, J., D. Codron, J. A. Lee-Thorp, M. Sponheimer, W. J. Bond, D. de Ruiter and R. Grant (2005). "Taxonomic, anatomical, and spatio-temporal variations in the stable carbon and nitrogen isotopic compositions of plants from an African savanna." Journal of Archaeological Science **32**(12): 1757-1772.

Cowling, R. and D. Richardson (1995). Fynbos: South Africa's Unique Floral Kingdom. Cape Town, University of Cape Town.

Cowling, R. M. (1983). "The occurrence of C_3 and C_4 grasses in fynbos and allied shrublands in the South Eastern Cape, South Africa." Oecologia **58**(1): 121-127.

Cowling, R. M., S. Proches and T. C. Partridge (2009). "Explaining the uniqueness of the Cape flora: incorporating geomorphic evolution as a factor for explaining its diversification." Molecular Phylogenetics and Evolution **51**(1): 64-74.

Cowling, S. A., P. M. Cox, C. D. Jones, M. A. Maslin, M. Peros and S. A. Spall (2008). "Simulated glacial and interglacial vegetation across Africa: implications for species phylogenies and trans-African migration of plants and animals." Global Change Biology **14**: 827-840.

d'Errico, F., C. Henshilwood, M. Vanhaeren and K. van Niekerk (2005). "Nassarius kraussianus shell beads from Blombos Cave: evidence for symbolic behaviour in the Middle Stone Age." Journal of Human Evolution **48**(1): 3-24.

d'Errico, F. and C. S. Henshilwood (2007). "Additional evidence for bone technology in the southern African Middle Stone Age." Journal of Human Evolution **52**(2): 142-163.

Dart, R. (1925). "Australopithecus africanus: the man-ape of South Africa." Nature **115**: 195-199.

Davies, K. C. and J. U. M. Jarvis (1986). "The burrow systems and burrowing dynamics of the mole rats Bathyergus suillus and Cryptomys hottentotus in the fynbos of the southwestern Cape, South Africa." Journal of Zoology **209**(1): 125-147.

De Graaff, G. (1981). "The rodents of southern Africa." Durban: Butterworths.

DeNiro, M. J. and S. Epstein (1978). "Influence of diet on the distribution of carbon isotopes in animals." Geochimica et Cosmochimica Acta **42**(5): 495-506.

Faith, J. T. (2011). "Ungulate community richness, grazer extinctions, and human subsistence behavior in southern Africa's Cape Floral Region." Palaeogeography, Palaeoclimatology, Palaeoecology **306**(3): 219-227.

Franz-Odendaal, T. A., J. A. Lee-Thorp and A. Chinsamy (2002). "New evidence for the lack of C_4 grassland expansions during the early Pliocene at Langebaanweg, South Africa." Paleobiology **28**(3): 378-388.

Goldblatt, P. (1997). "Floristic diversity in the Cape Flora of South Africa." Biodiversity and Conservation **6**(3): 359-377.

Goldblatt, P. and J. C. Manning (2002). "Plant Diversity of the Cape Region of Southern Africa." Annals of the Missouri Botanical Garden **89**(2): 281-302.

Henshilwood, C., F. D'Errico, M. Vanhaeren, K. van Niekerk and Z. Jacobs (2004). "Middle Stone Age Shell Beads from South Africa." Science **304**(5669): 404.

Henshilwood, C., C. Marean and H. Soodyall (2006). Remodeling the origins of modern human behavior. The Prehistory of Africa: Tracing the Lineage of Modern Man. Cape Town, Jonathan Ball Publishers**:** 31-48.

Henshilwood, C. S., F. d'Errico, K. L. van Niekerk, Y. Coquinot, Z. Jacobs, S. E. Lauritzen, . . . R. Garcia-Moreno (2011). "A 100,000-year-old ochre-processing workshop at Blombos Cave, South Africa." Science **334**(6053): 219-222.

Henshilwood, C. S., F. d'Errico and I. Watts (2009). "Engraved ochres from the middle stone age levels at Blombos cave, south Africa." Journal of Human Evolution **57**(1): 27-47.

Hynek, S. A., B. H. Passey, J. L. Prado, F. H. Brown, T. E. Cerling and J. Quade (2012). "Small mammal carbon isotope ecology across the Miocene-Pliocene boundary, northwestern Argentina." Earth and Planetary Science Letters **321-322**(0): 177-188.

Ingman, M., H. Kaessmann, S. Paàbo and U. Gyllensten (2000). "Mitochondrial genome variation and the origin of modern humans." Nature **408**(6813): 708-713.

Jacobs, Z. (2010). "An OSL chronology for the sedimentary deposits from Pinnacle Point Cave 13B, a punctuated presence." Journal of Human Evolution **59**(3): 289-305.

Kingdon, J., D. Happold, T. Butynski, M. Hoffmann, M. Happold and J. Kalina (2013). Mammals of Africa, A&C Black.

Klein, R. G. (1999). The Human Career: Human Biological and Cultural Origins. Chicago, University of Chicago Press.

Koch, P. L. (1997). "Isotopic reconstruction of past continental environments." Annual Review of Earth and Planetary Sciences **26**(1): 573-613.

Kohn, M. J., M. J. Schoeninger and J. W. Valley (1996). "Herbivore tooth oxygen isotope compositions: Effects of diet and physiology." Geochimica et Cosmochimica Acta **60**(20): 3889-3896.

Kuman, K. and R. J. Clarke (2000). "Stratigraphy, artefact industries and hominid associations for Sterkfontein, Member 5." Journal of Human Evolution **38**(6): 827-847.

Lahr, M. M. and R. Foley (1994). "Multiple dispersals and modern human origins." Evolutionary Anthropology: Issues, News, and Reviews **3**(2): 48-60.

Lahr, M. M. and R. A. Foley (1998). "Towards a theory of modern human origins: geography, demography, and diversity in recent human evolution." Yearbook of Physical Anthropology **41**: 137-176.

Lansing, S., A. L. Rector, K. E. Reed, J. Lee-Thorp and C. W. Marean (2009). Taphonomic, Taxonomic and Isotopic Analyses of A Marine Isotope Stage 6 Carnivore Den from Pinnacle Point, Mossel Bay, South Africa. Annual Meeting of the Paleoanthropology Society. Chicago, Ill.

Lee-Thorp, J. and N. J. Van Der Merwe (1987). "Carbon isotope analysis of fossil bone apatite." South African Journal of Science; v. **83**(11) p. 712-715

Lee-Thorp, J. A., J. C. Sealy and N. J. Van Der Merwe (1989). "Stable carbon isotope ratio differences between bone collagen and bone apatite, and their relationship to diet." Journal of Archaeological Science **16**(6): 585-599.

Lee-Thorp, J.A., Manning, L. and M. Sponheimer (1997) “Problems and prospects for carbon isotope analysis of very small samples of fossil tooth enamel” Bulletin de la Societe Geologique de France **168**: 767-773

Marean, C., P. Nilssen, K. Brown, A. Jerardino and D. Stynder (2004). "Paleoanthropological investigations of Middle Stone Age sites at Pinnacle Point, Mossel Bay (South Africa): Archaeology and hominid remains from the 2000 field season." PaleoAnthropology **5**(2): 14-83.

Marean, C. W. (2010). "Pinnacle Point Cave 13B (Western Cape Province, South Africa) in context: the Cape floral kingdom, shellfish, and modern human origins." Journal of Human Evolution **59**(3): 425-443.

Marean, C. W., Z. Assefa and A. B. Stahl (2005). The Middle and Upper Pleistocene African record for the biological and behavioral origins of modern humans African Archaeology. New York, Blackwell**:** 93-129.

Marean, C. W., M. Bar-Matthews, J. Bernatchez, E. Fisher, P. Goldberg, A. I. R. Herries, . . . H. M. Williams (2007). "Early human use of marine resources and pigment in South Africa during the Middle Pleistocene." Nature **449**: 905-908.

Marean, C. W., H. C. Cawthra, R. M. Cowling, K. J. Esler and J. De Vynck (2014). "Stone Age people in a changing South African Greater Cape Floristic Region." Fynbos: Ecology, Evolution, and Conservation of a Megadiverse Region: 164.

Matthews, T. (2004). The taxonomy and taphonomy of Mio-Pliocene and Late Middle Pleistocene micromammals from the Cape west coast, South Africa PhD Thesis, University of Cape Town, South Africa.

Matthews, T. (n.d.). A summary of the micromammal population from PP30 (Brown hyaena den). Unpublished report.

McBrearty, S. and A. S. Brooks (2000). "The revolution that wasn't: a new interpretation of the origin of modern human behavior." Journal of Human Evolution **39**: 453-563.

McDougall, I., F. H. Brown and J. G. Fleagle (2005). "Stratigraphic placement and age of modern humans from Kibish, Ethiopia." Nature **433**: 733-736.

Meadows, M. E. and A. J. Baxter (1999). "Late Quaternary Palaeoenvironments of the southwestern Cape, South Africa: a regional synthesis." Quaternary International **57-58**: 193-206.

Mills, M. G. L. (1990). Kalahari Hyenas : Comparative Behavioral Ecology of Two Species, The Blackburn Press.

Mitchell, P. (2002). The Archaeology of Southern Africa. Cambridge, Cambridge University Press.

Muller, M. J. and P. D. Tyson (1988). "Winter rainfall over the interior of South Africa during extreme dry years." South African Geographical Journal **70**: 20-30.

Oestmo, S. and C. W. Marean (2014). Pinnacle Point: Excavation and Survey Methods. In Smith C. (ed.) Encyclopedia of Global Archaeology, New York: Springer.

Partridge, T. C., P. B. deMenocal, S. A. Lorentz, M. J. Paiker and J. C. Vogel (1997). "Orbital forcing of climate over South Africa: a 200,000-year rainfall record from the Pretoria Saltpan." Quaternary Science Reviews **16**(10): 1125-1133.

Passey, B. H. and T. E. Cerling (2006). "In situ stable isotope analysis (^{13}C, ^{18}O) of very small teeth using laser ablation GC/IRMS." Chemical Geology **235**: 238-249.

Podelsak, D. W., A.-M. Torregrossa, J. R. Ehleringer, M. D. Dearing, B. H. Passey and T. E. Cerling (2008). "Turnover of oxygen and hydrogen isotopes in the body water, CO2, hair, and enamel of a small mammal." Geochimica et cosmochimica acta **72**(1): 19-35.

Reason, C. and M. Rouault (2005). "Links between the Antarctic Oscillation and winter rainfall over western South Africa." Geophysical Research Letters **32**(7): L07705.

Rector, A. L. and K. E. Reed (2010). "Middle and late Pleistocene faunas of Pinnacle Point and their paleoecological implications." Journal of Human Evolution **59**(3): 340-357.

Robb, G. N., S. Woodborne and N. C. Bennett (2012). "Subterranean sympatry: an investigation into diet using stable isotope analysis." PloS one **7**(11): e48572.

Scholz, C. A., T. C. Johnson, A. S. Cohen, J. W. King, J. A. Peck, J. T. Overpeck, M R. Talbot et al. (2007) "East African megadroughts between 135 and 75 thousand years ago and bearing on early-modern human origins." Proceedings of the National Academy of Sciences **104**(42):16416-16421

Sharp, Z. and T. Cerling (1996). "A laser GC-IRMS technique for in situ stable isotope analyses of carbonates and phosphates." Geochimica et Cosmochimica Acta **60**(15): 2909-2916.

Skinner, J. D. and C. T. Chimimba (2005). The mammals of the southern African sub-region, Cambridge University Press.

Skinner, J. D., M. A. Haupt, M. Hoffmann and H. M. Dott (1998). "Bone Collecting by Brown Hyaenas *Hyaena brunnea* in the Namib Desert: Rate of Accumulation." Journal of Archaeological Science **25**(1): 69-71.

Skinner, J. D. and R. J. Van Aarde (1991). "Bone collecting by brown hyaenas *Hyaena brunnea* in the central Namib Desert, Namibia." Journal of Archaeological Science **18**(5): 513-523.

Smith, B. N. and S. Epstein (1971). "Two Categories of $^{13}C/^{12}C$ Ratios for Higher Plants 1." Plant Physiology **47**(3): 380-384.

Sponheimer, M., & Lee-Thorp, J. A. (2001). “The oxygen isotope composition of mammalian enamel carbonate from Morea Estate, South Africa”. Oecologia **126**(2), 153-157.

Sponheimer, M. and J. A. Lee-Thorp (1999). "Oxygen Isotopes in Enamel Carbonate and their Ecological Significance." Journal of Archaeological Science **26**(6): 723-728.

Sponheimer, M., J. A. Lee-Thorp, D. J. DeRuiter, J. M. Smith, N. J. van der Merwe, K. Reed, . . . C. Heidelberger (2003a). "Diets of Southern African Bovidae: stable isotope evidence." Journal of Mammalogy **84**(2): 471-479.

Sponheimer, M., T. Robinson, L. Ayliffe, B. Passey, B. Roeder, L. Shipley, . . . J. Ehleringer (2003b). "An experimental study of carbon-isotope fractionation between diet, hair, and feces of mammalian herbivores." Canadian Journal of Zoology **81**(5): 871-876.

Stuut, J. B., X. Crosta, K. van der Borg and R. Schneider (2004). "Relationship between Antarctic sea ice and southwest African climate during the late Quaternary." Geology **32**(10): 909-912.

Thackeray, J. F., A. van de Venter, J. A. Lee-Thorp, C. T. Chimimba and J. Van Heerden (2003). "Stable carbon isotope analysis of modern and fossil samples of the South African rodent Aethomy namaquensis." Annals of the Transvaal Museum **40**: 43-46.

Tyson, P. D. (1999). "Atmospheric circulation changes and paleoclimates of southern Africa." South African Journal of Science **95**: 194-201.

Van Andel, T. H. (1989). "Late Pleistocene sea levels and human exploitation of the shore and shelf of southern South Africa." Journal of Field Archaeology **16**: 133-155.

Van Zinderen Bakker, E. (1976). "The evolution of Late-Quaternary palaeoclimates of southern Africa." Palaeoecology of Africa **9**: 160-202.

Vogel, J. C., A. Fuls and R. P. Ellis (1978). "The geographical distribution of Kranz grasses in South Africa." South African Journal of Science **74**: 209-215.

Wang, Y. and T. E. Cerling (1994). "A model of fossil tooth and bone diagenesis: implications for paleodiet reconstruction from stable isotopes." Palaeogeography, Palaeoclimatology, Palaeoecology **107**(3-4): 281-289.

White, T. D., B. Asfaw, D. DeGusta, H. Gilbert, G. D. Richards, G. Suwa and F. Clark Howell (2003). "Pleistocene Homo sapiens from Middle Awash, Ethiopia." Nature **423**(6941): 742-747.

Wiesel, I. (2007). "Predatory and foraging behaviour of brown hyenas (*Parahyaena brunnea* (Thunberg, 1820)) at Cape fur seal (Arctocephalus pusillus pusillus Schreber, 1776) colonies."

Yeakel, J. D., N. C. Bennett, P. L. Koch and N. J. Dominy (2007). "The isotopic ecology of African mole rats informs hypotheses on the evolution of human diet." **274**(1619): 1723-1730.

5. Stable carbon isotope analysis of micromammals from deposits straddling the MIS6-MIS5 transition at Pinnacle Point, South Africa suggest small but possibly significant vegetation changes at ~125 ka.

Introduction

Hypothesized changes in the composition of vegetation and the distribution of C_4 grasses due to shifts in the frequency and distribution of winter and summer rainfall during the terminal Pleistocene in South Africa are well documented (Klein, 1980; Lee-Thorp and Beaumont, 1995; Sealy, 1996; Chase and Meadows, 2007). What is less well documented is how past changes in these abiotic factors impacted the distribution of C_3 and C_4 vegetation during Middle Pleistocene glacial-interglacial transitions, and thus continuing to develop paleoenvironmental proxy records from the MIS6/MIS5e transition is crucial to our understanding of Middle Pleistocene fossil and archaeological contexts.

Reported here is a stable carbon isotope record obtained via laser ablation gas chromatograph isotope ratio mass spectrometry (LA-GC-IRMS) sampling of micromammal specimens from south Coast archaeological deposits that date to MIS6 and MIS5e. Micromammal fossil teeth are recognized as an abundant potential reservoir of paleoenvironmental proxy data at an extremely local scale (Gehler *et al.,* 2012; Hynek *et al.,* 2012; Kimura *et al.,* 2013; Royer *et al.,* 2013), and advances in mass spectrometry, including the use of laser ablation (Cerling and Sharp, 1996; Sharp and Cerling, 1996; Lindars *et al.,* 2001; Passey and Cerling, 2006; Grimes *et al.,* 2008), now permit enamel sampling of even very small specimens. Fossil micromammals 'sample' vegetation (by consuming it) on scales different from those of large mammals (Hynek *et al*, 2012), due

to unique aspects of their life histories, and the comparably small area over which micromammal assemblages are aggregated by predators such as owls (Andrews, 1990; Matthews, 2004).

The Sites

Although there are a handful of localities in South Africa that are attributed to MIS6 or early MIS5 age, geochronological control is largely lacking (Thompson *et al.*, 2010); the deposits in most well-dated coastal sites post-date MIS5e, likely the result of earlier sediments being washed out of low-lying caves during the MIS5e high sea stand (Hendey and Volman, 1986). Pinnacle Point 9C (PP9C) and Pinnacle Point 13B (PP13B) are two of the only archaeological localities in the southern Cape to have sediments that are terminal MIS6 and MIS5e in age. In PP9C, these sediments underlie and are older than the archaeological material, while at PP13B, the MIS6 and MIS5 sediments contain primarily fossiliferous material.

PP9C

Pinnacle Point 9C (PP9C) is part of a larger cave complex, PP9, at Pinnacle Point (Mossel Bay, Western Cape, South Africa, Figure 5.1) that occurs near the base of coastal cliffs comprised of Table Mountain Sandstone (TMS). The age of the formation of the PP9 complex is unknown, but U-Pb ages obtained from speleothem and TT-OSL ages produced from a secondary sandstone (not TMS) adhering to the back of the cave suggest that the complex is at least 850 ka, and PP9 is likely to have been formed by the same 1.1 – 1.0 mya high sea stand that cut other caves at the Pinnacle Point locality (Herries *et al.*,

in prep; Pickering *et al.*, 2013). The main cave of PP9, PP9A, is a large cave with a talus deposit of cliff collapse blocking the mouth, and the lowest point of the mouth is approximately 8 masl (Marean *et al.*, 2004); cave PP9B is a secondary cave near the south side of the mouth of PP9A, approximately 6m above the floor of PP9A, and is accessible without the use of ropes or specialized climbing equipment (Matthews *et al.*, 2011). The remaining cavities all have openings near the roof of PP9A. None is presently accessible without the use of fixed ropes (Matthews *et al*., 2011), although remnant dunes indicate that in the past large dunes abutting the cliff wall would have provided access to these upper cave portions by terrestrial animals (including *Homo*

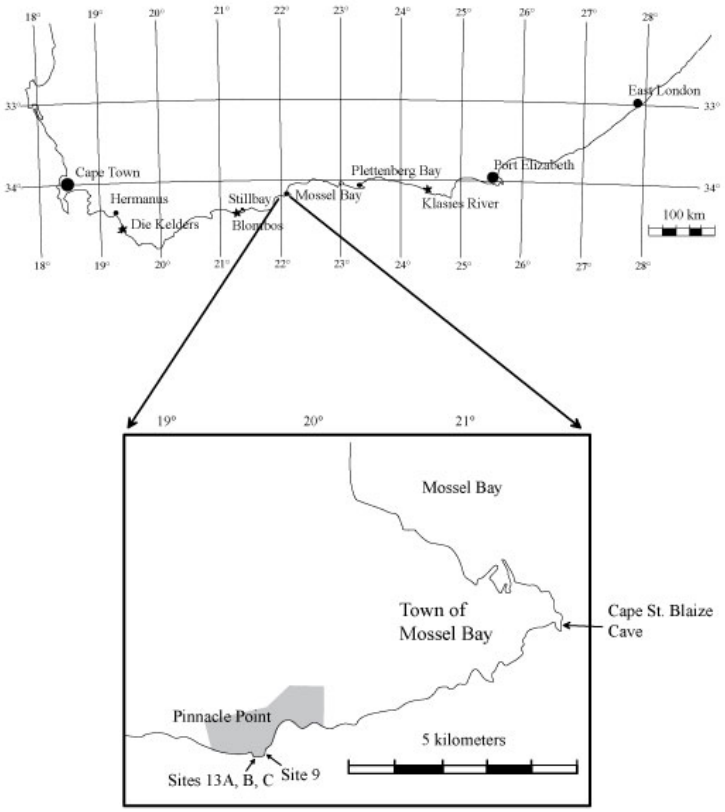

Figure 5.1. Map of South Africa, showing the location of Pinnacle Point. Inset: Map of Mossel Bay and Pinnacle Point, showing the location PP13B. (Figure credit: SACP4)

sapiens). The PP9C, PP9D, and PP9E cavities may thus all have been accessible for occupation at various points during the Pleistocene; however only PP9C has been excavated (Herries *et al.,* in prep).

The mouth of PP9C is >15 masl, above the height of the MIS5e high sea stand (+6.0m - + 8.0 m amsl; Carr *et al.,* 2010), and thus preserves MIS5e-and-earlier sediments. The oldest sedimentary deposits in PP9C are marine sands that are likely at least 600 ka (Herries *et al.,* in prep). PP9C preserves MIS8 and MIS7 sediments, as well as significant deposits that are MIS6 and MIS5e in age. Archaeological excavations of the PP9C deposits took place at two areas within the cave (one 50 cm^2 square was excavated in the entrance of the rear tunnel of the cave (the "RTE area"), and three 50 cm^2 excavation squares were placed at the back of the cave rear tunnel (the "RTR area") (Matthews *et al.,* 2011; Herries *et al.,* in prep). Although evidence for human occupation of the PP9C does not appear to pre-date 86 ± 4 ka (Herries *et al.,* in prep), excavations in the RTE and RTR areas exposed fossiliferous sediments dated by OSL to MIS6 and MIS5 (Matthews *et al*., 2011).

The "Brown Yellow Cave Sand" (BYCS) stratigraphic aggregate was excavated in the rear of PP9C in the RTR area. The BYCS is comprised primarily of aeolian sands, and contains abundant fossil micromammal material. An OSL sample taken from the BYCS section yielded an optical age of 130 ± 9 ka (Matthews *et al.,* 2011). Underlying the BYCS is the "Light Yellow Decalcified Sand" (LYDS), which lies at the mixed boundary of the MIS 19 raised beach and the BYCS (Herries *et al*., in prep). Fossiliferous material from this unit is likely similar in age to that from the BYCS, although the sample size is quite small (NISP = 10; Matthews *et al.*, 2011).

Overlying the BYCS in the RTR area is a second stratigraphic aggregate, the "Brown Yellow Surface Sand" (BYSS), that is contiguous with the BYCS (Herries *et al.*, in prep). Although there are no radiometric ages for the BYSS, it is likely close in age to the BYCS because the cave was closed to aeolian deposition by 129 ka; formation of clean speleothem at the back of the cave is evidence that PP9C was closed by the formation of a cave-sealing dune. The age of this speleothem growth has been dated by U-Th to 129.4 - 126.2 ka (Herries *et al.*, in prep).

Two stratigraphic aggregates were identified in the RTE area. The lower aggregate, the "Brown Yellow Dune Sand" (BYDS) has been aged by OSL to 126 ± 9 ka (Matthews *et al.*, 2011). Deposition of these dunes sands likely post-dates the closure of the cave indicated by the U-Th ages of the speleothem, as the micromammal material occurs throughout the deposits and shows strong evidence of being accumulated by either the spotted eagle owl (*Bubo africanus*) or the barn owl (*Tyto alba*) (Matthews *et al.*, 2011). Raptor accumulation would require at least partial opening of the cave for owl roosting, and it is common for caves that are partially sealed to have small opening near the roof between the cliff and the dune.

Overlying the BYDS is the "Olive Yellow Cave Sand" (OYCS). The OYCS is composed of quartzitic sand derived from roofspall (Herries *et al.*, in prep), and single-grain OSL of sediment sampled from the OYS yields an optical age of 120 ± 7 ka (Matthews *et al.*, 2011).

PP13B

Pinnacle Point 13B (PP13B) is an archaeological site located on the south coast of South Africa. PP13B is situated within a cave in a coastal cliff of the Table Mountain Sandstone (TMS) and its mouth has an elevation of ~15m asl. The cave itself is of unknown age, although the age of remnant deposits in another cave in the PP13 complex, PP13G (14.5 masl), suggest that the cave complex is at least 1 mya (Pickering *et al.*, 2013). All of the caves at the PP locality are thought to result from erosion of fault breccias within the TMS by high sea stands (Karkanas and Goldberg, 2010). The oldest deposits in PP13B, a boulder facies near the back (Western Area) of the cave (Figure 5.2) likely date to a regionally documented +13m ± 2m asl MIS 11 high-sea stand ~400 ka (Roberts *et al.*, 2012).

Basal sedimentary deposits in the Western Area of the cave are dated by TT-OSL to 349 ± 15 ka but are sterile of artifactual or fossil material (Marean *et al.*, 2010), and the majority of the archaeological deposits throughout the cave instead span MIS6 and MIS5 (Jacobs, 2010). MIS6 sediments are found in the lowermost deposits of the Western Area of the cave, and adhering as lightly cemented remnant (LC-MSA) on the north and south walls of the cave (Marean *et al.*, 2007; Marean *et al.*, 2010). MIS5 deposits occur in both the Western and in the Eastern (front) and Northeastern (north wall) Areas of the cave (Figure 5.2).

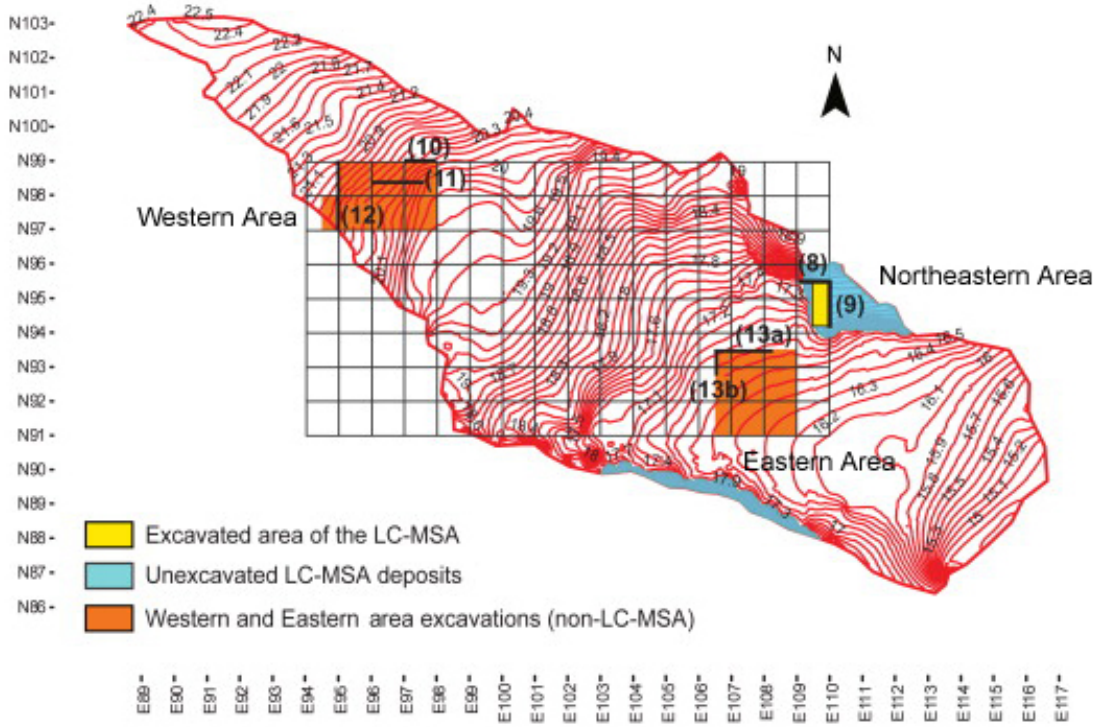

Figure 5.2. Map of the interior of the PP13B cave, showing Western, Eastern, and Northeastern excavation areas. Modified from Marean *et al.* (2010).

A dune sealed PP13B to occupation by ~90 ka, and the cave remained sealed until ~39 ka (Marean *et al.*, 2010). Archaeological deposits at PP13B are currently the only well-dated MIS6 Middle Stone Age (MSA) sequence in coastal southern Africa, and contain some of the earliest evidence for systematic use of pigments and marine resources by early *Homo sapiens* (Marean *et al.*, 2007).

Five stratigraphic units from PP13B have geochronological ages that suggest they temporally overlap with the sequence from PP9C. The "LC-MSA Middle" is an archaeology-bearing depositional unit excavated from the LC-MSA sediments adhering to the north wall of the PP13B cave. Shellfish remains and lithic tools are common

(Marean *et al.*, 2007), as are *in situ* hearths (Karkanas and Goldberg, 2010), although the MNI of large fauna is relatively small (Rector and Reed, 2010; Thompson, 2010). Single-grain OSL of a sample taken from the LC-MSA Middle provides an optical age of 125 ka ± 7 for the stratigraphic unit (Jacobs, 2010), with an adjusted minimum and maximum age range of 120 – 130 ka (Marean *et al.*, 2010) . The micromammal specimen count is comparably low (NISP = 10; Mattthews *et al*., 2009), and only three specimens were suitable for isotopic analysis, but as the dating on this stratigraphic aggregate it well constrained, it is included here. An overlying stratigraphic unit, the "LC-MSA Upper" is also MIS5e in age (Jacobs, 2010), but this unit is more heavily cemented than the underlying sediments, was partially excavated as blocks of cementation removed from the profile, and has very low specimen counts as a result; no micromammal specimens from the LC-MSA Upper were included in this analysis.

The "Light Brown Grey Sand 1" (LBG Sand 1) is an archaeological unit excavated in the Western Area of PP13B. The sedimentary matrix is a silty sand with some aeolian input and is between 12 and 20 cm thick (Karkanas and Goldberg, 2010). There is abundant artifactual material (Marean *et al*., 2010), both fragmentary and taxonomically identifiable large mammal remains (Rector and Reed, 2010; Thompson, 2010), and a comparably large micromammal sample (Matthews *et al.*, 2009). Four OSL samples were taken from the LBG Sand 1 stratigraphic unit. Two samples (sample #46459 and #46464) were taken from near the top of the unit, and resulted in optical ages of 98 ± 6 ka and 99 ± 4 ka respectively, while OSL samples taken from near the middle of the profile (#46463 and #46457) result in a weighted average optical age of 124 ± 5 ka (Jacobs, 2010). Given the comparable thickness of sediments, here the 99 ka ages from

the top of the LBG Sand 1 unit are treated as terminal ages, and OSL ages from the middle of the section as most applicable to the micromammal remains, and thus chronologically overlapping the stratigraphic aggregates from PP9C. Two other Western Area stratigraphic aggregates from PP13B, “DB Sand 4a” and “LBG Sand 2”, also likely date to MIS5e or late MIS6 on stratigraphic grounds (adjusted minimum age 117 ka, adjusted maximum age 166 ka; Marean *et al.,* 2010), but have comparably small micromammal samples (NISP = 8 and NISP = 7, respectively; Matthews *et al*., 2009). One specimen each of *Otomys* from the DB Sand 4a and the LBG Sand 2 were isotopically analyzed and are included here.

PP13B is approximately 250m southwest of PP9C in the same coastal exposures of TMS. Given the short distance between PP13B and PP9C, hypothetically contemporaneous deposits in both sites should contain similar proxy records, as the material aggregated in both caves would sample the same prevailing environmental conditions, and there is unlikely to be a significant change in vegetation and faunal communities over such a short distance. Thus, differences in proxy records between stratigraphic aggregates both within and between sites likely represent real temporal changes in the site-local paleoenvironmental conditions.

Chronological ordering of the deposits from which micromammal specimens were sampled.

Geochronology of the sites indicates that the deposits from PP9C, and the subset of deposits from PP13B sampled here, span the MIS6 to MIS5e transition (Marean *et al.*, 2010; Herries *et al.*, in prep). Within each site it is possible to produce a stratigraphically ordered sequence based on chronometric ages and the superimposition of sedimentary units. Putting the sequence between the two sites into an approximate chronological order is somewhat more complicated, as there are no shared 'marker horizons' between the two sets of deposits. Instead, indications of cave openings and closings (signaled by uranium-thorium ages from clean speleothem) and the chronometric ages obtained from over and underlying sediments are used constrain the OSL ages in such a way that the deposits from PP9C and PP13B may be placed in an approximate chronological ordering system (Table 5.1).

At PP13B, there is direct stratigraphic contact between the stratigraphic units in the Western Area from which micromammal specimens were sampled. The LBG Sand 2 directly underlies the DB Sand 4a, which in turn underlies the LBG Sand 1 (Marean *et al.*, 2010). Thus, while there are no direct geochronometric ages for the LBG Sand 2 and DB Sand 4a sediments, the law of superposition holds that, given that the sediments have not been reworked or redeposited as fill into more recent cuts, the LGB Sand 2 must be older than the DB Sand 4a, which is turn older than the LBG Sand 1, which has an adjusted maximum age of 134 ka, (Marean *et al.*, 2010). There is no excavated stratigraphic contact between these PP13B Western Area deposits and the LC-MSA

Middle, whose sediments are adhered to the northeast wall of the cave near the mouth (Figure 5.2). These deposits however have good chronometric control, and have a single-grain optical age of 125 ka ± 7 (Jacobs, 2010). Marean *et al.* (2010) ascribe an adjusted minimum age of 120 ka to the LC-MSA Middle, in part due to a weighted mean OSL age of 126 ± 4 ka for sediments from the overlying deposits. Based on optical ages, the LC-MSA Middle deposits are at least contemporaneous with the LBG Sand 1 sediments; it is likely that the LGB Sand 1 stratigraphic unit is actually somewhat younger than the LC-MSA Middle because OSL ages from the middle of the LBG Sand1 unit (124 ± 5 ka; Jacobs, 2010) overlap considerably with the optical ages for the LC-MSA Upper unit that overlies the LC-MSA Middle.

At PP9C, the BYCS has been dated by single grain OSL, with a weighted mean age of 130 ± 9 ka (Matthews *et al.*, 2011). It is stratigraphically contiguous with the BYSS, whose depositional terminus is indicated by clean speleothem formation that has been dated using U-Th to 129.4 - 126.2 ka (Herries *et al.*, in prep). Thus the BYCS and BYSS deposits in PP9C are likely older than the LC-MSA Middle and LBG Sand 1 deposits in PP13B. Given the PP13B stratigraphic units LBG Sand 2 and DB Sand 4a are likely older the ~125ka and younger than ~157 ka (Table 5.1) (Marean *et al*, 2010; Jacobs, 2010), the LBG Sand 2 and DB Sand 4a material is here treated as likely older than or contemporaneous to the PP9C BYCS and BYSS material.

The BYDS deposits from PP9C likely post-date the closure of the cave indicated by clean speleothem formation dating from 126.2 ka to 129.4 ka (Herries *et al.*, in prep), and the OSL age of 126 ± 9 ka for those deposits (Matthews *et al.*, 2011) likely makes them peri-contemporaneous with the PP13B LC-MSA Middle and LBG Sand 1 deposits.

The optical age of 120 ± 7 ka for the PP9C stratigraphic unit OYCS (Matthews *et* al., 2011) does not exclude it from contemporaneity with the BYDS, LC-MSA Middle or the LBG Sand 1 units; however, given the comparably more recent mean OSL age for the OYCS and the fact that it overlaid the older BYDS, the OYCS represents the youngest sediments from which fossiliferous material in this study was sampled.

Strat. Unit	Site	Adj. Min. Age[a]	Adj. Max. Age[a]	Weighted Mean OSL Age	OSL Age of overlying deposit	OSL Age of underlying deposit	Speleothem: cave open or closed?	Stratigraphic association
OYCS	PP9C			120 ± 7[b]		126 [b] □ 9		Overlies BYDS
LBG Sand 1	PP13B	94	134	124 ± 5[c]				Overlies DB Sand 4a
LC-MSA Middle	PP13B	120	130	125 ± 7[c]	126 ± 4[c]	162 ± 5[c]		
BYDS	PP9C			126 ± 9[b]	120 ± 7[b]		cave likely sealed 129.4 - 126.2[d]	Underlies OYCS
BYSS	PP9C					130 [b] □ 9	cave likely sealed 129.4 - 126.2[d]	Overlies BYCS
BYCS	PP9C			130 ± 9[b]			cave likely sealed 129.4 - 126.2[d]	Between BYSS & LYDS
LYDS	PP9C				130 ± 9[b]	MIS 19		Underlies BYCSS
DB Sand 4a	PP13B	117	166		124 ± 5[c]			Between LBG Sand 1 and LBG Sand 2
LBG Sand 2	PP13B	117	166			157 ± 8[c]		Underlies DB Sand 4a

Table 5.1. Geochronometric ages for deposits from which fossil micromammal specimens derive. All ages in thousands of years (ka). [a] Adjusted minimum and maximum ages from (Marean *et al.*, 2010); [b] OSL ages from (Matthews *et al.* , 2011); [c] OSL ages from (Jacobs, 2010); [d] Speleothem U-TH ages and indications of cave closure from (Herries *et al.*, in prep).

Materials and Methods

Micromammals: Fossil

Micromammal specimens are housed at the Diaz Museum, Mossel Bay, South Africa. Destructive analysis and temporary export permits were granted by the South African Heritage Resource Agency (SAHRA permits 80/12/03/013/52 and 80/12/03/012/52). Preliminary assessment of the suitability of individual specimens for isotopic analysis was undertaken in the field; loose and *in situ* catalogued teeth were macroscopically examined for indications of burning, staining, adhering organics or other signs of alteration. One hundred seventy-four teeth from PP9C that were identified to at least the generic level were classified as suitable for laser ablation; of these, 80 were exported per the requirements of the sampling permit, which stipulated that no more than half of the suitable specimens be exported at any one time. Three hundred thirty-six specimens from PP13B that were identified to at least the generic level were also classified as suitable for laser ablation; 163 specimens from all stratigraphic units at PP13B (including those not reported here) were exported for analysis. All specimens were returned to South Africa after analysis. A smaller sample of powdered enamel was retained from a subset of the larger teeth (primarily incisor specimens) for phosphoric acid digestion.

The taxonomic composition of the LA-GC-IRMS sample from PP9C is different from that of the PP9C micromammal assemblage as a whole. Insectivorous or omnivorous species were excluded from isotope sampling in order to eliminate potential interpretive problems that might arise from trophic fractionation of stable carbon and oxygen isotopes (see Chapter 3). Thus, although specimens attributed to Soricidae, as

well as murids belonging to the genera *Rhabdomys*, *Mystromys*, and *Steatomys* are important in paleoenvironmental reconstructions based on community structure (Matthews *et al.*, 2011), they are not included in the isotopic analysis due to either partial or complete insectivory. In both the RTE area and the RTR area, the number of species identified in the assemblage is comparably high, but the relative proportion of the respective assemblages represented by *Otomys* specimens is variable (Matthews *et al*., 2011). In the OYCS and the BYDS stratigraphic aggregates from the RTE area of PP9C, *Otomys* specimens comprise between 40% and 52% of the assemblage (OYCS *Otomys* NISP = 34, total NISP = 86; BYDS *Otomys* NISP = 11, total NISP = 21; Matthews *et al*., 2011). In the BYSS and BYCS deposits from the RTR area of the cave, the relative frequency of *Otomys* specimens are comparably lower (26%; BYSS *Otomys* NISP = 28, total NISP = 105; BYCS *Otomys* NISP = 96, total NISP = 362) (Matthews *et al.*, 2011). *Bathyergus* and *Gerbilliscus* are present in all units in low numbers.

The PP13B MIS5 micromammal community is dominated by representatives of the genus *Otomys*, especially in stratigraphic aggregates where the NISP is low (DB Sand 4a NISP = 8, LGB Sand 2 NISP = 7, LC-MSA NISP = 10; Matthews *et al*., 2009). In the LGB Sand 1, micromammal specimens are considerably more abundant (NISP = 210). More than 60% of the LGB Sand 1 micromammal sample is assigned to the genus *Otomys* (NISP = 132), but *M. varius*, *G. afra*, and *Rhabdomys* also occur with some frequency (Matthews *et al.*, 2009).

The sample of micromammal fossil specimens analyzed for LA-GC-IRMS is composed of the following five species; *Bathyergus suillus*, *Gerbilliscus afra*, *Aethomys namaquensis*, *Otomys irroratus*, and *Otomys saundersiae*, as well as nine specimens

identified only to the genus *Otomys*, and one specimen assigned to *Bathyergidae (non-specific)*. The specimen counts of the isotopic analysis for each stratigraphic aggregate, by taxon, are listed in Tables 5.1-5.7.

B. suillus is a member of the Bathyergidae, a family of burrowing rodents that has been extant in southern Africa since at least the Pliocene (Denys, 1998; Matthews *et al.*, 2006). *B. suillus* is an herbivore and consumes primarily geophytic material (Bennett and Faulkes, 2000), as well as aboveground grasses and sedges that it pulls into the burrow (Davies and Jarvis, 1986; Bennett and Faulkes, 2000). $\delta^{13}C_{enamel}$ values should reflect admixed stable carbon isotope compositions of above ground and below ground vegetation.

G. afra is also a burrowing taxon, with a diet similar to that of *B. suillus* (e.g. “grass, bulbs, and roots", Skinner and Chimimba, 2005) although they also consume seeds (Granjon and Dempster, 2013). *Gerbilliscus* specimens have been recovered from Plio-Pleistocene contexts at Sterkfontein (Gauteng, South Africa) (Avery, 2000), but are not found in Pliocene deposits at Langebaanweg on the West Coast of South Africa (Matthews, 2004); *G. afra* does however appear in Middle Pleistocene fossil assemblages from throughout the Western Cape (Matthews, 2004; Matthews *et al.*, 2005). Modern *Gerbilliscus sp.* is associated with xeric environments (Matthews, 2011), but distribution analysis of modern specimens by Campbell *et al.* (2011) suggests a wide range of vegetation and rainfall tolerance. Given the similarities in burrowing behavior and dietary ecology in *G. afra* and *B. suillus*, and the comparable ranges of these taxa, it is hypothesized that contemporaneous stable carbon and stable oxygen isotopes values will be similar between the two species.

There is one specimen of *A. namaquensis* included in the isotope analysis. This taxon is distributed across southern Africa and has no strong preference for specific habit types. Stomach contents of modern specimens show mixed gramnivore-granivore feeding (Monadjem, 1997). Stable carbon isotope data obtained from bone collagen extracted from modern *A. namaquensis* collected along a SW/NE transect across modern vegetation zones of South Africa has a range of ~12‰ VPDB (Thackeray *et al.*, 2003), with the lowest mean $\delta^{13}C_{collagen}$ values found in specimens from the Karroo and South Coast (C_3-dominant vegetation), and higher values found in Mpumalanga and Limpopo (where C_4 vegetation is more predominant). Modern *A. namaquensis* specimens collected from the Cradle Nature Reserve (Gauteng Province, ZA) by Codron *et al.* (2015) are quite depleted in ^{13}C (median $\delta^{13}C_{hair}$ values = -22.7‰), which is also consistent with the mean $\delta^{13}C_{collagen}$ value of -20‰ (n = 5) reported in Thackeray *et al.* (2003) for modern specimens from the region.

Otomys is a genus of murid distributed across sub-Saharan Africa. In southern Africa, the oldest specimens are Pliocene in age (Skinner and Chimimba, 2005; Taylor, 2013). All members of the genus are strictly herbivorous, and primarily gramnivorous (although many species also consume herbs in addition to grasses) (Taylor, 2013). Fossil specimens of *Otomys* recovered from Pinnacle Point are primarily attributed to either *O. irroratus* or *O. saundersiae* (Matthews *et al.*, 2011). *O. irroratus* is a preferential grass feeder than can also act as an herbivorous generalist (Skinner and Chimimba, 2005; Taylor, 2013). *O. saundersiae*, whose comparable smaller range overlaps with larger and more habitat-diverse range of *O. irroratus*, has similar dietary preferences.

Micromammals: Modern

Modern comparative data for the taxa sampled exist in two forms. Stable carbon and oxygen isotope data obtained from enamel apatite was generated by sampling modern specimens of *Otomys irroratus, Otomys saundersiae, B. suillus,* and *G. afra* from three localities in modern ecosystems on the south coast of South Africa (Chapter 3). $\delta^{13}C_{apatite}$ and $\delta^{18}O_{apatite}$ values from these specimens are summarized in Table 5.2. This $\delta^{13}C_{apatite}$ and $\delta^{18}O_{apatite}$ data is the most directly comparable to fossil material, as both modern and fossil data sets derive from sampling of the same biological tissue. Isotope fractionation and routing varies by tissue type; as a result the relationship between $\delta^{13}C_{tissue}$ values and $\delta^{13}C_{diet}$ values vary as a function of the tissue type being measured. The diet-to-tissue offsets for stable carbon are well characterized (see Chapter 3 for discussion), but converting between tissue types does introduce a level of uncertainty into the analysis.

A small but growing literature regarding the isotope ecology of modern small and micromammals can provide additional context for fossil data. Additional stable carbon, oxygen, and nitrogen isotope data for modern specimens of *Otomys irroratus*, *Otomys saundersiae, B. suillus, G. afra,* and *A. namaquensis* from the Western Cape can be found in Sealy and van der Merwe (1986), Thackeray *et al.* (2003), Yeakel *et al.* (2007), Robb *et al.* (2012), and van den Heuvel and Midgley (2014). Sample materials derive from a number of localities within the winter rainfall region, and tissue types sampled include hair, collagen, and bone apatite. In order to compare this data to $\delta^{13}C_{apatite\text{-}fossil}$ data, $\delta^{13}C_{hair}$ and $\delta^{13}C_{collagen}$ values must be converted using known diet-tissue spacing values. For sampling localities from the literature in which the authors gave coordinate data,

lat/long coordinates were superimposed using GIS onto the SANBI National Vegetation Map (Mucina *et al.*, 2006). Given that none of the modern specimens from the literature data set derive from localities close to PP, they are not therefore an ideal dataset against which to compare the PP fossil specimens, but they can be cautiously used to provide additional interpretive context. Values available in the literature have been converted to apatite-comparable $\delta^{13}C$ values and are summarized in Appendix B as well as Chapter 3 of this dissertation.

$\delta^{13}C$ values of atmospheric CO_2 have decreased by ~1.5‰ over the last 150 years due to the introduction of ^{13}C-depleted CO_2 into the atmosphere via fossil fuel burning (see Cerling and Harris, 1999 for discussion). Comparison of fossil and modern apatites requires correcting for the impact of this fossil fuel effect on the carbon isotope composition of sample specimens.

Taxon	Locality	n	$\delta^{13}C_{enamel}$ (‰ VPDB)	δ13C ‰ VPDB, "corrected"	$\delta^{18}O_{enamel}$ (‰ VSMOW)
B. suillus	Rein's Nature Reserve	1	-13.51	-12.01	20.9
G. afra	Rein's Nature Reserve	1	-8.9	-7.4	30.0
O. irroratus	Amisrus, Wilderness	1	-12.7	-11.2	26.0
O. irroratus	Amisrus, Wilderness	1	-7.1	-5.6	26.5
O. irroratus	Amisrus, Wilderness	1	-12.3	-10.8	27.9
O. irroratus	Amisrus, Wilderness	1	-11.5	-10	26.3
O. irroratus	Amisrus, Wilderness	1	-18.1	-16.6	26.4
O. irroratus	Amisrus, Wilderness	1	-16	-14.5	25.9
O. irroratus	Amisrus, Wilderness	1	-21.2	-19.7	25.0
O. irroratus	Wolwe River	1	-15	-13.5	27.2
O. irroratus	Wolwe River	1	-14.7	-13.2	28.1
O. irroratus	Wolwe River	1	-15	-13.5	29.4
O. irroratus	Wolwe River	1	-10.7	-9.2	25.5
O. irroratus	Wolwe River	1	-18.3	-16.8	27.3
O. irroratus	Wolwe River	1	-14.3	-12.8	26.7
O. irroratus	Wolwe River	1	-15.1	-13.6	24.9
O. irroratus	Wolwe River	1	-10.8	-9.3	27.3
O. irroratus	Wolwe River	1	-10.1	-8.6	25.2
O. irroratus	Wolwe River	2	-17.7	-16.2	29.9
O. saundersiae	Rein's Nature Reserve	1	-16.32	-14.8	32.4
O. saundersiae	Rein's Nature Reserve	1	-17.23	-15.7	32.7
O. saundersiae	Rein's Nature Reserve	1	-15.19	-13.7	33.7
O. saundersiae	Rein's Nature Reserve	1	-15.35	-13.9	33.9
O. saundersiae	Rein's Nature Reserve	1	-17.19	-15.7	32.5
O. saundersiae	Rein's Nature Reserve	1	-15.23	-13.7	33.7
O. saundersiae	Rein's Nature Reserve	1	-15.57	-14.1	33.9
O. saundersiae	Amisrus, Wilderness	2	-12	-10.5	21.9

Table 5.2. Conventional phosphoric acid digestion stable carbon and oxygen isotope data from modern micromammal specimens sampled within 50km of Pinnacle Point. Methodological details of sampling and environmental context can be found in Williams (Chapter 3).

Laser Ablation Gas Chromatograph Isotope Ratio Mass Spectrometry (LA-GC-IRMS):

LA-GC-IRMS measurements on fossil teeth from both PP9C and PP13B were made at the Stable Isotope Laboratory at Johns Hopkins University (Baltimore, MD), following the methodology described in Passey and Cerling (2006).

Specimens were mounted within a vacuum chamber, which was flushed with He gas prior to analysis. Ablation of individual specimens proceeded using a 30-watt CO_2 laser at 5% power. Ablation pit spot size was 30 μm, and laser dwell time was 0.01 s. These laser settings limit the depth of the ablation pit, which is necessary to insure that only enamel, and not dentine (which is more likely to have been altered by diagenesis in fossil specimens; Kohn *et al.*, 1999; Dauphin and Williams, 2004) is sampled in taxa in which the enamel is comparably thin (Passey and Cerling, 2006). Ablation-produced CO_2 sample size was increased by the production of multiple ablation pits for each specimen sample during a "run"; where preservation and available enamel surface permitted, between 20 and 30 ablation pits were produced. CO_2 produced by ablation is then aggregated into a single sample aliquot that is introduced into the mass spectrometer (Sharp and Cerling, 1996; Passey and Cerling, 2006).

Charring was observed during 29 ablation runs on specimens from the PP9C stratigraphic aggregates, and on 14 specimens from the PP13B deposits reported here; this data was excluded from the analysis, as charring indicates likely ablation of surface organics (Henry *et al.*, 2012 SOM). Nine additional data points were removed from the analysis due to large fraction blanks that result in a significant reduction in the precision of isotope measurement (Passey and Cerling, 2006).

The final analytical dataset for fossil micromammal material from PP9C is comprised of 78 LA-GC-IRMS sampling runs on 65 unique specimens, and from PP13B MIS5 deposits it is comprised of 26 LA-GC-IRMS runs on 24 unique specimens. Stable isotope ratio data obtained via LA-GC-IRMS are normalized to VPDB and VSMOW using the known values from injected CO_2 standards, following standardized procedures (Passey and Cerling, 2006).

Results

The results of the stable carbon isotope analyses of the PP9C and PP13B fossil material are presented below. Stable oxygen isotope ratio data has been included in the Tables 1-7, but are not discussed at length due to the difficulties both in interpreting bulk $\delta^{18}O_{carbonate}$ data without an ecological context (Bryant *et al.*, 1996; Sponheimer and Lee-Thorp, 1999) as well as the reduction in accuracy in stable oxygen isotope measurement using LA-GC-IRMS when compared to traditional phosphoric acid digestion techniques (Passey and Cerling, 2006).

PP9C RTR Area

Two *Otomys sp.* specimens from the LYDS were sampled using LA-GC-IRMS. $\delta^{13}C_{laser}$ values for the specimens are -13.4‰ and -11.2‰ VPDB.(Table 5.3)

Twenty-eight micromammal specimens were sampled from the 130 ± 9 ka BYCS stratigraphic aggregate (Table 5.4). *B. suillus* (*n* = 4), *G. afra* (*n* = 1), *O. irroratus* (*n* = 3),

O. saundersiae (*n* =19), and *Otomys sp.* (*n* = 1) are represented in the sample. *B. suillus* $\delta^{13}C_{laser}$ values range from -9.4‰ to -11.7‰ VPDB (mean = -10.9‰ VPDB, σ = 1.01). The one specimen of *G. afra* has a $\delta^{13}C_{laser}$ value of -8.0‰. *Otomys irroratus* $\delta^{13}C_{laser}$ values range from -11.3 to -12.4‰ (mean = -11.7‰ VPDB, σ = 0.62), while *O. saundersiae* specimen $\delta^{13}C_{laser}$ values are slightly, although not significantly, more depleted ($\delta^{13}C$ range = -10.9 to -14.9‰, mean = -12.5‰ VPDB, σ = 1.12). The single *Otomys sp.* specimen $\delta^{13}C_{laser}$ = -12.9‰ VPDB.

Taxon	Specimen ID	Tooth Type	fraction blank	$\delta^{13}C_{laser}$ ‰ VPDB	$\delta^{18}O_{laser}$ ‰ VSMOW
Otomys sp.	100459A	MU1	0.058448	-13.4	22.2
Otomys sp.	100459B	ML2/ML3/MU2	0.06488	-11.2	24.1

Table 5.3. LA-GC-IRMS-obtained stable carbon and oxygen isotope data from the LYDS units from PP9C. For all tables, "tooth type", ML = lower molar, MU = upper molar.

Fourteen fossil micromammal specimens were sampled from BYSS (peri-contemporaneous to the BYCS)(Table 5.5). The single specimen of *A. namaquensis* was sampled twice, and produced a mean $\delta^{13}C_{laser}$ value of -14.8‰ (σ = 0.92). Four total ablation runs were performed on 3 specimens of *B. suillus*; *B. suillus* $\delta^{13}C_{laser}$ values range from -8.1‰ to -9.6‰ VPDB (mean = -8.9‰ VPDB, σ = 0.15). Two specimens of *G. afra* are included in the isotope sample. There is a nearly 5‰ difference between the $\delta^{13}C_{laser}$ values of the *G. afra* specimens: fossil #100453D $\delta^{13}C_{laser}$ = -10.0‰ VPDB, fossil #100408C $\delta^{13}C_{laser}$ = -5.9‰ VPDB). The *G. afra* specimen #100408C has the most

^{13}C-enriched value of any specimen from any of the stratigraphic units reported here. Two different specimens of *O. irroratus* had $\delta^{13}C_{laser}$ values of -11.4‰ VPDB and -14.4‰ VPDB. The *O. saundersiae* specimen count is somewhat higher (n = 6), with a mean value for $\delta^{13}C_{laser}$ of -12.1‰ VPDB (σ = 0.62; $\delta^{13}C_{laser}$ values range from -10.8‰ to -13.6‰).

Taxon	Specimen ID	Tooth	fraction blank	$\delta^{13}C$ ‰ VPDB	$\delta^{18}O$ ‰ VSMOW
B. suillus	100428A	incisor	0.090849	-11.3	18.0
B. suillus	100461A	molar	0.096368	-11.7	18.9
B. suillus	100461B	molar	0.087003	-11.1	17.9
B. suillus	100500B	molar	0.10759	-9.4	19.0
G. afra	100438A	ML1	0.10626	-8.0	20.1
O. irroratus	100460c	ML1	0.056766	-10.9	22.6
O. irroratus	100460C	ML1	0.085005	-11.7	21.9
O. irroratus	100460E	MU3	0.080582	-12.4	22.4
O. irroratus	100460F	MU3	0.053529	-11.1	23.3
O. irroratus	100460F	MU3	0.054614	-11.6	23.1
O. saundersiae	100384	MU3	0.080644	-11.5	22.8
O. saundersiae	100419	MU3	0.056222	-12.6	22.7
O. saundersiae	100428C	MU3	0.13268	-13.1	21.6
O. saundersiae	100428D	MU1/MU2	0.13058	-12.9	23.3
O. saundersiae	100428D	MU1/MU2	0.13638	-13.3	23.0
O. saundersiae	100437H	MU3	0.069143	-12.0	22.0
O. saundersiae	100438D	ML1	0.098034	-13.3	21.4
O. saundersiae	100460K	MU3	0.075248	-11.7	22.8
O. saundersiae	100461c	ML1	0.047022	-12.2	21.2
O. saundersiae	100461c	ML1	0.052743	-11.3	21.9
O. saundersiae	100461C	ML1	0.070241	-11.9	22.6
O. saundersiae	100461d	ML1	0.062195	-13.7	21.4
O. saundersiae	100461e	ML1	0.062388	-10.9	21.7
O. saundersiae	100461f	ML1	0.055881	-13.9	21.8
O. saundersiae	100461F	ML1	0.10091	-13.9	23.1
O. saundersiae	100461g	MU3	0.095955	-12.0	27.3
O. saundersiae	100461g	MU3	0.1399	-11.3	26.5
O. saundersiae	100461h	MU3	0.063551	-12.8	20.9
O. saundersiae	100461h	MU3	0.10628	-11.1	19.5
O. saundersiae	100500c	MU3	0.079971	-11.0	19.8
O. saundersiae	100500d	MU3	0.053283	-12.8	23.0
O. saundersiae	100500d	MU3	0.080701	-12.1	23.3
O. saundersiae	100500E	MU3	0.11234	-11.6	23.4
O. saundersiae	100500F	MU3	0.092541	-12.5	27.8
O. saundersiae	100500F	MU3	0.099131	-12.1	27.7
O. saundersiae	100500G	ML1	0.10064	-14.9	20.9
O. saundersiae	100500j	ML1	0.04529	-14.3	20.6
O. saundersiae	100500j	ML1	0.063352	-14.3	20.1
Otomys sp.	100446c	MU3	0.055987	-12.9	20.6

Table 5.4. LA-GC-IRMS-obtained stable carbon and oxygen isotope data from the BYCS units from PP9C. Tooth types: ML = lower molar, MU = upper molar (e.g. ML1 = lower 1st molar)

Taxon	Specimen ID	Tooth Type	fraction blank	$\delta^{13}C_{laser}$ ‰ VPDB	$\delta^{18}O_{laser}$ ‰ VSMOW
A. namaquensis	100412a	ML1	0.11045	-15.4	22.5
A. namaquensis	100412A	ML1	0.11161	-14.1	23.7
B. suillus	100450a	molar	0.083225	-9.0	19.9
B. suillus	100450b	molar	0.073139	-8.1	20.6
B. suillus	100450B	molar	0.11206	-9.6	18.9
B. suillus	100453a	molar	0.052765	-8.7	19.1
G. afra	100408C	ML1	0.064694	-5.9	20.7
G. afra	100453D	MU1	0.07919	-10.0	21.5
O. irroratus	100422a	ML1	0.092355	-11.1	22.4
O. irroratus	100422c	MU3	0.087015	-14.4	21.5
O. saundersiae	100430	MU3	0.085477	-11.7	23.0
O. saundersiae	100399B	ML1	0.056202	-13.0	22.7
O. saundersiae	100412B	Ml1	0.070814	-12.5	25.6
O. saundersiae	100412C	molar	0.065644	-11.7	21.5
O. saundersiae	100412C	molar	0.080031	-11.2	22.4
O. saundersiae	100412c	ML1	0.13893	-13.6	24.1
O. saundersiae	100412D	MU3	0.065611	-10.8	24.3
O. saundersiae	100422d	ML1	0.083543	-11.7	24.1
O. saundersiae	100453c	MU3	0.04354	-11.8	23.7

Table 5.5. LA-GC-IRMS-obtained stable carbon and oxygen isotope data from the BYSS units from PP9C. Tooth types: ML = lower molar, MU = upper molar (e.g. ML1 = lower 1st molar)

PP9C RTE Area

Six individual specimens from the BYDS (126 ± 9 ka) were ablated (Table 5.6). All were assigned to the genus *Otomys*: *O. irroratus* (*n* = 3), *O. saundersiae* (*n* = 1), *Otomys sp.* (*n* = 2). This is just over half of the total number of *Otomys* specimens (*n* = 11) recovered from this stratigraphic aggregate. One specimen of *G. afra* was recovered from the deposits, but was not sampled. The *O. irroratus* specimens range in $\delta^{13}C_{laser}$ from -9.6‰ to -12.4‰ VPDB (mean = -11.3‰ σ = 0.55). Three replicate measures of *O. irroratus* specimen #100395D resulted in a measurement σ =0.5‰, and duplicate

measures on specimen #100421C resulted in σ = 0.7‰. The *O. saundersiae* specimen has a mean $\delta^{13}C_{laser}$ of -11.9‰ (σ = 0.9), while the *Otomys sp.* $\delta^{13}C_{laser}$ values range from -11.6‰ to -13.0‰ VPDB (mean = -12.2‰, σ = 0.9).

Six specimens from the OYCS (120 ± 7 ka) were sampled (Table 5.7). Five specimens are attributed to *O. irroratus* and have $\delta^{13}C_{laser}$ that range from -11.7 ‰ to -13.8‰ (mean = -12.4‰, σ = 0.9). One specimen of *B. suillus* was sampled, $\delta^{13}C_{laster}$ = -7.0‰ VPDB.

Taxon	Specimen ID	Tooth Type	fraction blank	$\delta^{13}C_{laser}$ ‰ VPDB	$\delta^{18}O_{laser}$ ‰ VSMOW
O. irroratus	100395D	MU3	0.052535	-10.9	24.2
O. irroratus	100421b	ML1	0.058831	-11.7	23.1
O. irroratus	100421B	ML1	0.081416	-11.7	21.7
O. irroratus	100421b	ML1	0.11245	-9.6	23.1
O. irroratus	100421C	ML1	0.071383	-12.4	22.9
O. irroratus	100421C	ML1	0.085177	-11.4	22.9
O. saundersiae	100426	MU3	0.083354	-12.5	23.6
O. saundersiae	100426	MU3	0.083454	-11.2	24.3
Otomys sp.	100448a	ML2/ML3/MU2	0.057632	-13.0	20.8
Otomys sp.	100448a	ML2/ML3/MU2	0.058474	-12.6	21.1
Otomys sp.	100448A	ML2/ML3/MU2	0.084961	-13.0	21.8
Otomys sp.	100448b	ML2/ML3/MU2	0.053697	-11.6	22.5

Table 5.6. LA-GC-IRMS-obtained stable carbon and oxygen isotope data from the BYDS units from PP9C. Tooth types: ML = lower molar, MU = upper molar (e.g. ML1 = lower 1st molar)

Taxon	Specimen ID	Tooth Type	fraction blank	$\delta^{13}C_{laser}$ ‰ VPDB	$\delta^{18}O_{laser}$ ‰ VSMOW
B. suillus	100452	molar	0.098652	-7.0	20.2
O. irroratus	100427A	MU3	0.077753	-11.7	22.5
O. irroratus	100427B	MU3	0.075439	-12.4	21.1
O. irroratus	100431A	ML1	0.064359	-12.5	23.1
O. irroratus	100431B	MU3	0.072738	-11.7	22.7
O. irroratus	100462B	ML1	0.08034	-13.8	21.7

Table 5.7. LA-GC-IRMS-obtained stable carbon and oxygen isotope data from the OYCS units from PP9C. Tooth types: ML = lower molar, MU = upper molar (e.g. ML1 = lower 1st molar)

PP13B

One micromammal specimen attributed to *O. irroratus* was sampled from the LBG Sand 2 (adjusted minimum age: 112 ka, adjusted maximum age: 166 ka; Marean et al, 2010). Measured values of $\delta^{13}C_{laser}$ = -14.8‰ VPDB (Table 5.8).

One micromammal specimen attributed to *O. irroratus* was also sampled from the DB Sand 4a (adjusted minimum age: 112 ka, adjusted maximum age: 166 ka; Marean et al, 2010). Measured values of $\delta^{13}C_{laser}$ = -13.6‰ (Table 5.8).

Three specimens from the LC-MSA Middle (125 ± 7 ka), two attributed to *O. irroratus*, and one to *Otomys sp*. were ablated (Table 5.8). *Otomys irroratus* $\delta^{13}C_{laser}$ values were -10.7‰ and -11.5‰ (mean $\delta^{13}C_{laser}$ = -11.1‰ VPDB, σ = 0.6). The *Otomys sp.* specimen $\delta^{13}C_{laser}$ = -13.4‰ VPDB.

Nineteen specimens from the LBG Sand 1 (124 ± 5 ka) produced data within acceptable instrumentation standards (Table 5.9). Ablation of one specimen of *G. afra* resulted in a $\delta^{13}C_{laser}$ value of -14.4‰ VPDB. Nine specimens of *O. irroratus* were ablated, and $\delta^{13}C_{laser}$ values ranged from -15.4‰ to -16.5‰ VPDB (mean $\delta^{13}C_{laser}$ = -15.9‰ VPDB, σ = 0.4). Nine *O. saundersiae* specimens were also ablated, and resultant values of $\delta^{13}C_{laser}$ range from -13.5‰ to -18.8‰ (mean $\delta^{13}C_{laser}$ = -15.7‰ VPDB, σ=1.6).

layer	Taxon	Specimen ID	Tooth Type	fraction blank	$\delta^{13}C_{laser}$ ‰ VPDB	$\delta^{18}O_{laser}$ ‰ VSMOW
LC-MSA Middle	*O. irroratus*	99205A	ML1	0.053435	-10.7	25.1
LC-MSA Middle	*O. irroratus*	99245	MU1	0.087093	-11.5	22.6
LC-MSA Middle	*Otomys sp.*	99617		0.061193	-13.4	23.5
DB Sand 4a	*O. irroratus*	99926A	ML1	0.076508	-13.6	22.5
LBG Sand 2	*O. irroratus*	99929	ML1	0.12946	-14.8	23.7

Table 5.8. LA-GC-IRMS-obtained stable carbon and oxygen isotope data from the LBG Sand2, DB Sand 4a, and LC-MSA Middle units from PP13B. Tooth types: ML = lower molar, MU = upper molar (e.g. ML1 = lower 1st molar)

Taxon	Specimen ID	Tooth Type	fraction blank	$\delta^{13}C_{laser}$ ‰ VPDB	$\delta^{18}O_{laser}$ ‰ VSMOW
G. afra	99851	MU1,2	0.1244	-14.4	21.0
O. irroratus	99920C	ML1	0.044269	-16.2	20.4
O. irroratus	100012A	ML1	0.054662	-16.7	19.5
O. irroratus	100012A	ML1	0.063394	-16.2	20.2
O. irroratus	99368A	MU3	0.063887	-15.4	22.5
O. irroratus	99938D	MU3	0.074114	-15.4	20.9
O. irroratus	99938C	ML1	0.079375	-15.7	19.9
O. irroratus	99920C	ML1	0.093027	-16.1	21.0
O. irroratus	99935	ML1	0.097408	-16.1	21.7
O. irroratus	99932	ML1	0.10399	-15.5	21.7
O. irroratus	100049A	ML1	0.11847	-16.0	22.7
O. irroratus	99938C	ML1	0.13961	-16.4	18.7
O. saundersiae	100037		0.046151	-14.3	21.4
O. saundersiae	99331A		0.059243	-14.9	21.0
O. saundersiae	99325D		0.061362	-15.5	21.4
O. saundersiae	99368C		0.063155	-16.7	23.1
O. saundersiae	99325E		0.066852	-15.2	21.9
O. saundersiae	99325D		0.078555	-16.5	21.2
O. saundersiae	100049B		0.098053	-18.8	18.4
O. saundersiae	99933		0.098858	-16.5	22.8
O. saundersiae	99317D		0.12186	-13.5	22.7

Table 5.9. LA-GC-IRMS-obtained stable carbon and oxygen isotope data from the LBG Sand 1 units from PP13B. Tooth types: ML = lower molar, MU = upper molar (e.g. ML1 = lower 1st molar)

Discussion

Inferring the stable isotope composition of the diet from $\delta^{13}C_{enamel/laser}$ values.

The Greater Cape Floristic Region (GCFR) encompasses the entirety of the modern winter and year round rainfall zones of southern Africa, and is characterized by a distinctive, ancient vegetation biome. Within the GCFR there is no universally agreed classification, but there is broad agreement that there are four major vegetation types or complexes (Rebelo *et al.*, 2006). All are ecosystems with relatively high plant species diversity, and the majority of plants—with the exception of the grasses—utilize C_3 photosynthesis (Cowling, 1983; Cowling and Richardson, 1995; Goldblatt, 1997; Goldblatt and Manning, 2002). Current grass composition in CFR areas is a mixture of C_3 and C_4 species, with C_4 grasses predominating only in areas of limited shrubby vegetation cover and typically receiving at least some summer rain (Cowling, 1983).

Although fynbos on average is a C_3 vegetation community (and thus the majority of plant taxa will have distinctively C_3 $\delta^{13}C$ values), not all vegetation in fynbos communities utilizes the C_3 photosynthetic pathway; in fact, significant components of grass in certain fynbos community types are C_4. Within ~50km of Pinnacle Point there are 17 distinct GCFR vegetation groups (Rebelo *et al.*, 2006; see this thesis, Chapter 2), and the range of available $\delta^{13}C_{plant}$ values varies within the vegetation communities as a function of the presence and absence of C_4 grass taxa. While C_4 grasses are extant in most of the present day plant communities proximate to Pinnacle Point, there are some plant communities that appear to be depauperate in C_4 taxa. More so, this dearth of

available C_4 biomass is reflected in the stable carbon isotopic composition of modern micromammal consumer tissue (Chapter 3).

Meta-analysis of the available $\delta^{13}C_{plant}$ data available in the literature (Chapter 2) indicates that in modern GCFR plant communities, the range of $\delta^{13}C_{plant}$ in C_3 plants is -31.3‰ to -18.30‰ VPDB ($\bar{x}$= -25.9‰, σ = 2.39), while the range of $\delta^{13}C_{plant}$ in C_4 taxa is -15.6‰ to -9.96‰ VPDB ($\bar{x}$= -12.34‰, σ = 1.12). The combustion of fossil fuels has depleted atmospheric CO_2 in ^{13}C by approximately 1.5-2‰, and the effect is mirrored in both plant and animal tissues (see Cerling and Harris, 1999). In preindustrial conditions, these ranges of plant $\delta^{13}C$ values are more likely to have been concomitantly higher, and that effect has here been adjusted for by correcting all modern ranges of $\delta^{13}C_{plant}$ values for this ^{13}C-depleted atmospheric CO_2 when comparing them to fossil material.

Enamel $\delta^{13}C$ values are offset from dietary $\delta^{13}C$ sources due to the fractionation of carbon isotopes by metabolic processes. In mammals $\delta^{13}C_{tissue}$ is enriched relative to $\delta^{13}C_{diet}$; the factor of this enrichment (ε*) likely varies to some degree between taxonomic groups as a function of body size, physiology, macronutrient composition of the diet, and metabolism (DeNiro and Epstein, 1978; Cerling and Harris, 1999; Jim *et al.*, 2004; Passey *et al*, 2005; Podlesak *et al*., 2008). Diet-apatite carbon isotope enrichment factors for for large-bodied mammals have been reported between ~12‰ and ~14‰ (Sullivan and Krueger, 1981; Lee-Thorp and Van Der Merwe, 1987; Lee-Thorp *et al.*, 1989; Cerling *et al.*, 1997; Cerling and Harris, 1999). For small mammals, it appears that the difference between diet and apatite tissue $\delta^{13}C$ may be smaller, as values obtained from rodents have ranged from about 9‰ (DeNiro and Epstein, 1978; Ambrose and Norr,

1993; Tieszen and Fagre, 1993) in laboratory rats and mice to about 11‰ and 11.5‰ for wood rats (Podelsak *et al.*, 2008) and voles (Passey *et al.,* 2005) respectively. This study follows Hynek *et al.* (2012) in using a small-mammal specific enrichment factor of $\varepsilon^*_{\text{apatite-diet}} = 11‰$, to reconstruct the $\delta^{13}C_{diet}$ of fossil rodents. δ_{diet} is calculated using the the following formula (see chapter 3 for the reference formulae used in the production of this formula):

$$\delta_{diet} = \left(\frac{1000 + \delta_{enamel}}{1 + \frac{\varepsilon^*_{\text{apatite-diet}}}{1000}} \right) - 1000$$

C_3 and C_4 dietary fraction in the fossil Micromammal material

Samples are discussed by stratigraphic unit, following the ordering described in Table 5.1 from oldest material to most recent.

LBG Sand 1 and DB Sand 4a

The one stable carbon isotope ratio data point from the LBG Sand 1 was obtained from a specimen of *O. irroratus*. The $\delta^{13}C$ value obtained from this specimen (-14.8‰ VPDB) results in a $\delta^{13}C_{diet}$ of -25.5‰ VPDB. This value is well within the pre-industrial adjusted $\delta^{13}C_{plant}$ ranges of GCFR C_3 plants (-29.8‰ to -16.8‰ VPDB). The same is true for the single *O. irroratus* specimen from the overlying DB Sand 4a ($\delta^{13}C_{diet}$ = -24.3‰).

LYDS

The two specimens attributed to *Otomys sp.* have $\delta^{13}C_{laser}$ values (-13.4‰, -11.2‰) that convert to $\delta^{13}C_{diet}$ values indicative of consumption of only C_3 plant matter ($\delta^{13}C_{diet}$ = -24.2‰, -22.0‰, respectively).

BYCS

All specimens of *O. irroratus* and *O. saundersiae* sampled from the BYCS have $\delta^{13}C_{enamel}$ values that indicate pure C_3 diets ($\delta^{13}C_{diet}$ range for *O. irroratus* = -23.2‰ to -21.7‰; $\delta^{13}C_{diet}$ range for *O. saundersiae* = -25.7‰ to -21.6‰; $\delta^{13}C_{diet}$ for *Otomys sp.* = -23.7‰). The specimens of burrowing rodents sampled (*B. suillus* and *G. afra*) are enriched in ^{13}C relative to the Otomyids sampled (Figure 5.3).

The two *B. suillus* specimens with the lowest values of $\delta^{13}C$ overlap with the higher end of the range of *Otomys* $\delta^{13}C$ values, and a Kruskal-Wallis test (with Dunn's multiple comparisons post-hoc test) comparing the *B. suillus*, *O. irroratus*, and *O. saundersiae* populations from the BYCS indicates that the median $\delta^{13}C$ values of these groups are not significantly different from one another (H = 5.164, p = 0.0756). All three *B. suillus* specimens have $\delta^{13}C_{diet}$ values that fall within the range of pure C_3 diets, but are somewhat more enriched in ^{13}C than the adjusted mean GCFR C_3 $\delta^{13}C_{plant}$ value, and thus a small C_4 dietary fraction is probable.

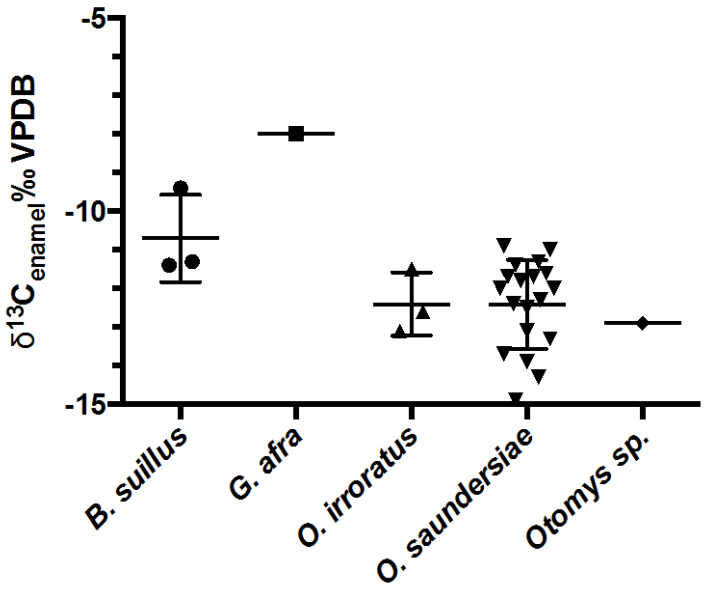

Figure 5.3. $\delta^{13}C_{laser}$ values, by taxon, of the specimens from PP9C stratigraphic unit BYCS.

The *G. afra* specimen in contrast is more than 4‰ enriched in ^{13}C, when compared to the mean $\delta^{13}C$ values of the *O. irroratus* and *O. saundersiae* populations. One-sample t-tests comparing the *O. irroratus* and *O. saundersiae* population mean $\delta^{13}C$ values to the "known" value of the *G. afra* specimen indicate that the stable carbon isotope ratio of the gerbillid specimen is significantly different from the Otomyid sample ($p_{O.\ saundersiae/G.\ afra} < 0.0001$; $p_{O.\ irroratus/G.\ afra} = 0.0113$). The reconstructed dietary value of $\delta^{13}C$ is still within the range of GCFR C_3 plants, but consumption of only higher values of $\delta^{13}C_{plant}$ is unlikely, and an admixture of dietary C_3 and C_4 fractions is indicated.

Single isotope, 2-source mixing modeling of dietary inputs using the Bayesian model "Stable Isotope Analysis in R" (SIAR; Parnell *et al.*, 2010, see "Supplemental Information", below, for a summary of the procedures used) supports the assessment of the OYCS *Otomys* populations as likely having diets with a very high C_3 fraction, while

the δ^{13}C values obtained from the *G. afra* specimen, and to a lesser degree the *B. suillus* population, suggest a larger dietary fraction of C_4 plants, and is evidence of mixed C_3/C_4 feeding (Figure 5.4).

Given that *Otomys* taxa are primarily gramnivorous, but include an unquantifiable fraction of herbaceous material in their diets (Skinner and Chimimba, 2005; Taylor, 2013), the strong signal of a primarily C_3 diet in the Otomyid specimens sampled from the BYCS is indicative of the presence of significant C_3 vegetation in the paleovegetation community these specimens inhabited. Bayesian modeling indicates that it is likely that less than 20% of the diet of any of the *Otomys* specimens sampled here derived from C_4 plant material (Figure 5.4).

Because *Otomys* consume significant grass, this ancient vegetation likely included a significant presence of C_3 grasses. Modern *Otomys* taxa also appear to sample a wide range of the vegetation present on the landscape (see Chapter 3, for discussion) (Figure 5.5). However, after adjusting for the fossil fuel effect, it appears that the BYCS *Otomys* specimens analyzed sample a much narrower range of dietary δ^{13}C values than do some modern populations from the same region. The BYCS fossil *Otomys* populations lack specimens with the lowest (closed vegetation) δ^{13}C values found in modern Otomyids from the region. This suggests that the vegetation communities the fossil *Otomys* sampled were lacking in the more ^{13}C-depleted floral elements, or were lacking in closed vegetation contexts, or both. The BYCS *Otomys* populations also do not have any specimens with whose $\delta^{13}C_{enamel}$ values overlap with the higher (larger dietary C_4 fraction) δ^{13}C values found in the modern Amisrus and Wolwe samples.

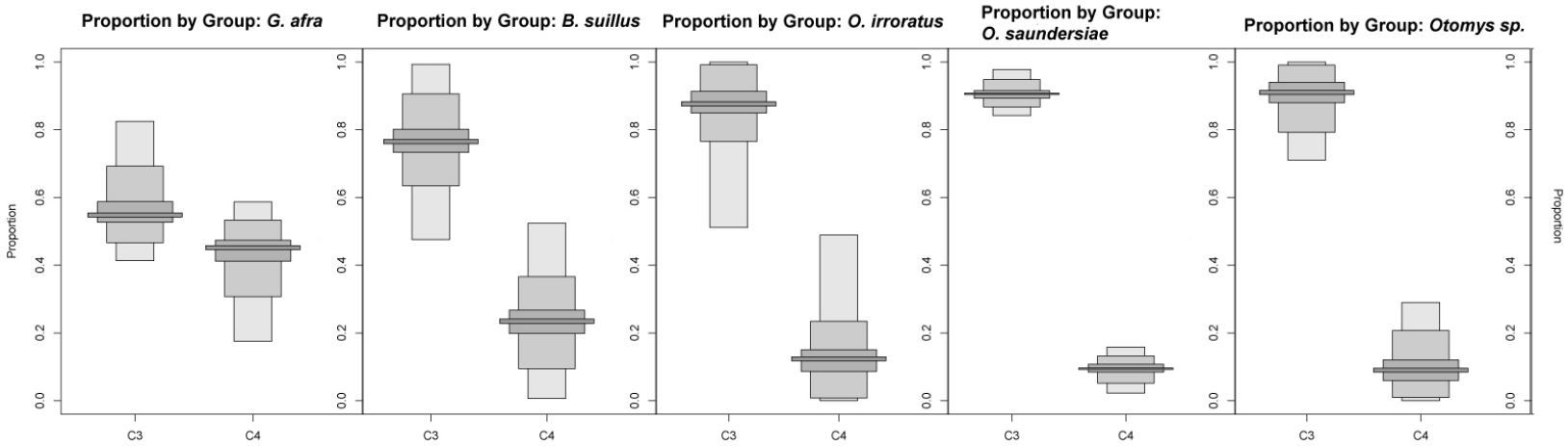

Figure 5.4. SIAR (Parnell *et* al., 2010) output, boxplots of end member source contributions to stable carbon isotope composition of micromammals, BYCS. Y-axis is the relative proportion of a dietary source in a given taxon's diet. 5%, 25%, 75% and 95% credibility intervals shown (Inger *et al.*, n.d.).

These modern, higher values of $\delta^{13}C_{enamel}$ have been attributed to the presence of C_4 grasses in vegetation communities within 3km (the foraging radius of the aggregating predator; Andrews, 1990; Matthews, 2004) of those modern localities (Chapter 3); if similar C_4 grasses were present on the landscape near PP9C at ~130 ka, the *Otomys* specimens sampled here are not intersecting them very often.

However, the presence of at least some C_4 vegetation within about 3km of the site at about 130 ± 9 ka is suggested by the higher values of $\delta^{13}C$ found in the sampled specimens of *B. suillus,* and especially *G. afra*. Both taxa consume the underground storage organs (USO) of plants, as well as some fraction of grasses. Between 20% and 60% of the diet of the *G. afra* specimen sampled here would have been composed of C_4 grasses or tubers (Figure 5.4), and thus indicates the presence of at least some patches of C_4 vegetation at the site during the time period spanned by the deposition of the BYCS sediments.

BYSS

The single specimen of *A. namaquensis* sampled from these sites derives from the BYSS stratigraphic unit, and the calculated $\delta^{13}C_{diet}$ for this specimen is -25.5‰ VPDB. This value is quite similar to the mean pre-industrial adjusted GCFR C_3 $\delta^{13}C_{plant}$ value (-24.4‰); it is likely that this specimen had a diet that consisted solely of C_3 plants, a conclusion that is also supported by the Bayesian modeling (Figure 5.6). All specimens of *O. irroratus* and *O. saundersiae* sampled from the BYSS also have $\delta^{13}C$ values that

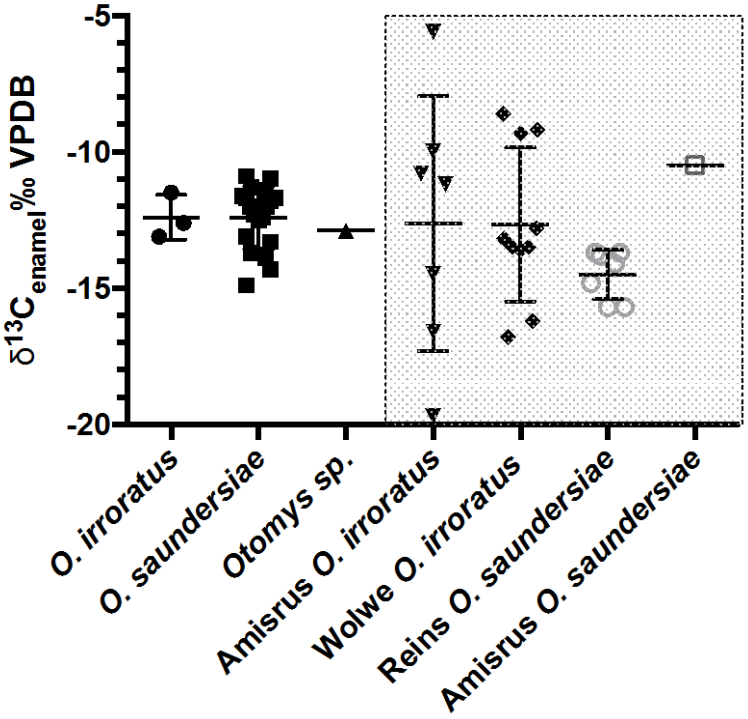

Figure 5.5. Comparison of the $\delta^{13}C_{laser}$ values for *Otomys* specimens from the BYCS (PP9C) to $\delta^{13}C_{enamel\text{-}conventional}$ values (shaded) measured on modern specimens derived from contexts near Pinnacle Point (Williams, in prep-b). Modern micromammal values have been corrected by +1.5‰ to account for the post-industrial depletion in ^{13}C of atmospheric CO_2.

suggest diets composed of primarily C_3 vegetation. ($\delta^{13}C_{diet}$ range for *O. irroratus* = -25.1‰ to – 21.9‰; $\delta^{13}C_{diet}$ range for *O. saundersiae* = -24.3‰ to -21.6‰). Single isotope, 2-source Bayesian modeling again indicates that the probable dietary proportions of C_3 vegetation are high, and the probable proportions of dietary C_4 grasses are low (Figure 5.6).

Small population sample sizes preclude statistical analysis, but the ranges of $\delta^{13}C_l$ values for *A. namaquensis*, *O. irroratus*, and *O. saundersiae* overlap with one another,

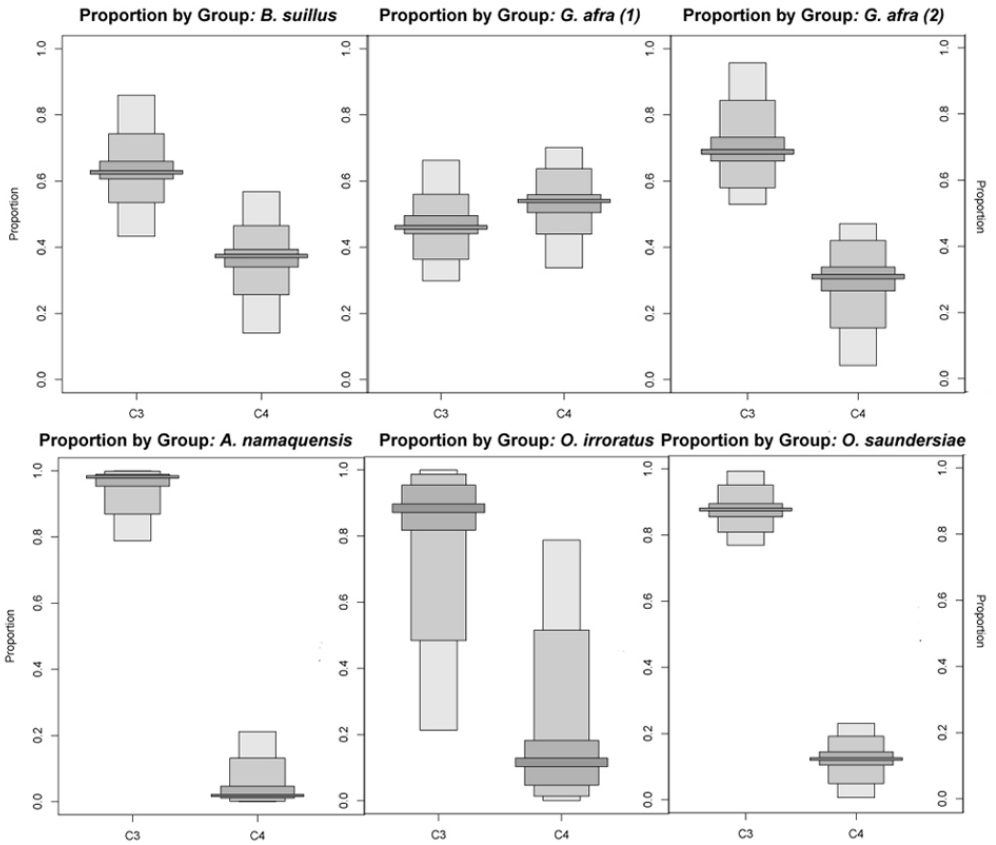

Figure 5.6. SIAR (Parnell *et* al., 2010) output, boxplots of end member source contributions to stable carbon isotope composition of micromammals, BYSS. Y-axis is the relative proportion of a dietary source in a given taxon's diet. 5%, 25%, 75% and 95% credibility intervals shown (Inger *et al.,* n.d.). *G. afra* specimens were treated as separate data points due to the large absolute difference in the specimen $\delta^{13}C_{laser}$ values. Grouping two *O. irroratus* specimens with dissimilar $\delta^{13}C$ values likely resulted in the wide range of proportional probabilities output for that taxon.

while the $\delta^{13}C$ values obtained from the *B. suillus* and *G. afra* specimens from this stratigraphic aggregate are again enriched in ^{13}C when compared to the *Otomys* and *Aethomys* specimens (Figure 5.7). Ranges of reconstructed $\delta^{13}C_{diet}$ for the *B. suillus* specimens are between -20.4‰ and -18.9‰ VPDB, while the two specimens of *G. afra* have $\delta^{13}C_{diet}$ values of -20.8‰ and -16.7‰. This latter value lies outside the range of adjusted 'pre-industrial- GCFR C_3 plant stable carbon isotope values, and is strongly

indicative of a large fraction of C_4 grass in this individual's diet. Output from SIAR suggests that ~30-70% of the ^{13}C-enriched *G. afra* specimen's diet came from C_4 grasses.

The pattern of relative depletion in ^{13}C in the *Otomys* and relative enrichment in the bathyergids and the gerbillids in the BYSS sample is similar to that seen in the BYCS, with which this unit is stratigraphically contiguous. The composition of the micromammal assemblages from both of these stratigraphic units is also similar (Matthews *et al.*, 2011), and together this further supports the hypothesis that these stratigraphic aggregates are roughly contemporaneous. Analysis of the stable carbon isotope data from BYSS also suggests a similar vegetation to that found in the BYCS. Modern *Otomys* taxa and *A. namaquensis* both consume grasses as a significant portion of their diets; if this is true for the fossil populations represented by the BYSS sample, the grasses that these micromammals were consuming were primarily C_3. Comparison of the fossil BYSS *Otomys* and *A. namaquensis* $\delta^{13}C_{laser}$ values with modern *Otomys* $\delta^{13}C_{enamel}$ values again suggests a comparably restricted range of tissue $\delta^{13}C$ values in the fossil gramnivores when compared to modern specimens from the region (Figure 5.8). If C_4 grasses are present in the habits occupied by the fossil *Otomys*, the sample analyzed here does not appear to have been consuming them with any frequency.

Again however, similar to the BYCS, *G. afra* and *B. suillus* $\delta^{13}C$ is suggestive of a significant dietary C_4 component, which indicates the C_4 vegetation must have been present in some patches proximate to the Pinnacle Point locality during the time period represented by the BYSS deposits.

BYDS

Only a small sample of *O. irroratus*, *O. saundersiae*, and *Otomys sp.* could be analyzed from the 126 ± 9 ka BYDS deposits. The range of $\delta^{13}C_{laser}$ values from all three taxa is quite restricted, but this may be an artifact of sample size. All $\delta^{13}C$ values obtained from BYDS taxa are consistent with diets composed primarily of C_3 vegetation, and Bayesian modeling suggests that C_3 vegetation was the primary contributor to all *Otomys* diets in the small sample population, although there is considerable uncertainty in the probabilistic proportions of C_3 and C_4 vegetation in the *Otomys sp.* specimens (Figure 5.9).

LC-MSA Middle

The sample from the LC-MSA Middle (125 ± 7 ka) is also quite small, and consists of two *O. irroratus* specimens whose reconstructed $\delta^{13}C_{diet}$ values are -21.5‰ and -22.2‰ VPDB, and one specimen attributed to *Otomys sp.* whose $\delta^{13}C_{diet}$ = -24.1‰. All specimens' dietary $\delta^{13}C$ values are suggestive of C_3-dominated diets, and Bayesian modeling indicatew that it is likely that >70% of all dietary carbon for these three specimens derived from C_3 plants (Figure 5.10).

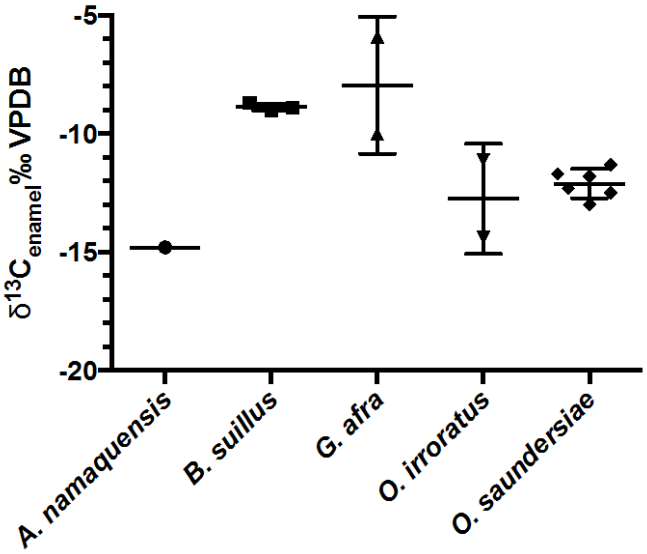

Figure 5.7. . $\delta^{13}C_{laser}$ values, by taxon, of the specimens from PP9C stratigraphic unit BYSS.

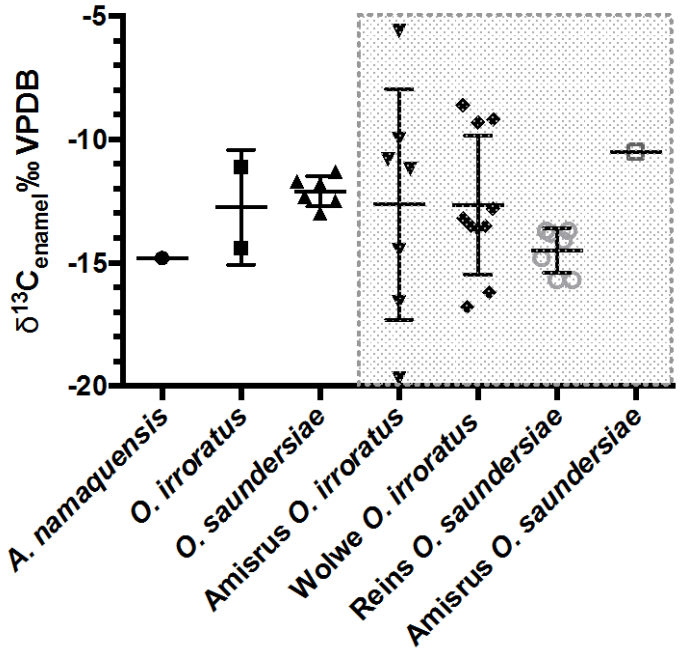

Figure 5.8. Comparison of the $\delta^{13}C_{laser}$ values for *Otomys* specimens from the BYSS (PP9C) to $\delta^{13}C_{enamel\text{-}conventional}$ values (shaded) measured on modern specimens derived from contexts near Pinnacle Point (Williams, in prep-b). Modern micromammal values have been corrected by +1.5‰ to account for the post-industrial depletion in ^{13}C of atmospheric CO_2.

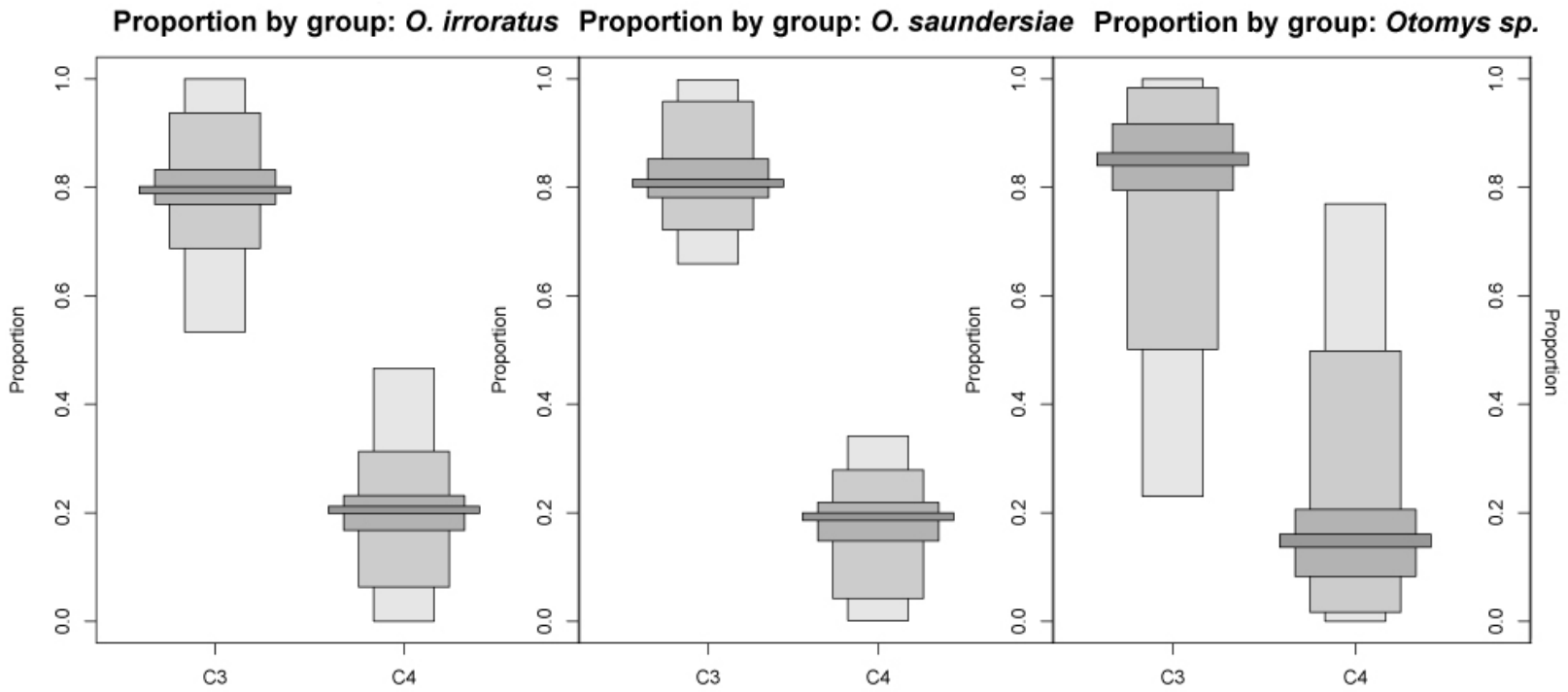

Figure 5.9. SIAR (Parnell *et* al., 2010) output, boxplots of end member source contributions to stable carbon isotope composition of micromammals, BYDS. Y-axis is the relative proportion of a dietary source in a given taxon's diet. 5%, 25%, 75% and 95% credibility intervals shown (Inger *et al.*, n.d.).

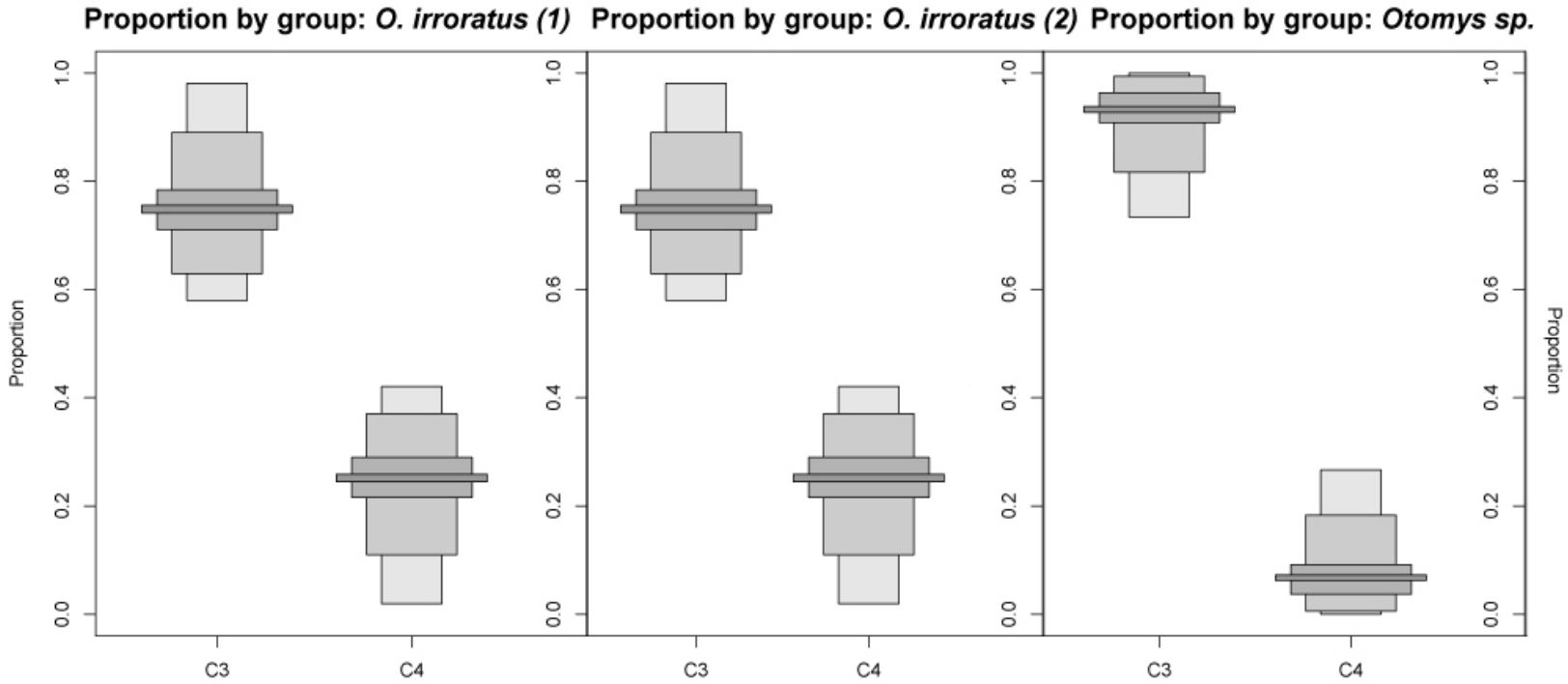

Figure 5.10. SIAR (Parnell *et* al., 2010) output, boxplots of source contributions to stable carbon isotope composition of micromammals, LC-MSA Middle. Y-axis is the relative proportion of a dietary source in a given taxon's diet. 5%, 25%, 75% and 95% credibility intervals shown (Inger *et al.*, n.d.). Two *O. irroratus* values of $\delta^{13}C_{laser}$ were treated as independent values due to small sample sizes; note they return very similar probable C_3/C_4 dietary proportions.

LBG Sand 1

The micromammals sampled from the LBG Sand 1 deposits at PP13B are 124 ± 5 ka in age (Jacobs, 2010). The sample is composed primarily of *O. irroratus* and *O. saundersiae* specimens, although a single *G. afra* specimen was also analyzed. Calculated $\delta^{13}C_{diet}$ values for *O. irroratus* range from -27.4‰ to -26.1‰ VPDB, while calculated $\delta^{13}C_{diet}$ values for *O. saundersiae* range from -27.4‰ to -24.2‰. All calculated *Otomys* $\delta^{13}C_{diet}$ values are more depleted in ^{13}C than the adjusted-for-fossil-fuel-effect mean GCFR C_3 $\delta^{13}C_{plant}$ value of -24.4‰. This strongly suggests that the *Otomys* diets were comprised entirely of C_3 vegetation. Bayesian modeling of the dietary inputs of the LBG Sand1 *Otomys* specimens supports this assertion (Figure 5.11); the probabilistic proportion of C_3 vegetation in the diets of the LBG Sand 1 *Otomys* specimens is greater than 90%. Examination of the histogram of probability distribution densities (Figure 5.12) shows that it is very likely that for both taxa, the fraction of C_3 vegetation in the diet was 1.0 (e.g. 100%). In the sample from all other stratigraphic aggregates presented here, *Otomys* specimens likely had a small (<20%) dietary fraction of C_4 grasses, but in the LBG Sand 1 it is highly likely that the *Otomys* specimens were consuming *no* C_4 grasses. Comparison of the fossil data from the LBG Sand1 with $\delta^{13}C_{enamel}$ values (adjusted for the fossil fuel effect, Figure 5.13) shows that the $\delta^{13}C_{laser}$ values of the LBG Sand 1 fossil *Otomys* population(s) overlap only with the most ^{13}C-depleted portion of the modern range of $\delta^{13}C_{enamel}$ values. Those ^{13}C-depleated modern specimens are

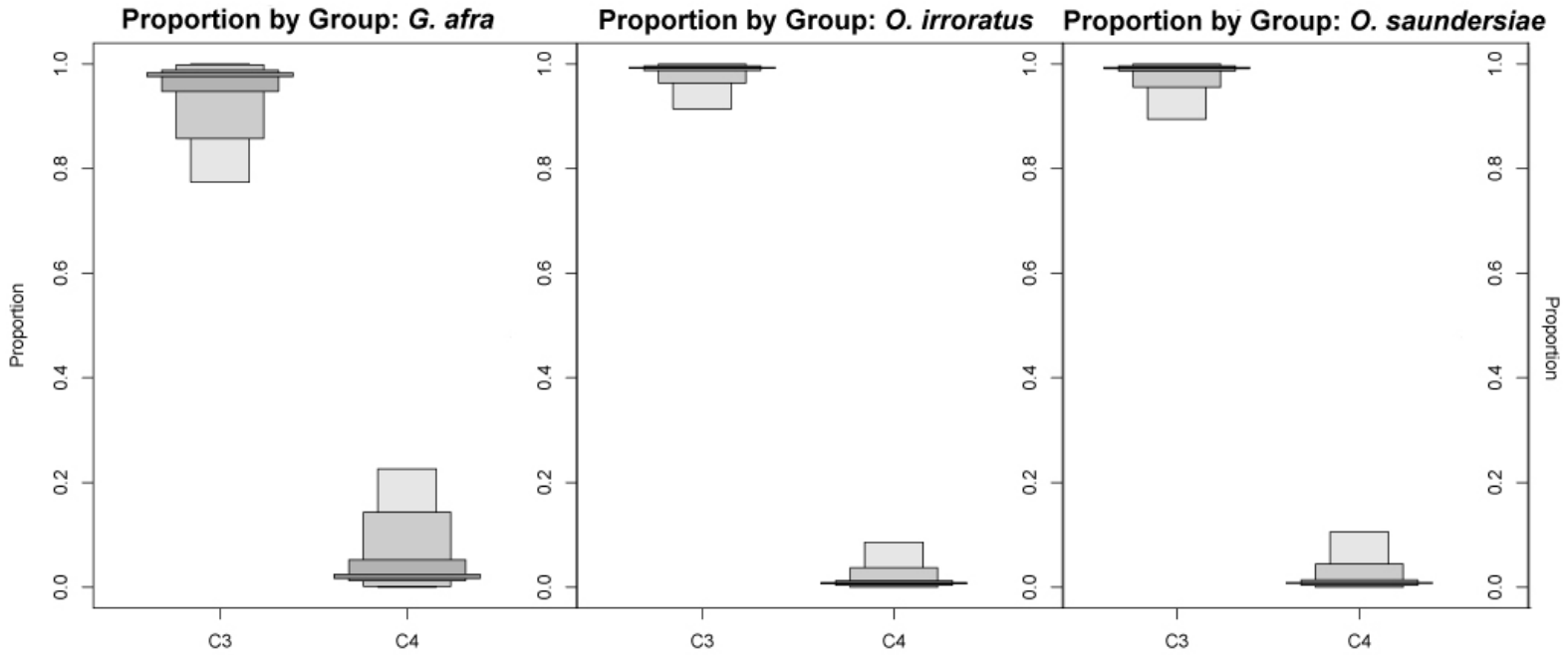

Figure 5.11. SIAR (Parnell *et* al., 2010) output, boxplots of end member source contributions to stable carbon isotope composition of micromammals, LBG Sand 1. Y-axis is the relative proportion of a dietary source in a given taxon's diet. 5%, 25%, 75% and 95% credibility intervals shown (Inger *et al.*, n.d.). Two *O. irroratus* values of $\delta^{13}C_{laser}$ were treated as independent values due to small sample sizes; note they return very similar probable C_3/C_4 dietary proportions.

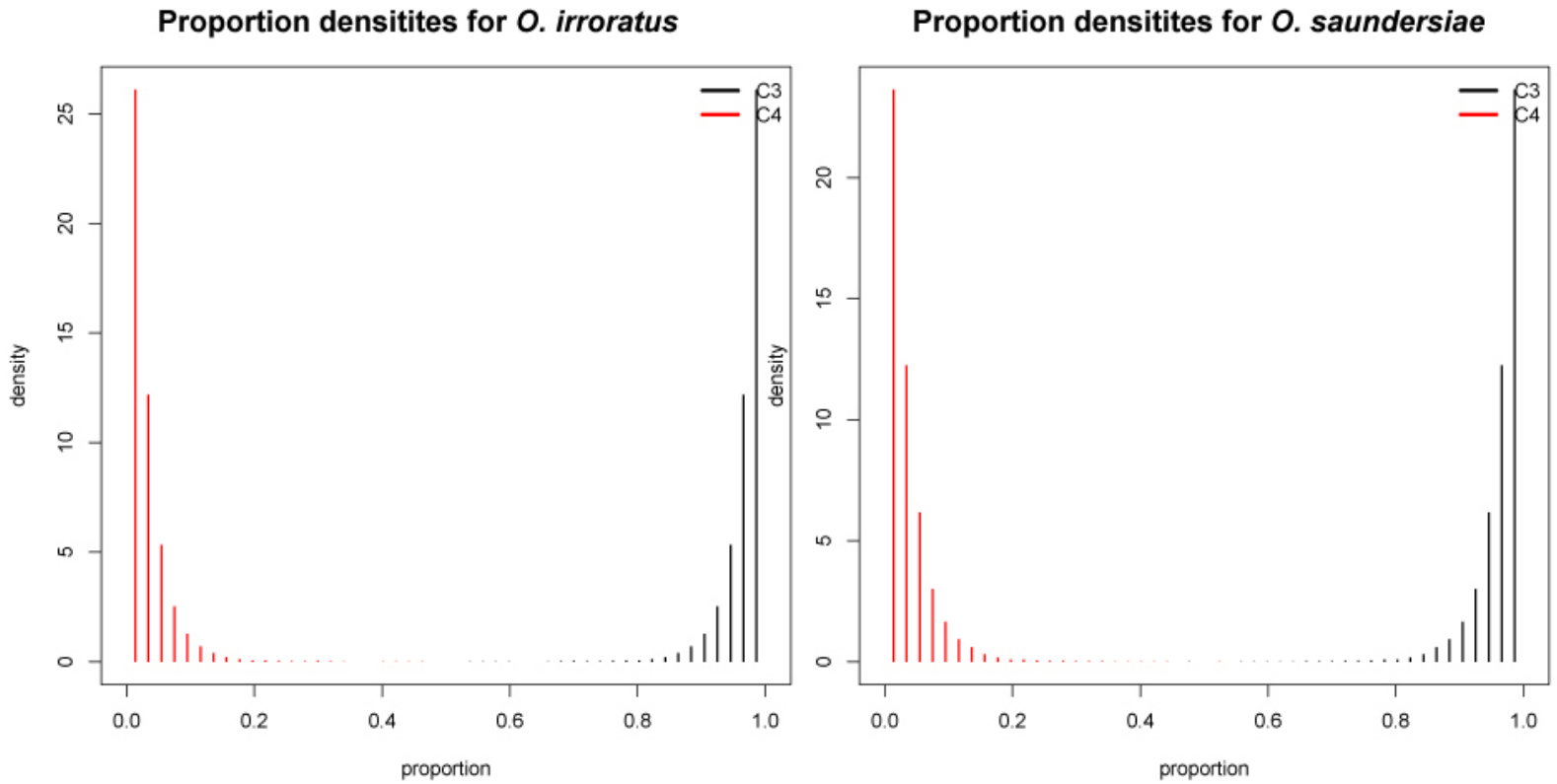

Figure 5.12. Histogram of probability densities for all possible solutions to C_3/C_4 dietary proportions. Note that for both taxa, probability densities are highest at C_3 = 100%, C_4 = 0%

derived from closed forest contexts and Canca Limestone Fynbos, both of which have very low frequencies of C_4 grasses (Williams, in prep-b; Williams, in prep-a).

The single *G. afra* specimen analyzed from this stratigraphic unit also has a value of calculated $\delta^{13}C_{diet}$ that indicates significant consumption of C_3 plant matter, and a relative absence of C_4 plants from the diet. The $\delta^{13}C_{enamel}$ value of *G. afra* specimen from the LBG Sand 1 is the most ^{13}C-depleted value yet recorded in the literature (Table 5.10). Calculated $\delta^{13}C_{diet}$ for this specimen is -25.12‰, which indicates little-to-no dietary C_4 fraction. This value of $^{13}C_{diet}$ is most similar to that of a (modern) specimen of *G. afra* reported by van den Heuvel and Midgley (2014) from an area where Koegelberg Sandstone Fynbos predominates, and where C_4 grass frequencies are reduced due to the presence of increased winter rain (Vogel *et al.,* 1978).

Taken together, stable carbon isotope data from the LBG Sand 1 specimens is strongly suggestive of a shift in local vegetation during the period of time represented by the deposits. C_4 grasses have no contribution to the diets of the gramnivore *Otomys* specimens, and also occur only at a much-reduced frequency in the diet of the *G. afra* specimen. More so, $\delta^{13}C_{lase}$ values for *Otomys* specimens are notably depleted relative to those from other stratigraphic aggregates (Figure 5.14). In all, this suggests a local vegetation during this time period that was lacking in any significant C_4 grass component, and may have had an increased availability of more ^{13}C-depleted vegetation on the landscape.

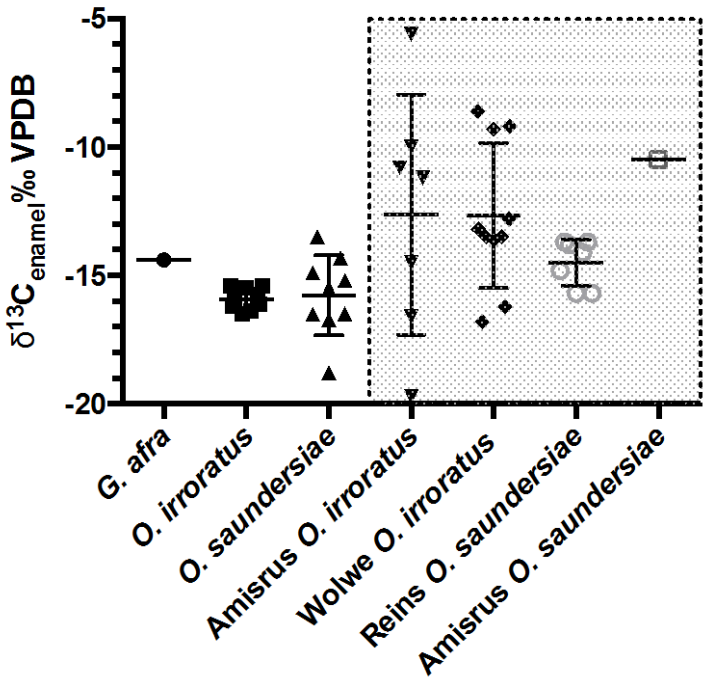

Figure 5.13. Comparison of the $\delta^{13}C_{laser}$ values for *Otomys* specimens from the LBG Sand 1 (PP13B) to $\delta^{13}C_{enamel\text{-}conventional}$ values (shaded) measured on modern specimens derived from contexts near Pinnacle Point (Williams, in prep-b). Modern micromammal values have been corrected by +1.5‰ to account for the post-industrial depletion in ^{13}C of atmospheric CO_2.

Taxon	Locality	n	$\delta^{13}C$ ‰ VPDB hair	δ13C ‰ VPDB enamel	δ13C ‰ VPDB "diet"	Citation
G. afra	Western Cape	3	-22.32		-25.0	van den Heuvel & Midgley, 2014
G. afra	Rein's Nature Reserve	1		-8.90	-19.7	Williams, in prep
G. afra	PP9C BYCS	1		-8	-18.8	this study
G. afra	PP9C BYSS	1		-5.9	-16.7	this study
G. afra	PP9C BYSS	1		-10	-20.8	this study
G. afra	PP13B LBG Sand 1	1		-14.4	-25.1	this study

Table 5.10. Published and unpublished stable carbon isotope ratio data for *G. afra*. $\delta^{13}C_{hair}$ values are converted to $\delta^{13}C_{diet}$ values following the procedure described in Williams (in prep-b). All $\delta^{13}C$ values are ‰VPDB

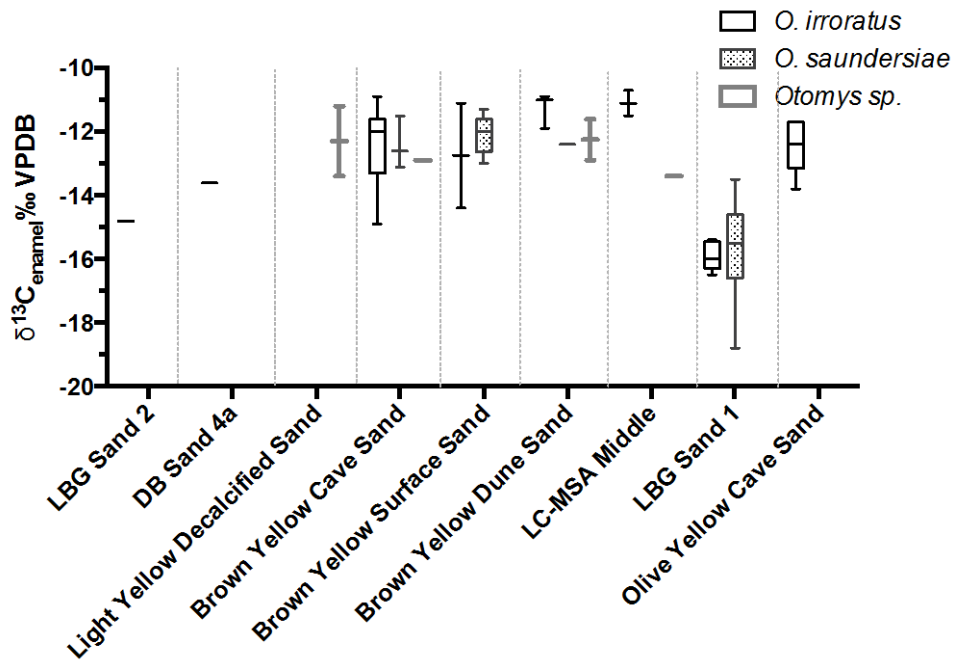

Figure 5.14. Comparison of all *Otomys* $\delta^{13}C_{laser}$ values across stratigraphic aggregates.

OYCS

Specimens from the 120 ± 7 ka deposits of the OYCS, resume the pattern seen in all pre-LBG Sand 1 deposits. *O. irroratus* specimens analyzed have calculated $\delta^{13}C_{diet}$ values that range from -24.6‰ to -22.4‰ VPDB, which suggests a significant C_3 dietary component, but are less depleted in ^{13}C than the *Otomys* specimens from the LBG Sand 1 (Figure 5.14). SIAR output indicates that C_4 plants contributed to <20% of OYCS *O. irroratus* diets (Figure 5.15). The one specimen of *B. suillus* has a calculated $\delta^{13}C_{diet}$ of -17.8‰, indicative of mixed feeding behavior. Bayesian single-data-point analysis results in a probability distribution that suggests C_4 vegetation comprised between 20% and 60% of this individual's diet.

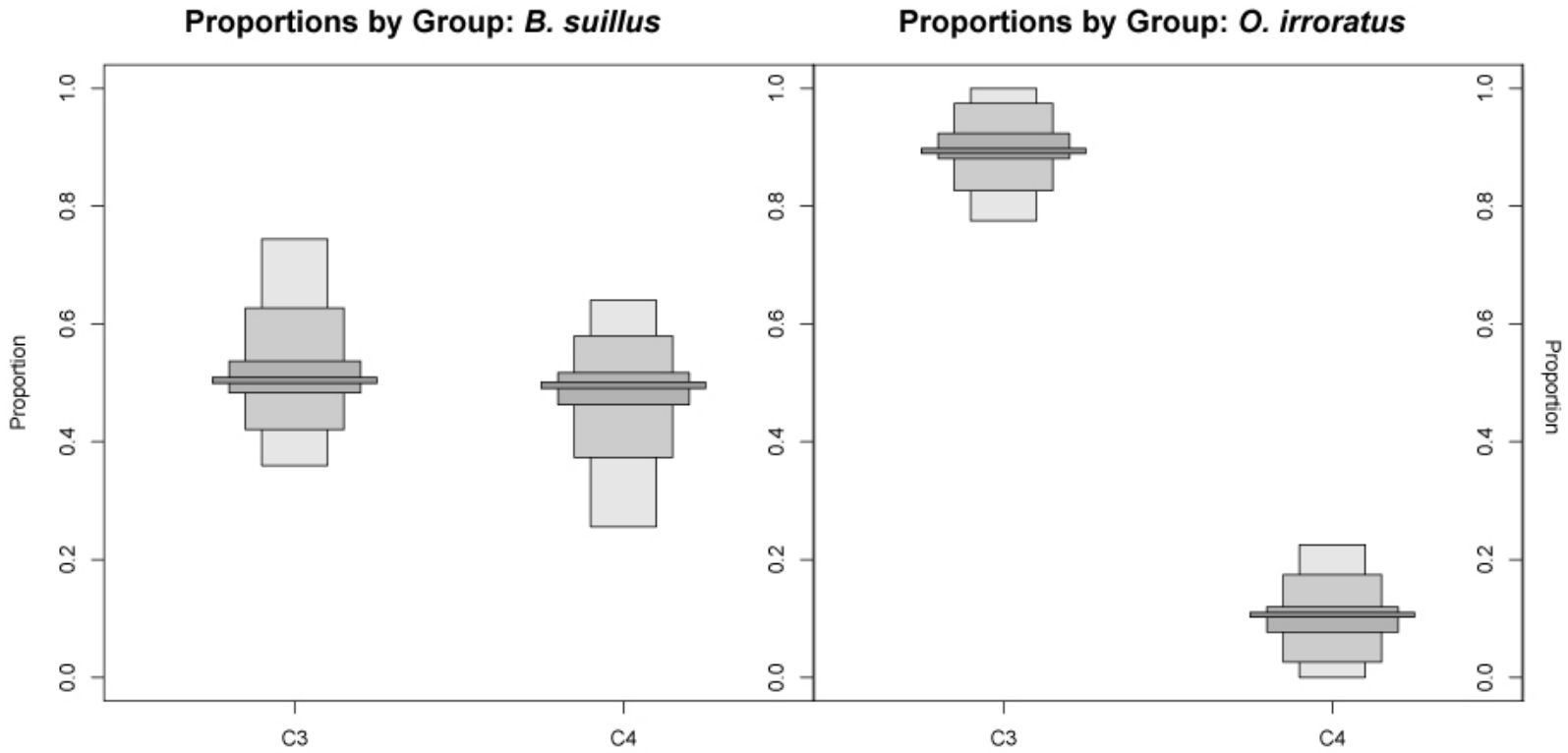

Figure 5.15. SIAR (Parnell *et* al., 2010) output, boxplots of end member source contributions to stable carbon isotope composition of micromammals, OYCS. Y-axis is the relative proportion of a dietary source in a given taxon's diet. 5%, 25%, 75% and 95% credibility intervals shown (Inger *et al.*, n.d.). Two *O. irroratus* values of $\delta^{13}C_{laser}$ were treated as independent values due to small sample sizes; note they return very similar probable C_3/C_4 dietary proportions.

Proportions of C_3/C_4 plants in *Otomys* diets from the OYCS are similar to those from all stratigraphic units described here, other than the LBG Sand 1. *Otomys* diets contain a significant grass component, but the *O. irroratus* specimens from the 120 ka time period appear to have been consuming only minimal amounts of C_4 grass. However, C_4 grasses are clearly present on the landscape, as they comprise a significant proportion of the diet of the *B. suillus* specimen.

Niche partitioning

Otomyinae specimens and specimens from varying groups of burrowing rodents (the Bathyergidae and the Gerbillinae) co-occur in four of the deposits sampled here, the BYCS (OSL age of 130 ± 9 ka), the BYSS (which is peri-contemporaneous with the BYCY on stratigraphic grounds), the LBG Sand 1 (OSL age of 124 ± 5 ka), and the OYCS (OSL age of 120 ± 7 ka). In all cases, the sample size of non-*Otomys* taxa is quite small. However, with the exception of the LBG Sand1, where it is likely that C_4 grasses were exceedingly rare in the paleovegetation community present in the immediate surroundings of Pinnacle Point during that time period, there is clear isotopic separation between $\delta^{13}C_{aser}$ values obtained from the *Otomys* and *A. namaquensis* and those obtained from the *B. suillus* and *G. afra* specimens. The values of $\delta^{13}C_{laser}$ for the larger-bodied burrowing rodents are (again with the exception of the *G. afra* from the LBG Sand 1) consistently more enriched in ^{13}C than those of the smaller-bodied cursorial rodents (Figure 5.16). Although all taxa sampled here consume only vegetation (and so the impact of insectivory on $\delta^{13}C$ values is negligible), it is possible that there are significant differences in dietary specialization between these taxa that result in isotopic niche

partitioning. Differences in stable carbon isotopic composition of tissues between micromammalian taxonomic groups with ostensibly similar diets has been observed in the Miocene of Pakistan (Kimura *et al.*, 2013), and modern South Africa (Codron *et al.*, 2015); both have been attributed to niche partitioning in syntopic micromammal populations. Although this data set is quite small, a similar pattern has also been observed in the modern Pinnacle Point-proximate micromammal specimens (Chapter 3).

It is thus hypothesized that the ^{13}C-depleted values seen in the *G. afra* specimen from the LBG Sand 1 is likely the result of a contraction of available $\delta^{13}C_{plant}$ values on the landscape at about 124 ka, and may represent a resultant restructuring of isotopic niches in the small mammal community during that time period. Given the limited sample sizes however, it is clear that more research explicitly structured to examine isotopic niche partitioning in fossil micromammal samples is needed.

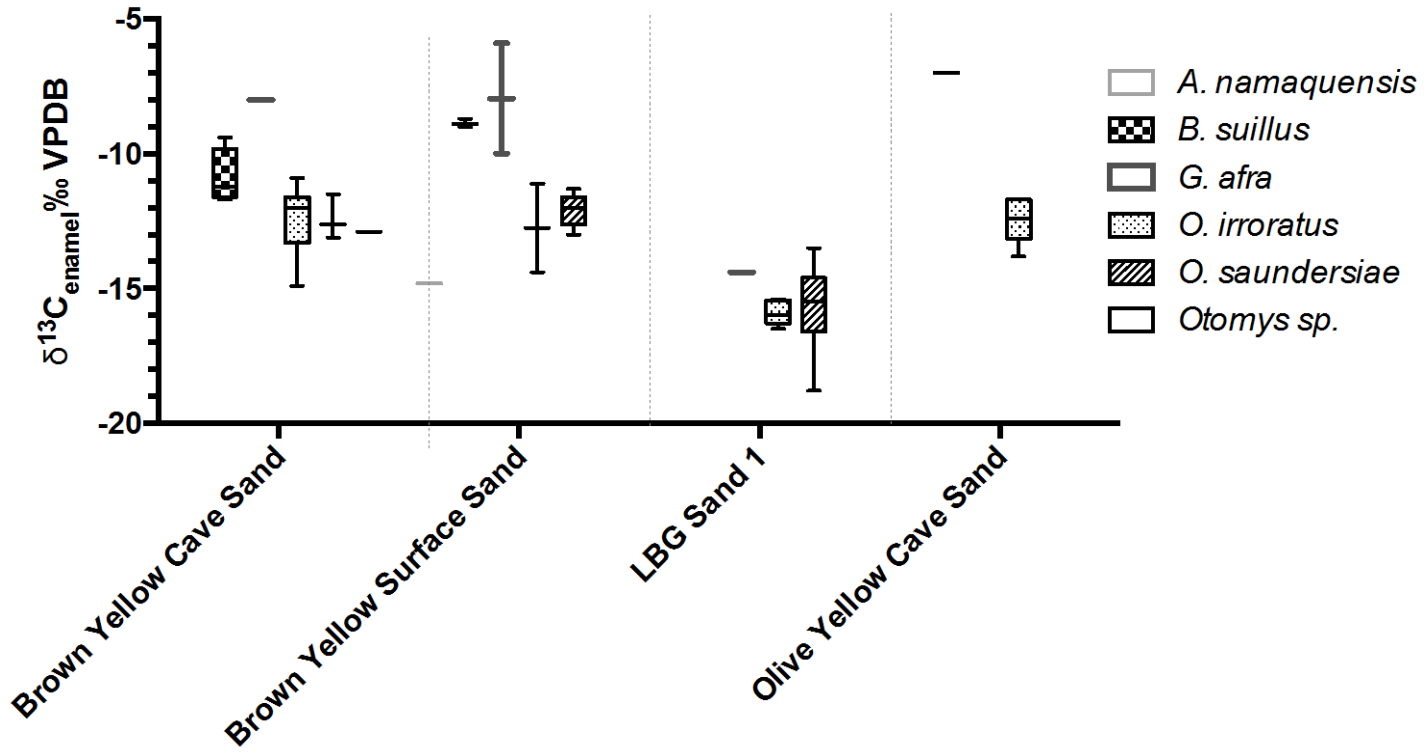

Figure 5.16. $\delta^{13}C_{laser}$ values for stratigraphic aggregates from which both large-bodies burrowing rodents (*B. suillus, G. afra*), and smaller-bodied cursorial rodents (*Otomys sp., O. irroratus, O. saundersiae, A. namaquensis*) were sampled.

Comparison to other climate and vegetation records

The micromammal stable carbon isotope record from the period spanning the MIS6 to MIS5e transition at Pinnacle Point is suggestive of a long period of relative stasis in the availability of C_3 and C_4 plants on the landscape, punctuated by a single 'episode' of reduced availability of C_4 biomass in the region.

At Pinnacle Point, glacial conditions had a direct impact on the physical landscape; the comparably shallow offshore Agulhas platform would have been exposed during periods of lowered sea level. A sea level model for the south coast of South Africa, pairing offshore bathymetry with a Pleistocene RSL curve (Fisher *et al.,* 2010), shows that for most of MIS6, the shoreline was between 20km – 97km distant from Pinnacle Point (Table 5.11). A rapid rise in sea level at about 128ka brought the sea to within 80 meters of the PP13B and PP9C sites. It is possible that some function of marine transgression altered abiotic factors in the region significantly enough to temporarily alter the local vegetation, resulting in more ^{13}C-depleted vegetation communities, possibly similar to some modern modern-day fynbos communities in their relative paucity of C_4 components. In fact, the $\delta^{13}C$ values of the fossil specimens from the LBG Sand 1 are most similar to the modern micromammal $\delta^{13}C$ values thought to have derived from Canca Limestone Fynbos or Southern Cape Dune Fynbos contexts (Chapter 2, Chapter 3), which occur around Pinnacle Point in near-coastal contexts in the present day. I hypothesize that the slight increase in C_4 in the diets of the PP micromammals during all other time periods may reflect some increase in C_4 components of local vegetation in response to increasing distance from the shore, but I cannot suggest a mechanism by

which only small increases of C_4 grasses in local vegetation (rather than large infiltrations expected due to changing atmospheric CO_2 concentrations) might occur.

Analysis of the PP9C micromammal community (Matthews *et al*, 2011) suggests the presence of somewhat dense vegetation, including a taller grass component, and relatively moist conditions, and this is consistent with the C_3-dominated, C_4-present vegetation suggested by the micromammal carbon isotope data from all non-LBG Sand 1 deposits. Specimens of *T. dolichurus*, an indicator taxon that is unique to thicket environments, and *D. mystacalis*, which inhabits closed "rank" vegetation, occur in the PP13B LBG Sand 1 micromammal assemblage (Matthews *et al.*, 2009); similarly, the $\delta^{13}C$ values obtained from all sampled LBG Sand 1 specimens are quite depleted and also suggest the presence of more closed vegetation communities at ~125 ka.

Whether the vegetation pattern suggested by the micromammal stable carbon isotope data is reflected in other regional paleovegetation proxies is difficult to assess. A regional speleothem record exists for the Pleistocene and Holocene at Pinnacle Point (Braun *et al.* ; Bar-Matthews *et al.*, 2010), but the current speleothem record lacks coverage for the time period represented by these deposits (Braun, personal communication). There is significant evidence for maintenance of C_3-dominated ecosystems along the Cape coast throughout the Pleistocene, in the form of high numbers of browsers in faunal assemblages from that period (Klein, 1980; Deacon, 1985)(Klein, 1980; Deacon, 1985). This maintenance of the these ecosystems is also suggested by the

Age, ka	avg RSL (m)	avg distance (km)
113	-26.69	1.27
114.5	-17.1	0.5
116	-11.42	0.5
117.5	-5.45	0.08
119	-1.16	0.08
121.4	2.2	0.08
123.9	6.3	0.08
126.3	4.91	0.08
128.8	-1.25	0.08
131.2	-29.39	1.27
132.7	-68.43	12.51
133.8	-84.62	29.64
134.9	-111.46	70.25
135.9	-125.54	93.48
137	-128.94	96.51
138.1	-127.05	94.66
139.1	-121.41	91.91
140.2	-117.27	84.44
141.3	-113.29	73.67
142.4	-108.6	67.09
143.4	-105.02	64.34
144.5	-103.84	60.79
146	-105.02	64.34
147.5	-113.28	73.67
149	-118.79	87.57
150.5	-119.99	91.11
152	-118.94	87.79
153.5	-111.98	71.02
155	-95.63	52.1
156.5	-76.94	22.59
158	-85.45	30.66

Table 5.11. Average sea level (m) and average distance to coast (in km from the mouth of PP13B) as a result of Pleistocene sea-level change for the time period spanned by the deposits sampled in this study. Data from (Fisher *et al.*, 2010)

very old plant lineages in the Cape Flora (Cowling *et al.*, 2009). Evidence for replacement of browsing species by grazing species at the LGM (Klein, 1980) suggests contraction of C_3 vegetation regimes during full glacial periods, but the micromammal stable carbon isotope record presented here indicates that that pattern might not hold for the glacial MIS6, at least in the Pinnacle Point region. There is certainly no evidence in the micromammal carbon isotope record of at least of a large-scale expansion of C_4-predominant vegetation into the region at any point between ~157 ka and ~120 ka.

Conclusions

Stable carbon isotope data obtained from Pleistocene fossil micromammals from MIS6 and MIS5e-ages deposits from two closely-situated sites at Pinnacle Point, South Africa indicates the presence of C_3-predominated vegetation in the area within ~3km of the sites for the duration of the terminal MIS6 as well as into MIS5e. For much of this time period, C_4 grasses are present in the diets of most micromammal taxa, although the proportional contribution varies between taxa, likely as a function of isotopic niche partitioning. At about 125ka, during the time period spanned by the deposition of the LBG Sand 1 unit at PP13B, there was probably a distinct shift in composition of the local vegetation communities; the $\delta^{13}C$ values of all LBG Sand 1 consumer tissues analyzed become markedly depleted in ^{13}C, when compared to the other MIS6/MIS5e assemblages. These LBG Sand 1 $\delta^{13}C$ values are so depleted that they overlap primarily with modern $\delta^{13}C$ values obtained from micromammals from comparably closed C_3 vegetation communities. Although sample sizes are small, even taxa that other modern

and fossil data suggest should have significant dietary C_4 grass fraction become primarily C_3 consumers. At no point in any of the MIS6/MIS5e PP micromammal assemblages is there evidence for vegetation predominant in C_4 grasses.

Rector and Verrelli (2010) have suggested that a model of "fynbos mosaicism" may be the most appropriate way to explain changes in the relative inputs of C_4 grasses into an ecosystem, rather than a full replacement by "grasslands". The MIS6/MIS5e PP9C and PP13B micromammal data certainly does not contradict such a model. Indeed, the data suggests that even in the face of marked changes in relative sea level and other climatic factors that characterize a shift from glacial to interglacial conditions, the observable fluctuation of C_4 grasses into and out of the local vegetation system may be comparably small, albeit significant.

Supplemental Information

Stable Isotope Analysis in R: Background

Mixing models in isotope geochemistry are traditionally used to determine the fractional component in a given sink of 2 or more isotope sources with known values of δX. Linear binary mixing models (those that incorporate only two sources) are straightforward, but make a number of assumptions, including that the isotopic composition of the 'end members' or reservoirs are known. In isotope ecology, there are several difficulties that arise from attempting to use linear mixing models to approximate the dietary contribution of sources to the isotopic composition of a consumer. Many of the problems are detailed in Phillips (2001); one of the more important issues to note is that linear mixing models do not accommodate uncertainty or variability in source, consumer, or enrichment factor values (Parnell *et al*., 2010).

In studies where researchers have been interested in examining the fractional component of C_4 vs. C_3 grass in an animal's diet using only measured values of $\delta^{13}C$, this issue can be 'resolved' by subsuming end members into categories (e.g. 'C_3 grass' and 'C_4 grass') and using the mean or median $\delta^{13}C$ for each of those groups as the end member value; thus, one isotope system and 2 isotopic reservoirs. The process however treats C_3 and C_4 grasses (or whichever dietary end members are being considered) as invariable, which is problematic, as in C_3 plants in particular there is a wide range in ‰ of $\delta^{13}C_{plant\ tissue}$ values. If one were to perform a series of linear mixing model calculations, shifting the assigned 'value' of C_3 plants within this range would

significantly alter the model-predicted frequencies of C_3 and C_4 plants (see Table 3.2, in Chapter 3 for an example of this).

Parnell *et al.,* (2010) briefly review the non-Bayesian solutions that have previously been employed in the literature, before introducing SIAR's Bayesian model, which is advantageous for a number of reasons, some of which are applicable to this research. Bayesian mixing models take into consideration all (entered) sources of error, including precision in isotope measurement, variability in metabolic fractionation, variability within a measured group (either consumers or dietary end members) (Parnell *et al.*, 2010). Although Bayesian models such as SIAR are most commonly uses to look at multi-source, multi-isotope systems, SIAR is appropriate for single isotope analysis as long as there is enough isotopic separation in source end-member values (Jackson, personal communication).

Stable Isotope Analysis in R: Procedures

The hyperdiversity of the GCFR in general and various GCFR plant communities in specific (Cowling *et al.*, 1997; Goldblatt, 1997; Goldblatt and Manning, 2002; Born *et al.,* 2007) presents a problem for isotopic dietary modeling of primary consumers: the number of possible food sources (e.g. plant taxa) well exceeds the number that can be handled even by complex models that still return fairly accurate results even when one or more of their underlying assumptions are violated (Parnell *et al*., 2010). It is logical to subsume dietary sources *a priori* into larger groups, but that can be problematic for a number of reasons (Phillips *et al.,* 2005); one of the suggested qualifications for *a priori* grouping is that the isotopic composition of grouped sources be statistically

indistinguishable from one another, often via use of a K nearest-neighbor (KNN) test (sensu Rosing *et al.,* 1998). KNN tests are not appropriate for the available GCFR stable carbon isotope dataset however, as there are no more than two or three entries for the vast majority of plant genera, and 88 genera are represented by only one specimen (Chapter 2). However, limited *a posteriori* testing of the available GCFR plant data set (Williams, unpublished data) supports the grouping of plant sources according to their photosynthetic anatomy, and the isotopic separation in $\delta^{13}C_{plant}$ values between C_3 and C_4 plants means that it is unlikely that the two 'sources' could be confounded.

Sources were grouped solely on the basis C_3 or C_4 anatomy, using source-vegetation community-wide averages and standard deviations in $\delta^{13}C_{plant}$ values, generating the values from the GSCIMS database presented in Chapter 2. Mean GCFR $\delta^{13}C_{plant}$ for C_3 taxa = -25.9‰, with a standard deviation of 2.39. Mean GCFR $\delta^{13}C_{plant}$ for C_4 taxa = -12.34‰, with a standard deviation of 1.12. Because values of $\delta^{13}C_{plant}$ were obtained from post-industrial plants, and because the stable carbon isotope composition of the modern atmosphere is depleted in ^{13}C by ~1.5-2‰ (see Cerling and Harris, 1999, for discussion), these GCFR mean $\delta^{13}C_{plant}$ values were then corrected by this factor, to approximate the isotopic composition of pre-industrial vegetation communities.

Thus, the source values entered into SIAR are: mean C_3 $\delta^{13}C$ = -24.4‰, σ = 2.39; mean C_4 $\delta^{13}C$ = -10.84‰, σ = 1.12. SIAR also incorporates the trophic enrichment factor (TEF) into the analysis. Here a TEF value of 11‰, σ = 0.1, from Podelsak *et al.* (2008), has been used. For consumer values, $\delta^{13}C_{laser}$ values were input into the model.

Where multiple data points exist for single taxa within a stratigraphic unit, the command “model1<-siarmcmcdirichletv4(data,sources,tef,concdep=0,500000,50000)” was used to run the model (Inger *et al.,* n.d.). In many cases there were single data points (e.g. a single specimen from a given taxon was sampled). In these cases, single specimen data was run on the model separately using the command “model1<-siarsolomcmcv4(data,sources,tef,concdep=0,500000,50000)” (Inger *et al.,* n.d.). Single data point outputs of Bayesian probability distribution-derived source proportions can then be compared to the similar outputs for the portion of the stable carbon isotope dataset that derived from multiple data points.

Chapter 5 References

Ambrose, S. H. and L. Norr (1993). Experimental evidence for the relationship of the carbon isotope ratios of whole diet and dietary protein to those of bone collagen and carbonate. Prehistoric Human Bone: Archaeology at the Molecular Level. New York, Springer-Verlag**:** 1-37.

Andrews, P. (1990). Owls, caves and fossils. London, London Natural History Museum Publications.

Avery, D. M. (2000). "Notes on the systematics of micromammals from Sterkfontein, Gauteng, South Africa." Paleontogica Africa **36:** 83-90

Bar-Matthews, M., C. W. Marean, Z. Jacobs, P. Karkanas, E. C. Fisher, A. I. R. Herries, . . . A. Ayalon (2010). "A high resolution and continuous isotopic speleothem record of paleoclimate and paleoenvironment from 90 to 53 ka from Pinnacle Point on the south coast of South Africa." Quaternary Science Reviews **29**(17): 2131-2145.

Bennett, N. C. and C. G. Faulkes (2000). African mole-rats: ecology and eusociality, Cambridge University Press.

Born, J., H. P. Linder and P. Desmet (2007). "The greater cape floristic region." Journal of Biogeography **34**(1): 147-162.

Braun, K., M. Bar-Matthews, A. Ayalon, C. Marean, I. Andy, R. Zahn and A. Matthews "Southern South African coastal and inland climate: the influence of sea level, SST and orbital parameters as recorded in speleothems." AGU Meetings, 2012

Bryant, J. D., P. L. Koch, P. N. Froelich, W. J. Showers and B. J. Genna (1996). "Oxygen isotope partitioning between phosphate and carbonate in mammalian apatite." Geochimica et Cosmochimica Acta **60**(24): 5145-5148.

Campbell, T. L., P. J. Lewis and J. K. Williams (2011). "Analysis of the modern distribution of South African Gerbilliscus (Rodentia: Gerbillinae) with implications for Plio-Pleistocene palaeoenvironmental reconstruction." South African Journal of Science **107**: 1-7.

Carr, A. S., M. D. Bateman, D. L. Roberts, C. V. Murray-Wallace, Z. Jacobs and P. J. Holmes (2010). "The last interglacial sea-level high stand on the southern Cape coastline of South Africa." Quaternary Research **73**(2): 351-363.

Cerling, T. E. and J. M. Harris (1999). "Carbon isotope fractionation between diet and bioapatite in ungulate mammals and implications for ecological and paleoecological studies." Oecologia **120**(3): 347-363.

Cerling, T. E., J. M. Harris, S. H. Ambrose, M. G. Leakey and N. Solounias (1997). "Dietary and environmental reconstruction with stable isotope analyses of herbivore tooth enamel from the Miocene locality of Fort Ternan, Kenya." Journal of Human Evolution **33**: 635-650.

Chase, B. M. and M. E. Meadows (2007). "Late Quaternary dynamics of southern Africa's winter rainfall zone." Earth-Science Reviews **84**(3-4): 103-138.

Codron, J., K. J. Duffy, N. L. Avenant, M. Sponheimer, J. Leichliter, O. Paine, . . . D. Codron (2015). "Stable isotope evidence for trophic niche partitioning in a South African savanna rodent community." Current Zoology 61 (3): 397-411

Cowling, R. (1983). "The occurrence of C_3 and C_4 grasses in fynbos and allied shrublands in the South Eastern Cape, South Africa." Oecologia **58**(1): 121-127.

Cowling, R. and D. Richardson (1995). Fynbos: South Africa's Unique Floral Kingdom. Cape Town, University of Cape Town.

Cowling, R. M., S. Proches and T. C. Partridge (2009). "Explaining the uniqueness of the Cape flora: incorporating geomorphic evolution as a factor for explaining its diversification." Molecular Phylogenetics and Evolution **51**(1): 64-74.

Cowling, R. M., D. M. Richardson, R. E. Schulze, M. T. Hoffman, J. J. Midgley and C. Hilton-Taylor (1997). "Species diversity at the regional scale." Vegetation of southern Africa: 447-473.

Dauphin, Y. and C. T. Williams (2004). "Diagenetic trends of dental tissues." Comptes Rendus Palevol **3**(6-7): 583-590.

Davies, K. C. and J. U. M. Jarvis (1986). "The burrow systems and burrowing dynamics of the molerats Bathyergus suillus and Cryptomys hottentotus in the fynbos of the southwestern Cape, South Africa." Journal of Zoology **209**(1): 125-147.

Deacon, H. J. (1985). "An introduction to the fynbos region, time scales and palaeoenvironments." CSIR Report **75**: 1-99.

DeNiro, M. J. and S. Epstein (1978). "Influence of diet on the distribution of carbon isotopes in animals." Geochimica et Cosmochimica Acta **42**(5): 495-506.

Denys, C. (1998). “Phylogenetic implications of the existence of two modern genera of Bathyergidae (Mammalia, Rodentia) in the Pliocene site of Langebaanweg (South Africa)”, Annals of the South African Museum **105**(5): 265-268

Fisher, E. C., M. Bar-Matthews, A. Jerardino and C. W. Marean (2010). "Middle and Late Pleistocene paleoscape modeling along the southern coast of South Africa." Quaternary Science Reviews **29**(1112): 1382-1398.

Gehler, A., T. Tutken and A. Pack (2012). "Oxygen and carbon isotope variations in a modern rodent community, implications for palaeoenvironmental reconstructions." PLoS1 e49531

Goldblatt, P. (1997). "Floristic diversity in the Cape Flora of South Africa." Biodiversity and Conservation **6**(3): 359-377.

Goldblatt, P. and J. C. Manning (2002). "Plant Diversity of the Cape Region of Southern Africa." Annals of the Missouri Botanical Garden **89**(2): 281-302.

Granjon, L. and E. R. Dempster (2013). "Genus Gerbilliscus: Gerbils". Mammals of Africa **III**. J. Kingdon, D. Happold, T. Butynskiet al, Bloomsbury.

Hendey, Q. B. and T. P. Volman (1986). "Last interglacial sea levels and coastal caves in the Cape Province, south Africa." Quaternary Research **25**(2): 189-198.

Henry, A. G., P. S. Ungar, B. H. Passey, M. Sponheimer, L. Rossouw, M. Bamford, . . . L. Berger (2012). "The diet of Australopithecus sediba; Supplementary Information." Nature **487**(7405): 90-93.

Herries, A.I.R, Z. Jacobs, M. Bar-Mathews, P. Karkanas, E. Fisher, R. Pickering, G. Goldberg, J. Thompson, T. Matthews, C.W. Marean (in prep) " One million year life history of a quartzite sea cave (PP9) at Pinnacle Point, southern Cape Coast, South Africa"

Hynek, S. A., B. H. Passey, J. L. Prado, F. H. Brown, T. E. Cerling and J. Quade (2012). "Small mammal carbon isotope ecology across the Miocene-Pliocene boundary, northwestern Argentina." Earth and Planetary Science Letters **321-322**(0): 177-188.

Inger, R., A. Jackson, A. Parnell and S. Bearhop. (n.d.). "SIAR V4 (Stable Isotope Analysis in R): An Ecologist's Guide." from https://http://www.tcd.ie/Zoology/research/research/theoretical/siar/SIAR_For_Ecologists.pdf.

Jacobs, Z. (2010). "An OSL chronology for the sedimentary deposits from Pinnacle Point Cave 13B, a punctuated presence." Journal of Human Evolution **59**(3): 289-305.

Jim, S., S. H. Ambrose and R. P. Evershed (2004). "Stable carbon isotopic evidence for differences in the dietary origin of bone cholesterol, collagen and apatite:

implications for their use in palaeodietary reconstruction." Geochimica et Cosmochimica Acta **68**(1): 61-72.

Karkanas, P. and P. Goldberg (2010). "Site formation processes at Pinnacle point Cave 13B (Mossel Bay, Western Cape Province, South Africa): resolving stratigraphic and depositional complexities with micromorphology." Journal of Human Evolution **59**(3): 256-273.

Kimura, Y., L. L. Jacobs, T. E. Cerling, K. T. Uno, K. M. Ferguson, L. J. Flynn and R. Patnaik (2013). "Fossil mice and rats show isotopic evidence of niche partitioning and change in dental ecomorphology related to dietary shift in late Miocene of Pakistan." PloS one **8**(8): e69308.

Klein, R. G. (1980). "Environmental and ecological implications of large mammals from upper pleistocene and holocene sites in southern africa." Annals of the South African Museum **81**: 223-283.

Kohn, M. J., M. J. Schoeninger and W. W. Barker (1999). "Altered states: effects of diagenesis on fossil tooth chemistry." Geochimica et cosmochimica acta **63**(18): 2737-2747.

Lee-Thorp, J. and N. J. Van Der Merwe (1987). "Carbon isotope analysis of fossil bone apatite." South African Journal of Science; v. **83**(11) p. 712-715

Lee-Thorp, J. A. and P. B. Beaumont (1995). "Vegetation and Seasonality Shifts during the Late Quaternary Deduced from 13C/12C Ratios of Grazers at Equus Cave, South Africa." Quaternary Research **43**(3): 426-432.

Lee-Thorp, J. A., J. C. Sealy and N. J. Van Der Merwe (1989). "Stable carbon isotope ratio differences between bone collagen and bone apatite, and their relationship to diet." Journal of Archaeological Science **16**(6): 585-599.

Marean, C. W., M. Bar-Matthews, J. Bernatchez, E. Fisher, P. Goldberg, A. I. R. Herries, . . . H. M. Williams (2007). "Early human use of marine resources and pigment in South Africa during the Middle Pleistocene." Nature **449**: 905-908.

Marean, C. W., M. Bar-Matthews, E. Fisher, P. Goldberg, A. Herries, P. Karkanas, . . . E. Thompson (2010). "The stratigraphy of the Middle Stone Age sediments at Pinnacle Point Cave 13B (Mossel Bay, Western Cape Province, South Africa)." Journal of Human Evolution **59**(3-4): 234-255.

Marean, C. W., P. J. Nilssen, K. Brown, A. Jerardino and D. Stynder (2004). "Paleoanthropological investigations of Middle Stone Age sites at Pinnacle Point, Mossel Bay (South Africa): Archaeology and hominid remains from the 2000 Field Season." Journal of Paleoanthropology **2**: 14-83.

Matthews, T. (2004). The taxonomy and taphonomy of Mio-Pliocene and Late Middle Pleistocene micromammals from the Cape west coast, South Africa PhD Thesis, University of Cape Town, South Africa.

Matthews, T., C. Denys and J. E. Parkington (2005). "The palaeoecology of the micromammals from the late middle Pleistocene site of Hoedjiespunt 1 (Cape Province, South Africa)." Journal of Human Evolution **49**(4): 432-451.

Matthews, T., C. Denys and J. E. Parkington (2006). "An analysis of the mole rats (Mammalia: Rodentia) from Langebaanweg (Mio-Pliocene, South Africa)." Geobios **39**(6): 853-864.

Matthews, T., C. Marean and P. Nilssen (2009). "Micromammals from the Middle Stone Age (92 - 167 ka) at Cave PP13B, Pinnacle Point, south coast, South Africa." Paleontol. Afr **44**: 112-120.

Matthews, T., A. Rector, Z. Jacobs, A. I. R. Herries and C. W. Marean (2011). "Environmental implications of micromammals accumulated close to the MIS6 to MIS5 transition at Pinnacle Point Cave 9 (Mossel Bay, Western Cape Province, South Africa)." Palaeogeography, Palaeoclimatology, Palaeoecology. **302**(3-4): 213-229

Monadjem, A. (1997). "Stomach contents of 19 species of small mammals from Swaziland." Ibis **113**: 194-202.

Mucina, L., M. C. Rutherford and L. W. Powrie (2006). Vegetation Atlas of South Africa, Lesotho and Swaziland. The Vegetation of South Africa, Lesotho, and Swaziland. Pretoria, South African National Biodiversity Institute**:** 748-790.

Parnell, A. C., R. Inger, S. Bearhop and A. L. Jackson (2010). "Source partitioning using stable isotopes: coping with too much variation." PloS one **5**(3): e9672.

Passey, B. H. and T. E. Cerling (2006). "In situ stable isotope analysis (13 C, 18 O) of very small teeth using laser ablation GC/IRMS." Chem. Geol **235**: 238-249.

Passey, B. H., T. F. Robinson, L. K. Ayliffe, T. E. Cerling, M. Sponheimer, M. D. Dearing, . . . J. R. Ehleringer (2005). "Carbon isotope fractionation between diet, breath CO2, and bioapatite in different mammals." Journal of Archaeological Science **32**(10): 1459-1470.

Phillips, D., S. Newsome and J. Gregg (2005). "Combining sources in stable isotope mixing models: alternative methods." Oecologia **144**(4): 520-527.

Phillips, D. L. (2001). "Mixing models in analyses of diet using multiple stable isotopes: a critique." Oecologia **127**(2): 166-170.

Pickering, R., Z. Jacobs, A. I. R. Herries, P. Karkanas, M. Bar-Matthews, J. D. Woodhead, . . . C. W. Marean (2013). "Paleoanthropologically significant South African sea caves dated to 1.1 - 1.0 million years using a combination of U-Pb, TT-OSL and palaeomagnetism." Quaternary Science Reviews **65**: 39-52.

Podelsak, D. W., A. M. Torregrossa, J. R. Ehleringer, M. D. Dearing, B. H. Passey and T. E. Cerling (2008). "Turnover of oxygen and hydrogen isotopes in the body water, CO2, hair, and enamel of a small mammal." Geochimica et cosmochimica acta **72**(1): 19-35.

Rebelo, A. G., C. Boucher, N. Helme, L. Mucina and M. C. Rutherford (2006). Fynbos Biome. The Vegetation of South Africa, Lesotho, and Swaziland. Pretoria, South African National Biodiversity Institute**:** 52-219.

Rector, A. L. and K. E. Reed (2010). "Middle and late Pleistocene faunas of Pinnacle Point and their paleoecological implications." Journal of Human Evolution **59**(3): 340-357.

Rector, A. L. and B. C. Verrelli (2010). "Glacial cycling, large mammal community composition, and trophic adaptations in the Western Cape, South Africa." Journal of Human Evolution **58**(1): 90-102.

Robb, G. N., S. Woodborne and N. C. Bennett (2012). "Subterranean sympatry: an investigation into diet using stable isotope analysis." PloS one **7**(11): e48572.

Roberts, D. L., P. Karkanas, Z. Jacobs, C. W. Marean and R. G. Roberts (2012). "Melting ice sheets 400,000 yr ago raised sea level by 13m: Past analogue for future trends." Earth and Planetary Science Letters **357-358**(0): 226-237.

Rosing, M. N., M. Ben-David and R. P. Barry (1998). "Analysis of stable isotope data: AK nearest-neighbors randomization test." The Journal of wildlife management 62(1): 380-388.

Royer, A. l., C. Lecuyer, S. Montuire, R. Amiot, S. Legendre, G. Cuenca-Bescis, . . . F. o. Martineau (2013). "What does the oxygen isotope composition of rodent teeth record?" Earth and Planetary Science Letters **361**: 258-271.

Sealy, J. (1996). "Seasonality of rainfall around the Last Glacial Maximum as reconstructed from carbon isotope analyses of animal bones from Nelson Bay Cave." South African Journal of Science **92**: 441-444.

Sealy, J. C. and N.J. van der Merwe (1986). "Isotope Assessment and the Seasonal-Mobility Hypothesis in the Southwestern Cape of South Africa [and Comments and Replies]." Current Anthropology: **27**(2): 135-150.

Sharp, Z. and T. Cerling (1996). "A laser GC-IRMS technique for in situ stable isotope analyses of carbonates and phosphates." Geochimica et Cosmochimica Acta **60**(15): 2909-2916.

Skinner, J. D. and C. T. Chimimba (2005). The mammals of the southern African sub-region, Cambridge University Press.

Sponheimer, M. and J. A. Lee-Thorp (1999). "Oxygen Isotopes in Enamel Carbonate and their Ecological Significance." Journal of Archaeological Science **26**(6): 723-728.

Sullivan, C. H. and H. W. Krueger (1981). "Carbon isotope analysis of separate chemical phases in modern and fossil bone." Nature **292:** 333-335

Taylor, P. J. (2013). “Genus Otomys: Vlei Rats”. Mammals of Africa Volume III: Rodents, Hares and Rabbits .Happold, D. C. D. (ed.). Bloomsbury Publishing, London, United Kingdom,

Thackeray, J. F., A. van der Venter, J. Lee-Thorp, C. T. Chimimba and J. van Heerden (2003). "Stable carbon isotope analysis of modern and fossil samples of the South African rodent Aethomys namaquensis." Annals of the Transvaal Museum **40**: 43-46.

Thompson, E., H. M. Williams and T. Minichillo (2010). "Middle and late Pleistocene Middle Stone Age lithic technology from Pinnacle Point 13B (Mossel Bay, Western Cape Province, South Africa)." Journal of Human Evolution **59**: 358-377.

Thompson, J. C. (2010). "Taphonomic analysis of the Middle Stone Age faunal assemblage from Pinnacle Point Cave 13B, Western Cape, South Africa." Journal of Human Evolution **59**(3-4): 321-339.

Tieszen, L. L. and T. Fagre (1993). Effect of diet quality and composition on the isotopic composition of respiratory CO2, bone collagen, bioapatite, and soft tissues. Prehistoric Human Bone, Springer**:** 121-155.

van den Heuvel, I. M. and J. J. Midgley (2014). "Towards an isotope ecology of Cape Fynbos small mammals." African Zoology **49**(2): 195-202.

Vogel, J. C., A. Fuls and R. P. Ellis (1978). "The geographical distribution of Kranz grasses in South Africa." South African Journal of Science **74**: 209-215.

Williams, H. M. (in prep-a). Isotope Ecology of the modern Greater Cape Floristic Region, with particular focus on the Pinnacle Point area: metadata analysis of the

modern floral stable carbon isotope record and the production of the GCFR-specific Stable Caron Isotope Metadata Set (GSCIMS). .

Williams, H. M. (in prep-b). Isotope Ecology of the modern Greater Cape Floristic Region: the modern micromammal record, with particular attention to new Pinnacle-Point Area-proximate data.

Yeakel, J. D., N. C. Bennett, P. L. Koch and N. J. Dominy (2007). "The isotopic ecology of African mole rats informs hypotheses on the evolution of human diet." **274**(1619): 1723-1730.

6. An MIS6-MIS5 stable carbon isotope record from fossil micromammal remains from the Middle Stone Age archaeological cave site PP13B, Pinnacle Point, South Africa.

Introduction

The archaeology of early modern humans in southern Africa has long sought to contextualize the behavior of *Homo sapiens* in an adaptive framework, where changes in material culture were the result of adaptation to changes in local abiotic and environmental factors. Paleoenvironmental proxy data derived directly from archaeological assemblages has provided direct contextual data for the ways in which changes in lithic procurement and production strategies, hunting intensity, butchering practices, and increased or decreased diet breadth, as well as other aspects of human material culture are linked to changing paleoenvironmental conditions (Deacon *et al.*; Klein, 1972; Klein, 1974; Klein, 1976; Klein *et al.*, 1983; Marean, 1986a; Marean, 1986b; Klein, 1989; Ambrose and Lorenz, 1990; Brown *et al.*, 2009; Brown, 2011; Brown *et al.*, 2012).

Pinnacle Point Cave 13B (Western Cape, South Africa) (PP13B) is a unique archaeological and paleoenvironmental record for the region, as it preserves what is currently the only well-dated archaeological sequence that predates MIS5 in age in coastal southern Africa. MIS6 and MIS5e deposits from PP13B contain the earliest evidence of a coastal adaptation in *Homo sapiens* (Marean *et al.*, 2007; Marean, 2011), and the lithic, faunal, and ochre assemblages provide a window into hominin material

culture and adaptive strategies along the south coast during this time period (Thompson, 2008; Thompson *et al.*, 2010; Thompson, 2010; Watts, 2010).

PP13B also sits at the confluence of the two major climate systems in South Africa, the Summer and Winter Rainfall Zones (SRZ and WRZ). There is significant evidence that the distributions of these rainfall zones were impacted by changing climatic parameters during previous glacial and interglacial periods (Van Zinderen Bakker, 1976; Tyson, 1999; Chase and Meadows, 2007). The structure of vegetation communities is tightly linked to the seasonality of rainfall (Vogel *et al.*, 1978; Cowling, 1983; Cowling *et al.*, 1994; Rutherford and Mucina, 2006; Cowling *et al.*, 2008); changes in the seasonality of distribution of rainfall would have had a significant impact on the vegetation communities near PP13B, which in turn would have significantly impacted the adaptive strategies of the hominins occupying the site.

As part of a multiproxy approach to paleoenvironmental reconstruction at PP13B, presented here are micromammal stable carbon isotope data for the MIS6 and MIS5 deposits from the cave obtained via laser ablation gas chromatograph isotope ratio mass spectrometry (LA-GC-IRMS). This record is then compared to other paleoenvironmental proxy records from the site, in order to explore the advantages and limitations of a micromammal isotope record in this context.

Stable carbon isotope data obtained from fossil and archaeological tooth enamel acts as a proxy for ancient vegetation because C_3 and C_4 photosynthetic pathways variably fractionate carbon and have distinct and non-overlapping values of $\delta^{13}C$ (Farquhar *et al.*, 1989a; Lee-Thorp, 1989). When animals consume C_3 and C_4 plants, these C_3 and C_4 signals are integrated into the consumer tissues, resulting in consumer

$\delta^{13}C_{tisue}$ values that reflect the relative proportions of C_3 and C_4 vegetation in the diet. For fossil and archeological material, enamel is the ideal consumer tissue to sample, as it is resistant to diagenetic alteration and retains a biogenic $\delta^{13}C$ signal even after fossilization (Lee-Thorp and Van Der Merwe, 1987; Lee-Thorp, 1989; Wang and Cerling, 1994; Sponheimer and Lee-Thorp, 1999; Nielsen-Marsh and Hedges, 2000; Lee-Thorp, 2002)

Micromammal $\delta^{13}C_{enamel}$ proxy records are a critical contribution to paleoenvironmental reconstruction as archaeological and fossil localities. Due to their reduced home ranges and accelerated growth, and the fact that different predators aggregate micromammal assemblages than aggregate large mammal assemblages (see Chapter 3, Chapter 4, for discussion), micromammals sample site-local vegetation on a scale that is distinct from large mammal records (Hynek *et al.*, 2012).

The site

Pinnacle Point 13B (PP13B) is an archaeological site situated in a cave in the coastal exposures of Paleozoic Table Mountain Sandstone along South Africa's south coast (Figure 6.1). The cave itself is at least 1mya (Pickering *et al.*, 2013), but the sediments and archeology contained within the cave are considerably younger (Jacobs, 2010; Marean, 2010; Marean *et al.*, 2010). Because the cave mouth is approximately 15 masl, it is likely that any deposits that predate the MIS11 high sea stand were washed out by storm surges or high tides during this period (*sensu* Hendey and Volman, 1986), when the ocean was +14m above present-day masl (Roberts *et al.*, 2012).

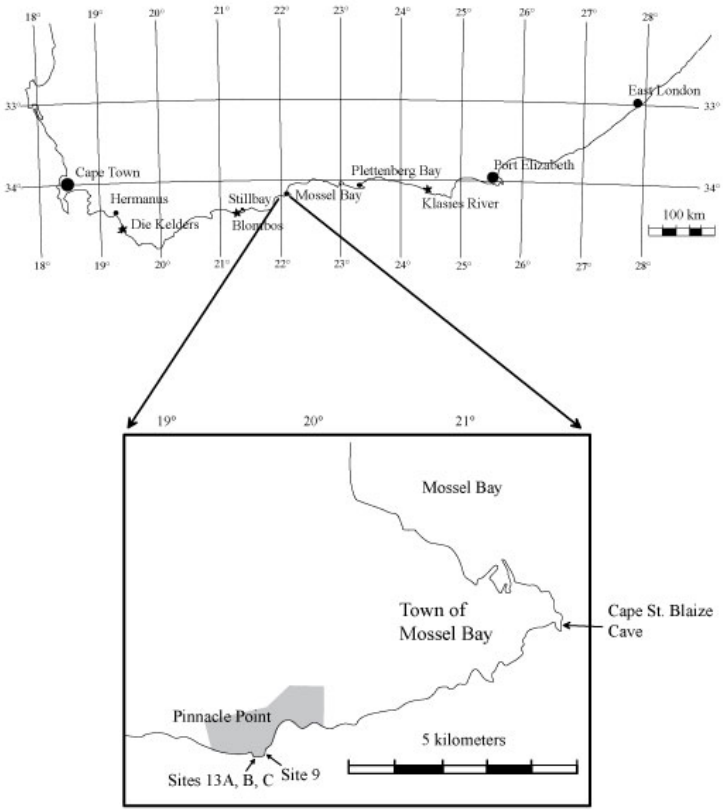

Figure 6.1. Map of South Africa, showing the location of Pinnacle Point. Inset: Map of Mossel Bay and Pinncale Point, showing the location PP13B. (Figure credit: SACP4)

Archaeological excavation of the site began in 2000, and proceeded for almost ten years. More detailed descriptions of the excavation procedures used are provided elsewhere (Marean *et al.*, 2004; Marean, 2010; Marean *et al.*, 2010; Bernatchez and Marean, 2011; Oestmo and Marean, 2015). At PP13B sedimentary units were excavated in 50cm quadrants within 1-meter squares, the southwest corner of which was tied into an arbitrary grid (MAP grid) (Marean *et al.*, 2010). Excavation did not occur in arbitrary level or spits, but rather followed the visible contours of the sedimentary stratigraphy. These smaller stratigraphic units were later grouped into larger "stratigraphic aggregates" based on geologic composition and micromorphology (Marean *et al.*, 2010). These

stratigraphic aggregates form the basic grouping parameter of the study presented here. Because the stratigraphic aggregates represent large spans of sedimentary deposition, the material retrieved from them has been subject to a palimpsest effect; however, because these stratigraphic aggregates represent distinct phases of deposition and can be well-dated by a number of geochronological techniques, they also function as distinct, temporally constrained sampling bins within a much larger chronological framework.

Excavation of the deposits, and of the archaeological, faunal, and geological material therein occurred in three areas of the cave: in the 'Eastern Area', which is located near the mouth of the cave; in the 'Western Area', located towards the rear of the cave; and in the "Northeastern Area" or the LC-MSA, in a section of exposed loosely consolidated sediments adhering to the northern wall of the cave near the mouth (Figure 6.2) (Marean *et al*., 2010). The oldest sediments occur in the back of the cave at the base of the Western Area excavation units. Karkanas and Goldberg (2010) suggest that while deposition was occurring in the back of the cave, human occupation at the front of the cave produced the archaeological and sedimentary deposits that would later become brecciated and form the LC-MSA. These LC-MSA sediments, with the exception of the remnant bulks adhering to the north and south walls near the front of the cave, were then eroded, and sedimentary deposition and human occupation near the front of the cave then produced the comparably more recent deposits of the Eastern Area (Karkanas and Goldberg, 2010).

Detailed description of site formation and depositional processes for the entire PP13B sequence can be found in Marean *et al.* (2010) and Karkanas and Goldberg (2010). I here give a brief overview of the literature describing the depositional

sequence, and summarize only those stratigraphic aggregates from which micromammal specimens were sampled for isotopic analysis. During excavation, all finds observed by excavators were plotted in 3-dimensional space using total station survey equipment, and all sediments removed from the archaeological deposits were sieved through nested 10mm, 3mm and 1.5mm screens to capture all fine material, which included significant numbers of micromammal remains (Matthews *et al.*, 2009; Marean *et al.*, 2010). Because excavated sediment was sieved by both quadrant and stratigraphic unit, the provenience of even the sieved micromammal remains can be traced to their respective stratigraphic aggregates with high fidelity. Description of the sedimentary contexts and their associated ages presented here places the stratigraphic aggregates into chronological order, beginning with the oldest sediments and ending with the most recent deposits (Table 6.1), instead of grouping them by the area of the cave from which they derive, which is instead noted parenthetically in the heading.

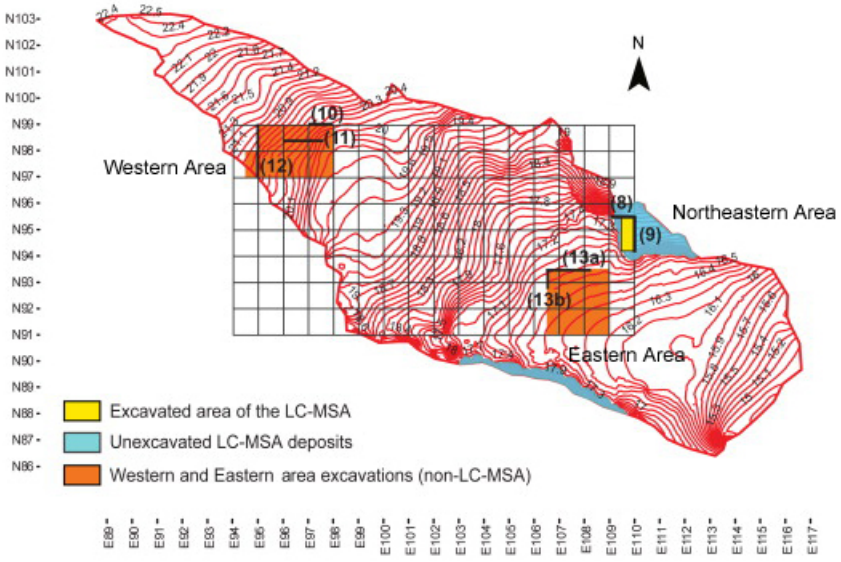

Figure 6.2. Map of the interior of the PP13B cave, showing Western, Eastern, and Northeastern excavation areas. Modified from Marean *et al.* (2010).

area	Stratigraphic Agg.	Adjusted min age[a]	Adjusted max age[a]	OSL age[b]	OSL σ[b]	U-Th age[c]	stratigraphic ordering	MIS[d]
Western Area	LB Sand 1	91	94	90	4	94.7	1	MIS5c
Western Area	DB Sand 2	91	102			102	2	MIS5c
Western Area	LB Sand 2	91	102				3	MIS5c
Western Area	DB Sand 3	91	102				4	MIS5c
Eastern Area	Shelly Brown Sand	91	98	94	3		5	MIS5c/MIS5d
Eastern Area	Roof Spall-Upper	91	98				6	MIS5c/MIS5d
Eastern Area	Roof Spall-Lower	106	114	110	5		7	MIS5d
Western Area	LBG Sand 1	94	134	124	5		8	MIS5e
NE Area	LC-MSA Middle	120	130	125	7		10	MIS5e
Western Area	DB Sand 4a	117	166				11	MIS6
Western Area	LBG Sand 2	117	166				12	MIS6
Western Area	DB Sand 4b	152	166	159	8		13	MIS6
Western Area	DB Sand 4c	152	349				15	MIS6+
NE Area	LC-MSA Lower	153	174	162	6		16	MIS6
Western Area	LB Silt	152	349	157	10		18	MIS6 - MIS10
Western Area	Laminated Facies	349	414	385	17		19	MIS10/MIS11

Table 6.1. Chronological ordering of the PP13B stratigraphic aggregates sampled for this study. Sequential ordering of deposits proceeded using both geochronological ages and stratigraphic association. Table produced using data provided by C.W. Marean and the SACP4 project. Gaps in the "stratigraphic ordering" column sequence indicate stratigraphic aggregates not sampled by this study. All ages are in thousands of years (ka) [a]Marean *et al.* (2010); [b] weighted mean optically stimulated luminescence (OSL) ages, Jacobs (2010); [c] Uranium-Thorium ages obtained from detached speleothem found within the sediments, Marean *et al.* SOM (2010); [d]Stratigraphic aggregates were associated with marine isotope stages using the criteria described in Table 1 in Thompson *et al.* (2010)

Boulder Facies and Laminated Facies (Western Area)

Directly dated regional geomorphic evidence places the MIS11 high sea stand at about +14 msl at ~390 ka (Roberts *et al.*, 2012). The basal units of PP13B are comprised of a boulder facies (sometimes described as a 'boulder beach') likely formed by this high sea stand. The boulder facies are overlain by an archaeologically sterile depositional unit called the "laminated facies" that have associated TT-OSL ages of 349 ± 15 ka (Marean *et al.*, 2010). The coastline would have been in or near the cave for the duration of the period represented by these sediments, with sea level regression moving the shoreline away from the site starting at about 370ka (Fisher *et al.*, 2010).

Fossil micromammal densities are low (number of individual specimens [NISP] = 6; Matthews *et al.*, 2009)(Table 6.2). One specimen of the micromammal *Otomys irroratus* from the Laminated Facies was sampled during this research, and although the sample size is small and MIS10 is outside of the general purview of this paper, this data point is included for completeness. The Laminated Facies are archaeologically sterile, but do contain small amounts of fossil bone (Marean *et al.*, 2010).

Taxon	South Pit Fill		Northeast Fill		LB Sand 1		DB Sand 2		LB Sand 2		DB Sand 3		LBG Sand 3	
	R	S	R	S	R	S	R	S	R	S	R	S	R	S
C. hottentotus														
G. afra					3	1	2	1			2	0		
O. irroratus	1	0			13	3	8	1	3	2	17	2		
O. saundersiae					7	2	4	3	1	1	1	1		
Otomys sp.														
n of other taxa	1	na	1	na	16	na	6	na	7	na	10	na	1	na
Total NISP	2	0	1	0	39	6	20	5	11	3	28	3	1	0

Taxon	DB Sand 4a		LBG Sand 1		LBG Sand 2		DB Sand 4b		DB Sand 4c		LB Silt		Laminated Facies	
	R	S	R	S	R	S	R	S	R	S	R	S	R	S
C. hottentotus														
G. afra			6	1							5	2		
O. irroratus	4	1	92	9	4	1	1	1	11	3	7	6		
O. saundersiae	1	0	33	9					4	1	27	5	1	1
Otomys sp.			7		3	0					13	0		
n of other taxa	3	na	72	na	0	na	0	na	3	na	7	na	5	na
Total NISP	8	1	210	18	7	1	1	1	18	4	59	13	6	1

Table 6.2. Western area taxonomic representation of the species targeted for isotopic analyses, by stratigraphic aggregate. Column heading “R” is the number of specimens recovered; column heading “S” is the number of specimens sampled for isotopic analysis.

LB Silt (Western Area)

The LB silt directly overlies the Laminated Facies in the Western Area of PP13B. Archaeology occurs at low densities (Marean *et al.*, 2010). Micromammals occur with some frequency (NISP = 59; Matthews *et al.*, 2009), while remains of large fauna appear to be rare (Thompson, 2008; Rector and Reed, 2010). The OSL sample taken from the base of the LB Silt deposit is saturated (Jacobs, 2010; Marean *et al.*, 2010), suggesting an age of >200 ka (Jacobs, 2010). Single grain OSL performed on a sample obtained from the profile near top of the unit returns an age of 157 ± 8 ka (Jacobs, 2010; Marean *et al.*, 2010); it is likely that the bulk of these deposits are thus at least MIS6 in age, but may be somewhat older (Table 6.1, Figure 6.3).

LC-MSA Lower (Northeastern Area)

The LC-MSA Lower represents some of the oldest well-dated Middle Stone Age (MSA) archaeological material from southern South Africa. The weighted mean optical age of the deposit is 162 ± 5 ka (Jacobs, 2010; Marean *et al.*, 2010). Distance-to-coast (Fisher *et al.*, 2010) was variable during this time period (Figure 6.4); however, the LC-MSA Lower contains some of the earliest evidence for shellfish procurement by ancient *Homo sapiens* (Marean *et al.*, 2007), and the presence of shellfish likely constrains the age of the deposits to a period of sea-level transgression at ~164 ka (Marean *et al.*, 2010).

Lithic remains (Thompson *et al.*, 2010), large mammal remains (Thompson, 2008; Rector and Reed, 2010; Thompson, 2010), and micromammal remains (Matthews *et al.*, 2009) are all abundant. The micromammal assemblage is dominated by *Otomys*

and other taxa that are non-specific in their habit preferences (Matthews *et al.*, 2009) (Table 6.3).

	LC-MSA Middle		LC-MSA Lower	
Taxon	**R**	**S**	**R**	**S**
C. hottentotus			1	1
G. afra			7	5
O. irroratus	4	2	13	9
O. saundersiae	3	0	24	15
Otomys sp.		1	9	0
n of other taxa	3	na	10	na
Total NISP	10	3	64	30

Table 6.3. Northeastern area taxonomic representation of the species targeted for isotopic analyses, by stratigraphic aggregate. Column heading "R" is the number of specimens recovered; column heading "S" is the number of specimens sampled for isotopic analysis. The one specimen analyzed as "*Otomys sp.*" From the LC-MSA Middle is either *O. saundersiae* or *O. irroratus*, although the attribution of the specimen is unclear.

DB Sand 4c (Western Area)

DB Sand 4c is the lowermost of a series of anthropogenic lenses interstratified with the LBG sands, and likely represent very short periods of occupation (Marean *et al.*, 2010; Marean, personal communication). There is no OSL age for this stratigraphic aggregate (Jacobs, 2010), but it must be older than depositional units above, including the DB Sand 4b, for which there is an OSL age of 159 ± 8 ka (Jacobs, 2010). These deposits are at a minimum MIS6 in age (e.g. older than 150 ka), but may be much older (Table 6.1), especially as micromorphology suggests a long-exposed surface within the aggregate (Marean *et al.*, 2010). The micromammal assemblage recovered from this stratigraphic aggregate (NISP = 18) is predominantly comprised of specimens from the genus *Otomys* (Matthews *et al.*, 2009) (Table 6.2).

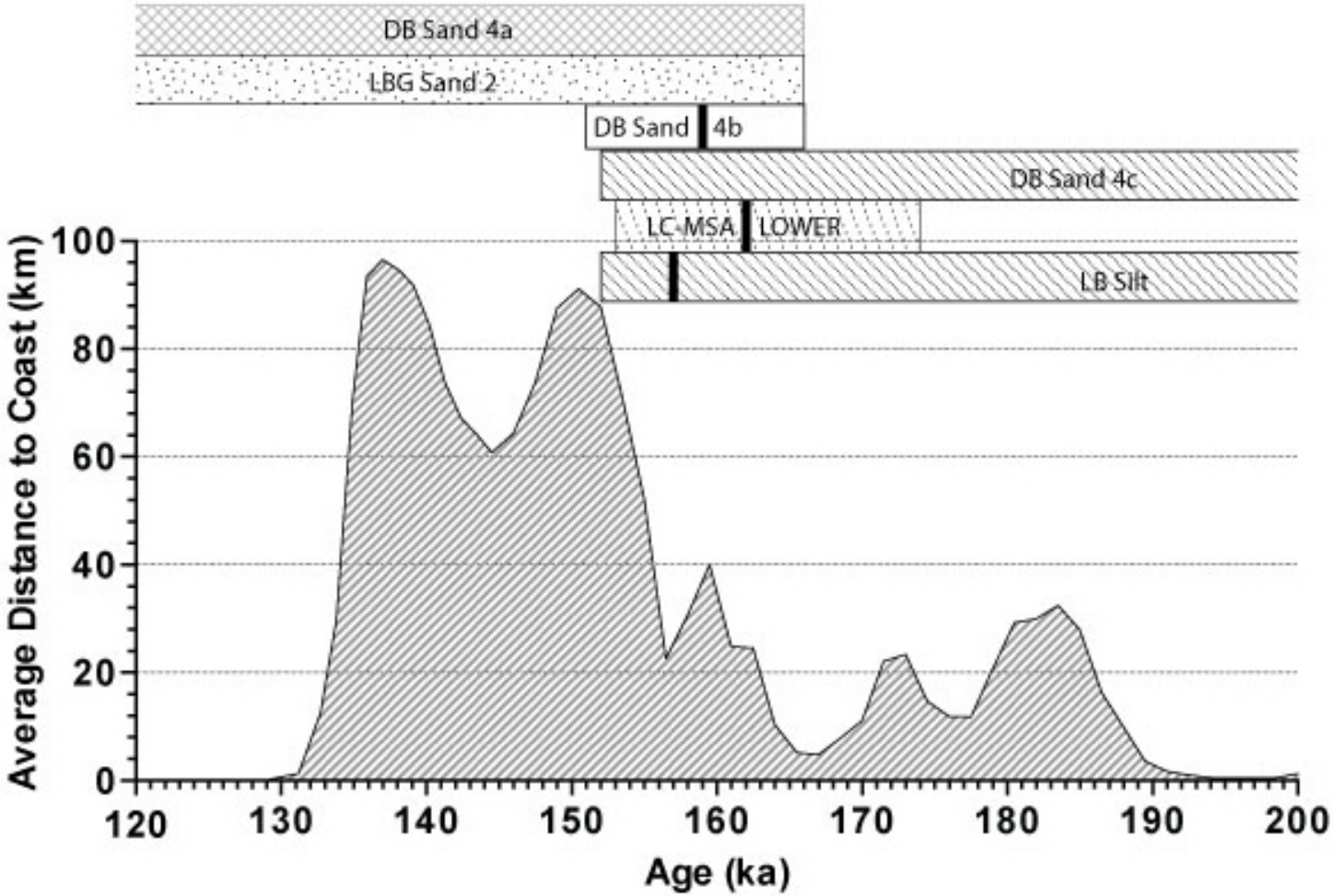

Figure 6.3. Mean distance-to-coast from PP13B during MIS6 - MIS11, with relevant PP13B stratigraphic aggregates superimposed. Sea level model data from Fisher *et al.* (2010, SOM Table 3.1). Minimum/maximum adjusted ages of PP13B deposits from Marean *et al.* (2010), as shown in Table 6.1. Thick horizontal bar within stratigraphic aggregate age ranges is the mean OSL age for those deposits (Jacobs 2010).

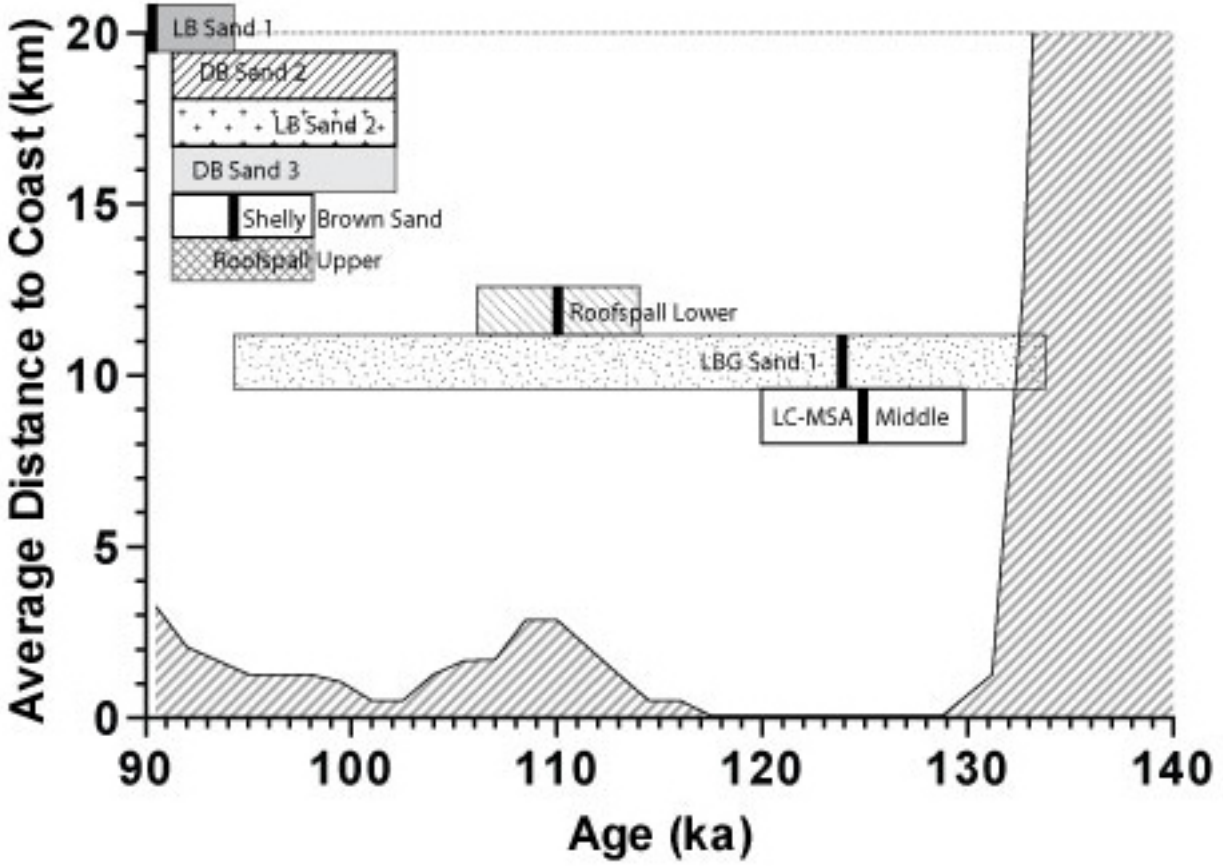

Figure 6.4. Mean distance-to-coast from PP13B during MIS5, with relevant PP13B stratigraphic aggregates superimposed. Sea level model data from Fisher *et al.* (2010, SOM Table 3.1). Minimum/maximum adjusted ages of PP13B deposits from Marean *et al.* (2010), as shown in Table 6.1. Thick horizontal bar within stratigraphic aggregate age ranges is the mean OSL age for those deposits (Jacobs 2010).

DB Sand 4b (Western Area)

Although more recent than DB Sand 4c (the here-unsampled stratigraphic aggregate LBG Sand 3 separates the two), DB Sand 4b is also MIS6 in age (OSL age 159 ± 8 ka; Jacobs, 2010). There is some evidence of anthropogenic burning in this layer (Marean *et al.*, 2010; but see Herries and Fisher, 2010). Identifiable micromammal specimens are singular (one specimen of *O. irroratus*; Matthews *et al*., 2009) (Table 6.2).

LBG Sand 2 (Western Area)

The LBG Sand 2 directly overlies the DB Sand 4b aggregate. There is no radiometric age obtained from direct sampling of the sediments (Jacobs, 2010). Given the stratigraphic position of the LBG Sand 2, it is certainly more recent than the underlying 159 ± 8 ka DB Sand 4b, and older than the MIS5e LGB Sand 1 deposits further up the sequence. Archaeology is not dense (Marean *et al.*, 2010), and large mammal remains appear to be quite rare (Thompson, 2008). Micromammal specimens are also comparably rare (NISP = 8) and again *Otomys* taxa predominate (Matthews *et al.*, 2009) (Table 6.2).

DB Sand 4a (Western Area)

There are no radiometric ages for the sediments from DB 4a. However ages from the overlying LBG Sand 1 (Table 6.1) constrain the age of these deposits to >124 ± 5 ka (Jacobs, 2010; Marean *et al*., 2010), and indicate that they are likely MIS6 in age. During the time span represented by the DB Sand 4a deposits, the sea was regressive, and the shoreline was likely never closer than 20km to the site (Fisher *et al.*, 2010).

DB Sand 4a is an anthropogenic layer with evidence of *in situ* burning (Marean *et*

al., 2010). A number of large mammal remains (Rector and Reed, 2010; Thompson, 2010) were present in the excavated deposits, and were found in association with hammerstones (Marean *et al.*, 2010), although lithic density is otherwise not high (Thompson *et al*., 2010). Micromammal remains are comparably rare (NISP = 8), and the assemblage is dominated by specimens of *Otomys* (Matthews *et al.*, 2009) (Table 6.2).

LC-MSA Middle (Northeastern Area)

The deposits of the LC-MSA Middle overlie those of the LC-MSA Lower, and are well dated, with an OSL age of 125 ± 7ka for this stratigraphic aggregate (Jacobs, 2010). The LC-MSA Lower is likely the first of two PP13B deposits that intersect a period of rapid marine transgression that occurred during MIS5e (Fisher *et al.,* 2010) (Figure 6.4).

Although the excavated area is small, lithics (Marean *et al.*, 2007; Thompson *et al.*, 2010) and abundant shellfish (Marean *et al.*, 2007; Marean *et al.*, 2010) were recovered from this unit. Remains of size 1, size 2, and size 3 mammals were also recovered during excavation (Thompson, 2008). Micromammal remains are still uncommon (NISP =10) and *Otomys* is again the predominant taxon (Matthews *et al.*, 2009) (Table 6.3).

LBG Sand 1 (Western Area)

The LBG Sand 1 deposits are also likely primarily MIS5e in age (Marean *et al.*, 2010), with OSL sampling in the profile near the middle of the excavated portion of the deposit returning a weighted mean age of 124 ± 5ka (Jacobs 2010). Optical ages from an

area with a diffuse contact of LGB Sand 1 and the overlying DB Sand 3 returns a significantly younger weighted mean age of 99 ± 4ka (Jacobs 2010), which may indicate two phases of sedimentary deposition, with truncation of the recent-most portion of the deposits in some excavated units (Jacobs, 2010; Marean *et al.*, 2010). The shoreline during the period represented by the LBG Sand 1 deposits was likely never more than 5km from the site (Fisher *et al*., 2010) (Figure 6.4).

Lithic densities are low in the LBG Sand 1 (Marean *et al.*, 2010), although a number of taxonomically identifiable large faunal remains were recovered (Rector and Reed, 2010). Micromammal remains are comparably more abundant than in many of the stratigraphic aggregates from PP13B (Matthews *et al.,* 2009) (Table 6.2).

Roofspall Lower (Eastern Area)

Single-grain OSL from samples collected from the Roofspall Lower facies have a weighted mean average age of 110 ± 4 ka (Jacobs, 2010), making the deposits MIS5d in age. The coast was near to the site for the duration of the depositional period (Fisher *et al*., 2010) (Figure 6.4). The Roofspall Lower forms the base of the archaeological deposits in the Eastern Area of PP13B (Marean *et al.*, 2010). Lithic artifacts are present but not abundant (Thompson *et al.*, 2010), and there is a reasonable sample of taxonomically identifiable large mammal remains (Rector and Reed, 2010; Thompson, 2010). There is a moderate amount of micromammal remains from the Roofspall Lower, with slightly increased diversity relative to the other depositional units (Matthews *et al.*, 2009) (Table 6.4).

Taxon	Shelly Brown Sand		Upper Roof Spall		Lower Roof Spall	
	R	S	R	S	R	S
C. hottentotus					1	
G. afra			2	1	1	2
O. irroratus	1	1	3	1	3	2
O. saundersiae			6	3	3	6
Otomys sp.			2	0		
n of other taxa	0	na	6	na	15	na
Total NISP	1	1	19	5	23	10

Table 6.4. Eastern area taxonomic representation of the species targeted for isotopic analyses, by stratigraphic aggregate. Column heading "R" is the number of specimens recovered; column heading "S" is the number of specimens sampled for isotopic analysis

Roofspall Upper (Eastern Area)

There are no radiometric ages for the Roofspall Upper aggregate, but its age is constrained by the underlying Roofspall Lower unit (110 ± 4ka) and the overlying Shelly Brown Sand aggregate (94 ± 3ka) (Jacobs, 2010; Marean *et al.*, 2010). This time period spans the end of MIS5d and the beginning of MIS5c. During the period represented by the Roofspall Upper facies, the coast was 1-4km from the site (Fisher *et al.*, 2010).

Blades and bladelets in a quartzite-predominate lithic assemblage are frequent (Thompson *et al.*, 2010). Large mammal remains are common (Thompson, 2010), and enough taxa could be identified to perform a correspondence analysis paleohabitat reconstruction (Rector and Reed, 2010). Micromammals are moderately abundant in the sediments (Table 6.4), with a taxonomic representation similar to that of the underlying Roofspall Lower Units (Matthews *et al.*, 2009).

Shelly Brown Sand (Eastern Area)

OSL dates the Shelly Brown Sand stratigraphic aggregate to 94 ± 3ka (Jacobs, 2010), and adjusted minimum and maximum ages for the deposit again span terminal MIS5d and the beginning of MIS5c (Marean *et al.,* 2010). Lithic and faunal artifactual densities are high, and marine shell is a frequent occurrence in the deposits (Marean *et al.*, 2010). A number of taxonomically identifiable large mammal specimens were recovered, although there were insufficient taxa represented to perform a correspondence analysis of the ancient habitat (Rector and Reed, 2010). Micromammal specimens are singular; one specimen of *O. irroratus* was recovered (Matthews *et al.,* 2009).

DB Sand 3 (Western Area)

DB Sand 3 directly overlies the LBG Sand 1. The OSL ages from the mixed contact between the LBG Sand 1 and the DB Sand 3 suggest a maximum age of ~99ka for this stratigraphic aggregate. (Jacobs, 2010) The minimum age of the unit is constrained by an OSL age of 90 ± 4 ka in the overlying LB Sand 1 (Jacobs, 2010). The sediments are thus likely MIS5c in age (Marean *et al.,* 2010). The DB Sand 3 is artifactually dense (Marean *et al.* 2010), and contains abundant large mammal remains (although in analyses the remains from the DB Sand 3 and DB Sand 2 are often subsumed into a single analytical unit, the DB Sand, or Upper DB sand to increase sample size; Reed and Rector, 2010; Thompson, 2010). Micromammal remains are somewhat abundant (NISP= 28) (Matthews *et al.* 2009).

LB Sand 2 (Western Area)

There are no direct radiometric ages on sediments from the LB Sand 2 (Jacobs, 2010), but the age of the deposits are similarly constrained by stratigraphy. Adjusted minimum and maximum ages for the LB Sand 2 is 91-102 ka (Marean *et al.*, 2010), making this stratigraphic aggregate MIS5c in age. Lithic material is again common in this deposit (Marean *et al.*, 2010; Thompson *et al.*, 2010), although NISP of large mammals is somewhat low (Reed and Rector, 2010). Micromammals are somewhat abundant (Table 6.2), and the assemblage from this depositional unit is predominately *Otomys* taxa that are nonspecific in their habitat preferences (Matthews *et al*,. 2009).

DB Sand 2 (Western Area)

DB Sand 2 is likely similar in age to the underlying LB Sand 2 and DB Sand 3 facies (Marean *et al.*, 2010). The minimum age of the deposit is constrained by an OSL age of 90 ± 4 ka obtained from sediments in the overlying LB Sand 1(Jacobs, 2010). Detached speleothem found within the deposits have a U-Th age of ~102 ka, providing a maximum age for the unit (Marean *et al.*, 2010). This deposit is thus likely MIS5c in age, and during the time of deposition the coastline was never more than 5km distant (Fisher *et al*., 2010) (Figure 6.4).

Lithic material is abundant in the DB Sand 2 (Marean *et al.*, 2010), as are faunal remains (Thompson, 2010). Correspondence analysis of the combined DB Sand 2/DB Sand 3 faunal assemblage has been used to produce a paleohabitat reconstruction for the MIS5c large fauna from PP13B (Reed and Rector, 2010). There are a moderate number

of micromammal specimens represented in this aggregate (Table 6.2), with habitat-nonspecific *Otomys* taxa again predominating (Matthews *et al.,* 2009).

LB Sand 1 (Western Area)

The most-recent material sampled from PP13B derives from the LB Sand 1 stratigraphic aggregate. A weighted mean OSL age of 90 ± 4 ka was obtained from analysis of two samples taken from the LB Sand 1 in profile (Jacobs, 2010). U-Th ages on clean speleothem that caps a remnant dune near the mouth of the cave indicates that PP13B was likely closed to human occupation and deposition by 91ka (Marean *et al.*, 2010), further constraining the age of LB Sand 1 deposits, which are thus MIS5c in age.

Lithic material is abundant (Marean *et al.*, 2010; Thompson *et al.* 2010), although the NISP of large fauna is quite low (Rector and Reed, 2010). Micromammal remains are somewhat abundant (see Table 6.2), and more individual taxa are represented in this assemblage, although *Otomys* specimens are still the most common (Matthews *et al.*, 2009).

Materials and Methods

Stable isotope analyses of micromammals

Stable isotope ecology of micromammal taxa is a growing area of research, with researchers now focused on the isotope ecology of both modern (Thackeray *et al.*, 2003; Robb *et al.*, 2012; Symes *et al.*, 2013; van den Heuvel and Midgley, 2014; Codron *et al.*, 2015) and fossil taxa (Hopley *et al.*, 2006; Yeakel *et al.*, 2007; Hynek *et al.*, 2012;

Kimura *et al.*, 2013). Advances in instrumentation (Sharp and Cerling, 1996; Passey and Cerling, 2006) have allowed researchers to sample enamel from very small specimens. For fossil and/or archaeological material, enamel is the often the only preserved biological material that retains a biogenic isotope ratio through time (Lee-Thorp and Van Der Merwe, 1987; Lee-Thorp, 1989; Kohn *et al.*, 1999; Sponheimer and Lee-Thorp, 1999).

Taxonomic Sampling

In order to track potential changes in the stable carbon isotope composition of micromammal populations over time at PP13B (and by extension possible changes in the relative contributions of C_3 and C_4 plants to their diets), it was necessary to develop a sampling strategy that sampled only taxa that were consistently represented throughout the sequence. Since there is evidence that $\delta^{13}C_{tissue}$ in rodents may vary between taxonomic groups even in similar vegetation contexts (Kimura *et al.*, 2013; Codron *et al.*, 2015; Chapter 3, this thesis), interspecific comparison of $\delta^{13}C$ values across geologic time is likely not appropriate, where as changes over time in the relative contribution of C_3 and C_4 plants to the diets within a given taxa may provide useful information about changes in the availability of these plants on the landscape.

Furthermore, restricting isotope sampling to taxa that are herbivorous controls for a number of factors that could potentially confound interpretation of the isotope analysis results. By sampling specimens that are only one trophic step removed from the vegetation on the landscape, the need to characterize the scale of trophic enrichment or depletion in ^{13}C from plants to insects to insectivores has been eliminated. This produces

a simpler and somewhat more straightforward vegetation proxy, and should serve to ensure that diet-to-tissue offsets will be more consistent across taxa analyzed.

The following four taxa were identified that met these criteria: *Gerbilliscus afra* (sometimes attributed to *T. afra*), *Otomys irroratus*, *Otomys saundersiae*, and *Otomys sp.* (e.g. specimens attributable only to the genus *Otomys* but not identifiable to species). At other sampling localities in the Pinnacle Point Region (Williams, in prep-b; Williams, in prep-d; Williams, in prep-c) the taxon *Bathyergus suillus* was also sampled for stable carbon isotope analysis; however, no specimens clearly attributed of *B. suillus* produced $\delta^{13}C$ data acceptable on quality control grounds, and so that taxon is not included in this study. The common mole rat, *Cryptomys hottentotus*, does not occur throughout the PP13B sequence, but was sampled from stratigraphic aggregates in which it did occur, in part to increase the possible range of vegetative niches covered by this research.

In modern contexts, *G. afra* is not associated with any particular environments, but prefers sandy substrates in which to burrow (Matthews *et al.*, 2009; Campbell *et al.*, 2011). Its diet is comprised primarily of grasses, bulbs, and roots (Skinner and Chimimba, 2005; Granjon and Dempster, 2013); $\delta^{13}C_{enamel}$ values obtained from *G. afra* should reflect admixed stable carbon isotope compositions of these plant groups available on the landscape.

C. hottentotus is a burrowing rodent that primarily consumes the underground storage organs (USO's) of plants. $\delta^{13}C_{enamel}$ values obtained from this taxon should reflect the stable carbon isotope compositions of geophytic plants available in the local vegetation.

Otomys as a genus are strictly herbivorous, and consume primarily grasses and grass seeds (Taylor, 2013), although leafy, non-grass plants may comprise a portion of their diet. *Otomys* molars are laminar and are particularly adapted to shearing; *Otomys* as a genus likely occupy a niche similar to Arvicoline rodents in the Northern Hemisphere (Taylor, 2013). *O. irroratus* is an herbivorous generalist with a primary grass constituent to its diet (Skinner and Chimimba, 2005; Taylor, 2013), while *O. saundersiae*, whose modern day range is somewhat reduced when compared to the *O. irroratus* it is often sympatric with, has similar dietary preferences. $\delta^{13}C$ values obtained from *Otomys* specimens should reflect admixed stable carbon isotope compositions of these grasses, grass seeds, and herbaceous vegetation present on the paleolandscape.

Data from a number of studies (Hynek *et al.*, 2012; Kimura *et al.*, 2013; Williams, in prep-b) indicate that within-taxon values of $\delta^{13}C$ are often disperse, suggesting that micromammals likely sample a broad range of the $\delta^{13}C_{plant}$ values available on the landscape (Hynek *et al*., 2012).

PP13B Fossil Micromammal Sample

Fossil micromammals from PP13B were sampled from all stratigraphic aggregates where taxa targeted by this study were represented. All efforts were made to maximize the specimen sample size from each depositional unit wherever possible, however, in many cases sample sizes were significantly constrained by the number of specimens represented in each assemblage. The sample sizes of the micromammal assemblages from the PP13B stratigraphic aggregates are quite varied, and range from only a few specimens recovered, to quite large assemblages (e.g. the LB Silt, the LC-

MSA Lower, the LBG Sand 1, and the LB Sand 1). The abundance of micromammal specimens recovered is almost certainly due in part to the intensity (or lack thereof) of human occupation in the cave, and the availability of suitable roosting sites within the cave for the assemblage-accumulating raptors. NISP of micromammals (from Matthews *et al*., 2009; Matthews *et al*., 2011), as well as the number of specimens sampled for isotopic analysis, are shown in Tables 2-4.

The number of micromammal specimens available for analysis was also further constrained by the suitability of individual specimens for isotopic analysis, as well as by the conditions of the destructive analysis sampling permit (SAHRA permit 80/12/03/012/52) and the desire to retain at least some specimens with un-ablated enamel for potential future analyses. The resultant specimen group samples all MIS5 and MIS6 stratigraphic aggregates from which micromammal remains were recovered.

The taxonomic composition of the entire PP13B micromammal assemblage has been described at length by Matthews *et al.* (2009). In general, taxonomic diversity is low, and the assemblages from most deposits are not diagnostic in terms of paleohabitat reconstruction. Incisor digestion patterns in deposits where incisor samples are large enough to diagnose patterns suggest that the accumulators of all micromammal assemblages are either barn owls (*Tyto alba;* LC-MSA Lower, all Western area facies, possibly the Eastern area facies), or spotted eagle owls (*Bubo africanus;* possibly the Eastern area) (Matthews *et al.*, 20009). Both of these predators have hunting radii of approximately 3km (Andrews, 1990; Matthews, 2004); the PP13B fossil micromammal assemblages thus likely sample an area approximately 28.25 km^2 during periods when the sea is more than 3km distant from the modern coast, and an area approximately ½ to 2/3

that size during periods when the coast is near to the cave (due to artificial truncation of the foraging range by the ocean itself; Figure 6.4).

Destructive analysis and temporary export permits were obtained from the South African Heritage Resource Agency (SAHRA permit 80/12/03/012/52). The PP13B micromammal specimens, which are permanently housed at the Diaz Museum, Mossel Bay, South Africa, were assessed for suitability for isotope analysis at the Diaz Museum prior to export. All excavated teeth attributed to the taxonomic groups targeted by this study were examined for signs of burning, significant gastric etching, or other signs of physical alteration. Three hundred and thirty-six specimens identifiable to at least the generic level were found suitable for laser ablation. The SAHRA permits stipulated that no more than half of the suitable specimens be exported at a given time; thus 163 specimens from PP13B stratigraphic aggregates were exported for analysis. All non-powdered specimens were returned to the Diaz Museum after analysis, and are retained there; a small set of powdered enamel samples drilled from the larger incisor teeth of some specimens was retained for phosphoric acid digestion, per the permit.

Laser Ablation Gas Chromatograph Isotope Ratio Mass Spectrometry (LA-GC-IRMS):

LA-GC-IRMS analysis of fossil micromammal teeth was performed by Williams at the Stable Isotope Laboratory at Johns Hopkins University (Baltimore, MD), following the methodology described in Passey and Cerling (2006). Ablation was performed on samples mounted within the helium-flushed sample chamber, using a CO_2 laser operating at 5% power. Each ablation 'run' performed on an individual specimen consisted of 20 to 30+ multiple ablation events that produced individual ablation pits on the enamel surface.

Laser targeting (controlled via computer) ensured that each ablation pit sampled only previously un-ablated enamel. Ablation spot size was set at 30 μm, with a laser dwell time of 0.01s. Dwell-time and spot size limit the depth of the ablation pit such that the underlying dentine (which may be diagenetically altered) is not inadvertently sampled (Passey and Cerling, 2006).

Ablation runs that resulted in char production were eliminated from the analysis; char is likely produced when the laser ablates organics remaining on the surface of the enamel (Henry *et al.*, 2012 SOM). Ablation runs that also had associated large fraction blanks, which result when insufficient sample CO_2 is introduced into the mass spectrometer, were also eliminated from the analysis. The final sampling counts in Tables 2-4 reflect this. $\delta^{13}C$ values reported here are normalized to VPDB using the procedures described in Passey and Cerling (2006).

Modern Plant Data

Vegetation communities from other regions in Africa have been extensively sampled to determine the range of available $\delta^{13}C_{plant}$ on the landscape (e.g. Tieszen and Imbamba, 1980; Boutton *et al.*, 1988; Tieszen, 1991; Cerling and Harris, 1999; Cerling *et al.*, 2003; Cerling *et al.*, 2004; Codron *et al.*, 2005; Symes *et al.*, 2013). The vegetation communities found in the region around Pinnacle Point in the present day all belong to biomes associated with the Greater Cape Floristic Region (GCFR), which are ancient and characterized by hyper-diverse vegetation communities with varying proportions of C_3 and C_4 plants (Cowling, 1983; Cowling *et al.*, 1994; Cowling and Richardson, 1995; Goldblatt, 1997; Goldblatt and Manning, 2002; Proches *et al.*, 2006; Cowling *et al.*,

2009). Most vegetation groups are characterized by a predominance of C_3 flora, but the percentage of C_4 grasses in the graminoid portion of these vegetation communities varies as a function of soil composition, shrub cover, temperature, and seasonality of rainfall (Vogel *et al.*, 1978; Cowling, 1983), and C_4 taxa are present in many vegetation communities (Cowling, 1983; Rebelo *et al.*, 2006).

There has as of yet been no systematic sampling of the GCFR vegetation to determine the range of C_3 $\delta^{13}C_{plant}$ values and C_4 $\delta^{13}C_{plant}$ values available in many of these communities. Meta-analysis of the available $\delta^{13}C_{plant}$ values extant in the literature (Chapter 2) can provide some baseline values for modern ranges of $\delta^{13}C_{plant}$ values in C_3 and C_4 plants in extant GCFR vegetation communities, and this chapter uses the values provided by that analysis (corrected for a 1.5-2‰ depletion in ^{13}C in modern atmospheric CO_2) as baseline end member values to which the $\delta^{13}C_{enamel}$ values obtained from the fossil specimens can be compared.

Results

The $\delta^{13}C_{laser/enamel}$ values obtained via LA-GC-IRMS are presented below. $\delta^{18}O_{laser}$ values are also listed in Tables 5-20, but are not discussed here. Where available, the tooth type sampled is also given in the tables. Stable carbon isotope data is organized by stratigraphic aggregate, starting with the oldest material and working forward in time. The micromammal $\delta^{13}C$ data for stratigraphic aggregates LC-MSA Middle, LBG Sand 1, DB Sand 4a, and LBG Sand 2 have also been presented and discussed in Chapter 5, in the context of more general patterns in micromammal stable isotope ecology at the MIS6-

Mis5e transition. It is included here as part of a full PP13B site-specific sequence, and its relationship to other PP13B-specific paleoenvironmental records is discussed in greater detail.

Laminated facies

One specimen of *O. irroratus* from the MIS6-MIS11-aged Laminated Facies was analyzed (Table 6.5). $\delta^{13}C_{laser}$ = -11.2‰ VPDB.

Strat Agg	Taxon	SACP4#	Tooth Type	fraction blank	δ13C ‰ VPDB	δ18O ‰ VSMOW
Laminated Facies	*O. irroratus*	99630	na	0.073198	-11.2	23.1

Table 6.5. $\delta^{13}C_{laser}$ and $\delta^{18}O_{laser}$ isotope data from the Laminated Facies micromammals. $\delta^{13}C$ values are ‰VPDB. $\delta^{18}O$ values are ‰VSMOW.

LB Silt

Thirteen specimens total were analyzed from the LB Silt, out of 59 identified specimens (22% of the total assemblage). Ablation of two specimens of *G. afra* produced $\delta^{13}C_{laser}$ values of -13.2‰ VPDB and -15.1‰ VPDB. Analysis of 6 specimens of *O. irroratus* resulted in a mean $\delta^{13}C$ value of -13.8‰ (σ = 0.4; range of $\delta^{13}C_{laser}$ values was -14.3‰ to -10.1‰). Analysis of 5 specimens of *O. saundersiae* resulted in a mean $\delta^{13}C$ value of -13.9‰ (σ = 1.2; range of $\delta^{13}C_{laser}$ values was -15.3‰ to -12.2‰) (Table 6.6).

LC-MSA Lower

Thirty specimens in total were sampled from the LC-MSA Lower (46.9% of the total micromammal assemblage from this unit). One specimen of *C. hottentottus* from the LC-MSA Lower was analyzed; $\delta^{13}C_{laser}$ = -10.3‰ VPDB. Five specimens of *G. afra* were sampled: $\bar{x}$ $\delta^{13}C_{laser}$ = -11.3‰ VPDB, σ = 1.1. $\delta^{13}C_{laser}$ values for *G. afra* specimens ranged from -12.8‰ to -10.2‰. Sampling of 9 specimens of *O. irroratus* resulted in a mean $\delta^{13}C_{laser}$ value of -13.2‰ VPDB, (σ = 1.3; range of $\delta^{13}C_{laser}$ values was -15.2‰ to -11.5‰). Fifteen *O. saundersiae* specimens were sampled: $\bar{x}$ $\delta^{13}C_{laser}$ = -11.8‰ VPDB, σ = 1.1, $\delta^{13}C_{laser}$ values ranged from -13.9‰ to -10.2‰ (Table 6.7).

Strat Agg	Taxon	SACP4#	Tooth Type	fraction blank	$\delta^{13}C$ ‰ VPDB	$\delta^{18}O$ ‰ VSMOW
LB Silt	*G. afra*	100044A	ML1	0.14652	-13.2	22.1
LB Silt	*G. afra*	99561A	ML1	0.063199	-15.1	20.1
LB Silt	*O. irroratus*	100044C		0.12318	-14.2	22.1
LB Silt	*O. irroratus*	99561B		0.083215	-13.9	23.1
LB Silt	*O. irroratus*	99561B		0.083786	-13.7	23.4
LB Silt	*O. irroratus*	99561C		0.082826	-14.3	22.1
LB Silt	*O. irroratus*	99641A		0.11061	-14.1	23.2
LB Silt	*O. irroratus*	99641A		0.1139	-13.5	23.6
LB Silt	*O. irroratus*	99641B		0.087758	-13.1	23.9
LB Silt	*O. irroratus*	99651B		0.11439	-13.8	22.5
LB Silt	*O. irroratus*	99651B		0.11727	-13.9	22.6
LB Silt	*O. saundersiae*	99641C		0.11439	-15.3	23.2
LB Silt	*O. saundersiae*	99697A		0.078054	-14.4	22.5
LB Silt	*O. saundersiae*	99697B		0.082302	-14.2	23.3
LB Silt	*O. saundersiae*	99820A		0.09393	-12.2	22.2
LB Silt	*O. saundersiae*	99820B		0.071333	-12.9	21.5
LB Silt	*O. saundersiae*	99820B		0.073147	-14.2	19.8

Table 6.6. $\delta^{13}C_{laser}$ and $\delta^{18}O_{laser}$ isotope data from the LB Silt micromammals. $\delta^{13}C$ values are ‰VPDB. $\delta^{18}O$ values are ‰VSMOW. For all tables, tooth type: ML = lower molar, MU = upper molar.

Strat Agg	Taxon	SACP4#	Tooth Type	fraction blank	δ13C ‰ VPDB	δ18O ‰ VSMOW
LC-MSA Lower	*C. hottentotus*	99348A	ML1/MU1	0.13538	-10.3	20.3
LC-MSA Lower	*G. afra*	99151	ML1	0.11279	-10.2	21.9
LC-MSA Lower	*G. afra*	99377	ML1	0.10635	-10.3	21.7
LC-MSA Lower	*G. afra*	99449	ML1,2,3	0.14409	-11.3	21.2
LC-MSA Lower	*G. afra*	99449	ML1,2,3	0.1481	-11.3	20.9
LC-MSA Lower	*G. afra*	99516A	ML1	0.082549	-11.8	21.6
LC-MSA Lower	*G. afra*	99516B	MU1	0.12114	-12.8	22.9
LC-MSA Lower	*O. irroratus*	99201		0.13059	-11.1	24.0
LC-MSA Lower	*O. irroratus*	99201		0.14668	-11.8	23.3
LC-MSA Lower	*O. irroratus*	99207		0.13677	-12.9	22.5
LC-MSA Lower	*O. irroratus*	99365		0.09064	-11.9	23.4
LC-MSA Lower	*O. irroratus*	99563		0.10626	-14.5	22.2
LC-MSA Lower	*O. irroratus*	99224A		0.069936	-13.6	22.1
LC-MSA Lower	*O. irroratus*	99346A		0.11651	-11.8	22.1
LC-MSA Lower	*O. irroratus*	99346A		0.14036	-11.6	22.6
LC-MSA Lower	*O. irroratus*	99346B		0.093582	-14.1	21.7
LC-MSA Lower	*O. irroratus*	99375A		0.084369	-13.5	22.0
LC-MSA Lower	*O. irroratus*	99375B		0.0931	-15.2	21.5
LC-MSA Lower	*O. saundersiae*	99144		0.093184	-11.0	22.2
LC-MSA Lower	*O. saundersiae*	99332		0.13291	-12.5	24.7
LC-MSA Lower	*O. saundersiae*	99358		0.080425	-12.1	21.8
LC-MSA Lower	*O. saundersiae*	99126A		0.081938	-12.9	22.1
LC-MSA Lower	*O. saundersiae*	99126B		0.072684	-12.6	24.2
LC-MSA Lower	*O. saundersiae*	99130A		0.075329	-10.2	25.5
LC-MSA Lower	*O. saundersiae*	99130B		0.070878	-11.4	22.1
LC-MSA Lower	*O. saundersiae*	99224B		0.07556	-10.3	22.6
LC-MSA Lower	*O. saundersiae*	99299A		0.040715	-13.8	23.6
LC-MSA Lower	*O. saundersiae*	99299A		0.046645	-13.9	22.8
LC-MSA Lower	*O. saundersiae*	99348C		0.082971	-11.3	24.8
LC-MSA Lower	*O. saundersiae*	99348D		0.080667	-12.0	23.9
LC-MSA Lower	*O. saundersiae*	99375C		0.070355	-10.4	21.2
LC-MSA Lower	*O. saundersiae*	99497C		0.078134	-11.1	23.0
LC-MSA Lower	*O. saundersiae*	99516C		0.088731	-13.2	23.7
LC-MSA Lower	*O. saundersiae*	99516C		0.098652	-13.6	22.8
LC-MSA Lower	*O. saundersiae*	99516C		0.11181	-13.8	23.3
LC-MSA Lower	*O. saundersiae*	99516D		0.11182	-11.1	24.4

Table 6.7. $\delta^{13}C_{laser}$ and $\delta^{18}O_{laser}$ isotope data from the LC-MSA Lower micromammals. $\delta^{13}C$ values are ‰VPDB. $\delta^{18}O$ values are ‰VSMOW.

DB Sand 4c

Four specimens (22% of the total assemblage from this unit) were analyzed. Sampling of three *O. irroratus* specimens resulted in a $\bar{x}$ $\delta^{13}C_{laser}$ = -14.2‰ VPDB, σ = 0.3. $\delta^{13}C_{laser}$ values for *O. irroratus* specimens ranged from -14.5‰ to -13.9‰. One specimen of *O. saundersiae* was analyzed, $\delta^{13}C_{laser}$ = -14.2‰ VPDB (Table 6.8).

DB Sand 4b

One *O. irroratus* specimen, representing the entire micromammal sample from this aggregate, was analyzed. $\delta^{13}C_{laser}$ = -15.6‰ VPDB (Table 6.9).

Strat Agg	Taxon	SACP4#	Tooth Type	fraction blank	δ13C ‰ VPDB	δ18O ‰ VSMOW
DB Sand 4c	*O. irroratus*	99583	ML1	0.04584	-13.9	22.6
DB Sand 4c	*O. irroratus*	100035A	ML1	0.087178	-14.2	19.5
DB Sand 4c	*O. irroratus*	100035B		0.093224	-14.5	22.5
DB Sand 4c	*O. saundersiae*	100041		0.13518	-14.2	24.6

Table 6.8. $\delta^{13}C_{laser}$ and $\delta^{18}O_{laser}$ isotope data from the DB Sand 4c micromammals. $\delta^{13}C$ values are ‰VPDB. $\delta^{18}O$ values are ‰VSMOW.

Strat Agg	Taxon	SACP4#	Tooth Type	fraction blank	δ13C ‰ VPDB	δ18O ‰ VSMOW
DB Sand 4b	*O. irroratus*	99904	MU3	0.10589	-15.6	21.6

Table 6.9. $\delta^{13}C_{laser}$ and $\delta^{18}O_{laser}$ isotope data from the DB Sand 4b micromammals. $\delta^{13}C$ values are ‰VPDB. $\delta^{18}O$ values are ‰VSMOW.

LBG Sand 2

One specimen of *O. irroratus* (14.3% of the total assemblage) was analyzed. $\delta^{13}C_{laser}$ = -14.8‰ VPDB (Table 6.10).

Strat Agg	Taxon	SACP4#	Tooth Type	fraction blank	δ13C ‰ VPDB	δ18O ‰ VSMOW
LBG Sand 2	*O. irroratus*	99929	ML1	0.12946	-14.8	23.7

Table 6.10. $\delta^{13}C_{laser}$ and $\delta^{18}O_{laser}$ isotope data from the LBG Sand 2 micromammals. $\delta^{13}C$ values are ‰VPDB. $\delta^{18}O$ values are ‰VSMOW.

DB Sand 4a

One *O. irroratus* specimen (representing 12.5% of the total assemblage from this unit) was sampled. $\delta^{13}C_{laser}$ = -13.6‰ VPDB (Table 6.11).

Strat Agg	Taxon	SACP4#	Tooth Type	fraction blank	δ13C ‰ VPDB	δ18O ‰ VSMOW
DB Sand 4a	*O. irroratus*	99926A	ML1	0.076508	-13.6	22.5

Table 6.11. $\delta^{13}C_{laser}$ and $\delta^{18}O_{laser}$ isotope data from the DB Sand 4a micromammals. $\delta^{13}C$ values are ‰VPDB. $\delta^{18}O$ values are ‰VSMOW.

LC-MSA Middle

Three specimens of *Otomys*, representing 30% of the total micromammal assemblage, were sampled. Two specimens were clearly attributed to *O. irroratus*, and $\delta^{13}C_{laser}$ values for those specimens are -10.7‰ VPDB and -11.5‰ VPDB. The taxonomic attribution of the third specimen was unclear, and so has been described here as *Otomys sp.*, although it belongs to either *O. irroratus* or *O. saundersiae*. The $\delta^{13}C_{laser}$ value of this specimen is -13.4‰. (Table 6.12).

Strat Agg	Taxon	SACP4#	Tooth Type	fraction blank	δ13C ‰ VPDB	δ18O ‰ VSMOW
LC-MSA Middle	*O. irroratus*	99245	MU1	0.087093	-11.5	22.6
LC-MSA Middle	*O. irroratus*	99205A	ML1	0.053435	-10.7	25.1
LC-MSA Middle	*Otomys sp.*	99617		0.061193	-13.4	23.5

Table 6.12. $\delta^{13}C_{laser}$ and $\delta^{18}O_{laser}$ isotope data from the LC-MSA Middle 4b micromammals. $\delta^{13}C$ values are ‰VPDB. $\delta^{18}O$ values are ‰VSMOW.

LBG Sand 1

Nineteen specimens representing 8.5% of the micromammal assemblage from this unit were analyzed. One specimen of *G.* afra was ablated, resulting in a $\delta^{13}C_{laser}$ value of -14.4‰ VPDB. Nine specimens of *O. irroratus* were analyzed; mean $\delta^{13}C_{laser}$ = -15.9‰ VPDB, σ=0.4 ($\delta^{13}C_{laser}$ values ranged from -15.4‰ to -16.5‰ VPDB). Nine *O. saundersiae* specimens were also sampled: mean $\delta^{13}C_{laser}$ = -15.7‰ VPDB, σ = 1.6 ($\delta^{13}C_{laser}$ values range from -18.8‰ to -13.5‰) (Table 6.13).

Roofspall Lower

Ten specimens (43.5% of the micromammal assemblage from this aggregate) were sampled. Two specimens of *G. afra* had $\delta^{13}C_{laser}$ values of -10.4‰ VPDB and -13.6‰ VPDB. The two *O. irroratus* specimens sampled had very disparate values of $\delta^{13}C_{laser}$ (-17.0‰ VPDB, -10.3‰VPDB). Six specimen of *O. saundersiae* were ablated: mean $\delta^{13}C_{laser}$ = -11.6‰ VPDB, σ = 0.8 ($\delta^{13}C_{laser}$ values for *O. saundersiae* range from -12.2‰ to -10.3‰) (Table 6.14).

Strat Agg	Taxon	SACP4#	Tooth Type	fraction blank	δ13C ‰ VPDB	δ18O ‰ VSMOW
LBG Sand 1	*G. afra*	99851	MU1,2	0.1244	-14.4	21.0
LBG Sand 1	*O. irroratus*	99932	ML1	0.10399	-15.5	21.7
LBG Sand 1	*O. irroratus*	99935	ML1	0.097408	-16.1	21.7
LBG Sand 1	*O. irroratus*	100012A	ML1	0.054662	-16.7	19.5
LBG Sand 1	*O. irroratus*	100012A	ML1	0.063394	-16.2	20.2
LBG Sand 1	*O. irroratus*	100049A	ML1	0.11847	-16.0	22.7
LBG Sand 1	*O. irroratus*	99368A	MU3	0.063887	-15.4	22.5
LBG Sand 1	*O. irroratus*	99920C	ML1	0.044269	-16.2	20.4
LBG Sand 1	*O. irroratus*	99920C	ML1	0.093027	-16.1	21.0
LBG Sand 1	*O. irroratus*	99938C	ML1	0.079375	-15.7	19.9
LBG Sand 1	*O. irroratus*	99938C	ML1	0.13961	-16.4	18.7
LBG Sand 1	*O. irroratus*	99938D	MU3	0.074114	-15.4	20.9
LBG Sand 1	*O. saundersiae*	99933		0.098858	-16.5	22.8
LBG Sand 1	*O. saundersiae*	100037		0.046151	-14.3	21.4
LBG Sand 1	*O. saundersiae*	100049B		0.098053	-18.8	18.4
LBG Sand 1	*O. saundersiae*	99317D		0.12186	-13.5	22.7
LBG Sand 1	*O. saundersiae*	99325D		0.061362	-15.5	21.4
LBG Sand 1	*O. saundersiae*	99325D		0.078555	-16.5	21.2
LBG Sand 1	*O. saundersiae*	99325E		0.066852	-15.2	21.9
LBG Sand 1	*O. saundersiae*	99331A		0.059243	-14.9	21.0
LBG Sand 1	*O. saundersiae*	99368C		0.063155	-16.7	23.1

Table 6.13. $\delta^{13}C_{laser}$ and $\delta^{18}O_{laser}$ isotope data from the LBG Sand 1 micromammals. $\delta^{13}C$ values are ‰VPDB. $\delta^{18}O$ values are ‰VSMOW.

Strat Agg	Taxon	SACP4#	Tooth Type	fraction blank	δ13C ‰ VPDB	δ18O ‰ VSMOW
Roof Spall-Lower	*G. afra*	99403	ML2	0.12535	-10.4	19.4
Roof Spall-Lower	*G. afra*	99225C	MU1	0.040959	-13.6	21.2
Roof Spall-Lower	*O. irroratus*	99537	MU3	0.069808	-17.0	20.0
Roof Spall-Lower	*O. irroratus*	99225A	MU1	0.071036	-10.3	20.7
Roof Spall-Lower	*O. saundersiae*	99293		0.064118	-10.3	22.6
Roof Spall-Lower	*O. saundersiae*	99553		0.15087	-12.2	21.1
Roof Spall-Lower	*O. saundersiae*	99225B		0.056625	-11.9	22.1
Roof Spall-Lower	*O. saundersiae*	99225B		0.060327	-12.5	21.7
Roof Spall-Lower	*O. saundersiae*	99239A		0.12718	-11.0	21.4
Roof Spall-Lower	*O. saundersiae*	99239A		0.13011	-11.1	20.9
Roof Spall-Lower	*O. saundersiae*	99239B		0.12192	-11.9	19.8
Roof Spall-Lower	*O. saundersiae*	99239B		0.13398	-11.8	19.2
Roof Spall-Lower	*O. saundersiae*	99241C		0.14414	-12.1	21.3

Table 6.14. $\delta^{13}C_{laser}$ and $\delta^{18}O_{laser}$ isotope data from the Roofspall Lower micromammals. $\delta^{13}C$ values are ‰VPDB. $\delta^{18}O$ values are ‰VSMOW.

Roofspall Upper

Five micromammal specimens from the Roofspall Upper were ablated (26.3% of the total assemblage). One specimen of *G. afra* had a $\delta^{13}C_{lase}$ value of -9.6‰ VPDB. The single *O. irroratus* specimen has a $\delta^{13}C_{laser}$ value of -10.5‰ VPDB, while the 3 specimens attributed to *O. saundersiae* had a mean $\delta^{13}C_{laser}$ = -13.1 ‰ VPDB, σ = 1.0 ($\delta^{13}C_{laser}$ values for *O. saundersiae* range from -14.1‰ to -12.1‰) (Table 6.15).

Strat Agg	Taxon	SACP4#	Tooth Type	fraction blank	δ13C ‰ VPDB	δ18O ‰ VSMOW
Roof Spall-Upper	*G. afra*	99413	ML1	0.077905	-9.6	21.5
Roof Spall-Upper	*O. irroratus*	99243A	MU3	0.073994	-10.5	23.5
Roof Spall-Upper	*O. saundersiae*	99362		0.14671	-13.2	20.7
Roof Spall-Upper	*O. saundersiae*	99243B		0.041564	-14.1	20.4
Roof Spall-Upper	*O. saundersiae*	99243C		0.051335	-12.4	22.6
Roof Spall-Upper	*O. saundersiae*	99243C		0.057104	-11.8	21.8

Table 6.15. $\delta^{13}C_{laser}$ and $\delta^{18}O_{laser}$ isotope data from the Roofspall Upper micromammals. $\delta^{13}C$ values are ‰VPDB. $\delta^{18}O$ values are ‰VSMOW.

Shelly Brown Sand

One specimen of *O. irroratus*, the only micromammal recovered from the Shelly Brown Sand, was ablated twice. $\bar{x}$ $\delta^{13}C_{laser}$ = -10.0‰ VPDB, σ = 0.3 (Table 6.16).

Strat Agg	Taxon	SACP4#	Tooth Type	fraction blank	δ13C ‰ VPDB	δ18O ‰ VSMOW
Shelly Brown Sand	*O. irroratus*	99541	MU3	0.054478	-9.8	24.0
Shelly Brown Sand	*O. irroratus*	99541	MU3	0.055538	-10.2	24.0

Table 6.16. $\delta^{13}C_{laser}$ and $\delta^{18}O_{laser}$ isotope data from the Shelly Brown Sand micromammals. $\delta^{13}C$ values are ‰VPDB. $\delta^{18}O$ values are ‰VSMOW.

DB Sand 3

Three *Otomys* specimens (10.7% of the assemblage from this aggregate) were sampled. *O. irroratus* values of $\delta^{13}C_{laser}$ were -11.8‰ and -14.9‰ VPDB. The $\delta^{13}C_{laser}$ value of the *O. saundersiae* specimen was -15.6‰ VPDB (Table 6.17).

Strat Agg	Taxon	SACP4#	Tooth Type	fraction blank	δ13C ‰ VPDB	δ18O ‰ VSMOW
DB Sand 3	*O. irroratus*	99768	ML1	0.076344	-11.8	22.6
DB Sand 3	*O. irroratus*	99775	MU3	0.12135	-14.9	23.1
DB Sand 3	*O. saundersiae*	99898		0.06728	-15.6	20.1

Table 6.17. $\delta^{13}C_{laser}$ and $\delta^{18}O_{laser}$ isotope data from the DB Sand 3 micromammals. $\delta^{13}C$ values are ‰VPDB. $\delta^{18}O$ values are ‰VSMOW.

LB Sand 2

Three *Otomys* specimens (27.3% of the assemblage) were sampled for the LB Sand 2. *O. irroratus* values of $\delta^{13}C_{laser}$ were -11.9‰ and -12.5‰ VPDB. The $\delta^{13}C_{laser}$ value of the single *O. saundersiae* specimen analyzed was -13.0‰ VPDB (Table 6.18).

Strat Agg	Taxon	SACP4#	Tooth Type	fraction blank	δ13C ‰ VPDB	δ18O ‰ VSMOW
LB Sand 2	*O. irroratus*	99913A	ML1	0.0588	-11.9	22.3
LB Sand 2	*O. irroratus*	99913B	ML1	0.059627	-12.5	21.1
LB Sand 2	*O. saundersiae*	99899		0.053797	-13.0	23.5

Table 6.18. $\delta^{13}C_{laser}$ and $\delta^{18}O_{laser}$ isotope data from the LB Sand 2 micromammals. $\delta^{13}C$ values are ‰VPDB. $\delta^{18}O$ values are ‰VSMOW.

DB Sand 2

Five micromammal specimens, representing 25% of the total micromammal assemblage from this aggregate, were analyzed. The $\delta^{13}C_{laser}$ value of the single *G. afra* specimen sampled was -8.9‰ VPDB. The $\delta^{13}C_{laser}$ value of the single *O. irroratus* specimen sampled was -11.8‰ VPDB. Sampling of three specimens of *O. saundersiae* resulted in a mean $\delta^{13}C_{laser}$ value of -12.9‰ for that taxon ($\sigma = 0.6$, $\delta^{13}C_{laser}$ values for *O. saundersiae* range from -13.3‰ to -12.2‰) (Table 6.19).

Strat Agg	Taxon	SACP4#	Tooth Type	fraction blank	δ13C ‰ VPDB	δ18O ‰ VSMOW
DB Sand 2	*G. afra*	99901E	MU1,2	0.028786	-8.9	24.4
DB Sand 2	*O. irroratus*	99901A	ML1	0.070277	-11.8	23.8
DB Sand 2	*O. saundersiae*	99908		0.1379	-12.2	21.3
DB Sand 2	*O. saundersiae*	99901C		0.05961	-13.3	21.4
DB Sand 2	*O. saundersiae*	99901C		0.06488	-13.2	22.1
DB Sand 2	*O. saundersiae*	99901D		0.1031	-13.1	21.0
DB Sand 2	*O. saundersiae*	99901D		0.10575	-13.2	21.6

Table 6.19. $\delta^{13}C_{laser}$ and $\delta^{18}O_{laser}$ isotope data from the DB Sand 2 micromammals. $\delta^{13}C$ values are ‰VPDB. $\delta^{18}O$ values are ‰VSMOW.

LB Sand 1

Six specimens (15.4% of the total assemblage) were ablated. $\delta^{13}C_{laser}$ of the *G. afra* specimen analyzed was -13.1‰ VPDB. Three *O. irroratus* specimens had a mean $\delta^{13}C_{laser}$ value of -13.0‰ (σ =1.9, $\delta^{13}C_{laser}$ values range from -15.1‰ to -11.3‰). Two specimens of *O. saundersiae* had $\delta^{13}C_{laser}$ values of -10.4‰ and -11.8‰VPDB (Table 6.20).

Strat Agg	Taxon	SACP4#	Tooth Type	fraction blank	δ13C ‰ VPDB	δ18O ‰ VSMOW
LB Sand 1	*G. afra*	99949	MU1	0.089735	-13.1	22.6
LB Sand 1	*O. irroratus*	99897	ML1	0.071467	-11.3	19.8
LB Sand 1	*O. irroratus*	99980	ML1	0.045328	-15.1	20.6
LB Sand 1	*O. irroratus*	99950A	MU3	0.06595	-12.5	22.3
LB Sand 1	*O. saundersiae*	99472		0.074283	-10.4	20.1
LB Sand 1	*O. saundersiae*	99950D		0.067914	-11.8	24.0

Table 6.20. $\delta^{13}C_{laser}$ and $\delta^{18}O_{laser}$ isotope data from the LB Sand 1 micromammals. $\delta^{13}C$ values are ‰VPDB. $\delta^{18}O$ values are ‰VSMOW.

Discussion

Many of the sample sizes from individual stratigraphic aggregates are quite small (Tables 2-4). This limits the ability of statistical analyses to robustly compare populations of $\delta^{13}C$ values between populations of samples. However, each micromammal specimen analyzed functions as a unique 'sampler' of vegetation on the landscape (*sensu* Hynek *et al.*, 2012), with individual $\delta^{13}C_{tissue}$ values representing the pooled stable carbon isotope composition(s) of dietary constituents for each specimen. Thus, if micromammals as a group tend to sample the range of vegetation and microhabitats on the landscape (at least within the hunting range of the aggregating predator), each discrete data point within a given stratigraphic aggregate can be treated as a "sample" of a the vegetation extant at a given site during a particular time period (Hynek *et al.*, 2012; Williams, in prep-b).

All measured $\delta^{13}C_{laser}$ values have first been converted to calculated $\delta^{13}C_{diet}$ values. $\delta^{13}C_{diet}$ is calculated by simple algebraic transformation using the equation (following Cerling and Harris, 1999; Passey *et al.*, 2005; see Chapter 3).

$$\delta_{diet} = \left(\frac{1000 + \delta_{enamel}}{1 + \frac{\varepsilon^*_{apatite\text{-}diet}}{1000}} \right) - 1000$$

In the case of micromammals, several trophic enrichment factors ($\varepsilon^*_{diet\text{-}apatite}$) have been measured, and range from about 9‰ to 11‰ (DeNiro and Epstein, 1978; Ambrose and Norr, 1993; Tieszen and Fagre, 1993; Passey *et al.*, 2005; Podelsak *et al.*, 2008), which is a fairly broad range. Unfortunately, $\varepsilon^*_{diet\text{-}apatite}$ has not been measured for any of the taxa

sampled here. However, a value of $\varepsilon^*_{\text{diet-apatite}}$ of 11‰ ± 0.1 has been measured in rodents with similar body size and ecology (Podelsak *et al.*, 2008) and has been used fruitfully by other researchers as a trophic enrichment factor in the analysis of fossil rodents (Hynek *et al.*, 2012), and that value of ε^* is also used here.

The calculated $\delta^{13}C_{diet}$ values are approximations of the stable carbon isotope composition of each individual specimen's diet. These values can then be compared to a known range of $\delta^{13}C_{plant}$ values for both C_3 and C_4 vegetation in order to assess whether there is input of significant dietary C_3 or C_4 vegetation into the dietary stable isotope composition of consumer tissue. C_3 and C_4 end member $\delta^{13}C_{plant}$ values are best approximated for the Pinnacle Point region using output from the GSCIMS metadata analysis of modern GCFR $\delta^{13}C_{plant}$ values (Williams, in prep-a), adjusted for a 1.5‰ depletion in ^{13}C in modern atmospheric CO_2 (and thus in plants) due to combustion of isotopically light fossil fuels during the last ~150 years. 'Corrected' GSCIMS values for GCFR plants are: C_3 $\delta^{13}C_{plant}$ range from -29.8‰ to –16.8‰ VPDB ($\bar{x}$= -24.4‰, σ = 2.39), while C_4 $\delta^{13}C_{plant}$ values range from -14.1‰ to -8.1‰ VPDB ($\bar{x}$= -10.8‰, σ = 1.12).

Fossil $\delta^{13}C_{diet}$ values are also compared to the fossil-fuel-adjusted $\delta^{13}C_{diet}$ values of specimens from three vegetation contexts in the Pinnacle Point region (Chapter 3). *O. irroratus* specimens from the modern context of Amisrus, in the Wilderness Forest near Knysna, sample both very closed C_3 vegetation associated with forests (the lower values of $\delta^{13}C$ found in this population) and more open vegetation from fynbos communities within the 3km of the sampling locality. Some Wolwe River *Otomys*

specimens sample more open C_3-predominant environments in which some C_4 grasses are present, when the narrow and comparably low values of $\delta^{13}C_{diet}$ in the *O. saundersiae* specimens from Rein's Nature Reserve reflect the habitat near this sampling locality: C_3-predominant GCFR in which C_4 grass is rare (Williams, in prep-b).

C_3 and C_4 proportions in micromammal diets, by stratigraphic aggregate

Laminated Facies

Calculated $\delta^{13}C_{diet}$ (using $\varepsilon^*_{diet\text{-}apatite}$ = 11‰) for *Otomys* individual sampled from the Laminated Facies is -21.9‰, several ‰ higher that the fossil-corrected GCFR mean C_3 $\delta^{13}C_{plant}$ value of -24.4‰, but within the 'corrected' range of all GCFR C_3 plants (-29.8‰ to –16.8‰ VPDB). Thus, the diet of this individual specimen is likely to have been wholly C_3.

LB Silt

Calculated $\delta^{13}C_{diet}$ for of the 11 *Otomys* specimens sampled from this layer range from -26.0‰ to -23.0‰. All *Otomys* values of $\delta^{13}C_{diet}$ are close to the 'corrected' mean GCFR C_3 $\delta^{13}C_{plant}$ value of -24.4‰; micromammal specimens with values of $\delta^{13}C_{diet}$ more depleted in ^{13}C than this mean C_3 plant value are certainly pure-C_3 consumers. (Figure 6.5). Calculated values of $\delta^{13}C_{diet}$ for the two specimens of *G. afra* analyzed are -23.9‰ VPDB and -25.8‰ VPDB; both of these values indicate a C_3 diet in both individuals. A Kruskal-Wallis one-way analysis of variance (with Dunn's post hoc test)

indicates the median values of $\delta^{13}C_{diet}$ of the *G. afra*, *O. irroratus,* and *O. saundersiae* populations sampled are not significantly different (H = 0.25, 2 d.f., p = 0.89).

The fossil micromammals from the LB Silt have values of $\delta^{13}C_{diet}$ that are quiet depleted in ^{13}C and intersect the lowest portion of $\delta^{13}C_{diet}$ ranges of modern micromammal specimens (Figure 6.5). The micromammal stable carbon isotope data from the sampled LB Silt specimens thus suggests that C_4 vegetation is likely not present in the diet of any of the taxa sampled, and was not intersected on the landscape during the period of time represented (early MIS6 or earlier) by any of the 13 specimens analyzed.

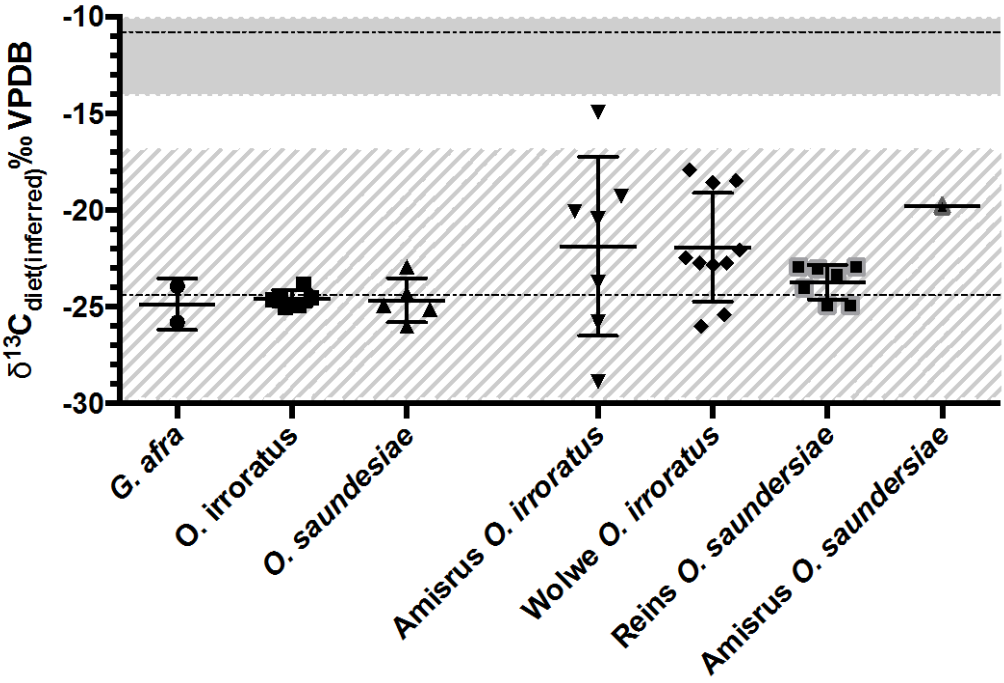

Figure 6.5. Calculated $\delta^{13}C_{diet}$ for the specimens sampled from the LB Silt (left) compared to fossil fuel adjusted values of modern specimens (right). Hashed band represents the range of fossil fuel adjusted GCFR C_3 $\delta^{13}C_{plant}$ values (horizontal dotted line is the mean). Shaded band represents the most-depleted portion of the range of fossil fuel adjusted GCFR C_4 $\delta^{13}C_{plant}$ values (horizontal dotted line is the mean).

LC-MSA Lower

Calculated $\delta^{13}C_{diet}$ for the *Otomys* specimens ranges from -25.9‰ to -20.9% VPDB. $\delta^{13}C_{diet}$ values of the *O. irroratus* specimens sampled are slightly depleted in ^{13}C relative to the values of $\delta^{13}C_{diet}$ in *O. saundersiae*, while *G. afra* $\delta^{13}C_{diet}$ values overlap with those of the *Otomys* specimens (Figure 6.6). A KW test indicates that the median $\delta^{13}C_{diet}$ value of the *O. irroratus* specimens are significantly lower than that of the *O. saundersiae* and *G. afra* populations, which probably reflects a slight difference in more closed versus more open C_3 vegetation in their diets.

Calculated $\delta^{13}C_{diet}$ for the *C. hottentotus* specimen is -21.0% VPDB, which is still within the range C_3 $\delta^{13}C_{plant}$ values, although it is somewhat higher than the range of $\delta^{13}C_{diet}$ values for the other taxa sampled here.

The values of $\delta^{13}C_{diet}$ calculated for the fossil specimens here overlap with the middle portion of the $\delta^{13}C$ dietary ranges of modern micromammal specimens from the region, and thus suggest diets with a minimal C_4 admixture. The more ^{13}C-depleted fossil specimens of *O. irroratus* and *O. saundersiae* may indicate dietary vegetation obtained from more closed contexts, while the highest values of $\delta^{13}C_{diet}$ in the *O. saundersiae* and *G. afra* specimens sampled may suggest primary C_3 consumption in slightly more open environments.

The LC-MSA Lower micromammal stable carbon isotope dataset suggests that all taxa sampled are consuming diets that are primarily C_3 in composition. C_4 grasses may occur in the local vegetation communities, but are not a primary constituent of the diet of

any of the taxa sampled here. The C_3 dietary signal of the *C. hottentotus* specimen $\delta^{13}C$ indicates the presence of C_3 geophytic plants on the landscape at about 164 ka.

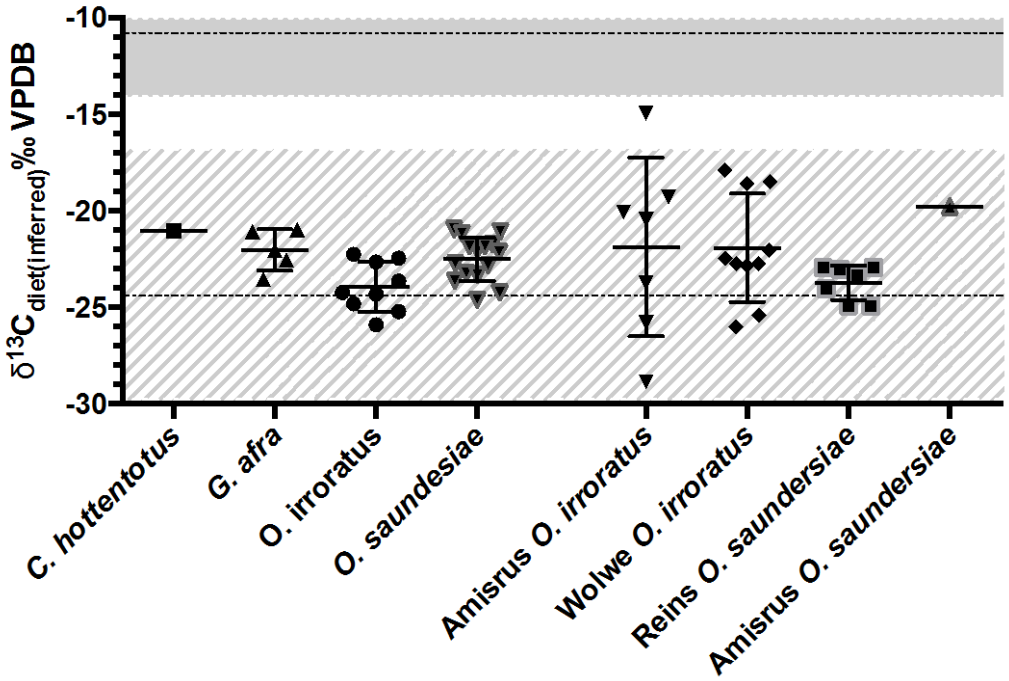

Figure 6.6. Calculated $\delta^{13}C_{diet}$ for the specimens sampled from the LC-MSA Lower (left) compared to fossil fuel adjusted values of modern specimens (right). Hashed band represents the range of fossil fuel adjusted GCFR C_3 $\delta^{13}C_{plant}$ values (horizontal dotted line is the mean). Shaded band represents the most-depleted portion of the range of fossil fuel adjusted GCFR C_4 $\delta^{13}C_{plant}$ values (horizontal dotted line is the mean).

DB Sand 4c

The sample of analyzed micromammal material from the DB Sand 4c is quite small (4 specimens). Calculated $\delta^{13}C_{diet}$ for the *Otomys* specimens from this unit suggest a diet composed exclusively of C_3 vegetation ($\delta^{13}C_{diet}$ values range from -25.2‰ to -24.6‰ VPDB. Fossil $\delta^{13}C_{diet}$ values are similar to those observed in the modern specimens from C_4-poor Limestone Fynbos (Figure 6.7). Thus the small micromammal

stable carbon isotope data suggests that the specimens here were intersecting or consuming no C_4 vegetation within their respective habitats.

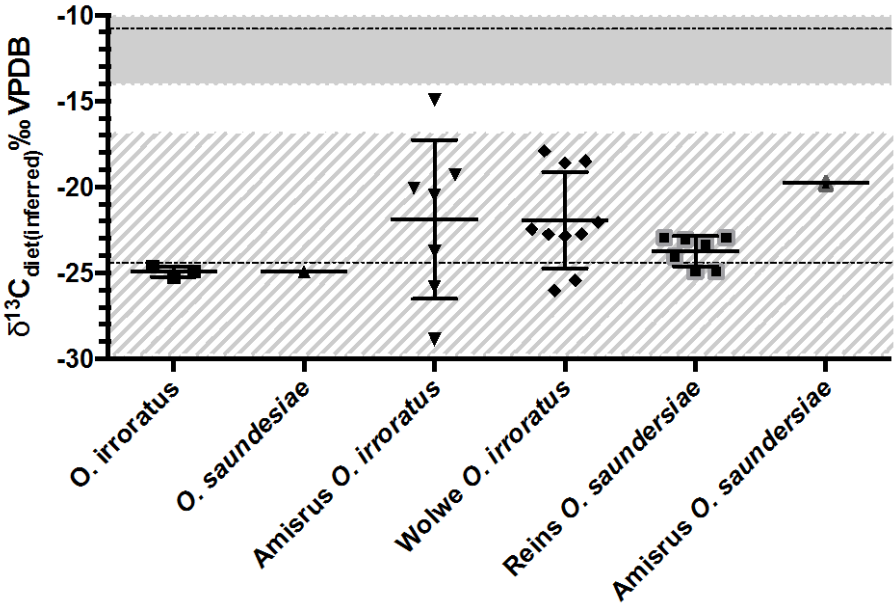

Figure 6.7. Calculated $\delta^{13}C_{diet}$ for the specimens sampled from the DB Sand 4c (left) compared to fossil fuel adjusted values of modern specimens (right). Hashed band represents the range of fossil fuel adjusted GCFR C_3 $\delta^{13}C_{plant}$ values (horizontal dotted line is the mean). Shaded band represents the most-depleted portion of the range of fossil fuel adjusted GCFR C_4 $\delta^{13}C_{plant}$ values (horizontal dotted line is the mean).

DB Sand 4b

Only one specimen of *O. irroratus* was available from DB Sand 4b for isotopic analysis. The $\delta^{13}C_{diet}$ value of this specimen is somewhat depleted in ^{13}C (-26.3‰ VPDB), and consistent with a pure C_3 diet in this specimen of *Otomys.*

LBG Sand 2

The calculated $\delta^{13}C_{diet}$ from the one analyzed specimen of *O. irroratus* from the LBG Sand 2 is quite low (-25.5‰ VPDB), and is indicative of a wholly-C_3 diet for this individual. Because the fossil value of $\delta^{13}C_{diet}$ is more depleted than that found in many modern specimens, it suggests that the vegetation comprising the diet of this specimen came from comparably closed environments.

DB Sand 4a

One specimen of *O. irroratus* was analyzed from the DB Sand 4a. The calculated $\delta^{13}C_{diet}$ value for this specimen is indicative of a primarily C_3 diet (Figure 6.8).

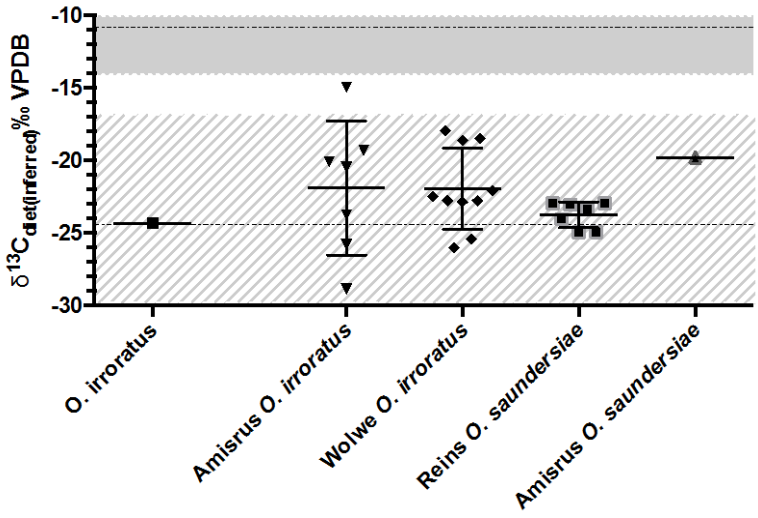

Figure 6.8. Calculated $\delta^{13}C_{diet}$ for the specimen sampled from the DB Sand 4a (left) compared to fossil fuel adjusted values of modern specimens (right). Hashed band represents the range of fossil fuel adjusted GCFR C_3 $\delta^{13}C_{plant}$ values (horizontal dotted line is the mean). Shaded band represents the most-depleted portion of the range of fossil fuel adjusted GCFR C_4 $\delta^{13}C_{plant}$ values (horizontal dotted line is the mean).

LC-MSA Middle

Calculated values of $\delta^{13}C_{diet}$ for the *Otomys* specimens sampled from the LC-MSA Middle indicate pure C_3 diets in these individuals (Figure 6.9). The small fossil sample population analyzed here appears to have not intersected C_4 vegetation within their habitats at about 125 ± 7 ka, near the transition from MIS6 to MIS5e.

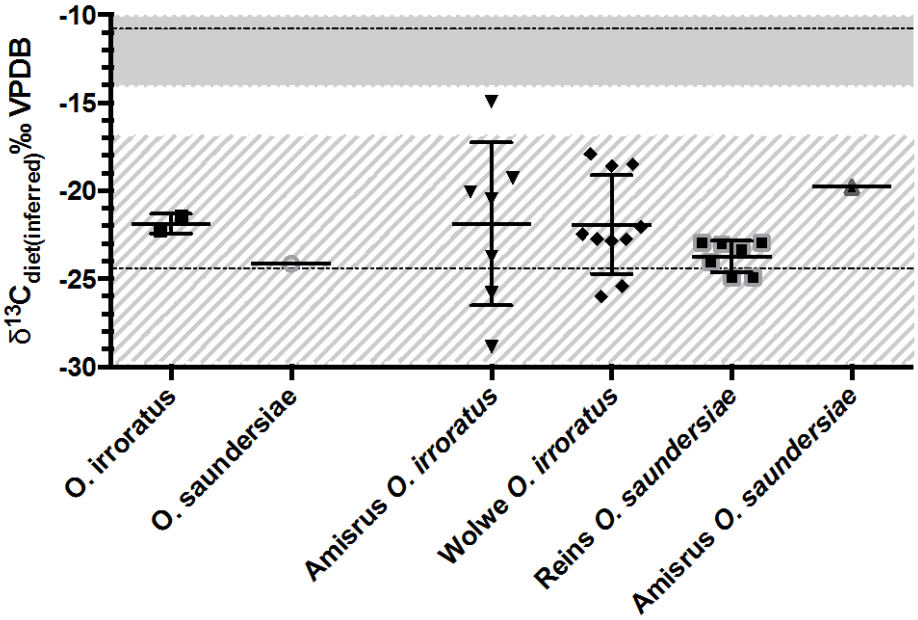

Figure 6.9. Calculated $\delta^{13}C_{diet}$ for the specimen sampled from the LC-MSA Middle (left) compared to fossil fuel adjusted values of modern specimens (right). Hashed band represents the range of fossil fuel adjusted GCFR C_3 $\delta^{13}C_{plant}$ values (horizontal dotted line is the mean). Shaded band represents the most-depleted portion of the range of fossil fuel adjusted GCFR C_4 $\delta^{13}C_{plant}$ values (horizontal dotted line is the mean).

LBG Sand 1

The 19 micromammal specimens analyzed from the LBG Sand stratigraphic aggregate have, as a group, values of $\delta^{13}C$ that are quite depleted in ^{13}C. Calculated $\delta^{13}C_{diet}$ values for *O. irroratus* range from -27.4‰ to -26.1‰ VPDB, while $\delta^{13}C_{diet}$ values

for *O. saundersiae* range from -27.4‰ to -24.2‰. Calculated $\delta^{13}C_{diet}$ for the *G. afra* specimen is -25.12‰ VPDB. All but one value of fossil $\delta^{13}C_{diet}$ are lower than the fossil fuel-adjusted GCFR C_3 mean $\delta^{13}C_{plant}$ value. A Mann-Whitney U test indicates that the meadian $\delta^{13}C_{diet}$ values of the *O. irroratus* and *O. saundersiae* are not significantly different from one another (p=0.81), while KW testing indicates that both populations are significantly depleted in ^{13}C compared to the modern values obtained from specimens sampling the low-C_4 Limestone Fynbos at Rein's Nature Reserve (H = 13.74, 2 d.f., p=0.001).

Calculated values of $\delta^{13}C_{diet}$ from all of the LBG Sand 1 fossil specimens overlap only with the most depleted individuals from modern contexts (Figure 6.10). One fossil specimen of *O. irroratus* has a $\delta^{13}C_{diet}$ value lower than even the most ^{13}C-depleted modern individual sampled from the closed forest context at Amisrus Wilderness.

These low fossil values of $\delta^{13}C_{diet}$ across all sampled taxa are indicative of closed C_3 vegetation proximate to PP13B at ~124 ± 5 ka. C_4 grasses, if present in the vegetation community, were not consumed by any of the individuals represented here. This reconstructed vegetation is notably different than what is suggested by the isotopic composition of specimens from sediments that bracket this time period. However, this interpretation of a closed vegetation is further supported by the presence of a single specimen of *T. dolichurus* in the micromammal assemblage from the LBG Sand 1, as well as one specimen of *D. mystacalis*. In modern GCFR environments, *T. dolichurus* and *D. mystacalis* inhabits closed vegetation such as thickets (Matthews *et al.*, 2009). The presence of these two taxa in this stratigraphic aggregate is thus concordant with stable

carbon isotope data from more habitat-neutral genera (such as *Otomys)* strongly indicating the presence of closed C_3 vegetation at the MIS5e transition.

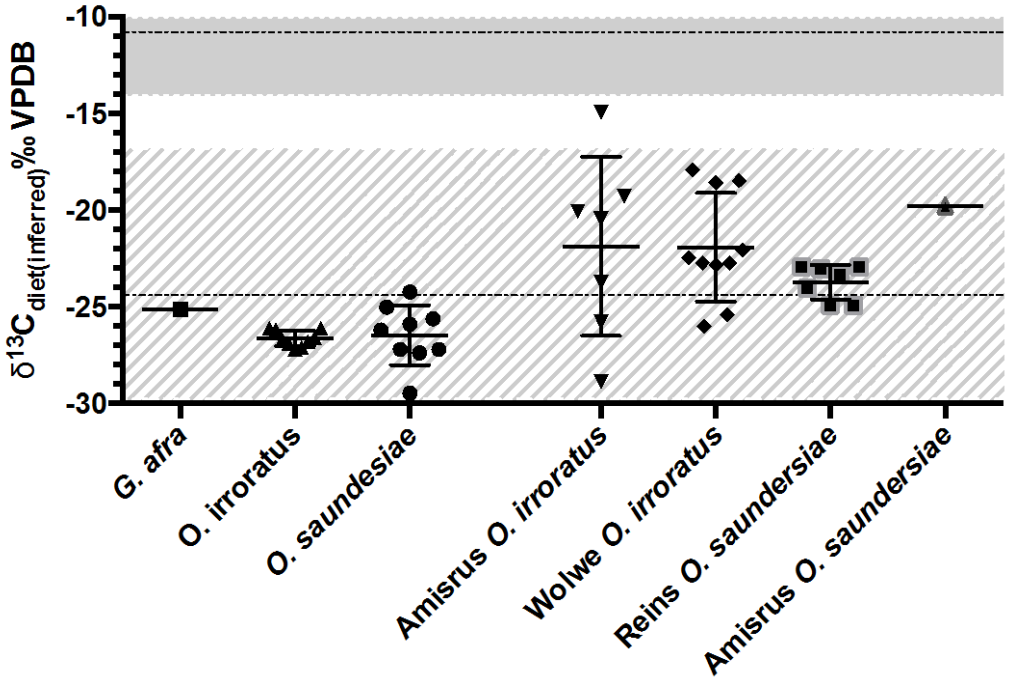

Figure 6.10. Calculated $\delta^{13}C_{diet}$ for the specimen sampled from the LBG Sand 1 (left) compared to fossil fuel adjusted values of modern specimens (right). Hashed band represents the range of fossil fuel adjusted GCFR C_3 $\delta^{13}C_{plant}$ values (horizontal dotted line is the mean). Shaded band represents the most-depleted portion of the range of fossil fuel adjusted GCFR C_4 $\delta^{13}C_{plant}$ values (horizontal dotted line is the mean).

Roofspall Lower

Two specimens of *G. afra*, two specimens of *O. irroratus*, and six specimens of *O. saundersiae* were analyzed. Calculated $\delta^{13}C_{diet}$ values for all taxa suggest C_3 diets (Figure 6.11). All $\delta^{13}C_{diet}$ values calculated for *G. afra* (-21.2‰ and -24.3‰) and *O. saundersiae* (mean = -22.4‰ VPDB, σ=0.8, range = -21.2‰ to -23.0‰) are greater than

the mean GCFR C_3 $\delta^{13}C_{plant}$ value of -24.4‰, but within the range of C_3 plant values reported (Cahpter 2), as is one value of *O. irroratus* $\delta^{13}C_{diet}$.

However, one *O. irroratus* specimen has a $\delta^{13}C_{diet}$ value that is quite low (-27.7‰ VPDB), and falls far below the 'corrected' range of $\delta^{13}C_{diet}$ in almost all modern micromammals sampled, with the exception of those from the most closed habitats (Table 6.14). On specimen of *T. dolichurus*, and two specimens of *D. mystacalis* occur in the larger micromammal assemblage from this stratigraphic aggregate, and their association with closed environments indicates that the ^{13}C-depleted $\delta^{13}C$ value of the fossil *O. irroratus* specimen is not anomalous.

This wide range of intraspecific variation in $\delta^{13}C$ seen in the admittedly small *Otomys* sample from this stratigraphic aggregate occurs in present-day micromammal communities where very closed and more open vegetation both occur within the foraging range of the aggregating predator (Chapter 3), and I hypothesize that this is also the case for the 110 ± 5ka Roofspall Lower assemblage. Thus the most ^{13}C-depleted specimen of *O. irroratus* samples a vegetation habitat within 3km of PP13B that was quite closed, while the other specimen of *O. irroratus*, as well as the specimens of *G. afra* and *O. saundersiae* were intersecting different C_3 vegetation communities where slightly more open conditions prevailed. This may indicate the presence of mosaic vegetation near PP13B at the end of MIS5e and the start of MIS5d.

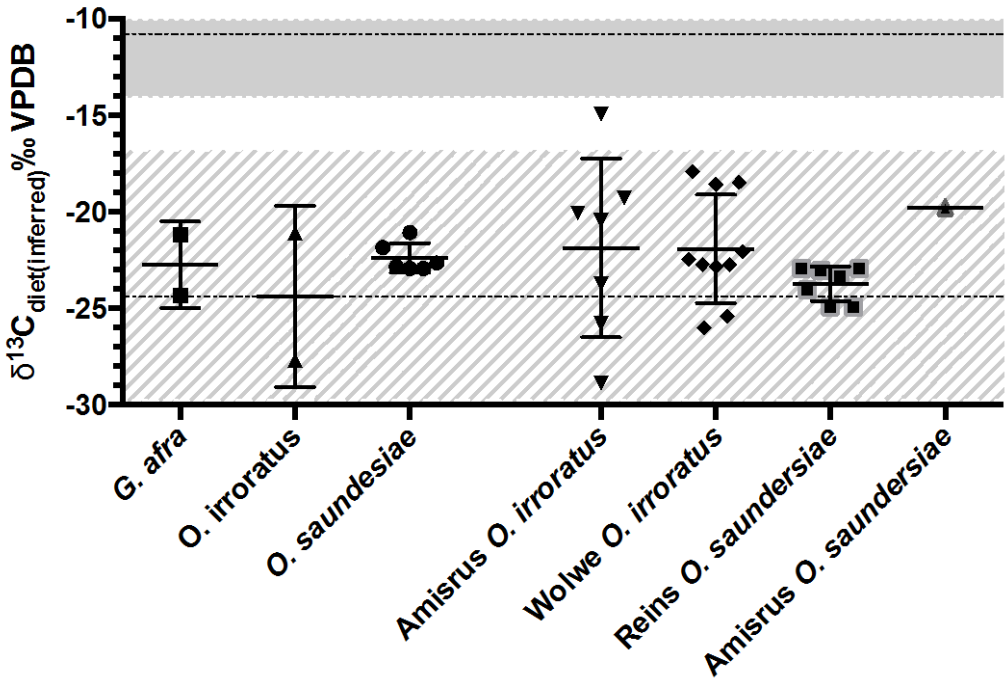

Figure 6.11. Calculated $\delta^{13}C_{diet}$ for the specimen sampled from the Roofspall Lower (left) compared to fossil fuel adjusted values of modern specimens (right). Hashed band represents the range of fossil fuel adjusted GCFR C_3 $\delta^{13}C_{plant}$ values (horizontal dotted line is the mean). Shaded band represents the most-depleted portion of the range of fossil fuel adjusted GCFR C_4 $\delta^{13}C_{plant}$ values (horizontal dotted line is the mean).

Roofspall Upper

One specimen of *G. afra* ($\delta^{13}C_{diet}$ = -20.4‰ VPDB), one specimen of *O. irroratus* ($\delta^{13}C_{diet}$ = -21.3‰ VPDB) and three specimens of *O. saundersiae* (mean $\delta^{13}C_{diet}$ = -23.9‰ VPDB, σ =1.0) all have dietary values of $\delta^{13}C$ that fall within the range of C_3 plants. The $\delta^{13}C_{diet}$ of the fossil *O. saundersiae* specimens overlaps with the 'corrected' modern $\delta^{13}C_{diet}$ value of *Otomys* specimens from the Rein's Nature Reserve sample (Figure 6.12), and a Mann-Whitney U test indicates that the meadian dietary values of $\delta^{13}C$ in these ancient and modern samples are not significantly different (p= 0.78),

suggesting that they sample vegetation communities with similar isotopic compositions. $\delta^{13}C_{diet}$ values in the *G. afra* and *O. irroratus* individuals are slightly higher, but all values suggest that the fossil micromammals sampled C_3 vegetation, with minimal or no input of C_4 grasses into their diets.

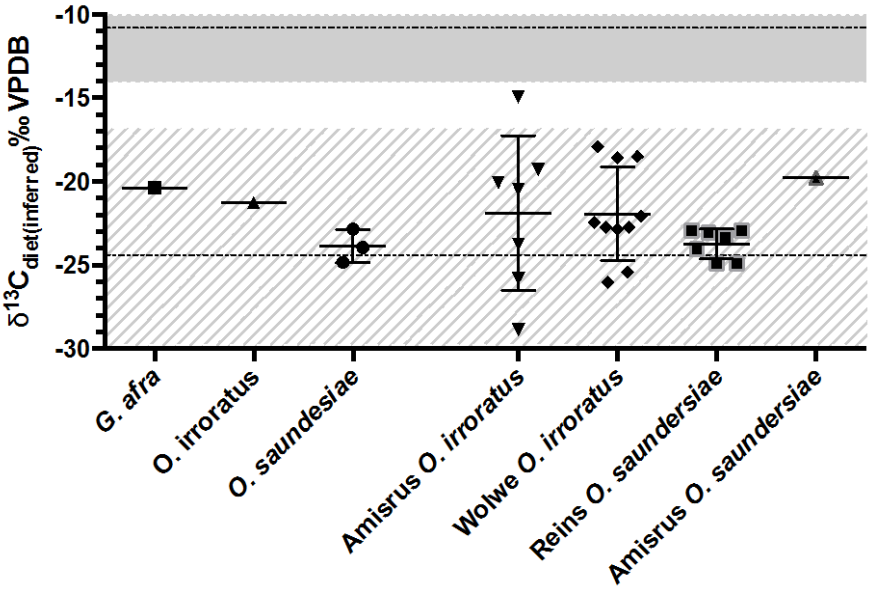

Figure 6.12. Calculated $\delta^{13}C_{diet}$ for the specimen sampled from the Roofspall Upper (left) compared to fossil fuel adjusted values of modern specimens (right). Hashed band represents the range of fossil fuel adjusted GCFR C_3 $\delta^{13}C_{plant}$ values (horizontal dotted line is the mean). Shaded band represents the most-depleted portion of the range of fossil fuel adjusted GCFR C_4 $\delta^{13}C_{plant}$ values (horizontal dotted line is the mean).

Shelly Brown Sand

One specimen of *O. irroratus* from the 94 ± 3 ka Shelly Brown Sand was available for analysis. The calculated $\delta^{13}C_{diet}$ value for this specimen, -20.8‰ VPDB, is consistent with a diet composed of C_3 vegetation, with some possible C_4 component.

DB Sand 3

Three specimens of *Otomys* sampled from the DB Sand 3 all have calculated values of $\delta^{13}C_{diet}$ that are consistent with C_3 diets (Figure 6.13).

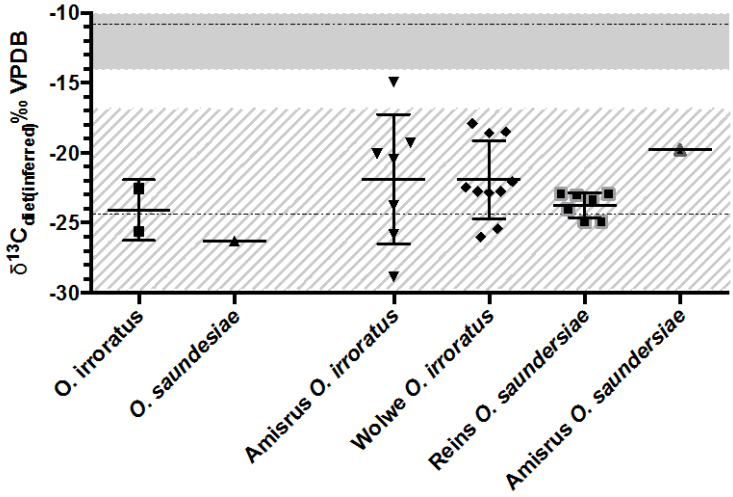

Figure 6.13. Calculated $\delta^{13}C_{diet}$ for the specimen sampled from the DB Sand 3 (left) compared to fossil fuel adjusted values of modern specimens (right). Hashed band represents the range of fossil fuel adjusted GCFR C_3 $\delta^{13}C_{plant}$ values (horizontal dotted line is the mean). Shaded band represents the most-depleted portion of the range of fossil fuel adjusted GCFR C_4 $\delta^{13}C_{plant}$ values (horizontal dotted line is the mean).

LB Sand 2

Two specimens of *O. irroratus* and one specimen of *O. saundersiae* for the LB Sand 4 were analyzed, and all have calculated $\delta^{13}C_{diet}$ values that indicate no significant input of C_4 grasses into any individual's diet. (Figure 6.14).

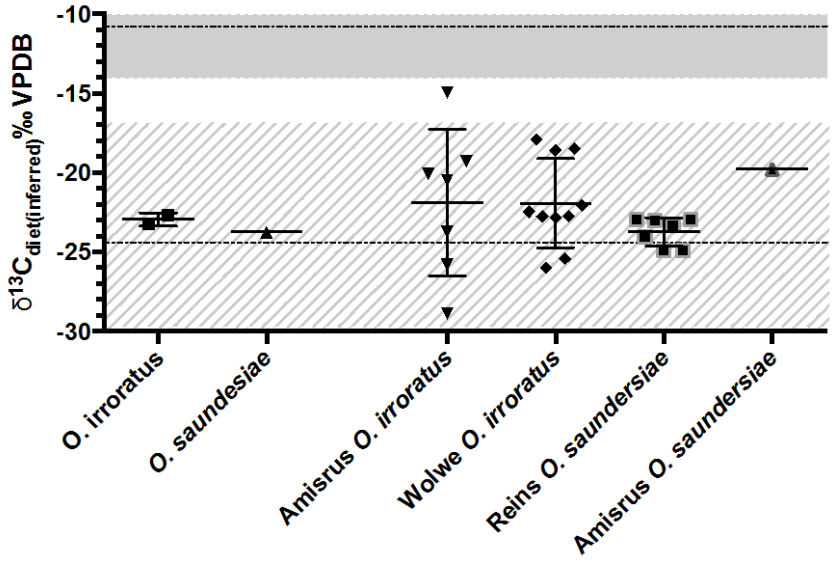

Figure 6.14. Calculated $\delta^{13}C_{diet}$ for the specimen sampled from the LB Sand 2 (left) compared to fossil fuel adjusted values of modern specimens (right). Hashed band represents the range of fossil fuel adjusted GCFR C_3 $\delta^{13}C_{plant}$ values (horizontal dotted line is the mean). Shaded band represents the most-depleted portion of the range of fossil fuel adjusted GCFR C_4 $\delta^{13}C_{plant}$ values (horizontal dotted line is the mean).

DB Sand 2

Otomys values of $\delta^{13}C_{diet}$ from fossil specimens taken from DB Sand 2 have values near to the mean 'corrected' GCFR C_3 $\delta^{13}C_{plant}$, indicating that the individuals representing these two taxa had diets that were composed of C_3 vegetation (Figure 6.15). Calculated $\delta^{13}C_{diet}$ for the single specimen of *G. afra* analyzed from this unit (-19.7‰) is enriched in ^{13}C relative to the syntopic *Otomys* taxa. The *G. afra* $\delta^{13}C_{diet}$ value still falls within the range of GCFR C_3 plant $\delta^{13}C$ values.

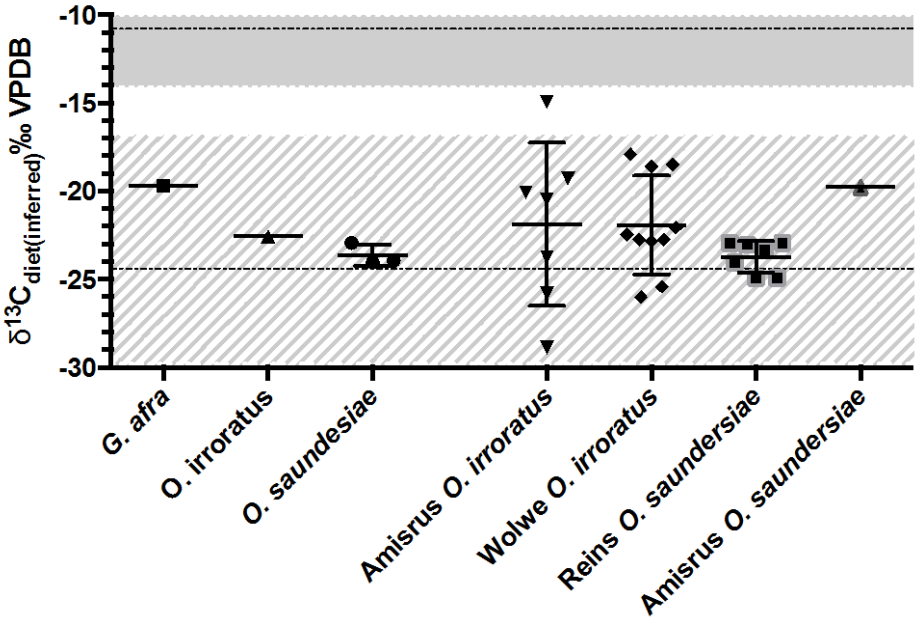

Figure 6.15. Calculated $\delta^{13}C_{diet}$ for the specimen sampled from the DB Sand 2 (left) compared to fossil fuel adjusted values of modern specimens (right). Hashed band represents the range of fossil fuel adjusted GCFR C_3 $\delta^{13}C_{plant}$ values (horizontal dotted line is the mean). Shaded band represents the most-depleted portion of the range of fossil fuel adjusted GCFR C_4 $\delta^{13}C_{plant}$ values (horizontal dotted line is the mean).

LB Sand 1

One $\delta^{13}C_{diet}$ value from *O. irroratus* (-25.8‰) overlaps with the more ^{13}C-depleted values obtained from modern *Otomys* in closed C_3 vegetation contexts, and may be indicative of slightly less open vegetation near to the PP13B at ~91ka, although it is not as strong a signal as is present in the LBG Sand 1 and Roofspall Lower units. (Figure 6.16). $\delta^{13}C_{diet}$ values of the remaining specimens are higher, but still well within the range of $\delta^{13}C$ values of GCFR C_3 plants. The source of the dietary carbon of all specimens sampled, *G. afra*, *O. irroratus*, and *O. saundersiae*, derived from C_3 plants.

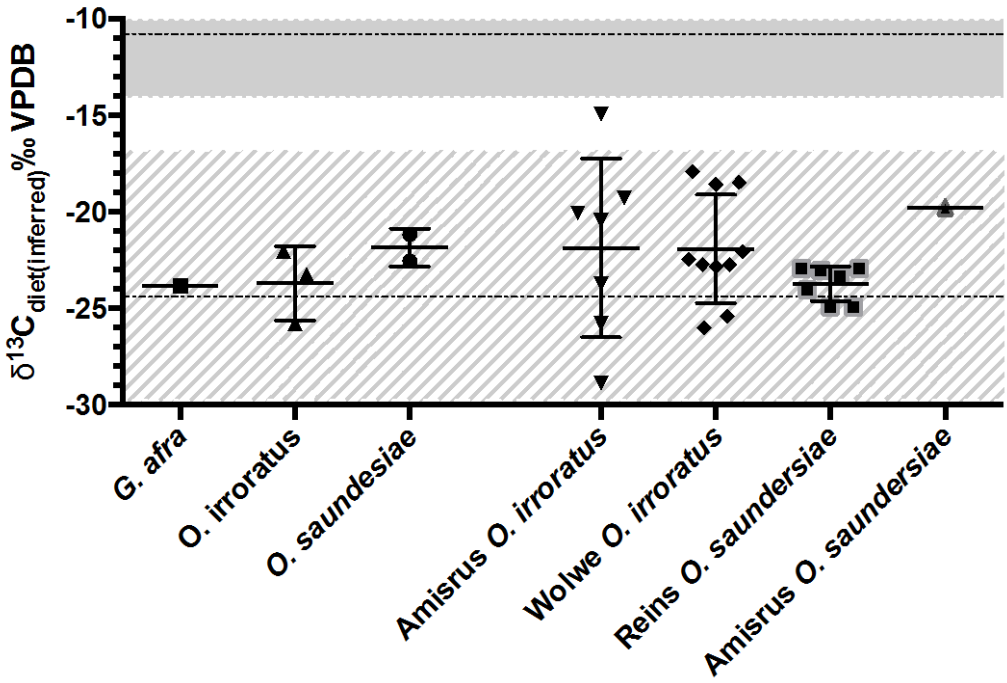

Figure 6.16. Calculated $\delta^{13}C_{diet}$ for the specimen sampled from the LB Sand 1 (left) compared to fossil fuel adjusted values of modern specimens (right). Hashed band represents the range of fossil fuel adjusted GCFR C_3 $\delta^{13}C_{plant}$ values (horizontal dotted line is the mean). Shaded band represents the most-depleted portion of the range of fossil fuel adjusted GCFR C_4 $\delta^{13}C_{plant}$ values (horizontal dotted line is the mean).

Intra-specific change through time:

Otomys

Measured values of $\delta^{13}C_{enamel}$ in *Otomys* specimens, both *O. irroratus* and *O. saundersiae*, appear to be fairly stable throughout the sequence, with the major exception of the $\delta^{13}C_{laser}$ values obtained from *Otomys* specimens from the LBG Sand 1 stratigraphic aggregate (Figure 6.17, Figure 6.18).

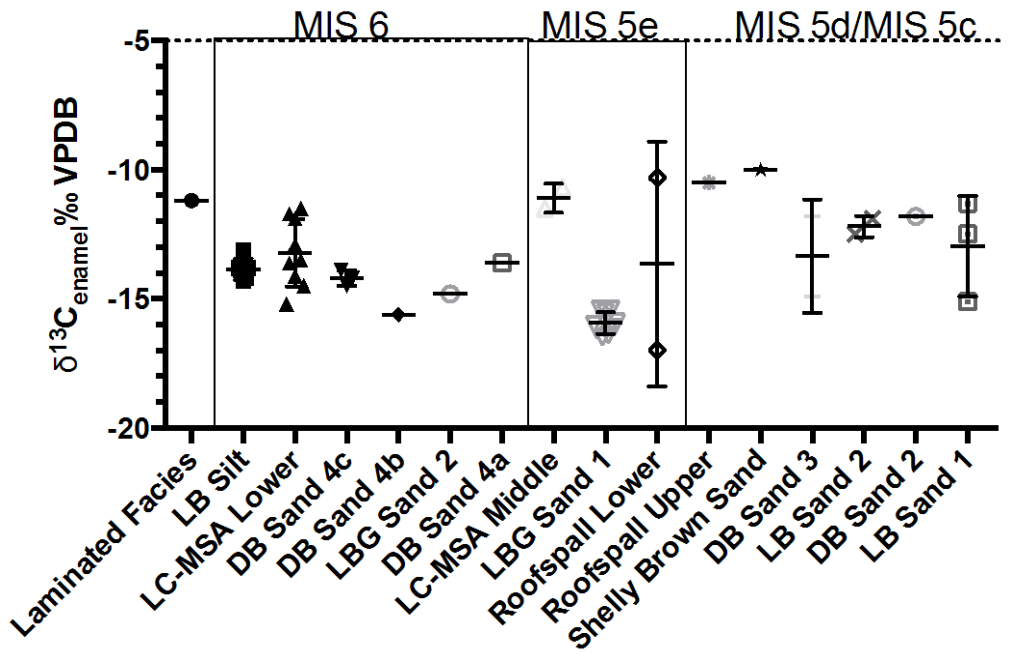

Figure 6.17. $\delta^{13}C_{laser}$ data from analyzed *Otomys irroratus* specimens from PP13B, by stratigraphic aggregate (oldest deposits left, most recent deposits right).

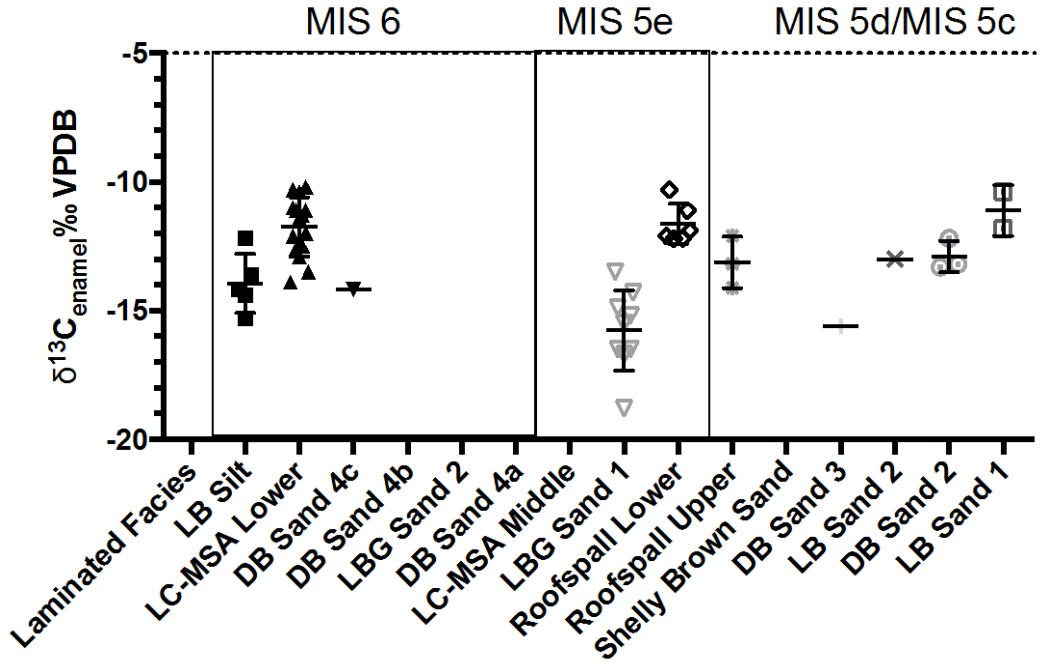

Figure 6.18. $\delta^{13}C_{laser}$ data from analyzed *Otomys saundersiae* specimens from PP13B, by stratigraphic aggregate (oldest deposits left, most recent deposits right).

In *O. irroratus*, populations of data large enough for non-parametric analysis occur in the MIS6 deposits of the LB Silt, the LC-MSA Lower, and the DB Sand 4c, and in the MIS5e LBG Sand 1. A KW test with Dunn's post hoc comparison indicates that the median $\delta^{13}C_{laser}$ values from the LBG Sand 1 are significantly different from those of the LB Silt and the LC-MSA Lower (although not the DB Sand 4c) (H =18.64, 3 d.f., p = 0.00). Very depleted values of $\delta^{13}C$ consistent with more closed C_3 vegetation are found only in specimens that post-date the MIS6/MIS5e transition (and are mostly restricted to MIS5e) (Figure 6.17). Marine transgression occurred fairly rapidly during this period, returning a long-distant coast back to the foot of the cliffs in which the cave is situated (Fisher *et al.*, 2010). Increasing moisture could have favored the development of denser vegetation communities in the region, producing the lower $\delta^{13}C_{plant}$ values often associated with closed canopies (Farquhar *et al.*, 1989b; Cerling and Harris, 1999) perhaps in the form of the thicket vegetation suggested by the presence of *T. dolichurus*. Alternately, increasing moisture and decreasing aridity could have resulted in fewer lighter values of $\delta^{13}C_{leaf}$ in C_3 plants (Kohn, 2010), thus reducing the mean C_3 $\delta^{13}C_{plant}$ values on the landscape.

O. irroratus MIS5d and MIS5c sample sizes are quite small, but seem to suggest a return to a less-dense vegetation during this period.

In *O. saundersiae*, a similar pattern to that seen in the *O. irroratus* $\delta^{13}C$ values is observed, although here the specimen count from the Roofspall Lower deposits is large enough to be included in a statistical analysis. A KW test comparing the medians of $\delta^{13}C_{laser}$ values from *O. saundersiae* populations sampled from the MIS6 LB Silt, and LC-MSA Lower; and the MIS5e LBG Sand 1 and Roofspall Lower deposits indicates

that the median LBG Sand 1 *O. saundersiae* $\delta^{13}C_{enamel}$ values are again significantly lower than those from the LC-MSA Lower and the Roofspall Lower Units (H = 22.81, 3 d.f., p = 0.00). Given the large size of the LBG Sand 1 stable carbon isotope sample, this systematic depletion in ^{13}C in LBG Sand 1 specimens is unlikely to be an artifact of sampling, especially given that small samples of specimens from MIS5d and MIS5c contexts appear to intersect a wider range of $\delta^{13}C$ values in plant tissues. If the systematically lower $\delta^{13}C_{enamel}$ values found in specimens from the LBG Sand 1 is not a sampling artifact, then it represents evidence for 1) a true decrease in the range of C_3 $\delta^{13}C_{leaf}$ values available on the paleolandscape, and 2) the presence of closed C_3 vegetation at or near to PP13B at about 125 ka.

Intra-specific change through time:

G. afra

G. afra sample sizes are considerably smaller than *Otomys* sample sizes throughout the PP13B sequence. Again measured values of $\delta^{13}C_{enamel}$ appear to be fairly stable throughout the sequence, although this occurs within a 5‰ range of $\delta^{13}C_{enamel}$. *G. afra* $\delta^{13}C_{enamel}$ values are somewhat lower in the MIS6 LB Silt assemblage than the slightly later MIS6 LC-MSA Lower (Figure 6.19), but no values of $\delta^{13}C_{laser}$ are, on their own, depleted in ^{13}C enough that they suggest closed-context vegetation as the primary dietary source. Even in the LBG Sand 1, where the *Otomys* $\delta^{13}C$ data suggests the presence of quite closed vegetation near to the site, the singular *G. afra* data point from this aggregate is not as significantly depleted (although neither is it as enriched in ^{13}C as

some *G. afra* specimens from the subsequent depositional units (Figure 6.19)). This may be in part related to the fact that *G. afra* prefers sandy substrates, and thus may be less likely to sample closed vegetation habitats where sediments may not be as loose.

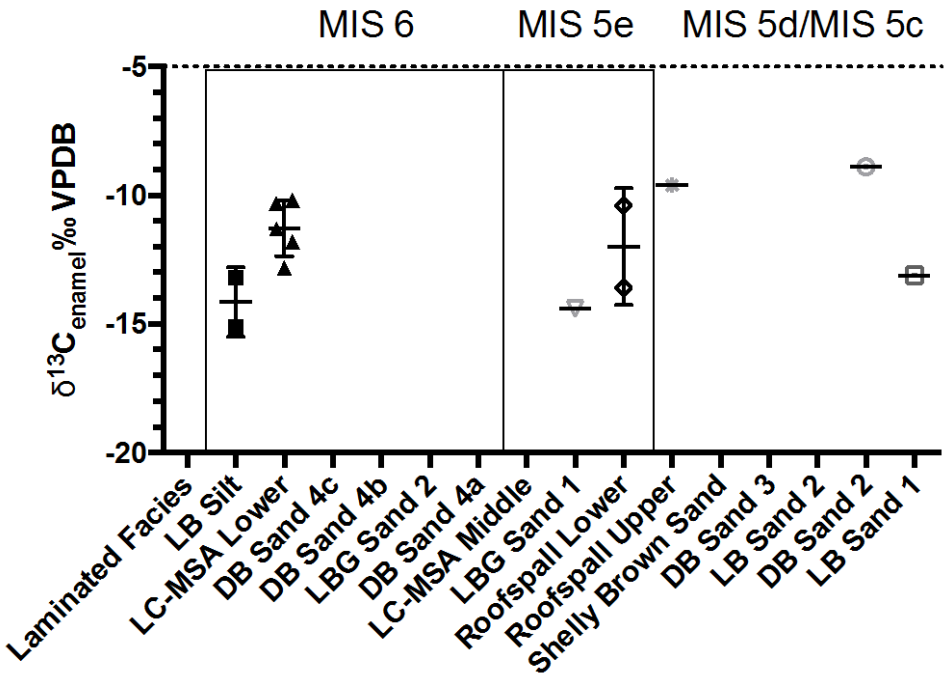

Figure 6.19. $\delta^{13}C_{laser}$ data from analyzed *G. afra* specimens from PP13B, by stratigraphic aggregate (oldest deposits left, most recent deposits right).

Niche Partitioning

In the majority of PP13B stratigraphic aggregates where different genera co-occur and were sampled, $\delta^{13}C_{enamel}$ values of the taxa overlap. (Figures 6-8, 12, 13, 15, 16, 18). The only exceptions occur in the LC-MSA Middle (where sample size = 3 specimens), the Roofspall Upper (where single *G. afra* and *O. irroratus* specimens are enriched in ^{13}C when compared to *O. saundersiae* from that aggregate), and the DB Sand 2 (where a

single *G. afra* specimen is about 4.5‰ enriched in ^{13}C when compared to the *Otomys* specimens from that unit).

In modern micromammal communities where niche partitioning has been explicitly studied, taxa occupying the same isotopic niche tend not to co-occur spatially (Codron *et al.*, 2015), although there is data to suggest that this is not always the case for all micromammals within a given community (Mauffrey and Catzeflis, 2003), especially when only a single isotope system is considered. In the case of carbon isotopes in particular, consumers can only inhabit some portion of the isotopic niche (in the form of plant $\delta^{13}C$) that is actually available on the landscape. If the range of $\delta^{13}C_{plant}$ in the local vegetation is quite narrow, it is logical that the isotopic niches of primary consumers will overlap to a significant degree. Conversely, in environments where both C_3 and C_4 vegetation co-exist there may be more latitude for primary consumers to inhabit different portions of the carbon isotopic niche, because the environmental niche itself is broader. Thus it is not surprising to see significant isotopic overlap in tissue $\delta^{13}C$ values between taxa in environments that appear to have primarily been C_3 in composition.

The lack of apparent niche partitioning seen in the assemblages from most aggregates at PP13B is quite different from the results seen in Chapter 5 for MIS6 and MIS5e taxa from PP9C, in part because the PP13B isotope sample lacks representatives of *B. suillus* (which were sampled at PP9C). *B. suillus* specimens, both fossil (Chapter 5) and modern (Yeakel *et al.*, 2007; Robb *et al.*, 2012) appear to frequently occupy a stable carbon isotope niche that is more enriched in ^{13}C than might be expected, even in C_3 contexts.

However at PP9C, *G. afra* are sometimes quite enriched in ^{13}C, which indicates that this taxon will consume C_4 grasses when they intersect such vegetation. Modern data is sparse (van den Heuvel and Midgley, 2014; Chapter 3, this thesis), but the large difference between the available data points (>5‰) suggests that there may be substantial variation in *G. afra* $\delta^{13}C_{diet}$ values across geographic space.

The PP9C and modern *G. afra* data thus suggests that *Otomys* and *Gerbilliscus* do not always have overlapping stable carbon isotopic niches in GCFR contexts, which raises the issue of why the $\delta^{13}C$ values overlap in the populations from the PP13B sediments. I hypothesize that the systematic overlap of *G. afra* $\delta^{13}C_{enamel}$ values with contemporaneous *Otomys* $\delta^{13}C_{enamel}$ values in the PP13B deposits may indicate a true reduction of C_4 grasses in the habitats these specimens sampled, but a large sample of modern and fossil isotope analyses are required to test this.

It could be argued that the strictly C_3 diet recorded in the *Otomys* specimens are however a function of niche partitioning. In a savanna biome in the Sterkfontein valley (Codron *et al*., 2015), *Otomys irroratus* $\delta^{13}C_{hair}$ values tend to indicate a 'preferred' C_3 niche (several dry season specimens however have $\delta^{13}C_{hair}$ values that indicate some consumption of C_4 grasses; Codron *et al.,* 2015). If *Otomys* have an isotopic niche that limits their consumption of C_4 grasses in favor of C_3 vegetation when the latter is abundant, this could limit the ability of carbon isotope analyses of fossil *Otomys* to detect C_4 grasses in the paleovegetation. On the other hand, other modern and Holocene specimens of *Otomys* from contexts where C_4 grasses are abundant have $\delta^{13}C_{tissue}$ values (Hopley *et al.*, 2006; Henry *et al.*, 2012) that appear to reflect a significant dietary fraction of C_4 vegetation. No extant data from any modern *Otomys* population however,

except for those from closed C_3 *environments in the southern Cape*, have $\delta^{13}C_{diet}$ values as low as the fossil specimens from the LBG Sand 1. Thus while it is impossible to exclude the possibility of C_4 vegetation on the paleoscape in this period based on the *Otomys* data alone (as absence of evidence is not evidence of absence), the carbon isotope data presented here does strongly suggest the presence of more closed C_3 vegetation communities at PP13B during MIS5e.

Comparison of PP micromammal data to other records

Rector and Reed (2010) performed correspondence analysis of the PP13B large fauna data to reconstruct environments for four of the stratigraphic aggregates, the LC-MSA Lower, the 'DBS Sand' (which is an aggregate DB Sands 2 and 3), the Upper Roofspall, and the LBG Sand 1. Results of their analysis indicate that the paleohabitats represented by the taxa in the large mammal assemblages are likely open shrubby grasslands. This conclusion further is supported by somewhat high frequencies of Alcelaphinae and Antilopinae (as a percentage of total bovids) present in the large mammal assemblages (Rector and Reed, 2010). $\delta^{13}C_{enamel}$ from micromammal specimens in the LC-MSA Lower, Roofspall Upper, and the upper DB Sand units (DB Sand 3 and BD Sand 2) indicate that the *Otomys* and *Gerbilliscus* specimens were consuming diets that were primarily C_3. The micromammal stable carbon isotope data from the LBG Sand 1 indicates that the specimens sampled were consuming C_3 vegetation from habitats that were quite closed.

Several possibilities arise from the comparison of the large mammal and micromammal data. The first is that the large mammals and micromammals analyzed

here sample different components of the same vegetation communities. If *Otomys* and *G. afra* isotopic niches are primarily C_3 even in the presence of C_4 grasses (as is the case for some *O. irroratus* specimens from the Sterkfontein Valley; Codron *et al.*, 2015), isotopic analysis of these taxa will fail to identify C_4 grasses even where they are present in ancient habitats. The existence of some modern *O. irroratus* specimens from GCFR contexts with very high $\delta^{13}C_{enamel}$ values (Chapter 3) suggests that *O. irroratus* on the south coast do at least on occasion consume C_4 grasses, but quantification of the frequency with which modern *Otomys* consume C_4 in various GCFR vegetation contexts needs to be further studied.

Alternately, it is possible that the PP13B micromammal specimens and large fauna are sampling different habitats within an ecotonal mosaic environment. As argued here and elsewhere (Hynek *et al.*, 2012), fossil accumulations of large and small mammals may sample vegetation on very different geographic scales (Figure 6.20). If there is considerable variability in the composition of vegetation over even comparably small geographic scales, it is just as likely that the accumulators of large faunal assemblages (humans and carnivores) and the accumulators of micromammal assemblages (raptors) will sample different habitats within the region as it is that they will sample similar habitats.

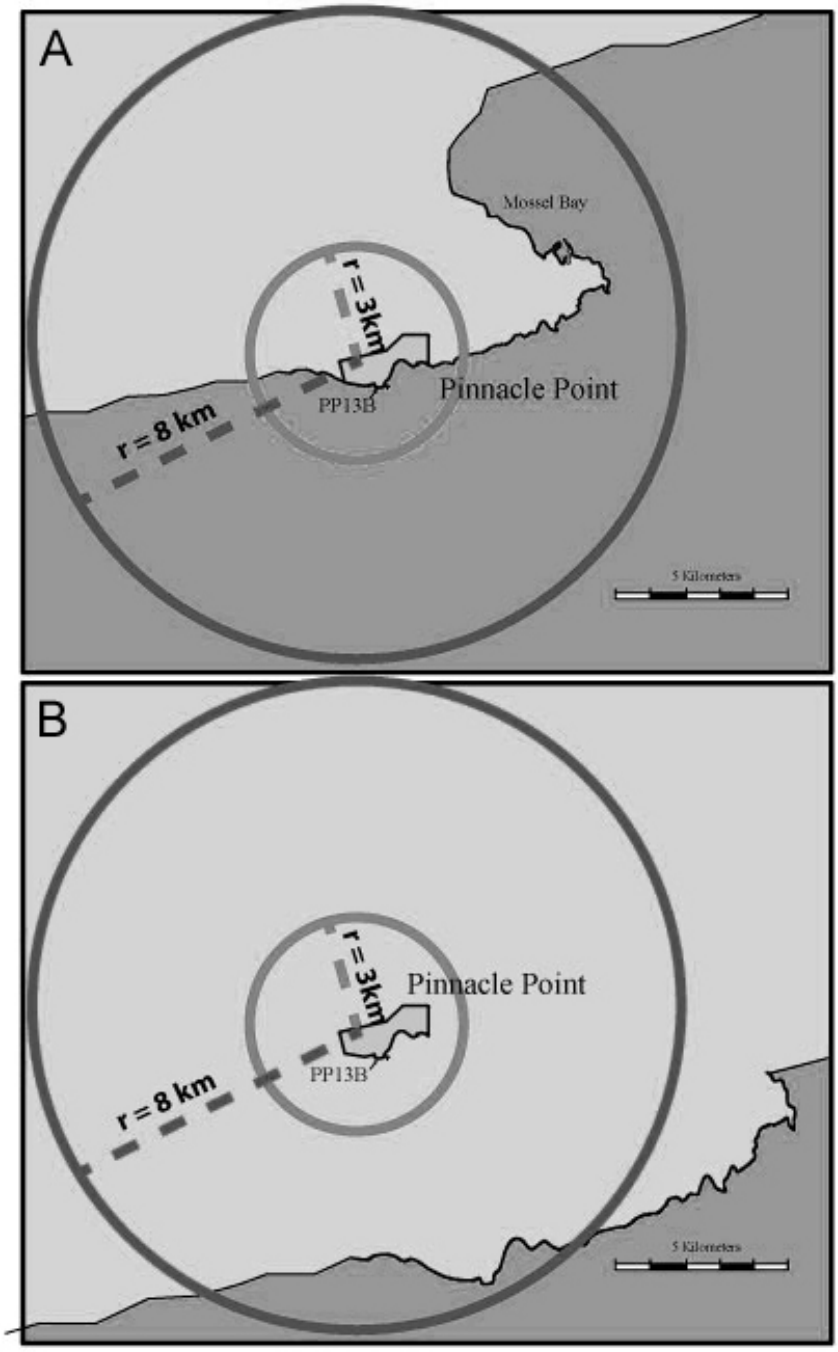

Figure 6.20. Cartoon of the foraging radius of owls (small circle) at PP13B during interglacial (A) and glacial (B) conditions. The larger circle represents the foraging range of large predators, such as hyaenids and humans. Note that the foraging areas are truncated when the coastline is proximate to the cave site.

Pleistocene speleothem records from the Pinnacle Point region (Braun *et al.*, 2012; Braun personal communication) also suggest varying inputs of C_3 and C_4 grasses into the vegetation near PP13B during MIS5 and MIS6, although there is a large gap in the record from 129.4 ka to 111.5 ka. Unpublished speleothem data provided by Braun shows troughs of quite low speleothem $\delta^{13}C$ values occuring in the record at 83 ka, 100 ka, and C_3 vegetation is likely present for most of the post-110 ka period, with exceptions at ~108 ka and ~92 ka, when Pinnacle Point speleothem $\delta^{13}C$ values become higher and overlap with the range of more C_4 $\delta^{13}C$ values recorded in the speleothem record from Cango Caves (see Bar-Matthews *et al.*, 2010 for discussion of the relationship between post-90 ka PP speleothem and the Cango record). From 150 ka to 129 ka, speleothem $\delta^{13}C$ values increased quite rapidly, and indicate a significant increase in C_4 grasses in the local vegetation. From ~150ka to ~200 ka, the $\delta^{13}C$ speleothem values from the Pinnacle Point record are fairly static at about -9‰ VPDB, and likely suggest vegetation where C_3 was predominant (Braun, unpublished data).

The relative imprecision in the ages of individual PP13B stratigraphic aggregates (plus or minus several thousand years for the OSL ages, and >50ka spans of time for the undated deposits) makes tying the PP13B micromammal data into the very precisely dated speleothem record somewhat complicated. Broadly, the presence of C_3 vegetation post 100 ka as indicated by the PP speleothem data are consistent with the results of the carbon isotope analysis of the micromammals from the MIS5d and MIS5c deposits. $\delta^{13}C_{enamel}$ values from micromammals from the PP13B MIS5d and MIS5e deposits are consistent with diets that are composed exclusively of C_3 vegetation. The $\delta^{13}C_{enamel}$ data

obtained from the MIS5d and MIS5c specimens are higher than the values of $\delta^{13}C_{enamel}$ obtained from the MIS5e LBG Sand 1 specimens, and there no are individuals in this part of the sample whose values of $\delta^{13}C_{enamel}$ are so depleted in ^{13}C that they suggest truly closed vegetation.

The long period of relative stasis in speleothem $\delta^{13}C$ values from 150 ka to 200 ka may be reflected in lack of change over time in the $\delta^{13}C_{enamel}$ values obtained from the populations of micromammals from the PP13B MIS6 deposits.

Phytoliths are not abundant in the PP13C deposits (Albert and Marean, 2012), but the general pattern of taxonomic representation is concordant with the inferred diets of the micromammal specimens. Grass phytolith abundances in particular are low through out the sequence, and phytoliths of C_4 grass appear primarily in sediments that are MIS5c in age; in the remaining samples, phytoliths of dicots and C_3 grasses are found (Albert and Marean, 2012). This suggests that C_4 grasses are rare near PP13B for much of the depositional sequence, a result that is mirrored in the lack of evidence for C_4 end member diets in the $\delta^{13}C_{enamel}$ sampling of the PP13B micromammals.

Conclusions

Enamel $\delta^{13}C$ data obtained from the PP13B micromammal taxa sampled here acts as a proxy for the carbon isotopic compostition of the diets of the *Otomys*, *Gerbilliscus*, and in one instance, *Cryptomys*, specimens sampled. Across all stratigraphic aggregates, inferred $\delta^{13}C_{diet}$ values suggest no significant input of C_4 vegetation into the diets of these taxa. Population values of inferred $\delta^{13}C_{diet}$ in individual taxa often overlap with those of other taxonomic groups within each depositional unit, suggesting that there carbon isotope niche partitioning in these samples is not observable.

During the LBG Sand 1 (at about 125 ka), the diets of the micromammal specimens sampled appear to incorporate more ^{13}C-depleted carbon than is indicated by the $\delta^{13}C_{enamel}$ values of specimens from any other stratigraphic aggregate sampled. Once the impact of relatively ^{13}C-depleted modern atmospheric CO_2 is accounted for in a modern comparative sample (Chapter 3), these lower fossil values of $\delta^{13}C_{enamel}$ overlap with the lowest values of $\delta^{13}C_{enamel}$ obtained from modern specimens that derive from relatively closed C_3 vegetative contexts. This suggests that the fossil specimens may have been consuming vegetation from similarly ^{13}C-depleted vegetation communities. The presence of closed-habitat indicator taxa, *T. dolichurus* and *D. mystacalis,* in the LBG Sand 1 and Roofspall Lower micromammal assemblages (Matthews *et al.*, 2009) supports this inference.

Other paleoenvironmental proxy data for the PP13B deposits, however, suggest the fluctuating presence of more open environments at PP13B during various phases of deposition (e.g. Rector and Reed, 2010), and speleothem records suggest the presence of

C_4 grasses in the regional vegetation, especially between 129 and 150 ka (Braun, unpublished data). If micromammal $\delta^{13}C_{enamel}$ values act as proxies for local vegetation, it possible that the $\delta^{13}C_{enamel}$ values obtained from taxa sampled here provide an incomplete picture of the local paleovegetation communities, especially in regards to the representation of C_4 grass in those communities. Alternately, the individual micromammal specimens may derive from specific habitats within a regional mosaic vegetation complex, and the inferred values of $\delta^{13}C_{diet}$ reflect this. While at PP13B, the possible inclusion of additional taxonomic groups was limited by the low taxonomic diversity of the micromammal assemblages themselves, in order to determine the whether the absence of evidence for C_4 grass in the diets of the *Otomys, Cryptomys,* and *Gerbilliscus* fossil specimens is the result of a narrow isotopic niche in these ancient micromammal communities, the sample of should be enlarged to include additional taxonomic groups wherever possible.

Chapter 6 References:

Albert, R. M. and C. W. Marean (2012). "The exploitation of plant resources by early Homo sapiens: the phytolith record from Pinnacle Point 13B Cave, South Africa." Geoarchaeology **27**(4): 363-384.

Ambrose, S. H. and K. G. Lorenz (1990). Social and ecological models for the middle stone age in southern africa. The emergence of modern humans: an archaeological perspective. Edinburgh, Edinburgh University Press**:** 3-33.

Ambrose, S. H. and L. Norr (1993). Experimental evidence for the relationship of the carbon isotope ratios of whole diet and dietary protein to those of bone collagen and carbonate. Prehistoric Human Bone: Archaeology at the Molecular Level. New York, Springer-Verlag**:** 1-37.

Andrews, P. (1990). Owls, caves, and fossils: predation, preservation, and accumulation of small mammal bones in caves, with an analysis of the pleistocene cave faunas from westbury-sub-mendip, somerset, UK. Chicago, University of Chicago Press.

Bar-Matthews, M., C. W. Marean, Z. Jacobs, P. Karkanas, E. C. Fisher, A. I. R. Herries, . . . A. Ayalon (2010). "A high resolution and continuous isotopic speleothem record of paleoclimate and paleoenvironment from 90 to 53 ka from Pinnacle Point on the south coast of South Africa." Quaternary Science Reviews **29**(17): 2131-2145.

Bernatchez, J. and C. W. Marean (2011). "Total station archaeology and the use of digital photography." SAA Archaeol. Rec **11**: 16-21.

Boutton, T. W., L. L. Tieszen and S. K. Imbamba (1988). "Seasonal changes in the nutrient content of East African grassland vegetation." African Journal of Ecology **28**: 103-115.

Braun, K., M. Bar-Matthews, A. Ayalon, C. Marean, I. Andy, R. Zahn and A. Matthews "Southern South African coastal and inland climate: the influence of sea level, SST and orbital parameters as recorded in speleothems." AGU Meetings, 2012

Brown, K. S. (2011). The Sword in the Stone: Lithic Raw Material Exploitation in the Middle Stone Age at Pinnacle Point Site 5-6, Southern Cape, South Africa. PhD Thesis, University of Cape Town.

Brown, K. S., C. W. Marean, A. I. R. Herries, Z. Jacobs, C. Tribolo, D. Braun, . . . J. Bernatchez (2009). "Fire as an engineering tool of early modern humans." Science **325**(5942): 859-862.

Brown, K. S., C. W. Marean, Z. Jacobs, B. J. Schoville, S. Oestmo, E. C. Fisher, . . . T. Matthews (2012). "An early and enduring advanced technology originating 71,000 years ago in South Africa." Nature **491**(7425): 590-593.

Campbell, T. L., P. J. Lewis and J. K. Williams (2011). "Analysis of the modern distribution of South African Gerbilliscus (Rodentia: Gerbillinae) with implications for Plio-Pleistocene palaeoenvironmental reconstruction." South African Journal of Science **107**: 1-7.

Cerling, T. E. and J. M. Harris (1999). "Carbon isotope fractionation between diet and bioapatite in ungulate mammals and implications for ecological and paleoecological studies." Oecologia **120**(3): 347-363.

Cerling, T. E., J. M. Harris and B. H. Passey (2003). "Diets of East African Bovidae based on stable isotope analysis." Journal of Mammalogy **84**(2): 456-470.

Cerling, T. E., J. A. Hart and T. B. Hart (2004). "Stable isotope ecology in the Ituri Forest." Oecologia **138**(1): 5-12.

Chase, B. M. and M. E. Meadows (2007). "Late Quaternary dynamics of southern Africa's winter rainfall zone." Earth-Science Reviews **84**(3-4): 103-138.

Codron, J., D. Codron, J. A. Lee-Thorp, M. Sponheimer, W. J. Bond, D. de Ruiter and R. Grant (2005). "Taxonomic, anatomical, and spatio-temporal variations in the stable carbon and nitrogen isotopic compositions of plants from an African savanna." Journal of Archaeological Science **32**(12): 1757-1772.

Codron, J., K. J. Duffy, N. L. Avenant, M. Sponheimer, J. Leichliter, O. Paine, . . . D. Codron (2015). "Stable isotope evidence for trophic niche partitioning in a South African savanna rodent community." Current Zoology 61 (3): 397-411

Cowling, R. (1983). "The occurrence of C_3 and C_4 grasses in fynbos and allied shrublands in the South Eastern Cape, South Africa." Oecologia **58**(1): 121-127.

Cowling, R. and D. Richardson (1995). Fynbos: South Africa's Unique Floral Kingdom. Cape Town, University of Cape Town.

Cowling, R. M., K. J. Esler, G. F. Midgley and M. A. Honig (1994). "Plant functional diversity, species diversity and climate in arid and semi-arid southern Africa." Journal of Arid Environments **27**(2): 141-158.

Cowling, R. M., S. Proches and T. C. Partridge (2009). "Explaining the uniqueness of the Cape flora: incorporating geomorphic evolution as a factor for explaining its diversification." Molecular Phylogenetics and Evolution **51**(1): 64-74.

Cowling, S. A., P. M. Cox, C. D. Jones, M. A. Maslin, M. Peros and S. A. Spall (2008). "Simulated glacial and interglacial vegetation across Africa: implications for species phylogenies and trans-African migration of plants and animals." Global Change Biology **14**: 827-840.

Deacon, H. J., J. Deacon, A. Scholtz, J. F. Thackeray, J. S. Brink and J. C. Vogel "Correlation of palaeoenvironmental data from the Late Pleistocene and Holocene deposits at Boomplaas cave, southern Cape." 339-351.

DeNiro, M. J. and S. Epstein (1978). "Influence of diet on the distribution of carbon isotopes in animals." Geochimica et Cosmochimica Acta **42**(5): 495-506.

Farquhar, G. D., J. R. Ehleringer and K. T. Hubick (1989a). "Carbon isotope descrimination and photosynthesis." Annual Review of Plant Physiology and Plant Molecular Biology **40**: 503-537.

Farquhar, G. D., J. R. Ehleringer and K. T. Hubick (1989b). "Carbon isotope discrimination and photosynthesis." Annual review of plant biology **40**(1): 503-537.

Fisher, E. C., M. Bar-Matthews, A. Jerardino and C. W. Marean (2010). "Middle and Late Pleistocene paleoscape modeling along the southern coast of South Africa." Quaternary Science Reviews **29**(11-12): 1382-1398.

Goldblatt, P. (1997). "Floristic diversity in the Cape Flora of South Africa." Biodiversity and Conservation **6**(3): 359-377.

Goldblatt, P. and J. C. Manning (2002). "Plant Diversity of the Cape Region of Southern Africa." Annals of the Missouri Botanical Garden **89**(2): 281-302
.

Granjon, L. and E. R. Dempster (2013). Genus Gerbilliscus: Gerbils. Mammals of Africa. Volume **III** J. Kingdon, D. Happold, T. Butynskiet al, Bloomsbury.

Hendey, Q. B. and T. P. Volman (1986). "Last interglacial sea levels and coastal caves in the Cape Province, south Africa." Quaternary Research **25**(2): 189-198.

Henry, A. G., P. S. Ungar, B. H. Passey, M. Sponheimer, L. Rossouw, M. Bamford, . . . L. Berger (2012). "The diet of Australopithecus sediba; Supplementary Information." Nature **487**(7405): 90-93.

Herries, A. I. and E. C. Fisher (2010). "Multidimensional GIS modeling of magnetic mineralogy as a proxy for fire use and spatial patterning: Evidence from the Middle Stone Age bearing sea cave of Pinnacle Point 13B (Western Cape, South Africa)." Journal of Human Evolution **59**(3): 306-320.

Hopley, P. J., A. G. Latham and J. D. Marshall (2006). "Palaeoenvironments and palaeodiets of mid-Pliocene micromammals from Makapansgat Limeworks, South Africa: A stable isotope and dental microwear approach." Palaeogeography, Palaeoclimatology, Palaeoecology **233**(3-4): 235-251.

Hynek, S. A., B. H. Passey, J. L. Prado, F. H. Brown, T. E. Cerling and J. Quade (2012). "Small mammal carbon isotope ecology across the Miocene-Pliocene boundary, northwestern Argentina." Earth and Planetary Science Letters **321-322**(0): 177-188.

Jacobs, Z. (2010). "An OSL chronology for the sedimentary deposits from Pinnacle Point Cave 13B, a punctuated presence." Journal of Human Evolution **59**(3): 289-305.

Karkanas, P. and P. Goldberg (2010). "Site formation processes at Pinnacle Point Cave 13B (Mossel Bay, Western Cape Province, South Africa): resolving stratigraphic and depositional complexities with micromorphology." Journal of Human Evolution **59**(3): 256-273.

Kimura, Y., L. L. Jacobs, T. E. Cerling, K. T. Uno, K. M. Ferguson, L. J. Flynn and R. Patnaik (2013). "Fossil mice and rats show isotopic evidence of niche partitioning and change in dental ecomorphology related to dietary shift in late Miocene of Pakistan." PloS one **8**(8): e69308.

Klein, R. G. (1972). "The late quaternary mammalian fauna of Nelson Bay Cave (Cape Province, South Africa): Its implications for megafaunal extinctions and environmental and cultural change." Quaternary Research **2**: 135-142.

Klein, R. G. (1974). "Environment and subsistence of prehistoric man in the Southern Cape province, South Africa." World Archaeology **5**: 249-289.

Klein, R. G. (1976). "The mammalian fauna of the Klasies River Mouth sites, southern Cape Province, South Africa." South African Archaeological Bulletin **31**: 75-98.

Klein, R. G. (1989). "Why Does Skeletal Part Representation Differ Between Smaller and Larger Bovids at Klasies River Mouth and Other Archeological Sites?" Journal of Archaeological Science **6**(4): 363-381.

Klein, R. G., H. J. Deacon, Q. B. Hendey and J. J. N. Lambrechts (1983). Palaeoenvironmental implications of quaternary large mammals in the fynbos region. Fynbos palaeoecology: a preliminary synthesis**:** 116-138.

Kohn, M. J. (2010). "Carbon isotope compositions of terrestrial C_3 plants as indicators of (paleo)ecology and (paleo)climate." Proceedings of the National Academy of Sciences of the United States of America **107**(46): 19691-19695.

Kohn, M. J., M. J. Schoeninger and W. W. Barker (1999). "Altered states: effects of diagenesis on fossil tooth chemistry." Geochimica et cosmochimica acta **63**(18): 2737-2747.

Tieszen, LL., S.K. Imbamba (1980). "Photosynthetic systems, carbon isotope discrimination and herbivore selectivity in Kenya." African Journal of Ecology **18**(4): 237-242.

Lee-Thorp, J. (2002). "Two decades of progress towards understanding fossilization processes and isotopic signals in calcified tissue minerals." Archaeometry **44**(3): 435-446.

Lee-Thorp, J. and N. J. Van Der Merwe (1987). "Carbon isotope analysis of fossil bone apatite." South African Journal of Science; v. **83**(11) p. 712-715

Lee-Thorp, J. A. (1989). "Stable carbon isotopes in deep time: the diets of fossil fauna and hominids." PhD Dissertation, University of Cape Town.

Marean, C., P. Nilssen, K. Brown, A. Jerardino and D. Stynder (2004). "Paleoanthropological investigations of Middle Stone Age sites at Pinnacle Point, Mossel Bay (South Africa): Archaeology and hominid remains from the 2000 field season." PaleoAnthropology **5**(2): 14-83.

Marean, C. W. (1986a). "On the seal remains from Klasies River Mouth: an evaluation of Binford's interpretation." Current Anthropology **27**(4): 365-368.

Marean, C. W. (1986b). "Seasonality and Seal Exploitation in the South-western Cape, South Africa." The African Archaeological Review **4**: 135-149.

Marean, C. W. (2010). "Pinnacle Point Cave 13B (Western Cape Province, South Africa) in context: the Cape floral kingdom, shellfish, and modern human origins." Journal of Human Evolution **59**(3): 425-443.

Marean, C. W. (2011). Coastal South Africa and the coevolution of the modern human lineage and the coastal adaptation. Trekking the Shore, Springer**:** 421-440.

Marean, C. W., M. Bar-Matthews, J. Bernatchez, E. Fisher, P. Goldberg, A. I. R. Herries, . . . H. M. Williams (2007). "Early human use of marine resources and pigment in South Africa during the Middle Pleistocene." Nature **449**: 905-908.

Marean, C. W., M. Bar-Matthews, E. Fisher, P. Goldberg, A. Herries, P. Karkanas, . . . E. Thompson (2010). "The stratigraphy of the Middle Stone Age sediments at Pinnacle Point Cave 13B (Mossel Bay, Western Cape Province, South Africa)." Journal of Human Evolution **59**(3-4): 234-255.

Matthews, T. (2004). The taxonomy and taphonomy of Mio-Pliocene and Late Middle Pleistocene micromammals from the Cape west coast, South Africa PhD Thesis, University of Cape Town, South Africa.

Matthews, T., C. Marean and P. Nilssen (2009). "Micromammals from the Middle Stone Age (92 - 167 ka) at Cave PP13B, Pinnacle Point, south coast, South Africa." Paleontol. Afr **44**: 112-120.

Mauffrey, J.-F. and F. Catzeflis (2003). "Ecological and isotopic discrimination of syntopic rodents in a neotropical rain forest of French Guiana." Journal of Tropical Ecology **19**(02): 209-214.

Nielsen-Marsh, C. M. and R. E. M. Hedges (2000). "Patterns of diagenesis in Bone 1: The effects of site environments." Journal of Archaeological Science **27**: 1139-1150.

Oestmo, S. and C. W. Marean (2015). Excavation and Survey at Pinnacle Point. Field Archaeology from Around the World, Springer**:** 123-126.

Passey, B. H. and T. E. Cerling (2006). "In situ stable isotope analysis (13 C, 18 O) of very small teeth using laser ablation GC/IRMS." Chemical Geology **235**: 238-249.

Passey, B. H., T. F. Robinson, L. K. Ayliffe, T. E. Cerling, M. Sponheimer, M. D. Dearing, . . . J. R. Ehleringer (2005). "Carbon isotope fractionation between diet, breath CO 2, and bioapatite in different mammals." Journal of Archaeological Science **32**(10): 1459-1470.

Phillips, D. and P. Koch (2002). "Incorporating concentration dependence in stable isotope mixing models." Oecologia **130**(1): 114-125.

Pickering, R., Z. Jacobs, A. I. R. Herries, P. Karkanas, M. Bar-Matthews, J. D. Woodhead, . . . C. W. Marean (2013). "Paleoanthropologically significant South African sea caves dated to 1.1 - 1.0 million years using a combination of U-Pb, TT-OSL and palaeomagnetism." Quaternary Science Reviews **65**: 39-52.

Podelsak, D. W., A.-M. Torregrossa, J. R. Ehleringer, M. D. Dearing, B. H. Passey and T. E. Cerling (2008). "Turnover of oxygen and hydrogen isotopes in the body water, CO2, hair, and enamel of a small mammal." Geochimica et cosmochimica acta **72**(1): 19-35.

Proches, S., R. M. Cowling, P. Goldblatt, J. C. Manning and D. A. Snijman (2006). "An overview of the Cape geophytes." Biological Journal of the Linnean Society **87**(1): 27-43.

Rebelo, A. G., C. Boucher, N. Helme, L. Mucina and M. C. Rutherford (2006). Fynbos Biome. The Vegetation of South Africa, Lesotho, and Swaziland. Pretoria, South African National Biodiversity Institute**:** 52-219.

Rector, A. L. and K. E. Reed (2010). "Middle and late Pleistocene faunas of Pinnacle Point and their paleoecological implications." Journal of Human Evolution **59**(3): 340-357.

Robb, G. N., S. Woodborne and N. C. Bennett (2012). "Subterranean sympatry: an investigation into diet using stable isotope analysis." PloS one **7**(11): e48572.

Roberts, D. L., P. Karkanas, Z. Jacobs, C. W. Marean and R. G. Roberts (2012). "Melting ice sheets 400,000 yr ago raised sea level by 13m: Past analogue for future trends." Earth and Planetary Science Letters **357-358**(0): 226-237.

Rutherford, M. C. and L. Mucina (2006). Introduction. The Vegetation of South Africa, Lesotho, and Swaziland. Pretoria, South African National Biodiversity Institute**:** 3-10.

Sharp, Z. and T. Cerling (1996). "A laser GC-IRMS technique for in situ stable isotope analyses of carbonates and phosphates." Geochimica et Cosmochimica Acta **60**(15): 2909-2916.

Skinner, J. D. and C. T. Chimimba (2005). The mammals of the southern African sub-region, Cambridge University Press.

Sponheimer, M. and J. A. Lee-Thorp (1999). "Alteration of enamel carbonate environments during fossilization." Journal of Archaeological Science **26**(2): 143-150.

Symes, C. T., J. W. Wilson, S. M. Woodborne, Z. S. Shaikh and M. Scantlebury (2013). "Resource partitioning of sympatric small mammals in an African forest-grassland vegetation mosaic." Austral Ecology **38**(6): 721-729.

Taylor, P. J. (2013). “Genus Otomys: Vlei Rats”. Mammals of Africa Volume III: Rodents, Hares and Rabbits .Happold, D. C. D. (ed.). Bloomsbury Publishing, London, United Kingdom,

Thackeray, J. F., A. van der Venter, J. Lee-Thorp, C. T. Chimimba and J. van Heerden (2003). "Stable carbon isotope analysis of modern and fossil samples of the South

African rodent Aethomys namaquensis." Annals of the Transvaal Museum **40**: 43-46.

Thompson, E., H. M. Williams and T. Minichillo (2010). "Middle and late Pleistocene Middle Stone Age lithic technology from Pinnacle Point 13B (Mossel Bay, Western Cape Province, South Africa)." Journal of Human Evolution **59**(3): 358-377.

Thompson, J. C. (2008). Zooarchaeological tests for modern human behavior at Blombos Cave and Pinnacle Point Cave 13B, southwestern Cape, South Africa, PhD Thesis, Arizona State University.

Thompson, J. C. (2010). "Taphonomic analysis of the Middle Stone Age faunal assemblage from Pinnacle Point Cave 13B, Western Cape, South Africa." Journal of Human Evolution **59**(3-4): 321-339.

Tieszen, L. L. (1991). "Natural variations in the carbon isotope values of plants: implications for archaeology, ecology, and paleoecology." Journal of Archaeological Science **18**(3): 227-248.

Tieszen, L. L. and T. Fagre (1993). Effect of diet quality and composition on the isotopic composition of respiratory CO2, bone collagen, bioapatite, and soft tissues. Prehistoric Human Bone, Springer**:** 121-155.

Tyson, P. D. (1999). "Atmospheric circulation changes and paleoclimates of southern Africa." South African Journal of Science **95**: 194-201.

van den Heuvel, I. M. and J. J. Midgley (2014). "Towards an isotope ecology of Cape Fynbos small mammals." African Zoology **49**(2): 195-202.

Van Zinderen Bakker, E. (1976). "The evolution of Late-Quaternary palaeoclimates of southern Africa." Palaeoecology of Africa **9**: 160-202.

Vogel, J. C., A. Fuls and R. P. Ellis (1978). "The geographical distribution of Kranz grasses in South Africa." South African Journal of Science **74**: 209-215.

Wang, Y. and T. E. Cerling (1994). "A model of fossil tooth and bone diagenesis: implications for paleodiet reconstruction from stable isotopes." Palaeogeography, Palaeoclimatology, Palaeoecology **107**(3-4): 281-289.

Watts, I. (2010). "The pigments from Pinnacle Point Cave 13B, Western Cape, South Africa." Journal of Human Evolution **59**(3): 392-411.

Williams, H. M. (in prep-a). Isotope Ecology of the modern Greater Cape Floristic Region, with particular focus on the Pinnacle Point area: metadata analysis of the

modern floral stable carbon isotope record and the production of the GCFR-specific Stable Caron Isotope Metadata Set (GSCIMS).

Williams, H. M. (in prep-b). Isotope Ecology of the modern Greater Cape Floristic Region: the modern micromammal record, with particular attention to new Pinnacle-Point Area-proximate data.

Williams, H. M. (in prep-c). Micromammal and large fauna stable isotopes from the MIS6 fossil hyena den Pinnacle Point 30 (south coast of South Africa) reveal differences in relative contribution of C_4 grasses to local paleovegetation on different geographic scales.

Williams, H. M. (in prep-d). Stable carbon isotope analysis of micromammals from deposits straddling the MIS6-MIS5 transition at Pinnacle Point, South Africa suggest small but possibly significant vegetation changes at ~125 ka.

Yeakel, J. D., N. C. Bennett, P. L. Koch and N. J. Dominy (2007). "The isotopic ecology of African mole rats informs hypotheses on the evolution of human diet." **274**(1619): 1723-1730.

7. Summary of Results and Conclusions

The modern GCFR south coast micromammal material

Stable carbon isotope analysis of fossil micromammal material is increasingly being explored as a fruitful paleoenvironmental proxy record (Thackeray *et al.*, 2003; Hopley *et al.*, 2006; Hynek *et al.*, 2012; Kimura *et al.*, 2013). Hynek *et al.* (2012) discuss the ability of micromammals to potentially sample a full range of $\delta^{13}C_{plant}$ available on a given landscape; however, different micromammal taxa have unique life histories (and potentially different isotopic niches) that may impact their utility in such studies. Thus production of modern $\delta^{13}C_{enamel}$ data for a variety of micromammal taxa and from a variety of vegetation communities is necessary in order to understand the ways in which micromammal $\delta^{13}C_{enamel}$ values reflect (or fail to reflect) the diversity of available $\delta^{13}C_{plant}$ on the landscape.

The modern micromammal data presented in this dissertation derived from specimens obtained from archived owl pellets collected in three vegetation contexts that occur along the south coast of South Africa (Chapter 3). Owl pellets were chosen specifically for this research, as the fossil and archaeological material to which they were to be compared also derived from raptor aggregations (Matthews *et al.*, 2009; Matthews *et al.*, 2011; Matthews, n.d.). The use of modern owl pellets simulated the palimpsest effect that might be found in archaeological assemblages, but limited the ability of the modern $\delta^{13}C_{enamel}$ data obtained from the micromammal specimens to be tightly correlated to specific vegetation communities, and instead meant that all vegetation

within a roughly 3km radius of the collection locality could have been sampled by the micromammals and their aggregating predator. This again simulated what would have occurred in archaeological and fossil raptor pellets, but did limit the ability of the study presented here to assess how well the taxa analyzed sampled an entire range of $\delta^{13}C_{plant}$ within a given vegetation community.

The Amisrus/Wilderness pellet collection locality was located within the Afrotemperate forests found near Knysna, where a canopy effect that would result in lower values of $\delta^{13}C_{plant}$ was expected, and where C_4 grasses should be comparably rare (Rebelo *et al*., 2006). The micromammals sampled from the Amisrus pellets however exhibited a wide range of $\delta^{13}C_{enamel}$ values (-21.2‰ to -7.1‰ VPDB), which indicated that while some individuals had inferred dietary $\delta^{13}C$ values that were consistent with closed-canopy environments, other individuals taken by the aggregating raptor had significant C_4 components to their diets that were unlikely to have been present in the vegetation immediate to the collection locality. GIS analysis indicated that other vegetation communities with C_4 components were present within the 3km foraging radius of owl, suggesting that the micromammals taken by raptors do in fact have the potential to sample a wide range of vegetation communities around a given site.

Micromammal specimens from the somewhat more open Wolwe River pellet collection locality lacked the lower $\delta^{13}C_{enamel}$ values that were present in the Amisrus sample population, suggesting that a lack of more closed environments might be visible in the $\delta^{13}C_{enamel}$ values of sample populations. Even without this closed C_3 component, Wolwe River *Otomys* specimens have a range of $\delta^{13}C_{enamel}$ values that is almost 10‰

wide, again indicating that this taxon sampled a considerable range of $\delta^{13}C_{plant}$ on the landscape. The majority of the Wolwe River individuals were however C_3 consumers, which may suggest that the presence of C_4 grasses (which were represented in the higher $\delta^{13}C_{enamel}$ values of a few individuals) will be under-represented when sampling this particular taxon.

This is contrasted with the micromammal sample from Rein's Nature reserve, which had no *Otomys* specimen with a $\delta^{13}C_{enamel}$ value suggestive of a dietary C_4 component. This is not unexpected, given that the primary vegetation in the vicinity of the pellet collection locality is Canca Limestone Fynbos, which has limited or absent C_4 elements (Rebelo *et al.*, 2006). *B. suillus* $\delta^{13}C_{enamel}$ data from Rein's nature reserve also indicated a strictly C_3 diet; in other regions of South Africa where *B. suillus* has been sampled, C_4 grasses are sometimes estimated to be a significant fraction of the taxon's diet (Robb *et al.*, 2012). The evidence for an absence of C_4 grasses in the diet of the Rein's *B. suillus* specimen thus suggests that lower $\delta^{13}C_{enamel}$ values measured in archaeological or fossil populations could be a useful proxy for a real paucity of C_4 in a given vegetation community—however, the sample size reported here is singular, and further work is clearly needed.

The modern micromammal stable carbon isotope data obtained from specimens collected along the south coast of the GCFR support the hypothesis that in general, generalist taxa tend to sample a wide range of $\delta^{13}C_{plant}$ on the landscape when it is available, and a narrower range of $\delta^{13}C_{plant}$ when certain floral elements are absent.

The fossil and archaeological micromammal material in context: Middle and Late Pleistocene paleoenvironments along the south coast

The archaeological micromammal specimens sampled and analyzed in this dissertation derived from a depositional sequence at sites Pinnacle Point 13B, Pinnacle Point 30, and Pinnacle Point 9C that spans much of the Middle and Late Pleistocene, from about > 200ka (the Laminated Facies and the LB Silt deposits from PP13B, MIS7/6 in age), to ~90 ka (the LB Sand 1 stratigraphic aggregate, also from PP13B, and which is likely MIS5c in age). Throughout the time period sampled, the micromammal specimens consistently have $\delta^{13}C_{enamel}$ values that indicate consumption of C_3 vegetation, and in most cases, only C_3 vegetation (Figure 7.1, Figure 7.2).

No *Otomys* specimen sampled, of the 182 $\delta^{13}C_{enamel}$ data points reported here, had tissue values consistent with anything other than a C_3 diet (Figure 7.2). Twenty-two stratigraphic aggregates contained specimens of *Otomys;* of those 16 aggregates had sufficient sample sizes to perform a Kruskal-Wallace one-way analysis of variance comparing the median $\delta^{13}C_{enamel}$ values between stratigraphic aggregates (H = 75.43, df= 15, p = <0.00001) (Given similarities in dietary ecology in modern specimens, *O. irroratus and O. saundersiae* were grouped for this analysis to increase sample size). Dunn's multiple comparison post-hoc test indicates that the grouped *Otomys* $\delta^{13}C_{enamel}$ values from the MIS5e LBG Sand 1 at PP13B are significantly different from those obtained from *Otomys* specimens in the rest of the PP sequence, but that the $\delta^{13}C_{enamel}$

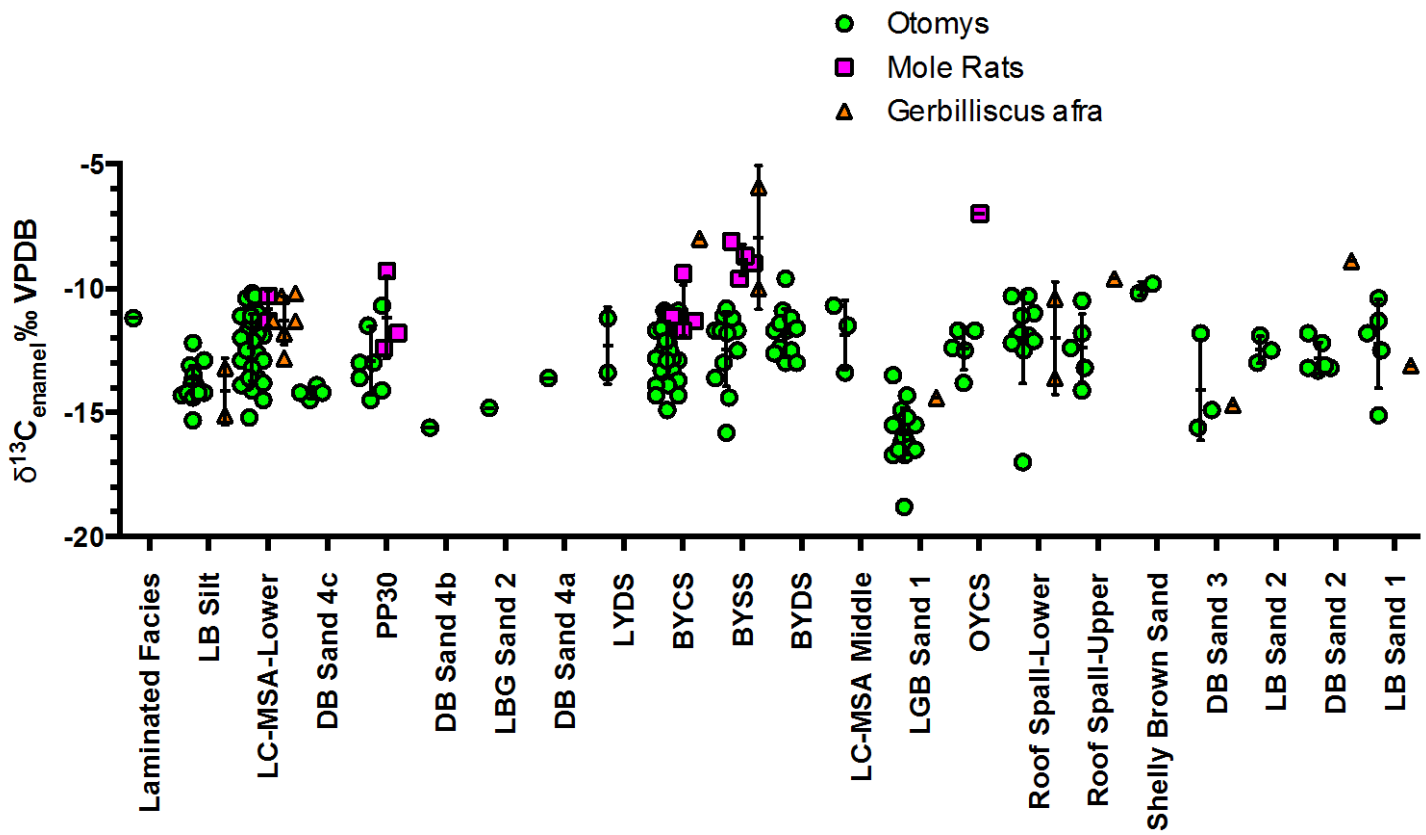

Figure 7.1. $\delta^{13}C_{enamel}$ values for all fossil and archaeological specimens from PP30, PP13B, and PP9C. See previous chapters for depositional ages for each stratigraphic aggregate.

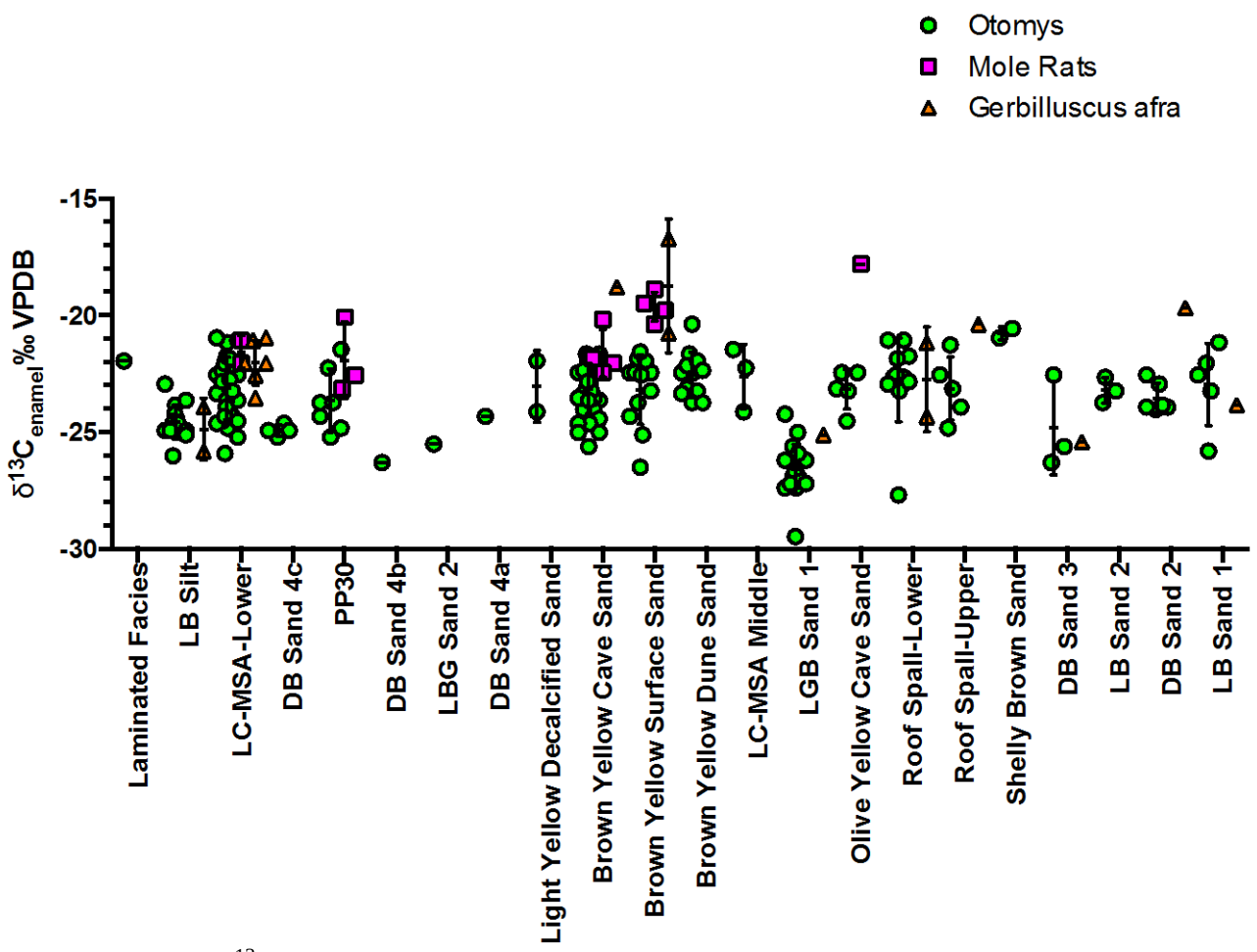

Figure 7.2. Transformed $\delta^{13}C_{diet}$ values for all fossil and archaeological specimens from PP30, PP13B, and PP9C. See previous chapters for depositional ages for each stratigraphic aggregate. $\delta^{13}C_{enamel}$ values are transformed to $\delta^{13}C_{diet}$ values following the procedures outlined in Chapters 5 and 6.

values of *Otomys* sample populations from the remaining aggregates are statistically similar. This strongly suggests that, for the duration of MIS6 and the majority of MIS5, there was no major change in the $\delta^{13}C$ composition of *Otomys* diets. The only clear exception to this pattern is found in the *Otomys* specimens from the LBG Sand 1 stratigraphic aggregate from PP13B, where $\delta^{13}C_{enamel}$ values are *lowest* when compared to the other fossil and archaeological $\delta^{13}C_{enamel}$ data from PP. When compared to $\delta^{13}C_{enamel}$ values of modern *Otomys* that have been corrected for modern ^{13}C-depletion of atmospheric CO_2, the LBG Sand 1 *Otomys* stable carbon isotope data suggests the presence of a unique paleoenvironmental condition present at PP13B at ~124 ka. Only a few specimens have $\delta^{13}C_{enamel}$ values that are consistent with some dietary fraction of C_4 grasses: the *G. afra* from the 130 ± 9 ka BYCS and the contiguous and likely 130 ka BYSS at PP9C; and some of the mole rat specimens from the BYSS at PP9C and from the 120 ± 7 ka OYCS at PP9C.

The oldest micromammal specimens date from between >200 ka to 159 ± 8 ka (Figure 7.3). The $\delta^{13}C_{enamel}$ values of all taxa sampled are indicative of C_3 diets in these specimens, with the exception of the highest value of $\delta^{13}C_{enamel}$ from a mole rat specimen from PP30 ($\delta^{13}C_{enamel}$ = -9.3‰ VPDB), and even this specimen is likely to have been primarily a C_3 consumer. Although it is possible that the limited range of $\delta^{13}C_{enamel}$ values in these specimens may be a function of isotopic niche partitioning (Williams, in prep), the fact that mole rat and *Gerbilliscus afra* specimens also have $\delta^{13}C_{enamel}$ values consistent with C_3 diets suggests the maintenance of C_3-dominated habitats in the PP region during MIS6. At 151 ka, stable carbon isotope data from PP30 large fauna

(provided by J.A. Lee-Thorp and discussed in chapter 4) are systematically slightly enriched in ^{13}C relative to both Pliocene Langebaanweg specimens and to fossil-fuel effect 'corrected' modern large fauna specimens, as well as to the micromammal specimens sampled from PP30. Although some of the difference between micromammal $\delta^{13}C_{enamel}$ values and large mammal $\delta^{13}C_{enamel}$ values may be attributable to differences in diet-tissue isotopic spacing between large and small fauna (see Sullivan and Krueger, 1981; Lee-Thorp and Van Der Merwe, 1987; Lee-Thorp *et al.*, 1989; Cerling *et al.*, 1997; Cerling and Harris, 1999; Podelsak *et al.*, 2008), the difference between the micromammal $\delta^{13}C_{enamel}$ values and the $\delta^{13}C_{ename;}$ values of the grazing fauna are large enough to indicate that the PP30 large mammals were sampling a paleovegetation in which some C_4 graze component was available. Differences in the vegetation sampled by the large mammals and micromammals can thus be hypothesized to have resulted from the different ranges of both the sampled fauna themselves, and the aggregating predators of both assemblages.

Stable carbon isotope data from the Middle Pleistocene large fauna from Elandsfontein on the West Coast reported by Luyt *et al.* (2000) suggest a maintenance of C_3-dominated vegetation even in the presence of other evidence for grassy habitats at that site. It appears that the paired micromammal and large mammal isotope data from PP30 suggests a similar scenario, where C_3 vegetation is the primary dietary component of all fauna during MIS6. Other types of paleoenvironmental proxy data from the south coast for MIS6 suggest the presence of open albeit shrubby environments during deposition of

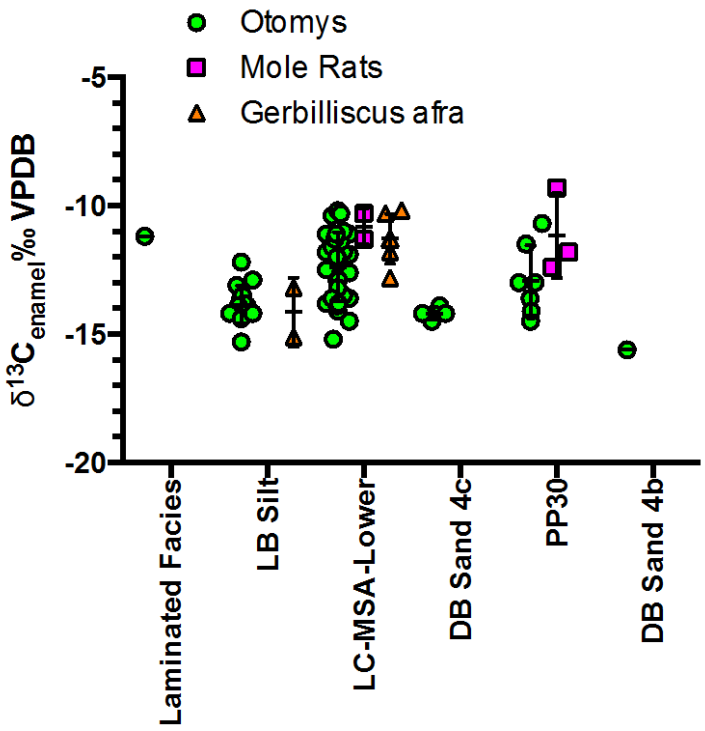

Figure 7.3. PP micromammal specimens from deposits that are MIS6 or older in age. Oldest stratigraphic aggregates are on the left, youngest stratigraphic aggregates are on the right.

the LC-MSA Lower and DB Sand aggregates at PP13B (Rector and Reed, 2010). The contrast between the micromammal stable carbon isotope data from the MIS6 aggregates in PP13B and paleoenvironmental reconstruction using large fauna is thus somewhat similar to the scenario seen in the PP30 data: the large mammalian fauna and the micromammals may have been sampling either a) different vegetation communities (possibly in an ecotonal context) or b) different components of the same vegetation community. Speleothem $\delta^{13}C$ from specimens sampled from the Pinnacle Point region are ~-9‰ VPBD for the duration of the 200ka to 148 ka period (Braun, personal communication), which is consistent with C_3-predominant vegetation in the immediate

area of the PP sites. Given the concordance between the speleothem and micromammal stable carbon isotope data, it is hypothesized that the C_4 component observed in the grazing large fauna from PP30 likely derives from somewhat more distant vegetation communities, almost certainly on the Paleo-Agulhas Plain.

Micromammal specimens from deposits that span the transition from MIS6 to MIS5e (Figure 7.4) are somewhat more variable than those from earlier in MIS6. Although the $\delta^{13}C_{enamel}$ values of the *Otomys* specimens, with the exception of the LGB Sand 1 (at 124 ± 5ka) do not change through this period, there is some small change seen in the $\delta^{13}C_{enamel}$ values of the *G. afra* specimens. The 130 ± 9 ka BYCS and BYSS *G. afra* specimen $\delta^{13}C_{enamel}$ values are between 0‰ – 4.3‰ VPDB higher than the most ^{13}C-enriched *G. afra* specimen from the 162 ± 6 ka LC-MSA Lower. In particular, one specimen of *G. afra* from the BYSS has a $\delta^{13}C_{enamel}$ value of -5.9‰ VPDB, which indicates a significant C_4 grass component in the diet of this individual. Sample sizes of *G. afra* throughout the sequence are small, so it is possible that the limited range of $\delta^{13}C_{enamel}$ values from the older LC-MSA specimens is a function of sample size, but the higher *G. afra* value from 130 ka is the only strong evidence of C_4 vegetation in the entire micromammal data set. This is however, indicative of the fact that some micromammal taxa certainly sample C_4 vegetation when it is present on the landscape, and results in the hypothesis that the lower $\delta^{13}C_{enamel}$ values found in the earlier and later *G. afra* sample may represent a more limited presence of C_4 in those vegetation communities. The more ^{13}C-enriched *G. afra* specimens occur in deposits that likely date to about 5ka prior the to start of MIS5e. A sea-level model for the PP region (Fisher *et al.*, 2010) indicates that at ~130ka the coastline was rapidly transgressing. If warmer conditions or increased year-

round or summer rainfall were associated with the sea level rise, this may explain this evidence for the presence of increased C_4 grasses in the Pinnacle Point area. Regardless of the cause, the higher $\delta^{13}C_{enamel}$ values from the 130 ka *G. afra* specimens are consistent with a rapid increase in Pinnacle Point speleothem $\delta^{13}C$ values at 130 ka that also suggest an increased penetration of C_4 grasses into local vegetation communities (Braun, personal communication). Speleothem $\delta^{13}C$ values are however quite high (-5.24 to -4.08‰ VPDB), suggesting vegetation communities that are quite C_4, and are thus inconsistent with the lower $\delta^{13}C_{enamel}$ values found in the *Otomys* specimens (Braun, unpublished data) (Figure 7.4). Given that the late MIS6/MIS5e *Otomys* specimens are likely to be quite local, and given that the speleothem also represents a local signal, it is difficult to resolve this discrepancy between the proxy records. Preferential occupation of a C_3 isotopic niche space by *Otomys* (*sensu* Codron *et al.*, 2015) may explain the low values of $\delta^{13}C_{enamel}$ measured in these specimens, but it also indicates that C_3 vegetation is still commonplace enough in the region to provide the primary dietary fraction for *O. irroratus* and *O. saundersiae*—and *Otomys* are common enough on the landscape to be a significant component of all micromammal assemblages (Matthews *et al.*, 2009; Matthews *et al.*, 2011).

Stable carbon isotope analysis of the micromammals from the LBG Sand 1 stratigraphic aggregate at PP13B suggest that the time period represented by this deposit intersects a somewhat unique vegetation or paleoenvironmental condition in the PP sequence. *Otomys* $\delta^{13}C_{enamel}$ values are depleted in ^{13}C relative to all other depositional units sampled from MIS6 and MIS5; these lower $\delta^{13}C_{enamel}$ values overlap with

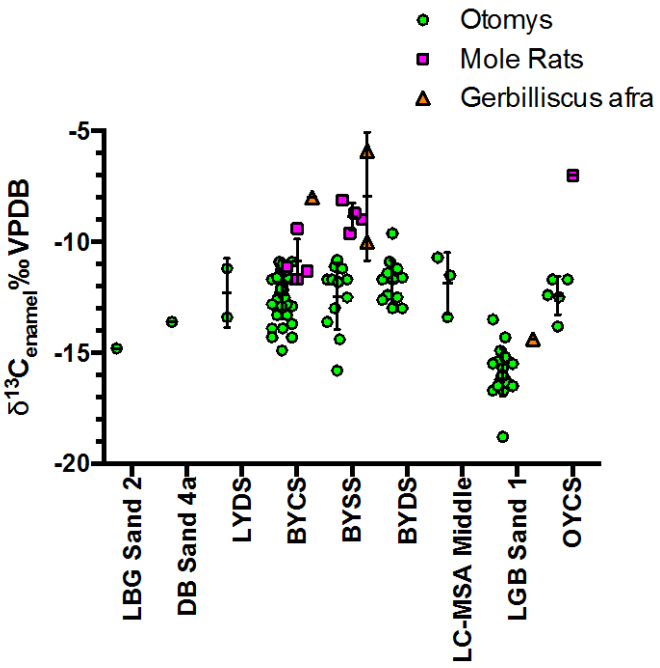

Figure 7.4. PP micromammal specimens from deposits that are late MIS6 or MIS5e in age. Oldest stratigraphic aggregates are on the left, youngest stratigraphic aggregates are on the right.

'corrected' modern *Otomys* $\delta^{13}C_{enamel}$ values from relatively closed contexts such as those found at Amisrus/Wilderness (Chapter 3). A number of factors can result in more ^{13}C-depleted values of $\delta^{13}C_{plant}$ (and as a result $\delta^{13}C_{enamel}$ of consumers), including the presence of very closed vegetation in which a canopy effect is occurring (Farquhar *et al.*, 1989), or decreased aridity (Kohn, 2010), and it is difficult to determine which factor may be a primary contributor to the decrease in $\delta^{13}C_{plant}$ values represented by the *Otomys* $\delta^{13}C_{enamel}$ data, in part because of a paucity of other paleoenvironmental records for the region during this time period (there is a gap in the current speleothem record at the time period represented by the LBG Sand 1; Braun, personal communication). The best corroborative evidence arises from the micromammal assemblage itself, where the presence of *T. dolichurus* and *D. mystacalis* in the LBG Sand 1 assemblage (Matthews *et*

al., 2009) likely indicate closed/thicket environments near to PP13B during the depositional period represented by this stratigraphic aggregate. LBG Sand 1 large faunal analyses still suggest the presence of more open environments at the site during this period (Rector and Reed, 2010), and thus it is again possible that the large mammals and micromammals are sampling different vegetation communities.

Micromammal specimens that post date the LBG Sand 1 anomaly (Figure 7.5) again have $\delta^{13}C_{enamel}$ values that are consistent with diets composed exclusively of C_3 vegetation, and with the exception of a single ^{13}C-depleted *Otomys* specimen from the Roofspall lower, show no evidence of the lower $\delta^{13}C_{enamel}$ values associated with very closed vegetation as in the LBG Sand 1. Pinnacle Point speleothem records for the 111 ka to 90 ka period again have lower $\delta^{13}C_{speleothem}$ values associated with the presence of C_3 vegetation near to the sites (although there is more variability in this portion of the record than for the MIS6 record; Braun, unpublished data).

Overall, the micromammal stable carbon isotope record from PP13B, PP30, and PP9C suggests that maintenance of C_3-dominated vegetation occurred for the duration of MIS6 and MIS5. The limited taxonomic diversity of the assemblage, and thus of the isotopic sample, may mean that some of this consistent C_3 signal is the result of the isotopic niche occupied by the taxa sampled. However, C_3 vegetation must still be present at the locality to produce the low $\delta^{13}C_{enamel}$ values seen in the micromammal

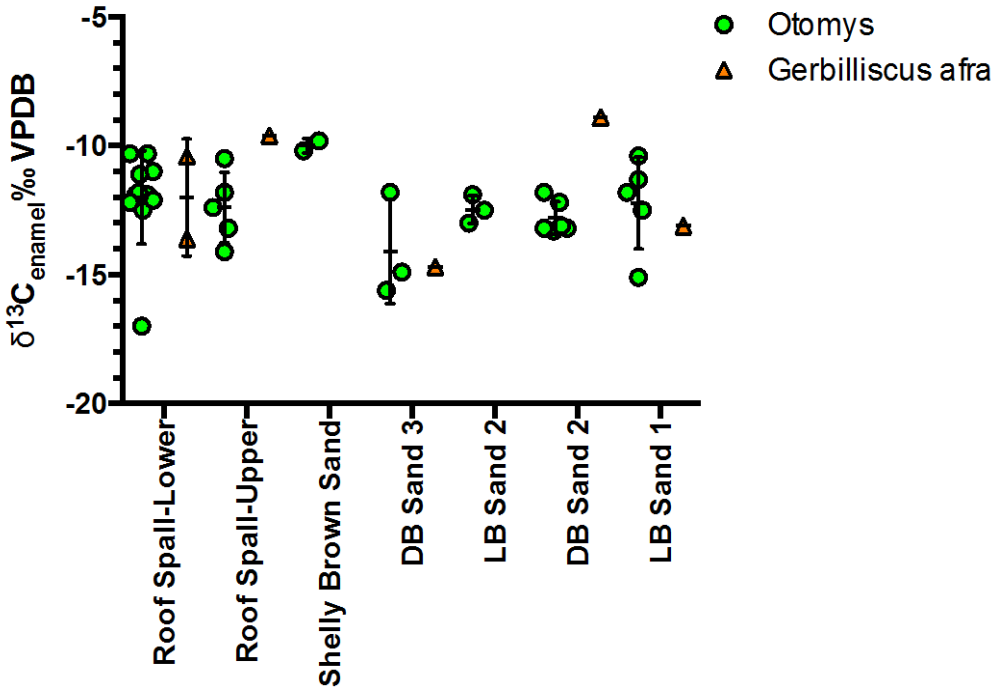

Figure 7.5. PP micromammal specimens from deposits that are MIS5e and younger in age. Oldest stratigraphic aggregates are on the left, youngest stratigraphic aggregates are on the right

sample; thus the presence of C_3 vegetation at PP for the duration of MIS6 and MIS5 is unequivocal, and instead the apparent absence of C_4 grasses cannot be taken as a true 'absence of evidence' on the landscape, but rather are only absent from the diets of the specimens sampled.

The maintenance of C_3 ecosystems, which are likely to be comprised of old and endemic GCFR floral elements, indicated by the micromammal stable carbon isotope record throughout MIS6 and MIS5 at Pinnacle Point suggest that the elements of GCFR vegetation communities that are appealing to hunter gatherers (Marean *et al.*, 2014) could have been present at PP during the occupation of PP13B and PP9C by early modern human groups. The enduring nature of these proabable GCFR elements would have

provided some environmental stability during these glacial and interglacial periods, and thus suggest that the south coast, at least proximate to Pinnacle Point, would have continued to be a viable refugium environment for *Homo sapiens* during this period due to the persistence of the predominantly C3 fynbos vegetation.

Directions for future research

This stable isotope analysis of modern and archaeological micromammals from the south coast of South Africa suggests several avenues for fruitful future research. Although the GSCIMS dataset produced by aggregation of published $\delta^{13}C$ values for GCFR plants provides a useful approximation of the range of stable carbon isotopic variation in Cape flora, it is by no means exhaustive, and suffers from several shortcomings discussed in Chapter 2. A dedicated floral sampling program should be undertaken to more accurately characterize the extent of geographic variation in $\delta^{13}C_{plant}$ values in C_3 and C_4 plants in the Greater Cape Floristic Region. Such datasets exist for Eastern Africa (Cerling and Harris, 1999; Cerling *et al.*, 2003; Cerling *et al.*, 2004) and northeastern Southern Africa (Codron *et al.*, 2005), but none yet have been produced for the GCFR. This is likely due in part to the hyper-diversity of Cape flora, and a number of different geographic regions and vegetation communities need to be sampled. The abundance of archaeological sites along the south coast makes it an ideal jumping off point for such studies, however, as isotopically well-characterized vegetation could provide modern contextual data for researchers looking to study micromammal and large fauna from MSA and LSA sites in the region.

Similarly, although a small stable carbon and oxygen isotope data set from modern south coast micromammals was presented here, the collection of that modern data (Chapter 3) was constrained by the need to have modern contextual data for a relatively limited number of archaeological and fossil micromammal taxa. Recent niche partitioning studies in other regions of South Africa (e.g. Codron et al., 2015) suggest that some micromammal taxa that, based on feeding ecology, should sample a complete range of vegetation types, may fail to do so. The limited data from the research presented here indicates that examining changes through time in stable isotope composition across multiple micromammal taxa may capture some elements of vegetation that may not be observed in the sampling of single taxa. Further isotopic sampling of a diversity of modern micromammal taxa from discrete vegetation communities in the south coast may further refine our ability to interpret $\delta^{13}C_{enamel}$ data from archaeological micromammal material.

Chapter 7 References:

Cerling, T. E. and J. M. Harris (1999). "Carbon isotope fractionation between diet and bioapatite in ungulate mammals and implications for ecological and paleoecological studies." Oecologia **120**(3): 347-363.

Cerling, T. E., J. M. Harris, S. H. Ambrose, M. G. Leakey and N. Solounias (1997). "Dietary and environmental reconstruction with stable isotope analyses of herbivore tooth enamel from the Miocene locality of Fort Ternan, Kenya." Journal of Human Evolution **33**: 635-650.

Codron, J., K. J. Duffy, N. L. Avenant, M. Sponheimer, J. Leichliter, O. Paine, . . . D. Codron (2015). "Stable isotope evidence for trophic niche partitioning in a South African savanna rodent community." Current Zoology 61 (3): 397-411

Farquhar, G. D., J. R. Ehleringer and K. T. Hubick (1989). "Carbon isotope discrimination and photosynthesis." Annual review of plant biology **40**(1): 503-537.

Fisher, E. C., M. Bar-Matthews, A. Jerardino and C. W. Marean (2010). "Middle and Late Pleistocene paleoscape modeling along the southern coast of South Africa." Quaternary Science Reviews **29**(11-12): 1382-1398.

Hopley, P. J., A. G. Latham and J. D. Marshall (2006). "Palaeoenvironments and palaeodiets of mid-Pliocene micromammals from Makapansgat Limeworks, South Africa: a stable isotope and dental microwear approach." Palaeogeography, Palaeoclimatology, Palaeoecology **233**(3): 235-251.

Hynek, S. A., B. H. Passey, J. L. Prado, F. H. Brown, T. E. Cerling and J. Quade (2012). "Small mammal carbon isotope ecology across the Miocene-Pliocene boundary, northwestern Argentina." Earth and Planetary Science Letters **321-322**(0): 177-188.

Kimura, Y., L. L. Jacobs, T. E. Cerling, K. T. Uno, K. M. Ferguson, L. J. Flynn and R. Patnaik (2013). "Fossil mice and rats show isotopic evidence of niche partitioning and change in dental ecomorphology related to dietary shift in late Miocene of Pakistan." PloS one **8**(8): e69308.

Kohn, M. J. (2010). "Carbon isotope compositions of terrestrial C_3 plants as indicators of (paleo)ecology and (paleo)climate." Proceedings of the National Academy of Sciences of the United States of America **107**(46): 19691-19695.

Lee-Thorp, J. and N. J. Van Der Merwe (1987). "Carbon isotope analysis of fossil bone apatite." South African Journal of Science; v. **83**(11) p. 712-715

Lee-Thorp, J. A., J. C. Sealy and N. J. Van Der Merwe (1989). "Stable carbon isotope ratio differences between bone collagen and bone apatite, and their relationship to diet." Journal of Archaeological Science **16**(6): 585-599.

Luyt, J., J. Lee-Thorp and G. Avery (2000). "New light on Middle Pleistocene west coast environments from Elandsfontein, Western Cape Province, South Africa." South African Journal of Science **96**(7).

Marean, C. W., M. Bar-Matthews, E. Fisher, P. Goldberg, A. Herries, P. Karkanas, . . . E. Thompson (2010). "The stratigraphy of the Middle Stone Age sediments at Pinnacle Point Cave 13B (Mossel Bay, Western Cape Province, South Africa)." Journal of Human Evolution **59**(3-4): 234-255.

Marean, C. W., H. C. Cawthra, R. M. Cowling, K. J. Esler and J. De Vynck (2014). "Stone Age people in a changing South African Greater Cape Floristic Region." Fynbos: Ecology, Evolution, and Conservation of a Megadiverse Region:.

Matthews, T. (n.d.). A summary of the micromammal population from PP30 (Brown hyaena den).

Matthews, T., C. Marean and P. Nilssen (2009). "Micromammals from the Middle Stone Age (92 - 167 ka) at Cave PP13B, Pinnacle Point, south coast, South Africa." Paleontol. Afr **44**: 112-120.

Matthews, T., A. Rector, Z. Jacobs, A. I. R. Herries and C. W. Marean (2011). "Environmental implications of micromammals accumulated close to the MIS6 to MIS5 transition at Pinnacle Point Cave 9 (Mossel Bay, Western Cape Province, South Africa)." Palaeogeography, Palaeoclimatology, Palaeoecology. **302**(3-4): 213-229

Podelsak, D. W., A.-M. Torregrossa, J. R. Ehleringer, M. D. Dearing, B. H. Passey and T. E. Cerling (2008). "Turnover of oxygen and hydrogen isotopes in the body water, CO2, hair, and enamel of a small mammal." Geochimica et cosmochimica acta **72**(1): 19-35.

Rebelo, A. G., C. Boucher, N. Helme, L. Mucina and M. C. Rutherford (2006). Fynbos Biome. The Vegetation of South Africa, Lesotho, and Swaziland. Pretoria, South African National Biodiversity Institute**:** 52-219.

Rector, A. L. and K. E. Reed (2010). "Middle and late Pleistocene faunas of Pinnacle Point and their paleoecological implications." Journal of Human Evolution **59**(3): 340-357.

Robb, G. N., S. Woodborne and N. C. Bennett (2012). "Subterranean sympatry: an investigation into diet using stable isotope analysis." PloS one **7**(11): e48572.

Sullivan, C. H. and H. W. Krueger (1981). "Carbon isotope analysis of separate chemical phases in modern and fossil bone." Nature **292:** 333-335

Thackeray, J. F., A. van der Venter, J. Lee-Thorp, C. T. Chimimba and J. van Heerden (2003). "Stable carbon isotope analysis of modern and fossil samples of the South African rodent Aethomys namaquensis." Annals of the Transvaal Museum **40**: 43-46.

Williams, H. M. (in prep). An MIS7-MIS4 stable carbon and oxygen isotope record from fossil micromammal remains from the Middle Stone Age archaeological cave site PP13B, Pinnacle Point, South Africa.

Comprehensive List of References

AGIS. (2007). "Agricultural Geo-Referenced Information System." Retrieved Jan, 2015, from http://www.agisagric.za.

Agenbag, L. (2006). A Study on an altitudinal gradient investigating the potential effects of climate change on Fynbos and the Fynbos Succulent Karoo Boundary Masters Thesis, University of Stellenbosch.

Albert, R. M. and C. W. Marean (2012). "The exploitation of plant resources by early Homo sapiens: the phytolith record from Pinnacle Point 13B Cave, South Africa." Geoarchaeology **27**(4): 363-384

Ambrose, S. H. (2006). "Howiesons Poort lithic raw material procurement patterns and the evolution of modern human behavior: A response to..." J Hum Evolution **50**(3), 365-369

Ambrose, S. and M. DeNiro (1986). "The isotopic ecology of East African mammals." Oecologia **69**(3): 395-406.

Ambrose, S. H. and K. G. Lorenz (1990). "Social and ecological models for the middle stone age in southern africa". In The emergence of modern humans: an archaeological perspective. Edinburgh, Edinburgh University Press**:** 3-33.

Ambrose, S. H. and L. Norr (1993). "Experimental evidence for the relationship of the carbon isotope ratios of whole diet and dietary protein to those of bone collagen and carbonate". Prehistoric Human Bone: Archaeology at the Molecular Level. New York, Springer-Verlag**:** 1-37.

Andrews, P. (1990). Owls, caves, and fossils: predation, preservation, and accumulation of small mammal bones in caves, with an analysis of the pleistocene cave faunas from westbury-sub-mendip, somerset, UK. Chicago, University of Chicago Press.

Araya, Y. N., J. Silvertown, D. J. Gowing, K. McConway, P. Linder and G. Midgley (2010). "Variation in $\delta^{13}C$ among species and sexes in the family Restionaceae along a fine-scale hydrological gradient." Austral Ecology **35**(7): 818-824.

Arneson, L. S. and S. E. MacAvoy (2005). "Carbon, nitrogen, and sulfur diet-tissue discrimination in mouse tissues." Canadian Journal of Zoology **83**(7): 989-995.

Avery, D. M. (1982). "Micromammals as palaeoenvironmental indicators and an interpretation of the Late Quaternary in the southern Cape Province, South Africa." Annals of the South African Museum **85**: 183-374.

Avery, D. M. (1983). "Palaeoenvironmental implications of the small Quaternary mammals of the fynbos region." Deacon, HJ, Hendey, QB & Lambrechts, JJN (eds.) Fynbos palaeoecology: a preliminary synthesis. S. Afr. Nat1. Scient. Progress Rep **75**: 139-155.

Avery, D. M. (1988). "Micromammals and paleoenvironmental interpretation in southern Africa." Geoarchaeology **3**(1): 41-52.

Avery, D. M. (1999). "A re-appraisal of micromammalian data from South Africa." Quaternary International **57-58**: 175-183.

Avery, D. M. (2000). "Notes on the systematics of micromammals from Sterkfontein, Gauteng, South Africa." Paleontogica Africa **36:** 83-90

Bar-Matthews, M., C. W. Marean, Z. Jacobs, P. Karkanas, E. C. Fisher, A. I. R. Herries, . . . A. Ayalon (2010). "A high resolution and continuous isotopic speleothem record of paleoclimate and paleoenvironment from 90 to 53 ka from Pinnacle Point on the south coast of South Africa." Quaternary Science Reviews **29**(17): 2131-2145.

Barham, L. S. and P. L. Smart (1996). "Current events: An early date for the Middle Stone Age of central Zambia." Journal of Human Evolution **30**(3): 287-290.

Barham, L. and P. Mitchell (2008). The first Africans: African archaeology from the earliest toolmakers to most recent foragers, Cambridge University Press.

Barrable, A., M. E. Meadows and B. C. Hewitson (2002). "Environmental reconstruction and climate modelling of the Late Quaternary in the winter rainfall region of the Western Cape, South Africa." South African Journal of Science **98**: 611-616.

Bender, M. M. (1971). "Variations in the $^{13}C/^{12}C$ ratios of plants in relation to the pathway of photosynthetic carbon dioxide fixation." Phytochemistry **10**(6): 1239-1244.

Bennett, N. C. and C. G. Faulkes (2000). African mole-rats: ecology and eusociality, Cambridge University Press.

Berger, L. R., D. J. de Ruiter, S. E. Churchill, P. Schmid, K. J. Carlson, P. H. G. M. Dirks and J. M. Kibii (2010). "Australopithecus sediba: A new species of Homo-like australopith from South Africa." Science **328**(5975): 195-204.

Berger, L. R., R. Lacruz and D. J. De Ruiter (2002). "Revised age estimates of Australopithecus-bearing deposits at Sterkfontein, South Africa." American Journal of Physical Anthropology **119**(2): 192-197.

Bernatchez, J. and C. W. Marean (2011). "Total station archaeology and the use of digital photography." SAA Archaeol. Rec **11**: 16-21.

Blome, M. W., A. S. Cohen, C. A. Tryon, A. S. Brooks and J. Russell (2012). "The environmental context for the origins of modern human diversity: A synthesis of regional variability in African climate 150,000 - 30,000 years ago." Journal of Human Evolution **62**(5): 563-592.

Bocherens, H., P. L. Koch, A. Mariotti, D. Geraads and J.-J. Jaeger (1996). "Isotopic Biogeochemistry (^{13}C, ^{18}O) of Mammalian Enamel from African Pleistocene Hominid Sites." Palaios **11**(4): 306-318.

Boom, A., A. S. Carr, B. M. Chase, H. L. Grimes and M. E. Meadows (2014). "Leaf wax n-alkanes and $\delta^{13}C$ values of CAM plants from arid southwest Africa." Organic Geochemistry **67**: 99-102.

Born, J., H. Linder and P. Desmet (2007). "The greater cape floristic region." Journal of Biogeography **34**(1): 147-162.

Boutton, T. W., L. L. Tieszen and S. K. Imbamba (1988). "Seasonal changes in the nutrient content of East African grassland vegetation." African Journal of Ecology **28**: 103-115.

Braun, K., M. Bar-Matthews, A. Ayalon, C. Marean, I. Andy, R. Zahn and A. Matthews "Southern South African coastal and inland climate: the influence of sea level, SST and orbital parameters as recorded in speleothems." AGU Meetings, 2012

Brown, K. S. (2011). The Sword in the Stone: Lithic Raw Material Exploitation in the Middle Stone Age at Pinnacle Point Site 5-6, Southern Cape, South Africa. PhD PhD, University of Cape Town.

Brown, K. S., C. W. Marean, A. I. R. Herries, Z. Jacobs, C. Tribolo, D. Braun, . . . J. Bernatchez (2009). "Fire as an engineering tool of early modern humans." Science **325**(5942): 859-862.

Brown, K. S., C. W. Marean, Z. Jacobs, B. J. Schoville, S. Oestmo, E. C. Fisher, . . . T. Matthews (2012). "An early and enduring advanced technology originating 71,000 years ago in South Africa." Nature **491**(7425): 590-593.

Bryant, J. D., P. L. Koch, P. N. Froelich, W. J. Showers and B. J. Genna (1996). "Oxygen isotope partitioning between phosphate and carbonate in mammalian apatite." Geochimica et Cosmochimica Acta **60**(24): 5145-5148

Campbell, T. L., P. J. Lewis and J. K. Williams (2011). "Analysis of the modern distribution of South African Gerbilliscus (Rodentia: Gerbillinae) with

implications for Plio-Pleistocene palaeoenvironmental reconstruction." South African Journal of Science **107**: 1-7.

Cann, R. L. (1988). "DNA and human origins." Annual Review of Anthropology **17**: 127-143.

Carr, A. S., A. Boom, H. L. Grimes, B. M. Chase, M. E. Meadows and A. Harris (2014). "Leaf wax n-alkane distributions in arid zone South African flora: environmental controls, chemotaxonomy and palaeoecological implications." Organic Geochemistry **67**: 72-84.

Carr, A. S., M. D. Bateman, D. L. Roberts, C. V. Murray-Wallace, Z. Jacobs and P. J. Holmes (2010). "The last interglacial sea-level high stand on the southern Cape coastline of South Africa." Quaternary Research **73**(2): 351-363

Cerling, T. E. and J. M. Harris (1999). "Carbon isotope fractionation between diet and bioapatite in ungulate mammals and implications for ecological and paleoecological studies." Oecologia **120**(3): 347-363.

Cerling, T. E., J. M. Harris and B. H. Passey (2003). "Diets of East African Bovidae based on stable isotope analysis." Journal of Mammalogy **84**(2): 456-470.

Cerling, T. E., J. A. Hart and T. B. Hart (2004). "Stable isotope ecology in the Ituri Forest." Oecologia **138**(1): 5-12.

Cerling, T. E. and J. M. Harris (1999). "Carbon isotope fractionation between diet and bioapatite in ungulate mammals and implications for ecological and paleoecological studies." Oecologia **120**(3): 347-363.

Cerling, T. E., J. M. Harris, S. H. Ambrose, M. G. Leakey and N. Solounias (1997). "Dietary and environmental reconstruction with stable isotope analyses of herbivore tooth enamel from the Miocene locality of Fort Ternan, Kenya." Journal of Human Evolution **33**: 635-650.

Chase, B. M. and M. E. Meadows (2007). "Late Quaternary dynamics of southern Africa's winter rainfall zone." Earth-Science Reviews **84**(3-4): 103-138.

Clark, J. D., Y. Beyene, G. WoldeGabriel, W. K. Hart, P. R. Renne, H. Gilbert, . . . K. R. Ludwig (2003). "Stratigraphic, chronological and behavioural contexts of Pleistocene Homo sapiens from Middle Awash, Ethiopia." Nature **423**(6941): 747-752.

Codron, D., J. A. Lee-Thorp, M. Sponheimer, D. de Ruiter and J. Codron (2006). "Inter- and intrahabitat dietary variability of chacma baboons (Papio ursinus) in South African savannas based on fecal δ13C, δ15N, and% N." American Journal of Physical Anthropology **129**(2): 204-214.

Codron, J., K. J. Duffy, N. L. Avenant, M. Sponheimer, J. Leichliter, O. Paine, . . . D. Codron (2015). "Stable isotope evidence for trophic niche partitioning in a South African savanna rodent community." Current Zoology **61** (3): 397-411

Codron, J., D. Codron, J. A. Lee-Thorp, M. Sponheimer, W. J. Bond, D. de Ruiter and R. Grant (2005). "Taxonomic, anatomical, and spatio-temporal variations in the stable carbon and nitrogen isotopic compositions of plants from an African savanna." Journal of Archaeological Science **32**(12): 1757-1772.

Cowling, R. and D. Richardson (1995). Fynbos: South Africa's Unique Floral Kingdom. Cape Town, University of Cape Town Press.

Cowling, R., D. Richardson and P. Mustart (1997). “Fynbos”. Vegetation of Southern Africa. R. M. Cowling, D. M. Richardson and S. M. Pierce. Cambridge, Cambridge University Press.

Cowling, R. M. (1983). "The occurrence of C_3 and C_4 grasses in fynbos and allied shrublands in the South Eastern Cape, South Africa." Oecologia **58**(1): 121-127.

Cowling, R. M. (1992). The Ecology of Fynbos: Nutrients, Fire and Diversity. Cape Town, Oxford.

Cowling, R. M., P. M. Holmes and A. G. Rebelo (1992). "The ecology of fynbos: nutrients, fire and diversity." Cape Town.: Oxford Univ. Press 411pp.. Contents include: Flora and vegetation, by RM Cowling & PM Holmes: 23-61.

Cowling, R. M., S. Proches and T. C. Partridge (2009). "Explaining the uniqueness of the Cape flora: incorporating geomorphic evolution as a factor for explaining its diversification." Molecular Phylogenetics and Evolution **51**(1): 64-74.

Cowling, R. M., D. M. Richardson, R. E. Schulze, M. T. Hoffman, J. J. Midgley and C. Hilton-Taylor (1997). "Species diversity at the regional scale." Vegetation of southern Africa: 447-473.

Cowling, R. M., K. J. Esler, G. F. Midgley and M. A. Honig (1994). "Plant functional diversity, species diversity and climate in arid and semi-arid southern Africa." Journal of Arid Environments **27**(2): 141-158.

Cowling, S. A., P. M. Cox, C. D. Jones, M. A. Maslin, M. Peros and S. A. Spall (2008). "Simulated glacial and interglacial vegetation across Africa: implications for

species phylogenies and trans-African migration of plants and animals." Global Change Biology **14**: 827-840

Craig, H. (1954) "Carbon-13 in plants and the relationships between carbon-13 and carbon-14 variations in nature" Journal of Geology **62**:115–149

Crowley, B. E., M. L. Carter, S. M. Karpanty, A. L. Zihlman, P. L. Koch and N. J. Dominy (2010). "Stable carbon and nitrogen isotope enrichment in primate tissues." Oecologia **164**(3): 611-626.

Cuenca Bescos, G. (2003). "The micromammal record as proxy of palaeoenvironmental changes in the Pleistocene of the Sierra de Atapuerca (Burgos, Spain)." Quaternary climatic changes and environmental crises in the Mediterranean Region: 133-138.

Dauphin, Y., P. Andrews, C. Denys, Y. Fernandez-Jalvo and T. Williams (2003). "Structural and chemical bone modifications in a modern owl pellet assemblage from Olduvai Gorge (Tanzania)." Journal of Taphonomy **1**: 209-232.

Dauphin, Y. and C. T. Williams (2004). "Diagenetic trends of dental tissues." Comptes Rendus Palevol **3**(6-7): 583-590.

Davies, K. C. and J. U. M. Jarvis (1986). "The burrow systems and burrowing dynamics of the molerats Bathyergus suillus and Cryptomys hottentotus in the fynbos of the southwestern Cape, South Africa." Journal of Zoology **209**(1): 125-147.

d'Errico, F., C. Henshilwood, M. Vanhaeren and K. van Niekerk (2005). "Nassarius kraussianus shell beads from Blombos Cave: evidence for symbolic behaviour in the Middle Stone Age." Journal of Human Evolution **48**(1): 3-24.

d'Errico, F. and C. S. Henshilwood (2007). "Additional evidence for bone technology in the southern African Middle Stone Age." Journal of Human Evolution **52**(2): 142-163.

De Graaff, G. (1981). The rodents of southern Africa. Durban: Butterworths

Dart, R. (1925). "Australopithecus africanus: the man-ape of South Africa." Nature **115**: 195-199.

Deacon, H. J. (1983). "Another look at the Pleistocene climates of South Africa." South African Journal of Science **79**: 325-328.

Deacon, H. J. (1985). "An introduction to the fynbos region, time scales and palaeoenvironments." CSIR Report **75**: 1-99.

Deacon, H. J., J. Deacon, A. Scholtz, J. F. Thackeray, J. S. Brink and J. C. Vogel "Correlation of palaeoenvironmental data from the Late Pleistocene and Holocene deposits at Boomplaas cave, southern Cape." 339-351.

DeNiro, M. J. and S. Epstein (1978). "Influence of diet on the distribution of carbon isotopes in animals." Geochimica et Cosmochimica Acta **42**(5): 495-506.

Denys, C. (1998). “Phylogenetic implications of the existence of two modern genera of Bathyergidae (Mammalia, Rodentia) in the Pliocene site of Langebaanweg (South Africa)”, Annals of the South African Museum **105**(5): 265-268

Faith, J. T. (2011). "Ungulate community richness, grazer extinctions, and human subsistence behavior in southern Africa's Cape Floral Region." Palaeogeography, Palaeoclimatology, Palaeoecology **306**(3): 219-227

Faith, J. T. (2013). "Taphonomic and paleoecological change in the large mammal sequence from Boomplaas Cave, western Cape, South Africa." Journal of Human Evolution **65**(6): 715-730.

Farquhar, G., M. O'Leary and J. Berry (1982). "On the Relationship Between Carbon Isotope Discrimination and the Intercellular Carbon Dioxide Concentration in Leaves." Functional Plant Biology **9**(2): 121-137.

Farquhar, G. D., J. R. Ehleringer and K. T. Hubick (1989). "Carbon isotope descrimination and photosynthesis." Annual Review of Plant Physiology and Plant Molecular Biology **40**: 503-537.

Fisher, E. C., M. Bar-Matthews, A. Jerardino and C. W. Marean (2010). "Middle and Late Pleistocene paleoscape modeling along the southern coast of South Africa." Quaternary Science Reviews **29**(1112): 1382-1398.

Flanagan, L. B., J. R. Brooks, G. T. Varney, S. C. Berry and J. R. Ehleringer (1996). "Carbon isotope discrimination during photosynthesis and the isotope ratio of respired CO2 in boreal forest ecosystems." Global Biogeochemical Cycles **10**(4): 629-640.

Franz-Odendaal, T. A., J. A. Lee-Thorp and A. Chinsamy (2002). "New evidence for the lack of C_4 grassland expansions during the early Pliocene at Langebaanweg, South Africa." Paleobiology **28**(3): 378-388.

Gehler, A., T. Tutken and A. Pack (2012). "Oxygen and carbon isotope variations in a modern rodent community, implications for palaeoenvironmental reconstructions." PLoS1 e49531

Goldblatt, P. (1997). "Floristic diversity in the Cape Flora of South Africa." Biodiversity and Conservation **6**(3): 359-377.

Goldblatt, P. and J. C. Manning (2002). "Plant Diversity of the Cape Region of Southern Africa." Annals of the Missouri Botanical Garden **89**(2): 281-302.

Granjon, L. and E. R. Dempster (2013). Genus Gerbilliscus: Gerbils. Mammals of Africa. J. Kingdon, D. Happold, T. Butynskiet al, Bloomsbury. Volume **III**.

Grun, R. and P. Beaumont (2001). "Border Cave revisited: a revised ESR chronology." Journal of Human Evolution **40**(6): 467-482.

Grun, R. and C. B. Stringer (1991). "Electron spin resonance dating and the evolution of modern humans." Archaeometry **33**(2): 153-199.

Heaton, T. H. E. (1999). "Spatial, Species, and Temporal Variations in the $^{13}C/^{12}C$ Ratios of C_3 Plants: Implications for Palaeodiet Studies." Journal of Archaeological Science **26**(6): 637-649.

Hedges, R. E. M. (2002). "Bone diagenesis: an overview of processes." Archaeometry **44**(3): 319-328.

Hendey, Q. B. and T. P. Volman (1986). "Last interglacial sea levels and coastal caves in the Cape Province, south Africa." Quaternary Research **25**(2): 189-198.

Henry, A. G., P. S. Ungar, B. H. Passey, M. Sponheimer, L. Rossouw, M. Bamford, . . . L. Berger (2012). "The diet of Australopithecus sediba; Supplementary Information." Nature **487**(7405): 90-93.

Henshilwood, C., F. D'Errico, M. Vanhaeren, K. van Niekerk and Z. Jacobs (2004). "Middle Stone Age Shell Beads from South Africa." Science **304**(5669): 404.

Henshilwood, C. S., F. d'Errico, K. L. van Niekerk, Y. Coquinot, Z. Jacobs, S. E. Lauritzen, . . . R. Garcia-Moreno (2011). "A 100,000-year-old ochre-processing workshop at Blombos Cave, South Africa." Science **334**(6053): 219-222.

Henshilwood, C. S., F. d'Errico and I. Watts (2009). "Engraved ochres from the middle stone age levels at Blombos cave, south Africa." Journal of Human Evolution **57**(1): 27-47.

Henshilwood, C., C. Marean and H. Soodyall (2006). Remodeling the origins of modern human behavior. The Prehistory of Africa: Tracing the Lineage of Modern Man. Cape Town, Jonathan Ball Publishers**:** 31-48.

Herries, A. I. and E. C. Fisher (2010). "Multidimensional GIS modeling of magnetic mineralogy as a proxy for fire use and spatial patterning: Evidence from the Middle Stone Age bearing sea cave of Pinnacle Point 13B (Western Cape, South Africa)." Journal of Human Evolution **59**(3): 306-320.

Herries, A.I.R, Z. Jacobs, M. Bar-Mathews, P. Karkanas, E. Fisher, R. Pickering, G. Goldberg, J. Thompson, T. Matthews, C.W. Marean (in prep) " One million year life history of a quartzite sea cave (PP9) at Pinnacle Point, southern Cape Coast, South Africa"

Hoare, D. B., L. Mucina, M. C. Rutherford, J. H. J. Vlok, D. I. W. Euston-Brown, A. R. Palmer, . . . R. A. Ward (2006). Albany Thicket Biome. The Vegetation of South Africa, Lesotho, and Swaziland. Pretoria, South African National Biodiversity Institute**:** 540-567

Hopley, P. J., A. G. Latham and J. D. Marshall (2006). "Palaeoenvironments and palaeodiets of mid-Pliocene micromammals from Makapansgat Limeworks, South Africa: a stable isotope and dental microwear approach." Palaeogeography, Palaeoclimatology, Palaeoecology **233**(3): 235-251.

Hynek, S. A., B. H. Passey, J. L. Prado, F. H. Brown, T. E. Cerling and J. Quade (2012). "Small mammal carbon isotope ecology across the Miocene-Pliocene boundary, northwestern Argentina." Earth and Planetary Science Letters **321-322**(0): 177-188.

Inger, R., A. Jackson, A. Parnell and S. Bearhop. (n.d.). "SIAR V4 (Stable Isotope Analysis in R): An Ecologist's Guide." from https://http://www.tcd.ie/Zoology/research/research/theoretical/siar/SIAR_For_Ecologists.pdf.

Ingman, M., H. Kaessmann, S. Paàbo and U. Gyllensten (2000). "Mitochondrial genome variation and the origin of modern humans." Nature **408**(6813): 708-713.

Jacobs, Z. (2010). "An OSL chronology for the sedimentary deposits from Pinnacle Point Cave 13B, a punctuated presence." Journal of Human Evolution **59**(3): 289-305.

Jarvis, J. U. M. (2013). Bathyergus suillus (Cape Dune Mole Rat). Mammals of Africa. J. Kingdon, D. Happold, T. Butynskiet al, Bloomsbury **III:** 646-648.

Jim, S., S. H. Ambrose and R. P. Evershed (2004). "Stable carbon isotopic evidence for differences in the dietary origin of bone cholesterol, collagen and apatite: implications for their use in palaeodietary reconstruction." Geochimica et Cosmochimica Acta **68**(1): 61-72.

Karkanas, P. and P. Goldberg (2010). "Site formation processes at Pinnacle point Cave 13B (Mossel Bay, Western Cape Province, South Africa): resolving stratigraphic and depositional complexities with micromorphology." Journal of Human Evolution **59**(3): 256-273.

Kesner, M., A. V. Linzey and C. T. Chimimba (2013). "*Aethomys namaquensis* (Namaqua Veld Rat)". Mammals of Africa. J. Kingdon, D. Happold, T. Butynski*et al.* Volume **III:** 370-371.

Kimura, Y., L. L. Jacobs, T. E. Cerling, K. T. Uno, K. M. Ferguson, L. J. Flynn and R. Patnaik (2013). "Fossil mice and rats show isotopic evidence of niche partitioning and change in dental ecomorphology related to dietary shift in late Miocene of Pakistan." PloS one **8**(8): e69308.

Kingdon, J., D. Happold, T. Butynski, M. Hoffmann, M. Happold and J. Kalina (2013). Mammals of Africa, A&C Black.

Klein, R. G. (1972). "The late quaternary mammalian fauna of Nelson Bay Cave (Cape Province, South Africa): Its implications for megafaunal extinctions and environmental and cultural change." Quaternary Research **2**: 135-142.

Klein, R. G. (1974). "Environment and subsistence of prehistoric man in the Southern Cape province, South Africa." World Archaeology **5**: 249-289.

Klein, R. G. (1976). "The mammalian fauna of the Klasies River Mouth sites, southern Cape Province, South Africa." South African Archaeological Bulletin **31**: 75-98.

Klein, R. G. (1989). "Why Does Skeletal Part Representation Differ Between Smaller and Larger Bovids at Klasies River Mouth and Other Archeological Sites?" Journal of Archaeological Science **6**(4): 363-381.

Klein, R. G. (1980). "Environmental and ecological implications of large mammals from upper pleistocene and holocene sites in southern africa." Annals of the South African Museum **81**: 223-283.

Klein, R. G. (1999). The Human Career: Human Biological and Cultural Origins. Chicago, University of Chicago Press.

Klein, R. G., H. J. Deacon, Q. B. Hendey and J. J. N. Lambrechts (1983). Palaeoenvironmental implications of quaternary large mammals in the fynbos region. Fynbos palaeoecology: a preliminary synthesis**:** 116-138.

Koch, P. L. (1998). "Isotopic reconstruction of past continental environments." Annual Review of Earth and Planetary Sciences **26**(1): 573-613.

Koch, P. L., N. Tuross and M. L. Fogel (1997). "The effects of sample treatment and diagenesis on the isotopic integrity of carbonate in biogenic hydroxylapatite." Journal of Archaeological Science **24**(5): 417-429.

Kohn, M. J., M. J. Schoeninger and W. W. Barker (1999). "Altered states: effects of diagenesis on fossil tooth chemistry." Geochimica et cosmochimica acta **63**(18): 2737-2747

Kohn, M. J. (2010). "Carbon isotope compositions of terrestrial C_3 plants as indicators of (paleo)ecology and (paleo)climate." Proceedings of the National Academy of Sciences of the United States of America **107**(46): 19691-19695.

Kohn, M. J., M. J. Schoeninger and J. W. Valley (1996). "Herbivore tooth oxygen isotope compositions: Effects of diet and physiology." Geochimica et Cosmochimica Acta **60**(20): 3889-3896.

Kohn, M. J., M. J. Schoeninger and W. W. Barker (1999). "Altered states: effects of diagenesis on fossil tooth chemistry." Geochimica et Cosmochimica Acta **63**(18): 2737-2747.

Körner, C., G. D. Farquhar and S. C. Wong (1991). "Carbon isotope discrimination by plants follows latitudinal and altitudinal trends." Oecologia **88**(1): 30-40.

Kuman, K. and R. J. Clarke (2000). "Stratigraphy, artefact industries and hominid associations for Sterkfontein, Member 5." Journal of Human Evolution **38**(6): 827-847

Lahr, M. M. and R. Foley (1994). "Multiple dispersals and modern human origins." Evolutionary Anthropology: Issues, News, and Reviews **3**(2): 48-60.

Lahr, M. M. and R. A. Foley (1998). "Towards a theory of modern human origins: geography, demography, and diversity in recent human evolution." Yearbook of Physical Anthropology **41**: 137-176.

Lansing, S., A. L. Rector, K. E. Reed, J. Lee-Thorp and C. W. Marean (2009). Taphonomic, Taxonomic and Isotopic Analyses of A Marine Isotope Stage 6 Carnivore Den from Pinnacle Point, Mossel Bay, South Africa. Annual Meeting of the Paleoanthropology Society. Chicago, Ill.

Latimer, A. M., J. A. Silander Jr, A. G. Rebelo and G. F. Midgley (2009). "Experimental biogeography: the role of environmental gradients in high geographic diversity in Cape Proteaceae." Oecologia **160**(1): 151-162.

Lee-Thorp, J. A. (1989). "Stable carbon isotopes in deep time: the diets of fossil fauna and hominids." PhD Dissertation, University of Cape Town.

Lee-Thorp, J. (2002). "Two decades of progress towards understanding fossilization processes and isotopic signals in calcified tissue minerals." Archaeometry **44**(3): 435-446.

Lee-Thorp, J. A. and P. B. Beaumont (1995). "Vegetation and seasonality shifts during the late Quaternary deduced from 13C/12C ratios of grazers at Equus Cave, South Africa." Quaternary Research **43**(3): 426-432.

Lee-Thorp, J. and N. J. Van Der Merwe (1987). "Carbon isotope analysis of fossil bone apatite." South African Journal of Science; v. **83**(11) p. 712-715

Lee-Thorp, J. A., J. C. Sealy and N. J. Van Der Merwe (1989). "Stable carbon isotope ratio differences between bone collagen and bone apatite, and their relationship to diet." Journal of Archaeological Science **16**(6): 585-599

Lee-Thorp, J.A., Manning, L. and M. Sponheimer (1997) “Problems and prospects for carbon isotope analysis of very small samples of fossil tooth enamel” Bulletin de la Societe Geologique de France **168**: 767-773

Lindars, E. S., S. T. Grimes, D. P. Mattey, M. E. Collinson, J. J. Hooker and T. P. Jones (2001). "Phosphate $\delta^{18}O$ determination of modern rodent teeth by direct laser fluorination: an appraisal of methodology and potential application to palaeoclimate reconstruction." Geochimica et Cosmochimica Acta **65**(15): 2535-2548.

Llorens, L., J. Peñuelas and M. Estiarte (2003a). "Ecophysiological responses of two Mediterranean shrubs, Erica multiflora and Globularia alypum, to experimentally drier and warmer conditions." Physiologia Plantarum **119**(2): 231-243.

Llorens, L., J. Penuelas and I. Filella (2003b). "Diurnal and seasonal variations in the photosynthetic performance and water relations of two co-occurring Mediterranean shrubs, Erica multiflora and Globularia alypum." Physiologia Plantarum **118**(1): 84-95.

Longinelli, A., P. Iacumin, S. Davanzo and V. Nikolaev (2003). "Modern reindeer and mice: revised phosphate-water isotope equations." Earth and Planetary Science Letters **214**(3-4): 491-498.

Lötter, D., E. A. van Garderen, M. Tadross and A. J. Valentine (2014). "Seasonal variation in the nitrogen nutrition and carbon assimilation in wild and cultivated Aspalathus linearis (rooibos tea)." Australian Journal of Botany **62**(1): 65-73.

Lutjeharms, J. R. E., P. M. S. Monteiro, P. D. Tyson and D. Obura (2001). "The oceans around southern Africa and regional effects of global change." South African Journal of Science **97**: 119-130.

Luyt, J., J. Lee-Thorp and G. Avery (2000). "New light on Middle Pleistocene west coast environments from Elandsfontein, Western Cape Province, South Africa." South African Journal of Science **96**(7).

Marean, C. W. (1986a). "On the seal remains from Klasies River Mouth: an evaluation of Binford's interpretation." Current Anthropology **27**(4): 365-368.

Marean, C. W. (1986b). "Seasonality and Seal Exploitation in the South-western Cape, South Africa." The African Archaeological Review **4**: 135-149.

Marean, C. W. (2010). "Pinnacle Point Cave 13B (Western Cape Province, South Africa) in context: the Cape floral kingdom, shellfish, and modern human origins." Journal of Human Evolution **59**(3): 425-443.

Marean, C. W. (2011). “Coastal South Africa and the co-evolution of the modern human lineage and coastal adaptations.” Trekking the Shore: Changing Coastlines and the Antiquity of Coastal Settlement. N. Bicho, J. A. Haws and L. G. Davis. New York, Springer: 421-440.

Marean, C. W. (2014). "The origins and significance of coastal resource use in Africa and Western Eurasia." Journal of Human Evolution **77**(0): 17-40.

Marean, C. W., Z. Assefa and A. B. Stahl (2005). The Middle and Upper Pleistocene African record for the biological and behavioral origins of modern humans African Archaeology. New York, Blackwell**:** 93-129.

Marean, C., P. Nilssen, K. Brown, A. Jerardino and D. Stynder (2004). "Paleoanthropological investigations of Middle Stone Age sites at Pinnacle Point, Mossel Bay (South Africa): Archaeology and hominid remains from the 2000 field season." PaleoAnthropology **5**(2): 14-83.

Marean, C. W., M. Bar-Matthews, J. Bernatchez, E. Fisher, P. Goldberg, A. I. R. Herries, . . . H. M. Williams (2007). "Early human use of marine resources and pigment in South Africa during the Middle Pleistocene." Nature **449**: 905-908.

Marean, C. W., M. Bar-Matthews, E. Fisher, P. Goldberg, A. Herries, P. Karkanas, . . . E. Thompson (2010). "The stratigraphy of the Middle Stone Age sediments at

Pinnacle Point Cave 13B (Mossel Bay, Western Cape Province, South Africa)." Journal of Human Evolution **59**(3-4): 234-255.

Marean, C. W., P. J. Nilssen, K. Brown, A. Jerardino and D. Stynder (2004). "Paleoanthropological investigations of Middle Stone Age sites at Pinnacle Point, Mossel Bay (South Africa): Archaeology and hominid remains from the 2000 Field Season." Journal of Paleoanthropology **2**: 14-83.

Marean, C. W., H.C. Cawthra, R.M. Cowling, K.J. Esler, E. Fisher, A. Milewski, A.J. Potts, E. Singels, and J. De Vynck (2014). "Stone Age People in a Changing South African Greater Cape Floristic Region". Fynbos: Ecology, Evolution, and Conservation of a Megadiverse Region. N. Allsopp, J. F. Colville and T. Verboom. Oxford, Oxford University Press: 164-199.

Maree, S., Faulkes, C. and Griffin, M. 2008. *Bathyergus suillus*. The IUCN Red List of Threatened Species 2008: e.T2620A9462799 Downloaded August 2012, from http://www.iucnredlist.org/details/2620/0.

Matthews, T. (2004). The taxonomy and taphonomy of Mio-Pliocene and Late Middle Pleistocene micromammals from the Cape west coast, South Africa PhD Thesis, University of Cape Town, South Africa.

Matthews, T. (n.d.). "A summary of the micromammal population from PP30 (Brown hyaena den)". Unpublished report.

Matthews, T., C. Denys and J. E. Parkington (2005). The palaeoecology of the micromammals from the late Middle Pleistocene site of Hoedjiespunt 1 (Cape Province, South Africa). Journal of Human Evolution **49**(4): 432-451

Matthews, T., C. Denys and J. E. Parkington (2006). "An analysis of the mole rats (Mammalia: Rodentia) from Langebaanweg (Mio-Pliocene, South Africa)." Geobios **39**(6): 853-864.

Matthews, T., C. Marean and P. Nilssen (2009). "Micromammals from the Middle Stone Age (92 - 167 ka) at Cave PP13B, Pinnacle Point, south coast, South Africa." Paleontol. Afr **44**: 112-120.

Matthews, T., A. Rector, Z. Jacobs, A. I. R. Herries and C. W. Marean (2011). "Environmental implications of micromammals accumulated close to the MIS6 to MIS5 transition at Pinnacle Point Cave 9 (Mossel Bay, Western Cape Province, South Africa)." Palaeogeography, Palaeoclimatology, Palaeoecology. **302**(3-4): 213-229

Mauffrey, J.-F. and F. Catzeflis (2003). "Ecological and isotopic discrimination of syntopic rodents in a neotropical rain forest of French Guiana." Journal of Tropical Ecology **19**(02): 209-214.

McBrearty, S. and A. S. Brooks (2000). "The revolution that wasn't: a new interpretation of the origin of modern human behavior." Journal of Human Evolution **39**: 453-563.

McDougall, I., F. H. Brown and J. G. Fleagle (2005). "Stratigraphic placement and age of modern humans from Kibish, Ethiopia." Nature **433**: 733-736.

Meadows, M. E. and A. J. Baxter (1999). "Late Quaternary Palaeoenvironments of the southwestern Cape, South Africa: a regional synthesis." Quaternary International **57-58**: 193-206.

Michaud, A. (2007, May 14, 2007). "d13C and d18O of Carbonates." 2014, from http://kfleb.asu.edu/Analytical/gIRMS/Instrumentandanalysis/Analytical/Methods/Carbonates.html.

Mills, M. G. L. (1990). Kalahari Hyenas : Comparative Behavioral Ecology of Two Species, The Blackburn Press.

Milton, S., R. Yeaton, W. Dean and J. Vlok (1997). "Succulent karoo." Vegetation of southern Africa **649**.

Minichillo, T. (2006). "Raw material use and behavioral modernity: Howiesons Poort lithic foraging strategies." Journal of Human Evolution **50**(3): 359-364.

Mitchell, P. (2002). The Archaeology of Southern Africa. Cambridge, Cambridge University Press.

Monadjem, A. (1997). "Stomach contents of 19 species of small mammals from Swaziland." Ibis **113**: 194-202.

Mooney, H. A., J. H. Troughton and J. A. Berry (1977). "Carbon isotope ratio measurements of succulent plants in southern Africa." Oecologia **30**(4): 295-305.

Mucina, L., M. C. Rutherford and L. W. Powrie (2006). Vegetation Atlas of South Africa, Lesotho and Swaziland. The Vegetation of South Africa, Lesotho, and Swaziland. Pretoria, South African National Biodiversity Institute**:** 748-790.

Muller, M. J. and P. D. Tyson (1988). "Winter rainfall over the interior of South Africa during extreme dry years." South African Geographical Journal **70**: 20-30.

Navarro, N., C. Lécuyer, S. Montuire, C. Langlois and F. Martineau (2004). "Oxygen isotope compositions of phosphate from arvicoline teeth and Quaternary climatic changes, Gigny, French Jura." Quaternary Research **62**(2): 172-182.

Nielsen-Marsh, C. M. and R. E. M. Hedges (2000). "Patterns of diagenesis in Bone II: Effects of acetic acid treatment and the removal of diagenetic CO2/3." Journal of Archaeological Science **27**: 1151-1159.

Oestmo, S. and C. W. Marean (2014). Pinnacle Point: Excavation and Survey Methods. In Smith C. (ed.) Encyclopedia of Global Archaeology, New York: Springer.

O'Leary, M. H. (1988). "Carbon isotopes in photosynthesis." BioScience: 328-336.

Parnell, A. and A. Jackson (2013). Stable Isotope Analysis in R. https://cran.r-project.org/web/packages/siar/siar.pdf

Parnell, A. C., R. Inger, S. Bearhop and A. L. Jackson (2010). "Source partitioning using stable isotopes: coping with too much variation." PloS one **5**(3): e9672.

Partridge, T. C., P. B. deMenocal, S. A. Lorentz, M. J. Paiker and J. C. Vogel (1997). "Orbital forcing of climate over South Africa: a 200,000-year rainfall record from the Pretoria Saltpan." Quaternary Science Reviews **16**(10): 1125-1133.

Passey, B. H. and T. E. Cerling (2006). "In situ stable isotope analysis (^{13}C, ^{18}O) of very small teeth using laser ablation GC/IRMS." Chemical Geology **235**: 238-249.

Passey, B. H., T. F. Robinson, L. K. Ayliffe, T. E. Cerling, M. Sponheimer, M. D. Dearing, . . . J. R. Ehleringer (2005). "Carbon isotope fractionation between diet, breath CO2, and bioapatite in different mammals." Journal of Archaeological Science **32**(10): 1459-1470.

Pearson, O. M. and F. E. Grine (1996). "Morphology of the Border Cave hominid ulna and humerus." South African Journal of Science **92**(5): 231-236.

Peeters, F. J., R. Acheson, G.-J. A. Brummer, W. P. De Ruijter, R. R. Schneider, G. M. Ganssen, . . . D. Kroon (2004). "Vigorous exchange between the Indian and Atlantic oceans at the end of the past five glacial periods." Nature **430**(7000): 661-665.

Phillips, D., S. Newsome and J. Gregg (2005). "Combining sources in stable isotope mixing models: alternative methods." Oecologia **144**(4): 520-527.

Phillips, D. L. (2001). "Mixing models in analyses of diet using multiple stable isotopes: a critique." Oecologia **127**(2): 166-170.

Phillips, D. and P. Koch (2002). "Incorporating concentration dependence in stable isotope mixing models." Oecologia **130**(1): 114-125.

Phillips, D. L., R. Inger, S. Bearhop, A. L. Jackson, J. W. Moore, A. C. Parnell, . . . E. J. Ward (2014). "Best practices for use of stable isotope mixing models in food-web studies." Canadian Journal of Zoology **92**(10): 823-835.

Pickering, R., Z. Jacobs, A. I. R. Herries, P. Karkanas, M. Bar-Matthews, J. D. Woodhead, . . . C. W. Marean (2013). "Paleoanthropologically significant South African sea caves dated to 1.1 - 1.0 million years using a combination of U-Pb, TT-OSL and palaeomagnetism." Quaternary Science Reviews **65**: 39-52.

Podelsak, D. W., A.-M. Torregrossa, J. R. Ehleringer, M. D. Dearing, B. H. Passey and T. E. Cerling (2008). "Turnover of oxygen and hydrogen isotopes in the body water, CO2, hair, and enamel of a small mammal." Geochimica et Cosmochimica Acta **72**(1): 19-35.

Proches, S., R. M. Cowling, P. Goldblatt, J. C. Manning and D. A. Snijman (2006). "An overview of the Cape geophytes." Biological Journal of the Linnean Society **87**(1): 27-43.

Radloff, F. G. T. (2008). The ecology of large herbivores native to the coastal lowlands of the Fynbos Biome in the Western Cape, South Africa, PhD Thesis, Stellenbosch University

Rau, A. J., J. Rogers, J. R. E. Lutjeharms, J. Giraudeau, J. A. Lee-Thorp, M. T. Chen and C. Waelbroeck (2002). "A 450-kyr record of hydrological conditions on the western Agulhas Bank Slope, south of Africa." Marine Geology **180**(1-4): 183-201.

Reason, C. and M. Rouault (2005). "Links between the Antarctic Oscillation and winter rainfall over western South Africa." Geophys. Res. Lett **32**(7): L07705.

Rebelo, A. G., C. Boucher, N. Helme, L. Mucina and M. C. Rutherford (2006). “Fynbos Biome”. The Vegetation of South Africa, Lesotho, and Swaziland. Pretoria, South African National Biodiversity Institute**:** 52-219..

Rector, A. L. and B. C. Verrelli (2010). "Glacial cycling, large mammal community composition, and trophic adaptations in the Western Cape, South Africa." Journal of Human Evolution **58**(1): 90-102.

Rector, A. L. and K. E. Reed (2010). "Middle and late Pleistocene faunas of Pinnacle Point and their paleoecological implications." Journal of Human Evolution **59**(3): 340-357.

Reed, D. N. (2003). Micromammal paleoecology: past and present relationships between African small mammals and their habitats PhD, Stony Brook University.

Reinecke, M. K. (2013). Links between lateral riparian vegetation zones and flow. PhD, Stellenbosch University.

Relethford, J. H. (2008). "Genetic evidence and the modern human origins debate." Heredity **100**(6): 555-563.

Robb, G. N., S. Woodborne and N. C. Bennett (2012). "Subterranean sympatry: an investigation into diet using stable isotope analysis." PloS one **7**(11): e48572.

Roberts, D. L., P. Karkanas, Z. Jacobs, C. W. Marean and R. G. Roberts (2012). "Melting ice sheets 400,000 yr ago raised sea level by 13m: Past analogue for future trends." Earth and Planetary Science Letters **357-358**(0): 226-237.

Rogers, K. L. and Y. Wang (2002). "Stable isotopes in pocket gopher teeth as evidence of a Late Matuyama climate shift in the southern Rocky Mountains." Quaternary Research **57**(2): 200-207.

Rohatgi, A. (2010). "WebPlotDigitizer." 3.6. 2014, from http://arohatgi.info/WebPlotDigitizer

Rosing, M. N., M. Ben-David and R. P. Barry (1998). "Analysis of stable isotope data: AK nearest-neighbors randomization test." The Journal of wildlife management 62(1): 380-388.

Royer, A., C. Lecuyer, S. Montuire, R. Amiot, S. Legendre, G. Cuenca-Bescos, . . . F. Martineau (2013). "What does the oxygen isotope composition of rodent teeth record?" Earth and Planetary Science Letters **361**: 258-271.

Rundel, P. W., K. J. Esler and R. M. Cowling (1999). Ecological and phylogenetic patterns of carbon isotope discrimination in the winter-rainfall flora of the Richtersveld, South Africa, Kluwer Academic Publ.

Rutherford, M. C. and L. Mucina (2006). Introduction. The Vegetation of South Africa, Lesotho, and Swaziland. Pretoria, South African National Biodiversity Institute**:** 3-10.

Saura, A., S. Mas and F. Lloret (2010). "Foliar stable carbon and nitrogen isotopes in woody Mediterranean species with different life form and post-fire regeneration." Plant Biology **12**(1): 125-133.

Schulze, E. D., R. Ellis, W. Schulze, P. Trimborn and H. Ziegler (1996). "Diversity, metabolic types and $\delta^{13}C$ carbon isotope ratios in the grass flora of Namibia in

relation to growth form, precipitation and habitat conditions." Oecologia **106**(3): 352-369.

Scholz, C. A., T. C. Johnson, A. S. Cohen, J. W. King, J. A. Peck, J. T. Overpeck, M R. Talbot et al. (2007) "East African megadroughts between 135 and 75 thousand years ago and bearing on early-modern human origins." Proceedings of the National Academy of Sciences **104**(42):16416-16421

Scott, L., E. S. Vrba, G. H. Denton, T. C. Partridge and L. H. Burckle (1995). Pollen evidence for vegetation and climatic change in southern Africa during the Neogene and Quaternary. Paleoclimate and evolution, with emphasis on human origins. New Haven and London, Yale University Press**:** 65-76.

Sealy, J. C. and van der Merwe (1986). "Isotope Assessment and the Seasonal-Mobility Hypothesis in the Southwestern Cape of South Africa [and Comments and Replies]." Current Anthropology: 135-150.

Sealy, J. (1996). "Seasonality of rainfall around the Last Glacial Maximum as reconstructed from carbon isotope analyses of animal bones from Nelson Bay Cave." South African Journal of Science **92**: 441-444.

Sharp, Z. and T. Cerling (1996). "A laser GC-IRMS technique for in situ stable isotope analyses of carbonates and phosphates." Geochimica et Cosmochimica Acta **60**(15): 2909-2916.

Skinner, J. D., M. A. Haupt, M. Hoffmann and H. M. Dott (1998). "Bone Collecting by Brown Hyaenas *Hyaena brunnea* in the Namib Desert: Rate of Accumulation." Journal of Archaeological Science **25**(1): 69-71.

Skinner, J. D. and R. J. Van Aarde (1991). "Bone collecting by brown hyaenas *Hyaena brunnea* in the central Namib Desert, Namibia." Journal of Archaeological Science **18**(5): 513-523.

Skinner, J. D. and C. T. Chimimba (2005). The mammals of the southern African sub-region, Cambridge University Press.

Smith, B. N. and S. Epstein (1971). "Two Categories of 13C/12C Ratios for Higher Plants 1." Plant Physiology **47**(3): 380-384.

Sponheimer, M. and J. A. Lee-Thorp (1999). "Oxygen Isotopes in Enamel Carbonate and their Ecological Significance." Journal of Archaeological Science **26**(6): 723-728.

Sponheimer, M., and Lee-Thorp, J. A. (2001). “The oxygen isotope composition of mammalian enamel carbonate from Morea Estate, South Africa”. Oecologia **126**(2), 153-157.

Sponheimer, M., J. A. Lee-Thorp, D. J. DeRuiter, J. M. Smith, N. J. van der Merwe, K. Reed, . . . C. Heidelberger (2003a). "Diets of Southern African Bovidae: stable isotope evidence." Journal of Mammalogy **84**(2): 471-479.

Sponheimer, M., T. Robinson, L. Ayliffe, B. Passey, B. Roeder, L. Shipley, . . . J. Ehleringer (2003b). "An experimental study of carbon-isotope fractionation between diet, hair, and feces of mammalian herbivores." Canadian Journal of Zoology **81**(5): 871-876.

Sponheimer, M. and J. A. Lee-Thorp (1999). "Oxygen Isotopes in Enamel Carbonate and their Ecological Significance." Journal of Archaeological Science **26**(6): 723-728.

Sponheimer, M. and J. A. Lee-Thorp (1999). "Alteration of enamel carbonate environments during fossilization." Journal of Archaeological Science **26**(2): 143-150.

Stewart, G. R., M. H. Turnbull, S. Schmidt and P. D. Erskine (1995). "^{13}C natural abundance in plant communities along a rainfall gradient: a biological integrator of water availability." Functional Plant Biology **22**(1): 51-55.

Stuut, J. B., X. Crosta, K. van der Borg and R. Schneider (2004). "Relationship between Antarctic sea ice and southwest African climate during the late Quaternary." Geology **32**(10): 909-912

Sullivan, C. H. and H. W. Krueger (1981). "Carbon isotope analysis of separate chemical phases in modern and fossil bone." Nature **292:** 333-335

Swap, R. J., J. N. Aranibar, P. R. Dowty, W. P. Gilhooly and S. A. Macko (2004). "Natural abundance of 13C and 15N in C_3 and C_4 vegetation of southern Africa: patterns and implications." Global Change Biology **10**(3): 350-358.

Symes, C. T., J. W. Wilson, S. M. Woodborne, Z. S. Shaikh and M. Scantlebury (2013). "Resource partitioning of sympatric small mammals in an African forest-grassland vegetation mosaic." Austral Ecology **38**(6): 721-729.

Taylor, P. J. (2013). “Genus Otomys: Vlei Rats”. Mammals of Africa Volume III: Rodents, Hares and Rabbits .Happold, D. C. D. (ed.). Bloomsbury Publishing, London, United Kingdom,

Thackeray, J. F. (1987). "Late Quaternary environmental changes inferred from small mammalian fauna, southern Africa." Climatic Change **10**(3): 285-305.

Thackeray, J. F., A. van der Venter, J. Lee-Thorp, C. T. Chimimba and J. van Heerden (2003). "Stable carbon isotope analysis of modern and fossil samples of the South

African rodent Aethomys namaquensis." Annals of the Transvaal Museum **40**: 43-46.

Thermo Finnigan (2002). Kiel Carbonate Device Operating Manual.

Thompson, E., H. M. Williams and T. Minichillo (2010). "Middle and late Pleistocene Middle Stone Age lithic technology from Pinnacle Point 13B (Mossel Bay, Western Cape Province, South Africa)." Journal of Human Evolution **59**: 358-377.

Thompson, J. C. (2008). Zooarchaeological tests for modern human behavior at Blombos Cave and Pinnacle Point Cave 13B, southwestern Cape, South Africa, PhD Thesis, Arizona State University.

Thompson, J. C. (2010). "Taphonomic analysis of the Middle Stone Age faunal assemblage from Pinnacle Point Cave 13B, Western Cape, South Africa." Journal of Human Evolution **59**(3-4): 321-339.

Tieszen, L. L., S.K. Imbamba. (1980). "Photosynthetic systems, carbon isotope discrimination and herbivore selectivity in Kenya." African Journal of Ecology **18**(4): 237-242.

Tieszen, L. L., M. M. Senyimba, K. I. Simeon and J. H. Troughton (1979). "The Distribution of C_3 and $\mathbf{C_4}$ Grasses and Carbon Isotope Discrimination along an Altitudinal and Moisture Gradient in Kenya." Oecologia **37**(3): 337-350.

Tieszen, L. L. and T. W. Boutton (1989). Stable carbon isotopes in terrestrial ecosystem research. Stable isotopes in ecological research, Springer**:** 167-195.

Tieszen, L. L. and T. Fagre (1993). Effect of diet quality and composition on the isotopic composition of respiratory CO2, bone collagen, bioapatite, and soft tissues. Prehistoric Human Bone, Springer**:** 121-155.

Tieszen, L. L. (1991). "Natural variations in the carbon isotope values of plants: implications for archaeology, ecology, and paleoecology." Journal of Archaeological Science **18**(3): 227-248.

Tishkoff, S. A. and B. C. Verrelli (2003). "Patterns of human genetic diversity: implications for human evolutionary history and disease." Annual Review of Genomics and Human Genetics **4**(1): 293-340.

Tryon, C. A. and S. McBrearty (2002). "Tephrostratigraphy and the Acheulian to Middle Stone Age transition in the Kapthurin Formation, Kenya." Journal of Human Evolution **42**(1/2): 211-236.

Tyson, P. D. (1999). "Atmospheric circulation changes and paleoclimates of southern Africa." South African Journal of Science **95**: 194-201.

Tutken, T., T. W. Vennemann, H. Janz and E. P. J. Heizmann (2006). "Palaeoenvironment and palaeoclimate of the Middle Miocene lake in the Steinheim basin, SW Germany: A reconstruction from C, O, and Sr isotopes of fossil remains." Palaeogeography, Palaeoclimatology, Palaeoecology **241**(3-4): 457-491

van Andel, T. H. (1989). "Late Pleistocene Sea Levels and the Human Exploitation of the Shore and Shelf of Southern South Africa." Journal of Field Archaeology **16**(2): 133-155.

van den Heuvel, I. M. and J. J. Midgley (2014). "Towards an isotope ecology of Cape Fynbos small mammals." African Zoology **49**(2): 195-202.

van Zinderen Bakker, E. (1976). "The evolution of Late-Quaternary palaeoclimates of southern Africa." Palaeoecology of Africa **9**: 160-202.

Verboom, G. A., J. K. Archibald, F. T. Bakker, D. U. Bellstedt, F. Conrad, L. L. Dreyer, . . . J. F. Henning (2009). "Origin and diversification of the Greater Cape flora: ancient species repository, hot-bed of recent radiation, or both?" Molecular Phylogenetics and Evolution **51**(1): 44-53.

Vogel, J. C. (1978). Recycling of carbon in a forest environment, Oecologia Plantarum **13:** 89-94.

Vogel, J. C., A. Fuls and R. P. Ellis (1978). "The geographical distribution of Kranz grasses in South Africa." South African Journal of Science **74**: 209-215.

Wang, Y. and T. E. Cerling (1994). "A model of fossil tooth and bone diagenesis: implications for paleodiet reconstruction from stable isotopes." Palaeogeography, Palaeoclimatology, Palaeoecology **107**(3-4): 281-289.

Watts, I. (2002). "Ochre in the Middle Stone Age of southern Africa: Ritualized display or hide preservative?" South African Archaeological Bulletin **57**: 1-14.

Watts, I. (2010). "The pigments from Pinnacle Point Cave 13B, Western Cape, South Africa." Journal of Human Evolution **59**(3): 392-411.

Weiguo, L., F. Xiahong, N. Youfeng, Z. Qingle, C. Yunning and A. N. Zhisheng (2005). "δ13C variation of C_3 and C_4 plants across an Asian monsoon rainfall gradient in arid northwestern China." Global Change Biology **11**(7): 1094-1100.

Werner, C. and C. Maguas (2010). "Carbon isotope discrimination as a tracer of functional traits in a Mediterranean macchia plant community." Functional Plant Biology **37**(5): 467-477.

West, A. G., J. J. Midgley and W. J. Bond (2001). "The evaluation of $\delta^{13}C$ isotopes of trees to determine past regeneration environments." Forest Ecology and Management **147**(2): 139-149.

White, T. D., B. Asfaw, D. DeGusta, H. Gilbert, G. D. Richards, G. Suwa and F. Clark Howell (2003). "Pleistocene *Homo sapiens* from Middle Awash, Ethiopia." Nature **423**(6941): 742-747.

Wiesel, I. (2007). "Predatory and foraging behaviour of brown hyenas (*Parahyaena brunnea* (Thunberg, 1820)) at Cape fur seal (Arctocephalus pusillus pusillus Schreber, 1776) colonies."

Wilkins, J., B. J. Schoville, K. S. Brown and M. Chazan (2012). "Evidence for early hafted hunting technology." Science **338**(6109): 942-946.

Williams, H. M. (in prep-a/Chapter 2). Isotope Ecology of the modern Greater Cape Floristic Region, with particular focus on the Pinnacle Point area: metadata analysis of the modern floral stable carbon isotope record and the production of the GCFR-specific Stable Caron Isotope Metadata Set (GSCIMS).

Williams, H. M. (in prep-b/Chapter 3). Isotope Ecology of the modern Greater Cape Floristic Region: the modern micromammal record, with particular attention to new Pinnacle-Point Area-proximate data.

Williams, H. M. (in prep-c/Chapter 4). Micromammal and large fauna stable isotopes from the MIS6 fossil hyena den Pinnacle Point 30 (south coast of South Africa) reveal differences in relative contribution of C_4 grasses to local paleovegetation on different geographic scales.

Williams, H. M. (in prep-d/Chapter 5). Stable carbon isotope analysis of micromammals from deposits straddling the MIS6-MIS5 transition at Pinnacle Point, South Africa suggest small but possibly significant vegetation changes at ~125 ka.

Yeakel, J. D., N. C. Bennett, P. L. Koch and N. J. Dominy (2007). "The isotopic ecology of African mole rats informs hypotheses on the evolution of human diet." Proceedings of the Royal Society B: Biological Sciences **274**(1619): 1723-1730.

APPENDIX A

METADATA SET OF PUBLISHED STABLE CARBON ISOTOPE DATA FOR PLANTS FROM THE GREATER CAPE FLORISTIC REGION (GSCIMS)

Appendix A. GSCIMS metadata, with sources

Collection Locality	Locality Specific	plant description	Taxon	photosynth.	Rainfall	n	δ13C permil VPDB	Citation	Notes
Northern Cape	Brandkaros	tree	*Acacia cf karoo*	C3	winter		-27.7	Rundel et al., 1999	values calculated from ΔC published values
Northern Cape	Akkerdisdraai	eudicot	*Acanthopsis disperma*	C3	winter		-27.6	Rundel et al., 1999	values calculated from ΔC published values
Little Karroo	Robertson Karroo	eudicot, succulent	*Adromischus mamillaris*	CAM	winter		-14.7	Mooney et al., 1977	
Little Karroo	Robertson Karroo	eudicot, succulent	*Adromischus mamillaris*	CAM	winter		-11.8	Mooney et al., 1977	
Eastern Cape	Grahamstown - Hell's Portal	eudicot, succulent	*Adromischus rhombifolius*	CAM	year-round		-14.5	Mooney et al., 1977	
Eastern Cape	Grahamstown - Hell's Portal	eudicot, succulent	*Adromischus rhombifolius*	CAM	year-round		-13.4	Mooney et al., 1977	
Western Cape	Diepwalle Forest	tree	*Afrocarpus falcatus*	C3			-29.1	West et al., 2001	values approximated from graphs in text
Western Cape	Diepwalle Forest	tree	*Afrocarpus falcatus*	C3			-24.9	West et al., 2001	values approximated from graphs in text
Western Cape	Diepwalle Forest	tree	*Afrocarpus falcatus*	C3			-24.5	West et al., 2001	values approximated from graphs in text
Western/Northern Cape	w/in GCFR	eudicot, succulent	*Aizoaceae*	CAM	winter		-18.7	Boom et al., 2014	
Western/Northern Cape	w/in GCFR	eudicot, succulent	*Aizoaceae*	CAM	winter		-16.3	Boom et al., 2014	
Western/Northern Cape	w/in GCFR	eudicot, succulent	*Aizoaceae*	FCAM	winter		-23.2	Boom et al., 2014	
Western Cape		monocot, geophytic	*Allium dregeanum*	C3		12	-24.7	Sealy and van der Merwe, 1986	
Western/Northern Cape	w/in GCFR	monocot, succulent	*Aloe dichomata*	CAM	winter		-18.7	Boom et al., 2014	
Western/Northern Cape	w/in GCFR	monocot, succulent	*Aloe dichomata*	CAM	winter		-15.4	Boom et al., 2014	
Eastern Cape	Grahamstown - Pluto's Vale	monocot, succulent	*Aloe ferox*	CAM	year-round		-14.7	Mooney et al., 1977	
Eastern Cape	Grahamstown - Pluto's Vale	monocot, succulent	*Aloe ferox*	CAM	year-round		-13.3	Mooney et al., 1977	
Western/Northern Cape	w/in GCFR	monocot, succulent	*Aloe maculata*	CAM	winter		-15.9	Boom et al., 2014	
Western Cape	Villiersdorp	monocot, succulent	*Aloe microstigma*	CAM	winter		-14.6	Mooney et al., 1977	
Western Cape	Villiersdorp	monocot, succulent	*Aloe microstigma*	CAM	winter		-14.5	Mooney et al., 1977	
Northern Cape	Akkerdisdraai	monocot, succulent	*Aloe ramosissima*	CAM	winter		-14.2	Rundel et al., 1999	values calculated from ΔC published values
Eastern Cape	Grahamstown - Pluto's Vale	monocot, succulent	*Aloe speciosa*	CAM	year-round		-17.0	Mooney et al., 1977	
Eastern Cape	Grahamstown - Pluto's Vale	monocot, succulent	*Aloe speciosa*	CAM/C3	year-round		-20.3	Mooney et al., 1977	
Northern Cape	Brandkaros	eudicot, succulent	*Anacampseros cf. papyracea*	CAM	winter		-16.8	Rundel et al., 1999	values calculated from ΔC published values
Eastern Cape	Grahamstown - Pluto's Vale	eudicot, succulent	*Anacampseros filamentosa*	CAM	year-round		-15.4	Mooney et al., 1977	
Namibia		grass	*Andropogon sp.*	C4		6	-11.8	Schulze et al., 1999	
Western Cape	New Years Peak	monocot, restionacea	*Anthochortus crinalis*	C3			-25.2	Araya et al., 2010	
Northern Cape	Hellskloof	eudicot, succulent	*Antimima sp.*	CAM/C3	winter		-19.5	Rundel et al., 1999	values calculated from ΔC published values
Western/Northern Cape	w/in GCFR	eudicot, succulent	*Antimima ventricosa cf.*	FCAM	winter		-21.3	Boom et al., 2014	
Western Cape		monocot, acquatic	*Aponogeton distyachos*	C3			-26.9	Sealy and van der Merwe, 1986	
Northern Cape	Akkerdisdraai	shrub, evergreen	*Aptosimum spinescens*	C3	winter		-25.4	Rundel et al., 1999	values calculated from ΔC published values
Western/Northern Cape	w/in GCFR	eudicot	*Argemone ochroleuca*	FCAM	winter		-27.6	Boom et al., 2014	
Western/Northern Cape	w/in GCFR	eudicot, succulent	*Aridaria noctiflora*	FCAM	winter		-22.7	Boom et al., 2014	
	Namib	monocot, grass	*Arstida junciformis*	C4	summer		-11.0	Schulze et al., 1996	
Western Cape	Within GCFR	bush	*Aspalathus linearis*	C3			-28.0	Lotter et al. 2014	
Western Cape	Within GCFR	bush	*Aspalathus linearis*	C3			-25.8	Lotter et al. 2014	
Western/Northern Cape	w/in GCFR	eudicot	*Asteraceae*	C3	winter		-29.0	Boom et al., 2014	
Northern Cape	Hellskloof	eudicot, succulent	*Astridia cf. hallii*	CAM/C3	winter		-18.2	Rundel et al., 1999	values calculated from ΔC published values
Northern Cape	Akkerdisdraai	eudicot, succulent	*Astridia longifolia*	CAM	winter		-16.4	Rundel et al., 1999	values calculated from ΔC published values
Western/Northern Cape	w/in GCFR	monocot	*Astroloba sp.*	CAM	winter		-14.1	Boom et al., 2014	
Northern Cape	McDougall's Bay	shrub, evergreen	*Atriplex cinerea*	CAM	winter		-13.6	Rundel et al., 1999	values calculated from ΔC published values
Northern Cape	Akkerdisdraai	shrub, evergreen	*Berkheya fruticosa*	C3	winter		-25.5	Rundel et al., 1999	values calculated from ΔC published values
Northern Cape	Akkerdisdraai	shrub, evergreen	*Blepharis capensis*	C3	winter		-22.0	Rundel et al., 1999	values calculated from ΔC published values
Northern Cape	Akkerdisdraai	tree	*Boschia albitrunca*	C3	winter		-26.2	Rundel et al., 1999	values calculated from ΔC published values
Eastern Cape	Fish River Karroid Scrub	tree/shrub	*Boscia oleoides*	C3	year-round		-24.1	Mooney et al., 1977	
-33.7233 19.17179	Molenaars	shrub/tree	*Brabejum stellatifolium*	C3			-29.5	Reinecke 2013	
-33.486433 19.529328	Sanddrifskloof	shrub/tree	*Brabejum stellatifolium*	C3			-28.7	Reinecke 2013	
Namib		monocot, grass	*Brachiaria serrata*	C4	summer		-11.5	Schulze et al., 1996	
Eastern Cape	Fish River Karroid Scrub	shrub	*Brachylaena ilicifolia*	C3	year-round		-24.3	Mooney et al., 1977	
Northern Cape	Brandkaros	eudicot, succulent	*Brownanthus neglectus*	CAM/C3	winter		-17.0	Rundel et al., 1999	values calculated from ΔC published values
Northern Cape	Akkerdisdraai	eudicot, succulent	*Brownanthus nucifer*	CAM	winter		-14.8	Rundel et al., 1999	values calculated from ΔC published values
Northern Cape	Hellskloof	eudicot, succulent	*Brownanthus pseudoschlichtianus*	CAM	winter		-13.9	Rundel et al., 1999	values calculated from ΔC published values
Eastern Cape	Grahamstown - Pluto's Vale	monocot, succulent, tu	*Bulbine caulescens*	C3	year-round		-26.4	Mooney et al., 1977	
Western Cape	Riverlands	monocot, restionacea	*Calopsis viminea*	C3			-26.9	Araya et al., 2010	
Western Cape	Riverlands	monocot, restionacea	*Cannomois acuminata*	C3			-27.5	Araya et al., 2010	
Little Karroo	Robertson Karroo	dicot, succlent	*Caralluma mammillaris*	CAM	winter		-14.4	Mooney et al., 1977	

Appendix A. GSCIMS metadata, with sources

Collection Locality	Locality Specific	plant description	Taxon	photosynth.	Rainfall	n	δ13C permil VPDB	Citation	Notes
Western Cape		dicot, succlent	*Carallluma mammillaris*	CAM			-14.4	Sealy and van der Merwe, 1986	
Western Cape		dicot, succlent	*Carallluma mammillaris*	CAM		1	-10.9	Sealy and van der Merwe, 1986	
Western Cape	Villiersdorp	dicot, succlent	*Carallluma sp.*	CAM	winter		-12.5	Mooney et al., 1977	
Western Cape		eudicot, succulent	*Carpabrotus sp.*	C3			-23.2	Sealy and van der Merwe, 1986	
Western/Northern Cape	w/in GCFR	eudicot, succulent	*Cephalophyllum cf*	FCAM	winter		-23.9	Boom et al., 2014	
Western/Northern Cape	w/in GCFR	eudicot, succulent	*Cephalophyllum sp.*	FCAM	winter		-22.2	Boom et al., 2014	
Northern Cape	Akkerdisdraai	eudicot, succulent	*Cephalophyllum sp.*	CAM/C3	winter		-18.2	Rundel et al., 1999	values calculated from ΔC published values
Northern Cape	Akkerdisdraai	eudicot, succulent	*Ceraria fruticulosa*	C3	winter		-21.1	Rundel et al., 1999	values calculated from ΔC published values
Northern Cape	Brandkaros	eudicot, succulent	*Ceraria fruticulosa*	CAM/C3	winter		-20.8	Rundel et al., 1999	values calculated from ΔC published values
Northern Cape	Akkerdisdraai	eudicot, succulent	*Ceraria namaquensis*	C3	winter		-21.8	Rundel et al., 1999	values calculated from ΔC published values
Western Cape	New Years Peak	monocot, restionacea	*Ceratocaryum fimbriatum*	C3			-27.7	Araya et al., 2010	
Western/Northern Cape	w/in GCFR	eudicot, succulent	*Cheiridopsis namaquanum*	CAM	winter		-13.6	Boom et al., 2014	
Northern Cape	Akkerdisdraai	eudicot, succulent	*Cheiridopsis robusta*	CAM/C3	winter		-18.7	Rundel et al., 1999	values calculated from ΔC published values
Western Cape	Riverlands	monocot, restionacea	*Chondropetalum nudum*	C3			-28.7	Araya et al., 2010	
Northern Cape	McDougall's Bay	monocot, grass	*Cladoraphis cyperoides*	CAM	winter		-12.8	Rundel et al., 1999	values calculated from ΔC published values
Western Cape		shrub	*Colpoon compressum*	C3			-26.2	Sealy and van der Merwe, 1986	
Northern Cape	Akkerdisdraai	eudicot, succulent	*Commiphora capensis*	C3	winter		-25.4	Rundel et al., 1999	values calculated from ΔC published values
Western/Northern Cape	w/in GCFR	eudicot, succulent	*Conophytum calculus*	CAM	winter		-14.8	Boom et al., 2014	
Northern Cape	Brandkaros	eudicot, succulent	*Conophytum saxetanum*	CAM	winter		-14.1	Rundel et al., 1999	values calculated from ΔC published values
Northern Cape	Akkerdisdraai	eudicot, succulent	*Conophytum sp.*	CAM	winter		-15.1	Rundel et al., 1999	values calculated from ΔC published values
Eastern Cape	Grahamstown - Pluto's Vale	eudicot, succulent	*Cotyledon orbiculata*	CAM	year-round		-13.7	Mooney et al., 1977	
Western Cape	Villiersdorp	eudicot, succulent	*Cotyledon orbiculata*	CAM	year-round		-11.0	Mooney et al., 1977	
Western Cape	Villiersdorp	eudicot, succulent	*Cotyledon orbiculata*	CAM	winter		-10.9	Mooney et al., 1977	
Western Cape	Villiersdorp	eudicot, succulent	*Cotyledon paniculata*	CAM	winter		-12.1	Mooney et al., 1977	
Western Cape	Villiersdorp	eudicot, succulent	*Cotyledon paniculata*	CAM/C3	winter		-16.9	Mooney et al., 1977	
Eastern Cape	Grahamstown - Hell's Portal	eudicot, succulent	*Cotyledon ramosissima*	CAM	year-round		-13.7	Mooney et al., 1977	
Northern Cape	Akkerdisdraai	eudicot, succulent	*Crassula sencea velutina*	CAM	winter		-13.3	Rundel et al., 1999	values calculated from ΔC published values
Eastern Cape	Grahamstown - Pluto's Vale	eudicot, succulent	*Crassula acutifolia*	CAM	year-round		-15.7	Mooney et al., 1977	
Eastern Cape	Grahamstown - Pluto's Vale	eudicot, succulent	*Crassula acutifolia*	CAM	year-round		-15.7	Mooney et al., 1977	
Eastern Cape	Grahamstown - Pluto's Vale	eudicot, succulent	*Crassula capitella thyrsifolia*	CAM/C3	year-round		-16.9	Mooney et al., 1977	
Eastern Cape	Grahamstown - Hell's Portal	eudicot, succulent	*Crassula cultrata*	CAM	year-round		-14.3	Mooney et al., 1977	
Eastern Cape	Grahamstown - Hell's Portal	eudicot, succulent	*Crassula cultrata*	CAM	year-round		-13.6	Mooney et al., 1977	
Northern Cape	Akkerdisdraai	eudicot, succulent	*Crassula deceptor*	CAM	winter		-14.5	Rundel et al., 1999	values calculated from ΔC published values
Eastern Cape	Grahamstown - Pluto's Vale	eudicot, succulent	*Crassula expansa*	CAM/C3	year-round		-20.3	Mooney et al., 1977	
Little Karroo	Robertson Karroo	eudicot, succulent	*Crassula flava*	CAM/C3	winter		-20.0	Mooney et al., 1977	
Northern Cape	Akkerdisdraai	eudicot, succulent	*Crassula fusca*	CAM	winter		-14.2	Rundel et al., 1999	values calculated from ΔC published values
Western Cape	Villiersdorp	eudicot, succulent	*Crassula lycopodioides*	CAM	winter		-12.8	Mooney et al., 1977	
Eastern Cape	Grahamstown - Pluto's Vale	eudicot, succulent	*Crassula lycopodioides*	CAM/C3	year-round		-18.7	Mooney et al., 1977	
Northern Cape	Akkerdisdraai	eudicot, succulent	*Crassula muscosa*	CAM/C3	winter		-18.2	Rundel et al., 1999	values calculated from ΔC published values
Eastern Cape	Grahamstown - Pluto's Vale	eudicot, succulent	*Crassula orbicula*	CAM	year-round		-15.9	Mooney et al., 1977	
Little Karroo	Robertson Karroo	eudicot, succulent	*Crassula orbicula*	CAM	winter		-11.0	Mooney et al., 1977	
Eastern Cape	Grahamstown - Pluto's Vale	eudicot, succulent	*Crassula perfoliata*	CAM	year-round		-15.0	Mooney et al., 1977	
Eastern Cape	Grahamstown - Pluto's Vale	eudicot, succulent	*Crassula perfoliata*	CAM	year-round		-14.8	Mooney et al., 1977	
Eastern Cape	Grahamstown - Pluto's Vale	eudicot, succulent	*Crassula perforata*	CAM	year-round		-13.1	Mooney et al., 1977	
Eastern Cape	Grahamstown - Pluto's Vale	eudicot, succulent	*Crassula portulacea*	CAM	year-round		-15.0	Mooney et al., 1977	
Eastern Cape	Grahamstown - Pluto's Vale	eudicot, succulent	*Crassula portulacea*	CAM	year-round		-14.3	Mooney et al., 1977	
Eastern Cape	Grahamstown - Hell's Portal	eudicot, succulent	*Crassula rupestris*	CAM	year-round		-14.1	Mooney et al., 1977	
Northern Cape	Akkerdisdraai	eudicot, succulent	*Crassula rupestris*	CAM	winter		-15.1	Rundel et al., 1999	values calculated from ΔC published values
Northern Cape	Akkerdisdraai	eudicot, succulent	*Crassula sp.*	CAM	winter		-14.7	Rundel et al., 1999	values calculated from ΔC published values
Northern Cape	Akkerdisdraai	eudicot, succulent	*Crassula subacaulis*	CAM	winter		-15.4	Rundel et al., 1999	values calculated from ΔC published values
Eastern Cape	Grahamstown - Pluto's Vale	eudicot, succulent	*Crassula tetragona*	CAM	year-round		-16.3	Mooney et al., 1977	
Eastern Cape	Grahamstown - Pluto's Vale	eudicot, succulent	*Crassula tetragona*	CAM	year-round		-14.7	Mooney et al., 1977	
Eastern Cape	Grahamstown - Pluto's Vale	eudicot, succulent	*Crassula tetragona robusta*	CAM	year-round		-15.8	Mooney et al., 1977	
Eastern Cape	Grahamstown - Pluto's Vale	eudicot, succulent	*Crassula tetragona robusta*	CAM	year-round		-12.9	Mooney et al., 1977	
Eastern Cape	Grahamstown - Pluto's Vale	eudicot, succulent	*Crassula trachysantha*	CAM	year-round		-16.9	Mooney et al., 1977	
Eastern Cape	Grahamstown - Pluto's Vale	eudicot, succulent	*Crassula trachysantha*	CAM	year-round		-14.9	Mooney et al., 1977	

Appendix A. GSCIMS metadata, with sources

Collection Locality	Locality Specific	plant description	Taxon	photosynth.	Rainfall	n	δ13C permil VPDB	Citation	Notes
Western/Northern Cape	w/in GCFR	eudicot, succulent	*Crassulaceae*	CAM	winter		-15.6	Boom et al., 2014	
Western/Northern Cape	w/in GCFR	eudicot, succulent	*Crassulaceae*	CAM	winter		-15.1	Boom et al., 2014	
Western/Northern Cape	w/in GCFR	eudicot, succulent	*Crassulaceae*	FCAM	winter		-23.2	Boom et al., 2014	
Western/Northern Cape	w/in GCFR	eudicot, succulent	*Crassulaceae*	FCAM	winter		-22.4	Boom et al., 2014	
Western Cape		monocot, geophytic	*Cyanella hyacinthoides*	C3		3	-26.4	Sealy and van der Merwe, 1986	
Namib		monocot, grass	*Cymbopogon dieterlenii*	C4	summer		-13.4	Schulze et al., 1996	
Namib		monocot, grass	*Cymbopogon excavatus*	C4	summer		-11.7	Schulze et al., 1996	
		monocot, grass	*Cymbopogon marginatus*	C4	x		see Cymbopogon entires		mentioned as a fynbos grass in Cowling 1983
Namib		monocot, grass	*Cymbopogon plurinodis*	C4	summer		-11.6	Schulze et al., 1996	
Namib		monocot, grass	*Cynodon dactylon*	C4	summer		-15.6	Schulze et al., 1996	mentioned as a fynbos grass in Cowling 1983
Gauteng	Rietondale Pretoria	monocot, grass	*Cynodon dactylon*	C4			-12.7	Vogel et al., 1978	value listed as reletive to SMOW; this is impossible and is probably PDB
Western Cape		dicot	*Cyphia digitata digitata*	C3			-23.0	Sealy and van der Merwe, 1986	
Eastern Cape	Grahamstown - Pluto's Vale	tree, succulent	*Cyphostemma quinatum*	CAM	year-round		-14.8	Mooney et al., 1977	
Eastern Cape	Grahamstown - Pluto's Vale	tree, succulent	*Cyphostemma quinatum*	CAM	year-round		-12.3	Mooney et al., 1977	
Northern Cape	Akkerdisdraai	eudicot	*Didelta carnosa*	C3	winter		-25.7	Rundel et al., 1999	values calculated from ΔC published values
Western/Northern Cape	w/in GCFR	eudicot	*Didelta sp.*	C3	winter		-26.6	Boom et al., 2014	
Northern Cape	Akkerdisdraai	shrub	*Didelta spinosa*	C3	winter		-24.9	Rundel et al., 1999	values calculated from ΔC published values
FIND ME	Namib	monocot, grass	*Digitaria eriantha*	C4	summer		-10.0	Schulze et al., 1996	
Western Cape		monocot, geophytic	*Dioscorea elephantipes*	C3			-28.2	Sealy and van der Merwe, 1986	
Northern Cape	Brandkaros	eudicot, succulent	*Dracophilus dealbatus*	CAM	winter		-16.6	Rundel et al., 1999	values calculated from ΔC published values
Northern Cape	Loeriesfontein	monocot, grass	*Dregeochloa calviniensis*	C3			-26.3	Vogel et al., 1978	value listed as reletive to SMOW; this is impossible and is probably PDB
Western/Northern Cape	w/in GCFR	eudicot, succulent	*Drosanthemum schoenlandium*	FCAM	winter		-22.8	Boom et al., 2014	
Northern Cape	Hellskloof	eudicot, succulent	*Drosanthemum sp.*	C3	winter		-18.3	Rundel et al., 1999	values calculated from ΔC published values
Northern Cape	Hellskloof	eudicot, succulent	*Drosanthemum sp.*	CAM/C3	winter		-22.2	Rundel et al., 1999	values calculated from ΔC published values
Northern Cape	Hellskloof	eudicot, succulent	*Drosanthemum uniflorum*	CAM	winter		-15.8	Rundel et al., 1999	values calculated from ΔC published values
Northern Cape	Akkerdisdraai	eudicot, succulent	*Eberlanzia stylosa*	C3	winter		-22.5	Rundel et al., 1999	values calculated from ΔC published values
Western Cape	New Years Peak	monocot, restionacea	*Elegia coleura*	C3			-27.2	Araya et al., 2010	
Western Cape	Riverlands	monocot, restionacea	*Elegia filacea*	C3			-28.0	Araya et al., 2010	
Western Cape	New Years Peak	monocot, restionacea	*Elegia filacea*	C3			-26.3	Araya et al., 2010	
Western Cape	New Years Peak	monocot, restionacea	*Elegia neesii*	C3			-26.5	Araya et al., 2010	
Namib		monocot, grass	*Elionurus muticus*	C4	summer		-11.6	Schulze et al., 1996	mentioned as a fynbos grass in Cowling 1983
KwaZulu-Natal	Zululand	monocot, grass	*Eragrostis capensis*	C4			-13.2	Vogel et al., 1978	value listed as reletive to SMOW; this is impossible and is probably PDB
Namib		monocot, grass	*Eragrostis curvula*	C4	summer		-13.0	Schulze et al., 1996	mentioned as a fynbos grass in Cowling 1983
KwaZulu-Natal	Rietondale Pretoria	monocot, grass	*Eragrostis curvula*	C4			-13.4	Vogel et al., 1978	value listed as reletive to SMOW; this is impossible and is probably PDB
Western/Northern Cape	w/in GCFR	monocot	*Eriospermum sp.*	C3	winter		-25.0	Boom et al., 2014	
Northern Cape	Akkerdisdraai	tree	*Euclea pseudebenus*	C3	winter		-25.2	Rundel et al., 1999	values calculated from ΔC published values
Eastern Cape	Grahamstown - Pluto's Vale	eudicot, succulent	*Euphorbia bothae*	CAM	year-round		-14.6	Mooney et al., 1977	
Eastern Cape	Grahamstown - Pluto's Vale	shrub, succulent	*Euphorbia burmannii*	CAM/C3	year-round		-18.3	Mooney et al., 1977	
Western Cape	Cape Preserve	eudicot, succulent	*Euphorbia caput-medusae*	CAM	winter		-13.3	Mooney et al., 1977	
Northern Cape	Akkerdisdraai	eudicot, succulent	*Euphorbia decussata*	C3	winter		-19.8	Rundel et al., 1999	values calculated from ΔC published values
Northern Cape	Akkerdisdraai	eudicot, succulent	*Euphorbia dregeana*	CAM	winter		-14.0	Rundel et al., 1999	values calculated from ΔC published values
Eastern Cape	Grahamstown - Pluto's Vale	eudicot, succulent	*Euphorbia gorgonis*	CAM	year-round		-12.9	Mooney et al., 1977	
Northern Cape	Akkerdisdraai	eudicot, succulent	*Euphorbia hamata*	CAM/C3	winter		-18.8	Rundel et al., 1999	values calculated from ΔC published values
Eastern Cape	Grahamstown - Pluto's Vale	eudicot, succulent	*Euphorbia inermis*	CAM	year-round		-14.9	Mooney et al., 1977	
Eastern Cape	Grahamstown - Pluto's Vale	eudicot, succulent	*Euphorbia inermis*	CAM	year-round		-13.4	Mooney et al., 1977	
Western/Northern Cape	w/in GCFR	eudicot, succulent	*Euphorbia loricata*	FCAM	winter		-23.6	Boom et al., 2014	
Western/Northern Cape	w/in GCFR	eudicot, succulent	*Euphorbia mauritanica*	FCAM	winter		-22.8	Boom et al., 2014	
Eastern Cape	Grahamstown - Pluto's Vale	shrub, succulent	*Euphorbia mauritanica*	CAM	year-round		-16.9	Mooney et al., 1977	
Little Karroo	Robertson Karroo	shrub, succulent	*Euphorbia mauritanica*	CAM	winter		-16.0	Mooney et al., 1977	
Western Cape	Villiersdorp	shrub, succulent	*Euphorbia mauritanica*	CAM/C3	winter		-22.0	Mooney et al., 1977	
Little Karroo	Robertson Karroo	eudicot, succulent	*Euphorbia nesemannii*	CAM	winter		-11.6	Mooney et al., 1977	
Eastern Cape	Grahamstown - Pluto's Vale	eudicot, succulent	*Euphorbia pentagona*	CAM	year-round		-14.9	Mooney et al., 1977	
Eastern Cape	Grahamstown - Hell's Portal	eudicot, succulent	*Euphorbia polygona*	CAM	year-round		-10.7	Mooney et al., 1977	
Eastern Cape	Grahamstown - Pluto's Vale	eudicot, succulent	*Euphorbia squarrosa*	CAM	year-round		-12.5	Mooney et al., 1977	
Eastern Cape	Grahamstown - Pluto's Vale	eudicot, succulent	*Euphorbia tetragona*	CAM	year-round		-16.9	Mooney et al., 1977	
Eastern Cape	Grahamstown - Hell's Portal	eudicot, succulent	*Euphorbia triangularis*	CAM	year-round		-14.7	Mooney et al., 1977	

Appendix A. GSCIMS metadata, with sources

Collection Locality	Locality Specific	plant description	Taxon	photosynth.	Rainfall	n	δ13C permil VPDB	Citation	Notes
Namib		monocot, true grass	*Eustachys paspaloides*	C4	summer		-12.6	Schulze et al., 1996	mentioned as a fynbos grass in Cowling 1983
Northern Cape	Akkerdisdraai	shrub, evergreen	*Ficus cordata*	C3	winter		-23.2	Rundel et al., 1999	values calculated from ΔC published values
Western Cape		dicot, geophytic	*Fockea comaru*	C3			-24.2	Sealy and van der Merwe, 1986	
Northern Cape	Akkerdisdraai	shrub, evergreen	*Forsskaolea candida*	C3	winter		-21.3	Rundel et al., 1999	values calculated from ΔC published values
Western/Northern Cape	w/in GCFR	shrub	*Galenia africana*	FCAM	winter		-23.8	Boom et al., 2014	
Northern Cape	Akkerdisdraai	shrub, evergreen	*Galenia ssarcophylla*	C3	winter		-26.0	Rundel et al., 1999	values calculated from ΔC published values
Little Karroo	Robertson Karroo	monocot, succulent	*Gasteria pillansii*	CAM	winter		-12.4	Mooney et al., 1977	
Northern Cape	Akkerdisdraai	eudicot	*Gazania lichtensteinii*	C3	winter		-25.3	Rundel et al., 1999	values calculated from ΔC published values
Eastern Cape	Fish River Karroid Scrub	bush	*Grewia robusta*	C3	year-round		-24.7	Mooney et al., 1977	
Western Cape		eudicot	*Grielum humufusum*	C3		5	-26.3	Sealy and van der Merwe, 1986	
Little Karroo	Robertson Karroo	monocot, succulent	*Haworthia margaritifera*	CAM	winter		-13.0	Mooney et al., 1977	
Little Karroo	Robertson Karroo	monocot, succulent	*Haworthia margaritifera*	CAM	winter		-12.1	Mooney et al., 1977	
Northern Cape	Akkerdisdraai	eudicot	*Heibenstreitia sp.*	C3	winter		-27.0	Rundel et al., 1999	values calculated from ΔC published values
Northern Cape	Akkerdisdraai	eudicot	*Heliophila sp.*	C3	winter		-28.2	Rundel et al., 1999	values calculated from ΔC published values
Namib		monocot, true grass	*Heteropogon contortus*	C4	summer		-12.1	Schulze et al., 1996	mentioned as a fynbos grass in Cowling 1983
Western Cape		eudicot, succulent	*Hoodia sp.*	CAM			-11.9	Sealy and van der Merwe, 1986	
Western Cape		parasite on succulent	*Hydnora africana*	achlorophyllous			-11.4	Sealy and van der Merwe, 1986	
Northern Cape	Akkerdisdraai	eudicot	*Hyperia sp.*	C3	winter		-24.2	Rundel et al., 1999	values calculated from ΔC published values
Northern Cape	Akkerdisdraai	shrub, evergreen	*Hypertelis salsoloides*	C3	winter		-22.8	Rundel et al., 1999	values calculated from ΔC published values
Western Cape		dicot	*Hypertelis salsoloides*	C3			-23.7	Sealy and van der Merwe, 1986	
Little Karroo	Robertson Karroo	dicot, succlent	*Hypertelis salsoloides*	C3	winter		-23.7	Mooney et al., 1977	
Western Cape	New Years Peak	monocot, restionacea	*Hypodiscus arescens*	C3			-28.1	Araya et al., 2010	
Western Cape	Riverlands	monocot, restionacea	*Hypodiscus willdenowia*	C3			-27.8	Araya et al., 2010	
Namib		monocot, true grass	*Imperata cylindrica*	C4	summer		-12.2	Schulze et al., 1996	mentioned as a fynbos grass in Cowling 1983
Northern Cape	Akkerdisdraai	eudicot	*Indigofera sp.*	C3	winter		-22.7	Rundel et al., 1999	values calculated from ΔC published values
Western Cape	Riverlands	monocot, restionacea	*Ischyrolepis capense*	C3			-28.2	Araya et al., 2010	
Western Cape	New Years Peak	monocot, restionacea	*Ischyrolepis curviramis*	C3			-26.8	Araya et al., 2010	
Western Cape	Riverlands	monocot, restionacea	*Ischyrolepis monanthos*	C3			-27.5	Araya et al., 2010	
Northern Cape	Akkerdisdraai	eudicot, succulent	*Jatropha orangeana*	C3	winter		-24.3	Rundel et al., 1999	values calculated from ΔC published values
Eastern Cape	Grahamstown - Pluto's Vale	dicot, succlent	*Kalanchoe rotundifolia*	CAM	year-round		-15.3	Mooney et al., 1977	
Northern Cape	Akkerdisdraai	monocot, grass	*Karoochloa sp.*	CAM	winter		-13.3	Rundel et al., 1999	values calculated from ΔC published values
Northern Cape	Akkerdisdraai	monocot, geophytic	*Lachenalia sp.*	C3	winter		-25.4	Rundel et al., 1999	values calculated from ΔC published values
Western Cape	Ceres	monocot, grass	*Lasiochola longifolia*	C3			-27.6	Vogel et al., 1978	value listed as reletive to SMOW; this is impossible and is probably PDB
Northern Cape	Akkerdisdraai	eudicot, succulent	*Leipoldtia schultzei*	C3	winter		-23.6	Rundel et al., 1999	values calculated from ΔC published values
Northern Cape	Hellskloof	eudicot, succulent	*Leipoldtia schultzei*	C3	winter		-22.4	Rundel et al., 1999	values calculated from ΔC published values
Northern Cape	Akkerdisdraai	eudicot, succulent	*Leipoldtia weigangiana*	C3	winter		-25.4	Rundel et al., 1999	values calculated from ΔC published values
Western Cape		dicot	*Leucadendron conocarpodendron*	C3		3	-28.6	van de Heuvel and Midgley, 2014	
Western Cape		dicot	*Leucadendron laureolum*	C3		6	-23.9	van de Heuvel and Midgley, 2014	
Western Cape		dicot	*Leucadendron salignum*	C3		6	-28.5	van de Heuvel and Midgley, 2014	
Western Cape		dicot	*Leucadendron salignum*	C3		3	-25.9	van de Heuvel and Midgley, 2014	
Western Cape		dicot	*Leucadendron sessile*	C3		6	-28.7	van de Heuvel and Midgley, 2014	
Western Cape		dicot	*Leucadendron sessile*	C3		2	-26.6	van de Heuvel and Midgley, 2014	
Western/Northern Cape	w/in GCFR	eudicot, succulent	*Lithops sp.*	CAM	winter		-14.8	Boom et al., 2014	
Western/Northern Cape	w/in GCFR	shrub	*Lycium ferocissimum*	C3	winter		-26.1	Boom et al., 2014	
Northern Cape	Brandkaros	eudicot, succulent	*Mesembryanthemum hypertrophicu*	CAM	winter		-12.7	Rundel et al., 1999	values calculated from ΔC published values
Northern Cape	Akkerdisdraai	eudicot, succulent	*Mesembryanthemum sp.*	CAM/C3	winter		-17.1	Rundel et al., 1999	values calculated from ΔC published values
Northern Cape	Hellskloof	eudicot, succulent	*Mesembryanthemum sp.*	CAM/C3	winter		-16.9	Rundel et al., 1999	values calculated from ΔC published values
Western/Northern Cape	w/in GCFR	eudicot, succulent	*Mesembryanthemum vaginatum*	CAM	winter		-17.0	Boom et al., 2014	
-33.7233 19.17179	Molenaars	shrub/tree	*Metrosideros angustifolia*	C3			-27.9	Reinecke 2013	
-33.486433 19.529328	Sanddrifskloof	shrub/tree	*Metrosideros angustifolia*	C3			-27.6	Reinecke 2013	
Northern Cape	Hellskloof	eudicot, succulent	*Mitrophyllum sp.*	C3	winter		-21.5	Rundel et al., 1999	values calculated from ΔC published values
Northern Cape	Akkerdisdraai	shrub, evergreen	*Monechma mollissimum*	C3	winter		-23.1	Rundel et al., 1999	values calculated from ΔC published values
Western/Northern Cape	w/in GCFR	eudicot, succulent	*Monilaria moniliformis*	FCAM	winter		-22.3	Boom et al., 2014	
Western Cape		monocot, geophytic	*Moraea fugax*	C3		3	-26.7	Sealy and van der Merwe, 1986	
Western Cape	33.25°S, 18.25°E		*multiple?*	C3			-25.6	Robb et al., 2012	
Western Cape	33.25°S, 18.25°E	eudicot	*multiple?*	C3			-28.8	Robb et al., 2013	

Appendix A. GSCIMS metadata, with sources

Collection Locality	Locality Specific	plant description	Taxon	photosynth.	Rainfall	n	δ13C permil VPDB	Citation	Notes
Western Cape	33.25°S, 18.25°E		*multiple?*	C3			-26.1	Robb et al., 2013	
Western Cape	33.25°S, 18.25°E	monocot	*multiple?*	C4? (grass not specified)			-12.6	Robb et al., 2013	
Northern Cape	Akkerdisdraai	eudicot	*Nemesia sp.*	C3	winter		-25.2	Rundel et al., 1999	values calculated from ΔC published values
Western Cape		dicot	*Nylandtia spinosa*	C3			-22.3	Sealy and van der Merwe, 1986	
Western Cape	Diepwalle Forest	tree	*Olea capensis macrocarpa*	C3			-30.5	West et al., 2001	values approximated from graphs in text
Western Cape	Diepwalle Forest	tree	*Olea capensis macrocarpa*	C3			-27.6	West et al., 2001	values approximated from graphs in text
Western Cape	Diepwalle Forest	tree	*Olea capensis macrocarpa*	C3			-27.4	West et al., 2001	values approximated from graphs in text
Western Cape	Diepwalle Forest	tree	*Olea capensis macrocarpa*	C3			-26.4	West et al., 2001	values approximated from graphs in text
Northern Cape	Akkerdisdraai	eudicot	*Osteospermum polycephalum*	C3	winter		-25.6	Rundel et al., 1999	values calculated from ΔC published values
Northern Cape	Akkerdisdraai	eudicot, succulent	*Othonna opima*	C3	winter		-24.3	Rundel et al., 1999	values calculated from ΔC published values
Northern Cape	Akkerdisdraai	eudicot, succulent	*Othonna sp.*	C3	winter		-25.7	Rundel et al., 1999	values calculated from ΔC published values
Northern Cape	Akkerdisdraai	eudicot	*Oxalis sp.*	C3	winter		-27.9	Rundel et al., 1999	values calculated from ΔC published values
Western Cape		eudicot	*Oxalis spp.*	C3			-26.4	Sealy and van der Merwe, 1986	
Northern Cape	Akkerdisdraai	tree	*Ozoroa concolor*	C3	winter		-22.3	Rundel et al., 1999	values calculated from ΔC published values
Northern Cape	Akkerdisdraai	eudicot, succulent	*Pachypodium namaquanum*	C3	winter		-23.2	Rundel et al., 1999	values calculated from ΔC published values
Eastern Cape	Grahamstown - Pluto's Vale	eudicot, succulent	*Pachypodium succelentum*	C3	year-round		-24.7	Mooney et al., 1977	
Eastern Cape	Grahamstown - Pluto's Vale	eudicot, succulent	*Pachypodium succelentum*	C3	year-round		-23.2	Mooney et al., 1977	
Namib	Ondangua	monocot, grass	*Panicum gilvum*	C4			-11.0	Vogel et al., 1978	
Northern Cape	Prieska	monocot, grass	*Panicum lanipea*	C4			-12.6	Vogel et al., 1978	
KwaZulu-Natal	Pretoria	monocot, grass	*Panicum phragmitoides*	C4			-12.7	Vogel et al., 1978	
Northern Cape	Akkerdisdraai	eudicot, succulent	*Pelargonium crithmifolium*	C3	winter		-24.9	Rundel et al., 1999	values calculated from ΔC published values
Northern Cape	Akkerdisdraai	eudicot, succulent	*Pelargonium klinghardtense*	C3	winter		-24.9	Rundel et al., 1999	values calculated from ΔC published values
Eastern Cape	Grahamstown - Pluto's Vale	eudicot, succulent	*Pelargonium peltatum*	CAM	year-round		-16.9	Mooney et al., 1977	
Western Cape	Jonaskop	shrub	*Phaenocoma prolifera*	C3			-26.9	Agenbag 2006	
Eastern Cape	Fish River Karroid Scrub	shrub	*Phyllanthus verrucosus*	C3	year-round		-25.6	Mooney et al., 1977	
Eastern Cape	Fish River Karroid Scrub	shrub	*Phyllanthus verrucosus*	C3	year-round		-24.4	Mooney et al., 1977	
Northern Cape	Akkerdisdraai	eudicot, succulent	*Phyllobolus sinuosus*	C3	winter		-21.1	Rundel et al., 1999	values calculated from ΔC published values
Northern Cape	Helskloof	eudicot, succulent	*Phyllobolus sp.*	CAM	winter		-13.7	Rundel et al., 1999	values calculated from ΔC published values
Northern Cape	Akkerdisdraai	eudicot	*Plexipus garipensis*	C3	winter		-24.0	Rundel et al., 1999	values calculated from ΔC published values
Western Cape	Jonaskop	shrub	*Podalyria sp*	C3			-27.0	Agenbag 2006	
Western Cape	Diepwalle Forest	tree	*Podocarpus latifolis*	C3			-27.5	West et al., 2001	values approximated from graphs in text
Western Cape	Diepwalle Forest	tree	*Podocarpus latifolis*	C3			-23.9	West et al., 2001	values approximated from graphs in text
Western Cape	Diepwalle Forest	tree	*Podocarpus latifolis*	C3			-23.6	West et al., 2001	values approximated from graphs in text
Western Cape	Diepwalle Forest	tree	*Podocarpus latifolis*	C3			-23.6	West et al., 2001	values approximated from graphs in text
Eastern Cape	Grahamstown - Pluto's Vale	shrub, succulent	*Portulacaria afra*	CAM/C3	year-round		-17.5	Mooney et al., 1977	
Western Cape		monocot	*Prionium serratum*	C3			-27.0	Sealy and van der Merwe, 1986	
Western Cape	Jonaskop 1550	bush	*Protea aurea*	C3			-31.1	Latimer et al., 2009	values calculated from sup figure
Western Cape	Nature's valley	bush	*Protea aurea*	C3			-29.5	Latimer et al., 2009	values calculated from sup figure
Western Cape	Swartberg Pass	bush	*Protea aurea*	C3			-29.2	Latimer et al., 2009	values calculated from sup figure
Western Cape	Jonaskop 950m	bush	*Protea aurea*	C3			-27.9	Latimer et al., 2009	values calculated from sup figure
Western Cape	Jonaskop 744m	bush	*Protea aurea*	C3			-26.0	Latimer et al., 2009	values calculated from sup figure
Western Cape	Jonaskop 1550	bush	*Protea mundii*	C3			-31.3	Latimer et al., 2009	values calculated from sup figure
Western Cape	Jonaskop 950m	bush	*Protea mundii*	C3			-29.7	Latimer et al., 2009	values calculated from sup figure
Western Cape	Nature's valley	bush	*Protea mundii*	C3			-29.5	Latimer et al., 2009	values calculated from sup figure
Western Cape	Swartberg Pass	bush	*Protea mundii*	C3			-29.4	Latimer et al., 2009	values calculated from sup figure
Western Cape	Jonaskop 744m	bush	*Protea mundii*	C3			-27.2	Latimer et al., 2009	values calculated from sup figure
Western Cape	Jonaskop 1550	bush	*Protea punctata*	C3			-29.7	Latimer et al., 2009	values calculated from sup figure
Western Cape	Nature's valley	bush	*Protea punctata*	C3			-29.3	Latimer et al., 2009	values calculated from sup figure
Western Cape	Swartberg Pass	bush	*Protea punctata*	C3			-28.4	Latimer et al., 2009	values calculated from sup figure
Western Cape	Jonaskop 950m	bush	*Protea punctata*	C3			-28.1	Latimer et al., 2009	values calculated from sup figure
Western Cape	Jonaskop 744m	bush	*Protea punctata*	C3			-25.8	Latimer et al., 2009	values calculated from sup figure
Western Cape	Jonaskop 950m	bush	*Protea subvestia*	C3			-27.3	Latimer et al., 2009	values calculated from sup figure
Northern Cape	Brandkaros	eudicot, succulent	*Psammophora modesta*	CAM	winter		-16.0	Rundel et al., 1999	values calculated from ΔC published values
Western/Northern Cape	w/in GCFR	eudicot	*Psilocaulon junceum*	CAM	winter		-17.5	Boom et al., 2014	
Northern Cape	Hellskloof	eudicot, succulent	*Psilocaulon sp.*	CAM	winter		-15.1	Rundel et al., 1999	values calculated from ΔC published values
Western Cape	New Years Peak	monocot, restionacea	*Restio bolusii*	C3			-25.9	Araya et al., 2010	

Appendix A. GSCIMS metadata, with sources

Collection Locality	Locality Specific	plant description	Taxon	photosynth.	Rainfall	n	δ13C permil VPDB	Citation	Notes
Western Cape	New Years Peak	monocot, restionacea	*Restio obscurus*	C3			-27.5	Araya et al., 2010	
Western Cape	New Years Peak	monocot, restionacea	*Restio pedicellatus*	C3			-27.1	Araya et al., 2010	
Northern Cape	Akkerdisdraai	shrub	*Rhus populifolia*	C3	winter		-24.2	Rundel et al., 1999	values calculated from ΔC published values
Northern Cape	Akkerdisdraai	tree	*Rhus undulata*	C3	winter		-22.7	Rundel et al., 1999	values calculated from ΔC published values
Western/Northern Cape	w/in GCFR	dicot, succlent	*Ruschia burtoieae*	FCAM	winter		-22.7	Boom et al., 2014	
Western Cape	Villiersdorp	dicot, succlent	*Ruschia caroli*	C3	winter		-23.7	Mooney et al., 1977	
Western Cape	Villiersdorp	dicot, succlent	*Ruschia caroli*	C3	winter		-23.1	Mooney et al., 1977	
Northern Cape	Akkerdisdraai	eudicot, succulent	*Ruschia schneideriana*	CAM	winter		-15.6	Rundel et al., 1999	values calculated from ΔC published values
Western/Northern Cape	w/in GCFR	eudicot, succulent	*Ruschia sp*	FCAM	winter		-24.0	Boom et al., 2014	
Western/Northern Cape	w/in GCFR	eudicot, succulent	*Ruschia sp.*	CAM	winter		-17.0	Boom et al., 2014	
Northern Cape	Akkerdisdraai	eudicot, succulent	*Ruschia sp.*	CAM/C3	winter		-18.3	Rundel et al., 1999	values calculated from ΔC published values
Northern Cape	Akkerdisdraai	eudicot, succulent	*Ruschia sp.*	CAM/C3	winter		-17.9	Rundel et al., 1999	values calculated from ΔC published values
Northern Cape	Hellskloof	eudicot, succulent	*Ruschia sp.*	CAM/C3	winter		-17.3	Rundel et al., 1999	values calculated from ΔC published values
Western/Northern Cape	w/in GCFR	eudicot, succulent	*Ruschia spinosa*	FCAM	winter		-24.2	Boom et al., 2014	
Western/Northern Cape	w/in GCFR	eudicot, succulent	*Ruschia stricta*	CAM	winter		-17.0	Boom et al., 2014	
Western/Northern Cape	w/in GCFR	eudicot, succulent	*Ruschia tumidula*	FCAM	winter		-24.0	Boom et al., 2014	
Western/Northern Cape	w/in GCFR	eudicot	*Ruschioid*	FCAM	winter		-23.5	Boom et al., 2014	
Western/Northern Cape	w/in GCFR	eudicot	*Ruschioid cf*	CAM	winter		-14.5	Boom et al., 2014	
Western/Northern Cape	w/in GCFR	eudicot	*Ruschioid cf*	FCAM	winter		-20.1	Boom et al., 2014	
-33.486433 19.529328	Sanddrifskloof	shrub/tree	*Salix mucronata*	C3			-30.5	Reinecke 2013	approximated
-33.7233 19.17179	Molenaars	shrub/tree	*Salix mucronata*	C3			-29.0	Reinecke 2013	approximated
Northern Cape	McDougall's Bay	shrub, evergreen	*Salsola nollothensis*	CAM	winter		-11.7	Rundel et al., 1999	values calculated from ΔC published values
Western/Northern Cape	w/in GCFR	eudicot	*Salsola tuberculata*	C4	winter		-13.6	Boom et al., 2014	
Eastern Cape	Grahamstown - Pluto's Vale	monocot, succulent	*Sansevieria thyrsiflora*	CAM	year-round		-13.0	Mooney et al., 1977	
Eastern Cape	Grahamstown - Pluto's Vale	monocot, succulent	*Sansevieria thyrsiflora*	CAM	year-round		-10.6	Mooney et al., 1977	
Northern Cape	Akkerdisdraai	eudicot, succulent	*Sarcocaulon crassicaule*	C3	winter		-25.6	Rundel et al., 1999	values calculated from ΔC published values
Northern Cape	Augrabies	eudicot, succulent	*Sarcostemma viminale*	CAM	winter		-13.2	Rundel et al., 1999	values calculated from ΔC published values
Northern Cape	Akkerdisdraai	tree	*Schotia afra*	C3	winter		-22.8	Rundel et al., 1999	values calculated from ΔC published values
Little Karroo	Robertson Karroo	eudicot, succulent	*Senecia radicans*	CAM/C3	winter		-16.7	Mooney et al., 1977	
Northern Cape	Akkerdisdraai	eudicot, succulent	*Senecio corymbiferus*	C3	winter		-22.2	Rundel et al., 1999	values calculated from ΔC published values
Northern Cape	Akkerdisdraai	eudicot, succulent	*Senecio longiflorus*	CAM/C3	winter		-17.5	Rundel et al., 1999	values calculated from ΔC published values
Western Cape	Jonaskop	shrub	*Serruria gremialis*	C3			-28.1	Agenbag 2006	
Namib		monocot, grass	*Setaria finita*	C4	summer		-11.6	Schulze et al., 1996	
Namib		monocot, grass	*Setaria flabellata*	C4			see Setaria entries		mentioned as a fynbos grass in Cowling 1983
Namib		monocot, grass	*Setaria ustilata*	C4	summer		-11.2	Schulze et al., 1996	
Northern Cape	Akkerdisdraai	eudicot	*Solanum sp*	C3	winter		-26.5	Rundel et al., 1999	values calculated from ΔC published values
Namib		monocot, grass	*Sporobolus africanus*	C4	summer		-13.1	Schulze et al., 1996	mentioned as a fynbos grass in Cowling 1983
Namib		monocot, grass	*Sporobolus fimbriatus*	C4	summer		-13.4	Schulze et al., 1996	mentioned as a fynbos grass in Cowling 1983
KwaZulu-Natal	Rietondale Pretoria	monocot, grass	*Sporobolus fimbriatus*	C4			-13.2	Vogel et al., 1978	value listed as reletive to SMOW; this is impossible and is probably PDB
Western Cape	New Years Peak	monocot, restionacea	*Staberoha cernua*	C3			-26.3	Araya et al., 2010	
Western Cape	Riverlands	monocot, restionacea	*Staberoha distachyos*	C3			-28.5	Araya et al., 2010	
Northern Cape	Akkerdisdraai	monocot, grass	*Stipagrostis sp.*	CAM	winter		-13.2	Rundel et al., 1999	values calculated from ΔC published values
Northern Cape	Hellskloof	eudicot, succulent	*Stoeberia arborescens*	CAM/C3	winter		-17.6	Rundel et al., 1999	values calculated from ΔC published values
Northern Cape	Akkerdisdraai	eudicot, succulent	*Stoeberia frutescens*	CAM	winter		-14.0	Rundel et al., 1999	values calculated from ΔC published values
Northern Cape	Akkerdisdraai	shrub, evergreen	*Sutera tomentosa*	C3	winter		-24.5	Rundel et al., 1999	values calculated from ΔC published values
Northern Cape	Hellskloof	eudicot, succulent	*Synaptophyllum juttae*	CAM/C3	winter		-16.7	Rundel et al., 1999	values calculated from ΔC published values
Northern Cape	Brandkaros	tree	*Tamarix usneoides*	C3	winter		-25.2	Rundel et al., 1999	values calculated from ΔC published values
Northern Cape	Akkerdisdraai	eudicot, succulent	*Tetragonia spicata*	C3	winter		-23.3	Rundel et al., 1999	values calculated from ΔC published values
Western Cape	Riverlands	monocot, restionacea	*Thamnochortus punctatus*	C3			-28.2	Araya et al., 2010	
Namib		monocot, grass	*Themeda triandra*	C4	summer		-11.6	Schulze et al., 1996	
Western/Northern Cape	w/in GCFR	eudicot	*Thesium sp*	C3	winter		-26.8	Boom et al., 2014	
Northern Cape	Akkerdisdraai	monocot, geophytic	*Trachyandra sp.*	C3	winter		-27.5	Rundel et al., 1999	values calculated from ΔC published values
Namib		monocot, grass	*Trachypogon spicatus*	C4	summer		-13.2	Schulze et al., 1996	mentioned as a fynbos grass in Cowling 1983
Eastern Cape	Grahamstown - Pluto's Vale	dicot, succlent	*Trichodiadema*	C3	year-round		-23.6	Mooney et al., 1977	
Namibia		grass	*Tristachya sp.*	C4		2	-11.0	Schulze et al., 1999	
Northern Cape	Akkerdisdraai	eudicot, succulent	*Tylecodon bucholzianus*	CAM	winter		-16.3	Rundel et al., 1999	values calculated from ΔC published values

Appendix A. GSCIMS metadata, with sources

Collection Locality	Locality Specific	plant description	Taxon	photosynth.	Rainfall	n	δ13C permil VPDB	Citation	Notes
Western/Northern Cape	w/in GCFR	eudicot, succulent	*Tylecodon cacalioides*	CAM	winter		-14.1	Boom et al., 2014	
Northern Cape	Akkerdisdraai	eudicot, succulent	*Tylecodon paniculatus*	CAM	winter		-13.2	Rundel et al., 1999	values calculated from ΔC published values
Northern Cape	Akkerdisdraai	eudicot, succulent	*Tylecodon rubrovenosus*	CAM	winter		-13.2	Rundel et al., 1999	values calculated from ΔC published values
Northern Cape	Hellskloof	succulent	*Unknown sp.*	CAM?	winter		-16.1	Rundel et al., 1999	values calculated from ΔC published values
Northern Cape	Akkerdisdraai	eudicot	*Ursinia sp.*	C3	winter		-28.1	Rundel et al., 1999	values calculated from ΔC published values
Western Cape		monocot, geophytic	*Watsonia pyramidata*	C3			see notes	Sealy and van der Merwe, 1986	
Western Cape	Riverlands	monocot, restionacea	*Willdenowia arescens*	C3			-28.8	Araya et al., 2010	
Northern Cape	Akkerdisdraai	shrub, evergreen	*Zygophyllum cf. macrocarpum*	C3	winter		-24.5	Rundel et al., 1999	values calculated from ΔC published values
Northern Cape	Akkerdisdraai	shrub, evergreen	*Zygophyllum cordifolium*	C3	winter		-24.9	Rundel et al., 1999	values calculated from ΔC published values
Northern Cape	Akkerdisdraai	shrub, evergreen	*Zygophyllum prismatocarpum*	C3	winter		-22.9	Rundel et al., 1999	values calculated from ΔC published values

APPENDIX B

SUMMARY OF PUBLISHED STABLE CARBON ISOTOPE DATA FROM MICROMMAMMALS FROM SOUTHERN AFRICA

Appendix B: Published stable carbon isotope data from the literature for South African micromammals.

Area	Taxon	n	$\delta^{13}C$ hair	$\delta^{13}C$ coll.	$\delta^{13}C$ enam.	Citation
W	*Acomys subspinosus*	37	-22.01			van den Heuvel & Midgley, 2014
CSA	*Aethomys namaquensis*	6		-17.5		Thackeray *et al*., 2003
G	*Aethomys namaquensis*	5		-20		Thackeray *et al*., 2003
L	*Aethomys namaquensis*	1		-14.1		Thackeray *et al*., 2003
M	*Aethomys namaquensis*	1		-10.8		Thackeray *et al*., 2003
M	*Aethomys namaquensis*	1		-12.9		Thackeray *et al*., 2003
W	*Aethomys namaquensis*	1		-20.6		Thackeray *et al*., 2003
W	*Aethomys namaquensis*	1		-21.4		Thackeray *et al*., 2003
W	*Aethomys namaquensis*	10	-22.86			van den Heuvel & Midgley, 2014
W	*Amblysomus hottentotus*	1	-11.35			van den Heuvel & Midgley, 2014
W	*Bathyergus suillus*		-22.3			Robb *et al*., 2012
W	*Bathyergus suillus*	1		-22.1		Sealy & van der Merwe, 1986
W	*Bathyergus suillus*	1		-20.3		Sealy & van der Merwe, 1986
W	*Bathyergus suillus*	1		-17.8		Sealy & van der Merwe, 1986
W	*Bathyergus suillus*	1		-19.2		Sealy & van der Merwe, 1986
W	*Bathyergus suillus*	1			-5.3	Yeakel *et al*. 2007
W	*Bathyergus suillus*	1			-3.4	Yeakel *et al*. 2007
W	*Bathyergus suillus*	1			-9.2	Yeakel *et al*. 2007
W	*Bathyergus suillus*	1			-5.5	Yeakel *et al*. 2007
W	*Bathyergus suillus*	1			-6.1	Yeakel *et al*. 2007
W	*Bathyergus suillus*	1			-3.3	Yeakel *et al*. 2007
W	*Bathyergus suillus*	1			-6.7	Yeakel *et al*. 2007
W	*Bathyergus suillus*	1			-3.7	Yeakel *et al*. 2007
W	*Bathyergus suillus*	1			-6.5	Yeakel *et al*. 2007
W	*Bathyergus suillus*	1			-9.1	Yeakel *et al*. 2007
W	*Bathyergus suillus*	1			-10.3	Yeakel *et al*. 2007
W	*Chrysochloris asiatica*	1	-21.7			van den Heuvel & Midgley, 2014
W	*Crocidura flavescens*	6	-20.93			van den Heuvel & Midgley, 2014

Table A. Available stable carbon isotope data from the literature for South African micromammals, *Acomys-Crocidura*. All $\delta^{13}C$ values ‰VPDB. Excludes data from Cordron et al. (2015), which is in press. Area codes: WC= Western Cape, CSA = Central southern Africa, G = Gauteng, L = Limpopo

Area	Taxon	n	δ13C hair	δ13C coll.	δ13C enam.	Citation
CSA	*Cryptomys damarensis*	1			-14.2	Yeakel *et al*. 2007
CSA	*Cryptomys damarensis*	1			-13.9	Yeakel *et al*. 2007
CSA	*Cryptomys damarensis*	1			-14.2	Yeakel *et al*. 2007
CSA	*Cryptomys damarensis*	1			-14.3	Yeakel *et al*. 2007
CSA	*Cryptomys damarensis*	1			-14	Yeakel *et al*. 2007
CSA	*Cryptomys damarensis*	1			-13.7	Yeakel *et al*. 2007
CSA	*Cryptomys damarensis*	1			-14.1	Yeakel *et al*. 2007
CSA	*Cryptomys damarensis*	1			-14.1	Yeakel *et al*. 2007
CSA	*Cryptomys damarensis*	1			-14.1	Yeakel *et al*. 2007
CSA	*Cryptomys damarensis*	1			-13.3	Yeakel *et al*. 2007
KZN	*Cryptomys h. natalensis*	1			-8.3	Yeakel *et al*. 2007
KZN	*Cryptomys h. natalensis*	1			-8	Yeakel *et al*. 2007
KZN	*Cryptomys h. natalensis*	1			-8.7	Yeakel *et al*. 2007
KZN	*Cryptomys h. natalensis*	1			-4.7	Yeakel *et al*. 2007
KZN	*Cryptomys h. natalensis*	1			-6.3	Yeakel *et al*. 2007
KZN	*Cryptomys h. natalensis*	1			-13.2	Yeakel *et al*. 2007
KZN	*Cryptomys h. natalensis*	1			-10.9	Yeakel *et al*. 2007
G	*Cryptomys h. pretoriae*	1			-9.1	Yeakel *et al*. 2007
G	*Cryptomys h. pretoriae*	1			-14.7	Yeakel *et al*. 2007
G	*Cryptomys h. pretoriae*	1			-14.6	Yeakel *et al*. 2007
G	*Cryptomys h. pretoriae*	1			-13.8	Yeakel *et al*. 2007
G	*Cryptomys h. pretoriae*	1			-14.2	Yeakel *et al*. 2007
G	*Cryptomys h. pretoriae*	1			-14.3	Yeakel *et al*. 2007
G	*Cryptomys h. pretoriae*	1			-14.2	Yeakel *et al*. 2007
WC	*Cryptomys hottentotus*		-27			Robb *et al.*, 2012
WC	*Cryptomys hottentotus*	1	-23.44			van den Heuvel & Midgley, 2014
M	*Dendromus mesomelas*	2	-19.8			Symes *et al.*, 2013
M	*Dendromus mesomelas*	4	-23.6			Symes *et al.*, 2013
M	*Dendromus mystacalis*	1	-22.2			Symes *et al.*, 2013
WC	*Elephantulus edwardii*	8	-22.86			van den Heuvel & Midgley, 2014

Table B. Available stable carbon isotope data from the literature for South African micromammals, *Crytomys-Elephantulus*. All $\delta^{13}C$ values ‰VPDB. Excludes data from Cordron et al. (2015), which is in press. Area codes: WC= Western Cape, CSA = Central southern Africa, G = Gauteng, L = Limpopo, KZN = KwZulu-Natal

Area	Taxon	n	δ13C hair	δ13C coll.	δ13C enam.	Citation
WC	*Georychus capensis*		-25.8			Robb *et al.,* 2012
WC	*Georychus capensis*	1			-14.6	Yeakel *et al*. 2007
WC	*Georychus capensis*	1			-14.4	Yeakel *et al*. 2007
WC	*Georychus capensis*	1			-15.6	Yeakel *et al*. 2007
WC	*Georychus capensis*	1			-15.4	Yeakel *et al*. 2007
WC	*Georychus capensis*	1			-15.8	Yeakel *et al*. 2007
WC	*Georychus capensis*	1			-14.4	Yeakel *et al*. 2007
WC	*Georychus capensis*	1			-14.4	Yeakel *et al*. 2007
WC	*Gerbilliscus afra*	3	-22.32			van den Heuvel & Midgley, 2014
M	*Grammomys dolichurus*	5	-23.2			Symes *et al.,* 2013
M	*Grammomys dolichurus*	2	-23.2			Symes *et al.,* 2013
M	*Grammomys dolichurus*	1	-21.9			Symes *et al.,* 2013
M	*Graphiurus murinus*	3	-24.1			Symes *et al.,* 2013
M	*Graphiurus murinus*	3	-24.1			Symes *et al.,* 2013
WC	*Graphiurus ocularis*	2	-21.82			van den Heuvel & Midgley, 2014
G	*Mastomys sp.*	1			-14.6	Henry *et al.,* 2012
G	*Mastomys sp.*	1			-14.3	Henry *et al.,* 2012
G	*Mastomys sp.*	1			-8.1	Henry *et al.,* 2012
G	*Mastomys sp.*	1			-15.3	Henry *et al.,* 2012
G	*Mastomys sp.*	1			-14.1	Henry *et al.,* 2012
G	*Mastomys sp.*	1			-15.1	Henry *et al.,* 2012
G	*Mastomys sp.*	1			-16	Henry *et al.,* 2012
G	*Mastomys sp.*	1			-6.2	Henry *et al.,* 2012
G	*Mastomys sp.*	1			-10.2	Henry *et al.,* 2012
L	*Mastomys sp.*				-2.2	Hopley *et al.,* 2006
L	*Mastomys sp.*				-7.3	Hopley *et al.,* 2006
L	*Mastomys sp.*				-2.2	Hopley *et al*., 2006
G	*Micaelamys*	1			-14.9	Henry *et al.,* 2012
G	*Micaelamys*	1			-13.9	Henry *et al.,* 2012
G	*Micaelamys*	1			-10.9	Henry *et al.,* 2012
G	*Micaelamys*	1			-15.2	Henry *et al.,* 2012
G	*Micaelamys*	1			-13.5	Henry *et al.,* 2012
G	*Micaelamys*	1			-12.6	Henry *et al.,* 2012

Table C. Available stable carbon isotope data from the literature for South African micromammals, *Georychus-Micaelamys*. All $\delta^{13}C$ values ‰VPDB. Excludes data from Cordron et al. (2015), which is in press. Area codes: WC= Western Cape, CSA = Central southern Africa, G = Gauteng, L = Limpopo, KZN = KwZulu-Natal. *Micaelamys* is an alternate generic designation for *Aethomys*, but has been retained in this table as that is the genus assigned to these specimens by their analysts.

Area	Taxon	n	δ13C hair	δ13C coll.	δ13C enam.	Citation
M	*Mus minutoides*	4	-21.3			Symes *et al.,* 2013
WC	*Mus minutoides*	13	-22.78			van den Heuvel & Midgley, 2014
WC	*Myomys verreauxii*	6	-22.98			van den Heuvel & Midgley, 2014
L	*Myosorex sp.*				-6.8	Hopley *et al.,* 2006
L	*Myosorex sp.*				-6	Hopley *et al.,* 2006
L	*Myosorex sp.*				-3	Hopley *et al.,* 2006
M	*Myosorex varius*	3	-23.2			Symes *et al.,* 2013
M	*Myosorex varius*	3	-15.6			Symes *et al.,* 2013
M	*Myosorex varius*	5	-20.8			Symes *et al.,* 2013
WC	*Otomys irroratus*	2	-25.24			van den Heuvel & Midgley, 2014
G	*Otomys sp.*	1			-3.2	Henry *et al.,* 2012
G	*Otomys sp.*	1			-8.5	Henry *et al.,* 2012
G	*Otomys sp.*	1			-5.5	Henry *et al.,* 2012
G	*Otomys sp.*	1			-5.9	Henry *et al.,* 2012
G	*Otomys sp.*	1			-4.6	Henry *et al.,* 2012
L	*Otomys sp.*				-3.6	Hopley *et al.,* 2006
L	*Otomys sp.*				-2.8	Hopley *et al.,* 2006
L	*Otomys sp.*				-2.8	Hopley *et al.,* 2006
M	*Rhabdomys pumilio*	4	-20.9			Symes *et al.,* 2013
M	*Rhabdomys pumilio*	3	-22.8			Symes *et al.,* 2013
WC	*Rhabdomys pumilio*	13	-22.49			van den Heuvel & Midgley, 2014
G	*Steatomys*	1			-11.5	Henry *et al.,* 2012
G	*Steatomys*	1			-1.7	Henry *et al.,* 2012
G	*Steatomys*	1			-0.2	Henry *et al.,* 2012
G	*Steatomys*	1			0.7	Henry *et al.,* 2012
M	*Suncus varilla*	2	-24.6			Symes *et al.,* 2013
WC	*Suncus varilla*	1	-22.53			van den Heuvel & Midgley, 2014

Table D. Available stable carbon isotope data from the literature for South African micromammals, *Mus-Suncus*. All $\delta^{13}C$ values ‰VPDB. Excludes data from Cordron et al. (2015), which is in press. Area codes: WC= Western Cape, CSA = Central southern Africa, G = Gauteng, L = Limpopo, KZN = KwZulu-Natal.